

**Some Aspects of Atmospheric Circulation,
Moisture and Heat Budgets at Selected
Areas Over Arabian Sea**

THESIS SUBMITTED TO
THE COCHIN UNIVERSITY OF SCIENCE AND TECHNOLOGY
FOR THE DEGREE OF
DOCTOR OF PHILOSOPHY
IN
METEOROLOGY

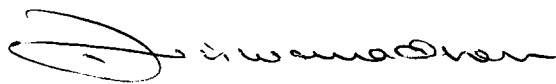
By
P. G. MEENA

PHYSICAL OCEANOGRAPHY AND METEOROLOGY DIVISION
SCHOOL OF MARINE SCIENCES
COCHIN UNIVERSITY OF SCIENCE AND TECHNOLOGY
COCHIN 682 016

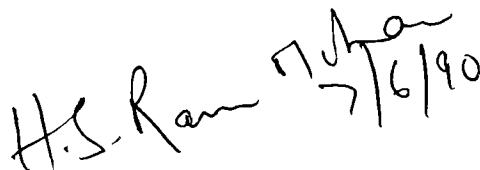
MAY 1990

CERTIFICATE

This is to certify that this thesis is an authentic record of research work carried out by Smt. P.G.MEENA in the School of Marine Sciences for the Ph.D. degree of the Cochin University of Science and Technology and no part of it has previously formed the basis for the award of any degree in any University.



D.V.VISWANADHAM
Principal Supervising Teacher
Reader in Meteorology
Department of Geophysics
Banaras Hindu University.



H.S.RAM MOHAN
Co-Supervising Teacher
Reader in Meteorology
School of Marine Sciences
Cochin University of Science and Technology.

C O N T E N T S

PREFACE

LIST OF FIGURES

CHAPTER	I	:	INTRODUCTION, LITERATURE REVIEW, MATERIALS AND METHODS	1
CHAPTER	II	:	ATMOSPHERIC CIRCULATION OVER ARABIAN SEA	49
CHAPTER	III	:	STUDIES ON MOISTURE BUDGET	72
CHAPTER	IV	:	STUDIES ON HEAT BUDGET	93
CHAPTER	V	:	SEA SURFACE TEMPERATURE AND ITS RELATION TO RAINFALL	115
CHAPTER	VI	:	SUMMARY AND CONCLUSIONS	126
REFERENCES				134

APPENDIX

PREFACE

The heavy concentration of the monsoon rain in the four month period (June - September), the large variability in the behaviour of the monsoon from year to year and the non-availability of irrigation facilities over large areas of the country, makes the Indian economy critically dependent on the timely arrival and withdrawal of the monsoon and on a good space-time distribution of the monsoon rainfall. Monsoon dynamics and processes in the Indian Ocean appear to be related to the El Nino-Southern Oscillation events, which show that the Indian summer monsoon has to be viewed as a part of the planetary scale general circulation. In view of the vital linkage of the summer monsoon to the Indian economy and its influence on the global atmospheric circulation, the energetics of the Arabian Sea area of the Indian Ocean, which play a major role in the sequence of events leading to the Indian summer monsoon is subjected to a detailed study.

On account of the interaction between the atmosphere and the ocean at the air sea interface, circulation systems of the atmosphere and the ocean are coupled. The latent and sensible heat fluxes from the ocean to the atmosphere constitute a significant energy source for atmospheric circulation. The evaporation over the sea is influenced by the sea surface temperature (S S T) and the

(ii)

Arabian sea surface temperatures undergo a sustained cooling of several degrees between April and August every year. Since the southwesterly monsoon flow carries the moisture from the Arabian Sea to the Indian sub-continent, the variations in the sea surface temperatures over the Arabian Sea are expected to lead to the variations in the available moisture over the sub-continent. Therefore, it is proposed to examine if there exists a link between the sea surface temperature variation over the Arabian Sea and the monsoon rainfall over the west coast of India. Detailed variations in the moisture and heat budgets over some parts of the Arabian Sea are also studied.

For the sake of convenience, the thesis is divided into six chapters. The first chapter comprises of the introduction, the review of literature and the methodology. The second chapter deals with the circulation patterns over the area of study; the third chapter consists of moisture budget studies while the fourth chapter is concerned with the heat budget studies. The influence of Arabian sea surface temperature on rainfall along the west coast of India is presented in the fifth chapter. The overall summary and conclusions are briefly presented in the final chapter. Variations of certain derived parameters are discussed with minute details in view of their importance, while that of some other parameters are limited to the discussion of the important features only.

LIST OF FIGURES

<u>Fig.No.</u>	<u>Name</u>	<u>Following Pg.No.</u>
FIG.1	MAP SHOWING THE AREAS OF STUDY.	37
FIG.2.1(a)	WEATHER MAP FOR 11TH JUNE 1977.	51
FIG.2.1(b)	WEATHER MAP FOR 05TH JULY 1977.	52
FIG.2.1(c)	WEATHER MAP FOR 25TH MAY 1979.	53
FIG.2.1(d)	WEATHER MAP FOR 11TH JUNE 1979.	55
FIG.2.2(a)	VERTICAL VARIATION OF SPECIFIC HUMIDITY AT 00 GMT DURING PHASE-I	55
FIG.2.2(b)	VERTICAL VARIATION OF SPECIFIC HUMIDITY AT 12 GMT DURING PHASE-I	55
FIG.2.2(c)	VERTICAL VARIATION OF SPECIFIC HUMIDITY AT 00 GMT DURING PHASE-II	56
FIG.2.2(d)	VERTICAL VARIATION OF SPECIFIC HUMIDITY AT 12 GMT DURING PHASE-II	56
FIG.2.2(e)	VERTICAL VARIATION OF SPECIFIC HUMIDITY AT 00 GMT DURING PHASE-III	56
FIG.2.2(f)	VERTICAL VARIATION OF SPECIFIC HUMIDITY AT 12 GMT DURING PHASE-III	56
FIG.2.2(g)	VERTICAL VARIATION OF SPECIFIC HUMIDITY AT 00 GMT DURING PHASE-IV	56
FIG.2.2(h)	VERTICAL VARIATION OF SPECIFIC HUMIDITY AT 12 GMT DURING PHASE-IV	56
FIG.2.3(a)	VERTICAL VARIATION OF ZONAL AND MERIDIONAL WIND AT 00 GMT DURING PHASE-I	57
FIG.2.3(b)	VERTICAL VARIATION OF ZONAL AND MERIDIONAL WIND AT 12 GMT DURING PHASE-I	57
FIG.2.3(c)	VERTICAL VARIATION OF ZONAL AND MERIDIONAL WIND AT 00 GMT DURING PHASE-II	58
FIG.2.3(d)	VERTICAL VARIATION OF ZONAL AND MERIDIONAL WIND AT 12 GMT DURING PHASE-II	58

<u>Fig.No.</u>	<u>Name</u>	<u>Following Pg.No.</u>
FIG.2.3(e)	VERTICAL VARIATION OF ZONAL AND MERIDIONAL WIND AT 00 GMT DURING PHASE-III	58
FIG.2.3(f)	VERTICAL VARIATION OF ZONAL AND MERIDIONAL WIND AT 12 GMT DURING PHASE-III	58
FIG.2.3(g)	VERTICAL VARIATION OF ZONAL AND MERIDIONAL WIND AT 00 GMT DURING PHASE-IV	59
FIG.2.3(h)	VERTICAL VARIATION OF ZONAL AND MERIDIONAL WIND AT 12 GMT DURING PHASE-IV	59
FIG.2.4(a)	VARIATION OF PRECIPITABLE WATER VAPOUR DURING PHASE-I	60
FIG.2.4(b)	VARIATION OF PRECIPITABLE WATER VAPOUR DURING PHASE-II	61
FIG.2.4(c)	VARIATION OF PRECIPITABLE WATER VAPOUR DURING PHASE-III	61
FIG.2.4(d)	VARIATION OF PRECIPITABLE WATER VAPOUR DURING PHASE-IV	61
FIG.2.5(a)	VARIATION OF KINETIC ENERGY DURING PHASE-I	62
FIG.2.5(b)	VARIATION OF KINETIC ENERGY DURING PHASE-II	62
FIG.2.5(c)	VARIATION OF KINETIC ENERGY DURING PHASE-III	63
FIG.2.5(d)	VARIATION OF KINETIC ENERGY DURING PHASE-IV	63
FIG.2.6(a)	VERTICAL TIME SECTION OF (a) VORTICITY, (b) DIVERGENCE and (c) VERTICAL VELOCITY DURING PHASE-I	64
FIG.2.6(b)	VERTICAL TIME SECTION OF (a) VORTICITY, (b) DIVERGENCE and (c) VERTICAL VELOCITY DURING PHASE-II	65
FIG.2.6(c)	VERTICAL TIME SECTION OF (a) VORTICITY, (b) DIVERGENCE and (c) VERTICAL VELOCITY DURING PHASE-III	68

<u>Fig.No.</u>	<u>Name</u>	<u>Following Pg.No.</u>
FIG.2.6(d)	VERTICAL TIME SECTION OF (a) VORTICITY, (b) DIVERGENCE and (c) VERTICAL VELOCITY DURING PHASE-IV	70
FIG.3.1(a)	DAY-TO-DAY VARIATIONS OF RATE OF EVAPORATION FOR PHASE-I	75
FIG.3.1(b)	DAY-TO-DAY VARIATIONS OF RATE OF EVAPORATION FOR PHASE-II	76
FIG.3.1(c)	DAY-TO-DAY VARIATIONS OF RATE OF EVAPORATION FOR PHASE-III	76
FIG.3.1(d)	DAY-TO-DAY VARIATIONS OF RATE OF EVAPORATION FOR PHASE-IV	76
FIG.3.2	DIURNAL VARIATION OF RATE OF EVAPORATION FOR THE FOUR PHASES	77
FIG.3.3	DAY-TO-DAY VARIATIONS OF AVERAGE EVAPORATION DURING THE FOUR PHASES	78
FIG.3.4(a)	DAY-TO-DAY VARIATIONS OF SUM OF MOISTURE FLUX FROM SURFACE TO 200 mbs DURING PHASE-I	79
FIG.3.4(b)	DAY-TO-DAY VARIATIONS OF SUM OF MOISTURE FLUX FROM SURFACE TO 200 mbs DURING PHASE-II	80
FIG.3.4(c)	DAY-TO-DAY VARIATIONS OF SUM OF MOISTURE FLUX FROM SURFACE TO 200 mbs DURING PHASE-III	80
FIG.3.4(d)	DAY-TO-DAY VARIATIONS OF SUM OF MOISTURE FLUX FROM SURFACE TO 200 mbs DURING PHASE-IV	80
FIG.3.5(a)	DAY-TO-DAY VARIATIONS OF SUM OF MOISTURE FLUX FROM SURFACE TO 700 mbs DURING PHASE-I	81
FIG.3.5(b)	DAY-TO-DAY VARIATIONS OF SUM OF MOISTURE FLUX FROM SURFACE TO 700 mbs DURING PHASE-II	82
FIG.3.5(c)	DAY-TO-DAY VARIATIONS OF SUM OF MOISTURE FLUX FROM SURFACE TO 700 mbs DURING PHASE-III	82

<u>Fig.No.</u>	<u>Name</u>	<u>Following Pg.No.</u>
FIG.3.5(d)	DAY-TO-DAY VARIATIONS OF SUM OF MOISTURE FLUX FROM SURFACE TO 700 mbs DURING PHASE-IV	82
FIG.3.6(a)	DAY-TO-DAY VARIATIONS OF SUM OF MOISTURE FLUX FROM 700 TO 200 mbs DURING PHASE-I	83
FIG.3.6(b)	DAY-TO-DAY VARIATIONS OF SUM OF MOISTURE FLUX FROM 700 TO 200 mbs DURING PHASE-II	83
FIG.3.6(c)	DAY-TO-DAY VARIATIONS OF SUM OF MOISTURE FLUX FROM 700 TO 200 mbs DURING PHASE-III	84
FIG.3.6(d)	DAY-TO-DAY VARIATIONS OF SUM OF MOISTURE FLUX FROM 700 TO 200 mbs DURING PHASE-IV	84
FIG.3.7(a)	DIURNAL VARIATION OF SUM OF MOISTURE FLUX FROM SURFACE TO 200 mb DURING PHASE-I	85
FIG.3.7(b)	DIURNAL VARIATION OF SUM OF MOISTURE FLUX FROM SURFACE TO 200 mb DURING PHASE-II	85
FIG.3.7(c)	DIURNAL VARIATION OF SUM OF MOISTURE FLUX FROM SURFACE TO 200 mb DURING PHASE-III	86
FIG.3.7(d)	DIURNAL VARIATION OF SUM OF MOISTURE FLUX FROM SURFACE TO 200 mb DURING PHASE-IV	86
FIG.3.8(a)	DAY-TO-DAY VARIATIONS OF NET MOISTURE FLUX DIVERGENCE DURING PHASE-I	88
FIG.3.8(b)	DAY-TO-DAY VARIATIONS OF NET MOISTURE FLUX DIVERGENCE DURING PHASE-II	88
FIG.3.8(c)	DAY-TO-DAY VARIATIONS OF NET MOISTURE FLUX DIVERGENCE DURING PHASE-III	88
FIG.3.8(d)	DAY-TO-DAY VARIATIONS OF NET MOISTURE FLUX DIVERGENCE DURING PHASE-IV	88

<u>Fig.No.</u>	<u>Name</u>	<u>Following Pg.No.</u>
FIG.3.9(a)	DIURNAL VARIATION OF NET MOISTURE FLUX DURING PHASE-I & II	89
FIG.3.9(b)	DIURNAL VARIATION OF NET MOISTURE FLUX DURING PHASE-III & IV	90
FIG.3.10	DAY-TO-DAY VARIATIONS OF AVERAGE NET MOISTURE FLUX DURING THE FOUR PHASES	91
FIG.3.11	DAY-TO-DAY VARIATIONS OF RATE OF PRECIPITATION DURING THE FOUR PHASES	92
FIG.4.1(a)	DAY-TO-DAY VARIATIONS OF THE RATE OF SENSIBLE HEAT DURING PHASE-I	95
FIG.4.1(b)	DAY-TO-DAY VARIATIONS OF THE RATE OF SENSIBLE HEAT DURING PHASE-II	95
FIG.4.1(c)	DAY-TO-DAY VARIATIONS OF THE RATE OF SENSIBLE HEAT DURING PHASE-III	96
FIG.4.1(d)	DAY-TO-DAY VARIATIONS OF THE RATE OF SENSIBLE HEAT DURING PHASE-IV	96
FIG.4.2(a)	DIURNAL VARIATION OF RATE OF SENSIBLE HEAT DURING PHASE-I	97
FIG.4.2(b)	DIURNAL VARIATION OF RATE OF SENSIBLE HEAT DURING PHASE-II	97
FIG.4.2(c)	DIURNAL VARIATION OF RATE OF SENSIBLE HEAT DURING PHASE-III	98
FIG.4.2(d)	DIURNAL VARIATION OF RATE OF SENSIBLE HEAT DURING PHASE-IV	98
FIG.4.3(a)	DAY-TO-DAY VARIATIONS OF HEAT FLUX DURING PHASE-I	99
FIG.4.3(b)	DAY-TO-DAY VARIATIONS OF HEAT FLUX DURING PHASE-II	100
FIG.4.3(c)	DAY-TO-DAY VARIATIONS OF HEAT FLUX DURING PHASE-III	101
FIG.4.3(d)	DAY-TO-DAY VARIATIONS OF HEAT FLUX DURING PHASE-IV	101
FIG.4.4(a)	DIURNAL VARIATION OF HEAT FLUX DURING PHASE-I	102

<u>Fig.No.</u>	<u>Name</u>	<u>Following Pg.No.</u>
FIG.4.4(b)	DIURNAL VARIATION OF HEAT FLUX DURING PHASE-I	102
FIG.4.4(c)	DIURNAL VARIATION OF HEAT FLUX DURING PHASE-II	103
FIG.4.4(d)	DIURNAL VARIATION OF HEAT FLUX DURING PHASE-II	103
FIG.4.4(e)	DIURNAL VARIATION OF HEAT FLUX DURING PHASE-III	104
FIG.4.4(f)	DIURNAL VARIATION OF HEAT FLUX DURING PHASE-IV	105
FIG.4.4(g)	DIURNAL VARIATION OF HEAT FLUX DURING PHASE-IV	105
FIG.4.5(a)	DAY-TO-DAY VARIATIONS OF NET HEAT FLUX DIVERGENCE DURING PHASE-I	107
FIG.4.5(b)	DAY-TO-DAY VARIATIONS OF NET HEAT FLUX DIVERGENCE DURING PHASE-II	107
FIG.4.5(c)	DAY-TO-DAY VARIATIONS OF NET HEAT FLUX DIVERGENCE DURING PHASE-III	108
FIG.4.5(d)	DAY-TO-DAY VARIATIONS OF NET HEAT FLUX DIVERGENCE DURING PHASE-IV	108
FIG.4.6(a)	DIURNAL VARIATION OF NET HEAT FLUX DIVERGENCE DURING PHASE-I	109
FIG.4.6(b)	DIURNAL VARIATION OF NET HEAT FLUX DIVERGENCE DURING PHASE-II	110
FIG.4.6(c)	DIURNAL VARIATION OF NET HEAT FLUX DIVERGENCE DURING PHASE-III	110
FIG.4.6(d)	DIURNAL VARIATION OF NET HEAT FLUX DIVERGENCE DURING PHASE-IV	111
FIG.4.7	DAY-TO-DAY VARIATIONS OF AVERAGE OF NET HEAT FLUX DIVERGENCE	112
FIG.4.8	DAY-TO-DAY VARIATIONS OF RATE OF RADIATIVE COOLING	113
FIG.5.1	MAP SHOWING THE AREA STUDY	116

CHAPTER I

1.1 INTRODUCTION

The importance of the summer monsoon in influencing the Indian economy can hardly be over emphasised. This monsoon which prevails over India during June to September exhibits substantial inter-annual variations which lead to either drought conditions or flood situations. The origin of it can best be described as follows.

During the Northern summer, the south east trades from Southern Hemisphere recurve while crossing the Equator and come into Southern Asia as south west monsoon with three main branches, one in the Arabian Sea, one in the Bay of Bengal and one in the South China Sea. Of these the air current over Arabian Sea is more intense and steady. Most parts of South Asia, particularly India, receives most of its annual rainfall during this monsoon period. Krishnamurthy et al (1981) consider onset vortex over Arabian Sea as a characteristic circulation feature heralding the onset of the Indian Summer Monsoon. Pearce and Mohanty (1984) concluded that the onset consists of a moisture building up stage and a subsequent intensification of winds over the Arabian Sea and increased latent heat release.

The different ways in which the ocean could influence the climate can be described as due to the physical and thermal properties of water. Because of the large volume, heat capacity and absorptivity of these water sources, they form an important source of heat and moisture to the atmosphere. The oceans have a large thermal inertia which cause a time lag between the absorption, redistribution and release of the solar energy and hence effectively influence the variations in climate.

The ocean and the atmosphere together act as a coupled system in a complex manner and controls one another. Various studies have indicated that tropical oceans have greater influence on the general circulation of the atmosphere than extra tropical oceans. Among the tropical oceans, the Indian Ocean sector is unique in its characteristics because of its spectacular seasonal changes. On account of its complexity, the studies of moisture and heat budget would become doubly important in the Arabian Sea. The monsoon experiments MONSOON-77 and MONEX-79 provided data and details necessary for a better understanding of the meteorology over the Indian Ocean. The Indian Summer Monsoon characterised by the seasonal reversal of wind is believed to be caused by the differential heating of land and sea which in turn is due to the asymmetric continentality and seasonal march of the sun, and hence the Arabian

Sea with its complex S S T pattern might feedback the overlying atmosphere. Hastenrath (1985) describes that pressure over land and wind speed over Arabian Sea act inversely, before the onset of the monsoon. It was also inferred that the region of warmest water and surface pressure moves northward in the Indian Ocean from February to July.

The evaporation over the sea which is the principal moisture source of the atmosphere is influenced by the sea surface temperature. The dramatic cooling of the Arabian Sea by a few degrees from April to August every year poses some serious questions about the mutual role of the monsoon and the Arabian Sea surface temperature. It is logical to think that these changes of evaporation and the consequent sea surface temperature changes might be associated either directly or indirectly with the rainfall received over the country in general and along the westcoast of India in particular. It will not be out of context to state that probably Arabian Sea surface temperature may be one of the potential predictors of the rainfall over India, although most of the proposed indicators seem to be more controlled by the monsoon rather than controlling it. However this should not defer investigators from exploring the possible indicators that influence the behaviour of monsoon. The numerous ongoing studies towards this end are the best examples for a determined effort to arrive atleast at stati-

stical indicators for predicting the monsoon. The results of these studies differ, mainly because of the difference in the data sets and approaches to the problem. Since this aspect is still open for further studies, an attempt is made to study the relation between Arabian Sea surface temperature and the rainfall along the West coast of India. West coast is chosen for the study because, the influence of Arabian Sea surface temperature should be more in this region since the monsoon enters the country through this coast.

The detailed objectives of the thesis are presented hereunder.

1. To study over the stationary ship polygon positions in Arabian Sea during 1977 and 1979, the diurnal and day to day variations of -
 - (a) Specific humidity, precipitable water vapour, wind, vorticity, divergence, vertical velocity and kinetic energy.
 - (b) Moisture budget including the evaporation and the moisture flux divergence.
 - (c) Heat budget including sensible heat and heat flux divergence.

2. To study the relation between Arabian Sea surface temperature and the monsoon rainfall along the west coast of India for a six year period including the MONEX years.

1.2 REVIEW OF LITERATURE

This section constitutes the literature available on earlier studies in the field. However to give a very detailed literature survey on monsoons is not only a very difficult task but also beyond the scope of the present study. For the sake of completeness a brief survey of the recent studies only are presented which may not be exhaustive but adequate enough to present the knowledge in this field.

From the various studies in the recent years, the role of oceans in influencing the atmospheric processes have become quite evident. During the last few decades, there have been many attempts (Pisharoty, (1965, 1981), Bhumralkar (1978), Shukla (1975, 1976, 1986) to find some oceanic parameters as predictors for the Indian Summer Monsoon. Although the relative importance of these parameters is still in dispute, studies made by Bunker* (1965), Pisharoty (1965, 1981), Ramage (1966, 1971), Ananthakrishnan (1968), Das (1968, 1985, 1986), Rao and Desai (1971), Rao (1970), Bhumralkar (1978), Krishnamurthy (1978), Sharma et al

(1980), Cadet and Reverdin (1981), Joseph (1981), Ramanathan (1981), Keshavamurthy (1982), Kraus and Hauson (1983) and Joseph and Pillai (1984, 1986) have given a deeper insight into the processes involved.

In general, any large water body acts as a significant source of water vapour to the atmosphere. However, only when the motion field develops low level convergence, this water vapour is transported aloft. For further moistening of the air column, convergence in the middle level is equally important. Circulation parameters such as wind, divergence, vorticity, kinetic energy, vertical velocity, and amount of water vapour in the atmosphere above the area have therefore been studied. Ramage (1966), Findlater (1969(a) and 1969(b)), Ali (1980), Bhide et al (1982) and Mooley and Parthasarathy (1983) have studied the different circulation parameters influencing the Indian monsoon. Das (1962), studied the east-west Walker cells in the Indian longitudes. Shukla and Sajnani (1971) pointed out that with all the limitations in the wind data accuracy and grid length used for finite difference technique, the computed divergence depicts reasonable values which are also synoptically consistent and exhibit systematic changes from day to day and from one level to another.

Wyrtki (1971) produced an Oceanographic atlas using the IIOE data, which serves as a valuable reference to the

values of different meteorological parameters over the Arabian Sea area. Bhumralkar (1974) reported that air-sea exchanges over the sea do not control the fluctuations of the monsoon but are themselves influenced by the variations of the monsoon flow. Appa Rao and Murthy (1977) evaluated the values of the precipitable water, mean and eddy transport of moisture and the vergence patterns over the Indian sub-continent, during two contrasting summer monsoons. They noted that in a good monsoon year there were (a) increased zonal and meridional transports, (b) stronger divergence and convergence patterns and (c) marginally higher precipitable water compared to a bad monsoon year.

Using MONEX-'79 dropsonde data, over the Arabian Sea and Indian West coast region, Ali (1980) analysed charts for a 48 hour period and found that a low level strong wind current with high shearing values is present in the southwest monsoon current. The speed of this current decreases steadily with height and finally around 500 mb level, the zonal direction was reversed from westerly to easterly. Rao and Webdell (1981) estimated the divergence, vorticity and humidity of air columns at various locations in the Arabian Sea. They pointed out that the areas of weak vertical velocities were characterised by low level convergence while that of divergence by gentle subsidence. Sinha and Sharma (1981) have presented a review on the different methods of

solving the omega equation to calculate the vertical velocity. Studies by Cadet and Reverdin (1981) and Cadet (1983), showed that the establishment of the strong circulation associated with the onset of monsoon is followed with a lag of 2 to 3 days, by a temperature drop of 2°C. There is also a significant positive correlation between the intensity of the wind over the Arabian Sea and monsoon activity over Central India. Ramanathan (1981, 1982) have studied the onset of monsoon and the atmospheric boundary layer over the Arabian Sea using MONEX '79 data. He found that the day to day variations of the parameters showed two periods of convective activity - one at the beginning of the onset period and the other during the active monsoon period, both being in June.

Bhide et al (1982) observed that during the onset phase of 1979 summer monsoon, organised convective synoptic scale systems such as (a) an easterly wave, (b) a cyclonic Vortex (on 8-9 June) and (c) a cyclonic circulation produced disturbed weather situation during June 1977. Chuchkalov (1982) have discussed the vertical structure of the Arabian Sea in different synoptic situations, taking into consideration the complex layer structure of the tropical and equatorial atmosphere. Howland and Sikdar (1983) studied the wind fields over the Arabian Sea for 1979 using a variety of data sources. They employed the kinematic method

to calculate divergence and O'Brien's technique to adjust the divergence of a column of atmosphere to calculate vertical velocity. They found that, the kinematic profiles of wind, divergence and vertical velocity undergo almost a complete reversal during the monsoon season.

There had been many attempts to relate the monsoon rainfall with the tropical circulation features. Mooley and Parthasarathy (1983) have found a wet and dry index for the Indian monsoon rainfall and correlated them with the tropical circulation features such as Southern Oscillation and El-Nino.

Bavadekar (1984) has explained the methods to compute the water vapour flux along a boundary wall and also has tabulated the moisture budget values for different years.

Ray and Bedi (1985) investigated the thermodynamic and kinematic structure of the troposphere over the Arabian Sea and Bay of Bengal during the Southwest monsoon season, making use of the ship polygon data taken during MONEX '79. They found that during the pre-onset phase, the flow was rather weak with dominantly subsiding motion and low moisture content while the onset phase was characterised by an increase in the kinetic energy as well as moisture content over the Arabian Sea. The height of the level of non-

divergence over Arabian Sea during pre-onset period was around 700 mb. The above mentioned studies gave a suitable background knowledge on the circulation and synoptic features over the Arabian Sea during the southwest monsoon months.

Moisture budget studies generally involve the computation of evaporation and latent heat flux together with moisture divergence or convergence by wind. Pisharoty (1965) was among the first to compute the water vapour budget of the lower troposphere over the Arabian Sea. He considered a cuboidal volume with its bottom at the sea level, and top at 450 mb level, eastern boundary along 42°E , western boundary along 75°E , northern boundary along 26°N and southern boundary along the equator. He computed net fluxes of water vapour across the equator into the sea and from the Arabian Sea across the Westcoast of India. His estimates suggested that more than half of the moisture crossing the West coast of India, was supplied by evaporation from the Arabian Sea and the remainder originating in the Southern Hemisphere and crossing the equator, between 42° and 75°E .

Saha (1970), using additional data recomputed the moisture fluxes across the equatorial box of rectangular volume over the above mentioned area and contrary to

Pisharoty's results found that the flux of water vapour across the equator is about 30% larger than the evaporation over the Arabian Sea. Saha and Suryanarayana (1972) computed the mean monthly values of vertical fluxes of sensible and latent heat from the surface of Indian Ocean for a five year period and showed that in 1967, the area under negative sensible heat flux extended southward to almost equator and to 70°E longitude. They found that the pattern is comparable to that during 1964 in areas extent as well as magnitude and both were good monsoon years. Their investigation on evaporation flux over Arabian sea showed that the region of low flux values coincided with the regions of upwelling and cold sea surface. Saha and Bavadekar (1973) later on studied the budget of water vapour of the lower troposphere (below 450 mb) by computing both mean and eddy motions. They used the following equation to compute fluxes

$$F = \frac{1}{g} \int_{p_t}^{p_b} \int_0^L v(p, l) q(p, l) dl dp$$

(The symbols have their usual meanings). The horizontal as well as vertical walls were divided into many segments and then integrated. Relative magnitudes of net cross-equatorial flux of water vapour into the volume and evaporation from the surface of the Arabian Sea appear to suggest that on an average the former may be about 30 percent larger than the latter.

Bhumralkar (1978) has shown that there was considerable increase in moisture content downstream of the monsoon air mass over the Eastern Arabian Sea before it strikes the West coast of India. Hastenrath and Lamb (1980) also found that a large portion of the moisture evaporating from Southern Tropical Indian Ocean during the northern summer is being carried northward across the equator in the lower layers of the monsoon flow.

Studies by Peixoto and Oort (1983) indicated the importance of the Tropical South Indian Ocean and the subordinate role of the Arabian Sea as a water vapour source for the Indian summer monsoon.

Cadet (1981) and Cadet and Reverdin (1981) examined the water vapour transport over the Indian Ocean and reported that 70% of the water vapour crossing the West coast of India come from the Southern Hemisphere and the remaining could be from the Arabian Sea evaporation. More than 50% of the total cross equatorial moisture flow was through the region between 45° and 60° E. Thus, it can be seen that, there are differences of opinion about the source region of moisture for the monsoon flow.

It may be mentioned that most of the above studies had been based on sparse upper air observations and availability of ISMEX-73 data helped many more to work on this

aspect. Jambunathan and Ramamurthy (1975) noticed no significant difference in temperature and moisture contents, between active and weak monsoons in the very lower atmosphere during 1973. Using same data, Pant (1977) calculated the heat and moisture fluxes over the Arabian sea area and concluded that during disturbed weather conditions, sensible heat flux shows a decrease. He also found a well defined diurnal variation for the sensible heat with a maximum positive flux around midnight and minimum around mid-day. In a similar study but using climatological data, Rao et al (1977) reported that during monsoon break there is a net loss of heat over Northern Arabian Sea and a net heat gain over the Bay of Bengal.

Saha and Bavadekar (1977) extended their earlier study (1973) using a nine year (1964-72) data set and got good correlations (0.87) between net moisture flux across the West coast of India south of Bombay and the monsoon rainfall. A later study by Bavadekar and Khaladkar (1982) for contrasting monsoon seasons revealed that zonal transport of moisture during good monsoon period is more in the West coast sector, south of Bombay.

Ghosh et al (1978) also using ISMEX-73 data calculated the water vapour budget over the Arabian Sea and drew conclusions supporting Pisharoty (1965). They further

reported that evaporation exceeded precipitation in the East Arabian Sea near the West coast of India and also found that there are no significant changes in the fluxes across the Equator at 50°E between active and weak monsoon periods.

Rao et al (1981) found that greater evaporation occurred over the Arabian Sea area before the onset of monsoon and after complete onset, there is a decrease in evaporation by 30 to 40 percent.

Ramanadham et al (1981) using MONSOON-77 data found that the latent heat flux associated with the onset vortex over Arabian sea is larger than that associated with a depression over north Bay of Bengal.

Rao et al (1981) compared estimated evaporation values over the Arabian Sea with rainfall derived from satellites for the three summer seasons of 1973, 1974 and 1977. They found that the total precipitation over Arabian Sea was only 40% of the evaporation during these seasons and they hypothesised that the remaining part might have been transported into the Indian sub-continent.

In yet another study, Bavadekar (1982) has calculated the monthly mean transfer of water vapour in the layer below 700 mb for India, for the years 1962-1972, and correlated them with summer monsoon rainfall. The correlations were negative or small positive values for different periods

Murakami et al (1983) evaluated the water vapour budget over the Arabian Sea and showed that the evaporation and precipitation over the Arabian Sea nearly balance each other. Hence the importance of cross-equatorial moisture transport in the south west monsoon rainfall of India is emphasized.

By 1981, MONEX data sets were available and there was a spurt in the studies, on the energy budgets especially over the Arabian Sea. Nitta (1980) estimated the energy budget over Bay of Bengal and found that the magnitude of latent heat flux is generally an order higher than the heat flux. Mohanty et al (1982b) and Mohanty and Singh (1983) studied the influence of heat, moisture and moist static energy over the Arabian Sea and adjoining area on the onset and activities of the Indian summer monsoon. Their studies indicated the significant increase in the net enthalpy, latent heat energy, moist static energy and a number of other budget parameters well in advance of the onset of monsoon over Kerala coast. The vertical distribution of the budget parameters revealed that the secondary maxima of horizontal heat and moisture flux divergence observed during active monsoon period in the upper troposphere are replaced by a minimum during weak monsoon period. They also found that the cross-equatorial flow influences the intensity of

the monsoon and there was an excess of condensation over evaporation over the Arabian Sea.

Chowdhury and Karmakar (1982) examined the mean vertical profiles of atmospheric energy using MONEX-79 data. The variations of enthalpy, dry static energy and latent heat with height showed that the influx of moisture remains mainly concentrated in the lower troposphere and becomes zero by 200 mb.

Howland and Sikdar (1983), calculated the moisture budget for pre-monsoon and monsoon onset conditions in the North Eastern Arabian sea using a variety of aerological data taken during MONEX-79. They used the bulk aerodynamic method to calculate the evaporation and for moisture budget used the following equation;

$$P = E - 1/g \int_p^R \nabla \cdot q \, v \, dp$$

where P is precipitation, E is evaporation and the last term is the horizontal transport of moisture. They noted that there was good increase in the specific humidity (5 g/Kg), and evaporation with the onset of the monsoon. Their results also highlight the importance of cross equatorial moisture flux especially west of 60°E.

As in the above study, Sadharam (1987) estimated the heat and moisture budgets of the atmosphere over the Central

Equatorial Indian Ocean. He used the flux of latent heat across the boundary walls of the area of study, evaporation and precipitation terms for moisture budget computations and sensible heat, heat due to precipitation, flux of dry static energy and radiational heating for heat budget. The time mean net flux divergence of latent heat was found to be about -0.366×10^{13} Cals/Sec. and that of the dry static energy -0.471×10^{13} Cals/Sec. He also reported that the contributions from the eddy terms are in general higher for heat budget than those for moisture budget.

Computation of the water vapour budget in a large monsoon area based on 15 years data by Oort (1985) showed that in the Indian monsoon region, the source of water vapour is Arabian Sea and the sink is North East India. It was also found that the difference between precipitation and evaporation is large and positive during April to October in a wide area over the Indian Ocean, comprising the South China Sea and Philippines.

In a recent study Sadharam and Rameshkumar (1988) remarked that the mean rates of evaporation and precipitation over the Arabian Sea during different monsoon seasons do not vary much suggesting that the contribution of evaporation from Arabian Sea towards the moisture flux across the West coast of India is less. They also suggested that only

detailed informations on evaporation and precipitation fields over the Arabian Sea under different phases could shed more light on this problem.

Many of the above mentioned studies suggest that the cross equatorial moisture flux is an important source of moisture for the Indian Summer monsoon rainfall, although the role of evaporation from Arabian Sea is quite significant. The differences in the data, period, and techniques must be the reason for the contradictory results reported by them. Refined satellite data may prove to be a more reliable and extensive source of data. Simon and Desai (1986) using GOES and TIROS-N data successfully determined the evaporation and sensible heat values over the Indian Ocean and related them to the onset and progress of Indian Summer Monsoon.

An immense and continuous flow of energy streams from the sun. Of this, some portions of the earth receive more energy than they return to space, while others return more than they receive, but the earth system as a whole is neither warming nor cooling. Consequently, there must be a transfer of energy between various parts of this system. The role of oceans in this, is of utmost importance, as evidenced by the studies of Rao et al (1978, 1981) Basu and Parel (1984), Mohanty et al (1982a) and many others more.

Hastenrath and Lamb (1979) suggested that the hydrosphere operates, as an effective heat exporter in the northern hemisphere, equatorial belt of the Indian Ocean and the adjacent tropical seas, whereas it acts as a heat importer in the higher latitudes of the Southern Indian Ocean.

A bimodal variation in temperature and heat storage in the surface layer in a large area in the Arabian sea was reported by Colborn (1975). Hastenrath and Lamb (1980) in another study, presented the heat budget of the Indian Ocean. They found that during the Northern summer, the radiative heat input at the top of the atmosphere and the precipitational heating of the atmosphere are much larger for the Northern Indian Ocean and smaller to the south of the Equator and vice versa during Northern winter. They also saw that the Northern Indian Ocean water body (except the more northerly region), experiences a good heat gain, during Northern winter.

Duing and Leetma (1980) computed the heat budget of the Arabian Sea during south west monsoon season and found that contrary to other geographically similar water bodies, Arabian Sea is characterised by a pronounced summer cooling. The quantum of lowering is as high as 10°C between May and July off Somalia coast and about 2 to 3°C off Indian West coast. Their study indicated that radiation overbalances the

evaporative cooling. This was contrary to the earlier findings by Colon (1962), that the evaporative heat loss would be greater than heat gain due to incoming radiation during the peak of the monsoon. Ramanadham et al (1981) studied the surface heat budget parameters using MONSOON-77 data. They found that the accumulation of energy in the surface layers of the sea encourages evaporation leading to a fall in the pressure over the region. During MONSOON-77 Rao et al (1981) found that greater evaporation has occurred along the West coast of India before the onset of the monsoon, and after the onset has set up, there is a decrease in evaporation by 30 to 40 percent.

Studies by Nuzhdin (1982) on the energetics of the atmosphere and ocean during MONEX-79 revealed that conditions which promote the onset of monsoon such as evaporation, transfer of sensible heat into the atmosphere and updrafts of warm and moist air masses are characteristic of the Central Arabian Sea whereas it was the reverse in the Western Arabian Sea. It has also been observed that lower than normal enthalpy in the Central Arabian Sea, favours the south west monsoon to set in.

Making use of the MONEX ship data for a continuous period Mohanty et al (1982a) computed the time variation of the surface energy parameters over the Arabian sea.

Murthy et al (1983) estimated the heat loss due to evaporation, back radiation and sensible heat transfer over the East Central Arabian Sea during two typical monsoon days and found that the surface heat loss accounted only about 40% of the total heat loss in the surface layer.

Rao et al (1985) using surface marine meteorological and solar radiation data collected during MONSOON-77 estimated the surface heat budget components at selected areas over North Indian Ocean. They found that energy input into the atmosphere from the ocean during disturbed weather is approximately double the corresponding value during fair-weather period.

Using satellite data Ali et al (1987) showed that the net heat gain at the ocean surface follows mainly the resultant pattern of both the shortwave radiation absorbed at the surface and the latent heat flux.

Studies by Singh and Singh (1988) on the vertical distribution of heat and momentum fluxes over the East coast of India during MONEX-79, revealed that these fluxes show remarkable changes with latitude in different layers of the atmosphere.

The above investigations reveal that the ocean-atmosphere coupling is very strong in the monsoonal Indian

Ocean. As already mentioned by Golovastov et al (1982), it has become evident that the knowledge of the interannual variability of the thermodynamics of ocean waters in the Indian Ocean is very important for developing and improving the methods of long-range prediction of weather and ocean processes.

The Indian monsoon is the most dominant feature of tropical circulations, set up and maintained by large-scale seasonal temperature differences between the ocean and the continent. Bjerknes (1966)* was the first to discuss about the temperature anomalies over the Equatorial oceans and their possible effect upon atmospheric circulation in this region. Recent evidences suggest that the variability in the intensity, frequency, inception and termination of Indian Summer Monsoon, might be associated with changes in the surface temperature of the Arabian Sea.

Saha (1970, 1974) showed that there exists a well defined zonal anomaly of SST between the equatorial West and East Indian Ocean. It was suggested that this anomaly affects the ocean atmosphere exchange and hence the low level air circulation over the Arabian Sea and therefore change the distribution of rainfall along the West coast and peninsular India.

Sastry and D'Souza (1970) found that the large spatial variations in surface temperature exceeding 11°C are due to processes such as radiation imbalance, intense upwelling off Somalia coast and complex intermingling of various water masses. Studies made by McPhaden (1975) also gave the importance of Somalia coast upwelling, offshore advection, advection of relatively cool water from the Southern Hemisphere, reduced insolation, enhanced evaporation and entrainment of thermocline water into surface mixed layer, in the evolution of SST over Arabian Sea during the South West Monsoon.

Jambunathan and Ramamurthy (1975) showed that over the Arabian Sea, the sea surface temperatures were higher than the air temperatures during active monsoon and vice versa while during weak monsoon period. Keshavamurthy et al (1975), Anjaneyulu (1981) and Shukla (1983) from their studies came to the same conclusion, that the ocean surface was relatively warmer during the months of April, May and June for good monsoon years as compared to the deficient monsoon years and it was relatively colder in the months of September, October and November. The differences in the surface temperature anomalies between good monsoon years and the deficient monsoon years for August, September and October were larger than those for April, May and June which suggest that during good monsoon years, the sea is cooled

more. Rao et al (1976) also noticed that sea surface temperatures are high during May-June while a lowering is observed in the month of July.

Fieux and Stommel (1977) analysed historic ship reports from the Arabian Sea to determine the mean variations in space and time of the SST during the onset of summer monsoon along 10°N for the period 1900-1967 and found that sea surface temperature anomalies are present but they are destroyed by the onset in May.

Sensitivity of model-simulated rainfall over India during the south west monsoon to SST anomalies over the Arabian Sea has been studied by Shukla (1975, 1976) with the GFDL model, by Washington et al (1977) with NCAR model and again by Shukla (1981) with the GLAS model. Shukla, in his earlier study, demonstrated that colder SST anomalies would increase rainfall over India. Sikka and Raghavan (1976) commented that the GFDL model does not estimate rainfall well.

Rao et al (1976) studied the thermal structure of the North West Indian Ocean in relation to the monsoon, using ISMEX 1973 data and showed that SSTs were higher in May, over Arabian Sea and that there was a decrease of SST ranging from 0.5°C in the Northern Arabian Sea to 3°C or more in the Western Arabian Sea, and a general increase in

the thickness of the mixed layer, from May to June or even July.

Saha and Bavadekar (1976) found that the correlation coefficient between the net moisture flux across the West coast of India, south of Bombay and the coastal monsoon rainfall was 0.87 and that for north of Bombay was only 0.14.

Ramage (1977) reported that observations at Canton Island and elsewhere in the tropics fail to support the idea that high SSTs cause high local rainfall. Washington et al (1977) and Druyan (1982 a,b) in similar studies using models, found that the small anomalies of sea surface temperature are able to generate only local effects. Their results showed increased (decreased) vertical velocity and precipitation over regions of warm (cold) anomalies.

Shukla and Mishra (1977) calculated the correlation coefficients between SST anomalies at about 10°N between 60° and 70°E and the seasonal mean rainfall over the Indian subdivisions. They found that the correlations between SST during July and rainfall during August over the Central and Western India were positive and significant.

Barnett (1978) tried to find the precursors of the variations in the global circulations like monsoons in sea

surface temperatures using a relatively large amount of data and concluded that they do influence each other.

Raghavan et al (1978) examined the relation between July 1964 SST in the West Arabian Sea and Indian Summer Monsoon and found that during a weak monsoon over India the sea surface experienced a significant drop in temperature over a larger area compared to that for a strong monsoon period. Weare (1979) from his studies concluded that a warmer Arabian Sea or Indian Ocean was weakly associated with decreased rainfall and increased pressure over much of the Indian subcontinent. He explained that periods of higher SSTs which is expected to lead to deeper monsoon low pressure are usually accompanied by periods of higher than average pressure over the subcontinent which would tend to offset the effects of temperature variations.

Anjaneyulu (1980) studied the monthly surface temperature at 16 representative areas over Arabian Sea for the period from 1961 to 1967 in relation to Indian monsoon activity and found that the positive anomalies of SST during May over the West and the adjoining Central Arabian Sea, though small in value were associated with subsequent good monsoon and vice versa. He also found that in good monsoon years, the difference between the highest SST during the premonsoon and the lowest SST during the monsoon in areas

off Arabia and Somalia were large and also suggested that the negative anomalies of SST during August over the Western Arabian Sea and the adjoining Central Arabian Sea were associated with good monsoon and vice versa during weak monsoon year. Ranjit Singh (1980) repeated the above calculations for the years, 1961, 1964, 1965 and 1966 and found that there was a general fall in surface temperature values ranging from 1 to 3°C during monsoon months in most of the areas.

Studies by Browen et al (1980), confirmed that the summer monsoon seasonal sea surface temperature changes are mainly influenced by mixing and heat loss at the surface.

Rao et al (1980) determined the time variation of SST and moisture over the Arabian Sea during the period from 25 May to 15 June 1973, covering the pre-onset phase of the southwest monsoon. They reported that its onset was associated with a decrease in the SST, especially north of 5°N. They also noticed a significant change in the SST and moisture distribution between the 27th and 28th and a progressive shift of the area of maximum moisture towards North East.

Studies by Joseph (1981) indicated that monsoon failures during the decade 1964-73 were followed by above normal SST over large areas of the North Indian Ocean, which

persisted for one year. He described it as, a bad monsoon warms up the North Indian Ocean, through decreased upwelling along the Somalia and Arabian Coasts and weaker surface winds over the Arabian Sea and Bay of Bengal causing reduced mixing, evaporative cooling, and cloud cover. The warm sea was found to cause the formation of a warm anticyclone in the upper troposphere over the Indian seas during the following winter and the pre-monsoon seasons. This was followed by a good monsoon which lead to cooling of the North Indian Ocean.

Pisharoty (1981) studied some aspects of the relation between SST and monsoon rainfall. He suggested that medium range forecasting of some of the features of the monsoon would be feasible using the SST over the Arabian Sea.

Mishra (1981) used SST derived from the satellites NOAA-5 and TIROS-N, for a period of 3 years and observed that during a good southwest monsoon season, the cold waters from the equatorial region of the Indian Ocean advected into the Arabian Sea by early May to form the South west monsoon current.

Ramesh Babu et al (1981) got good autocorrelation values, for the upper part of the sea temperature values, over the North East Arabian Sea for the pre-monsoon and

monsoon period. This feature was more prominent during monsoon period.

Datta et al (1982) from their studies on SST and moisture distribution over Arabian Sea during pre-onset and onset phase found that there is a definite indication of increase of moisture, north eastwards at the time of onset of monsoon, which is contrary to earlier findings. The onset of monsoon was also found to be associated with decrease in the SST especially north of 5°N and upto 65°E . Murthy et al (1983) also found this lowering of SST in the East Central Arabian Sea during onset period.

Much work had been done by scientists - Kung and Sharif (1982) and Kraus and Hauson (1983) to find the possibility of using sea surface temperatures and SST anomalies in long range forecasting of the Indian summer monsoon. Later on Pathak (1982) compared the SST observations from ships and TIROS-N satellite. They found that the TIROS-N derived SST were lower than the in situ observations during MONEX period over the North Indian ocean. Barnett (1984) studied the long term trends in sea surface temperature over oceans during this century, and found that the values were contaminated by a systematic conversion from bucket to injection measurements.

Khalsa (1983) found that the maximum in SST anomaly is not correlated spatially or temporally in any consistent manner with the sum of latent and sensible heat fluxes or rainfall from high reflective clouds.

The correlation between drought and wet indices over Indian sub-continent and SST anomaly over Eastern Equatorial Pacific for monsoon and post monsoon were found to be generally significant. Studies made by Mooley and Parthasarathy (1983) show that a positive and direct correlation exists between Drought Index (IDI) and a negative or inverse correlation between wet index (IWI) for India and SST of Arabian Sea. A possible explanation given by them for this was that a warmer Equatorial Eastern Pacific would suggest upward air motion over this area and this upward moving air may ultimately compensate for decreased ascent over the Eastern Indian Ocean or the Western Pacific Ocean leading to reduced activity of the summer monsoon or a higher than average drought index for India.

Cadet and Diehl (1984) saw that warmer (colder) SST due to weaker (stronger) circulation over the Arabian sea was related to below (above) normal rainfall over India.

Gadgil et al (1984) investigated the interaction between the large scale convective system associated with the continental Inter Tropical Convergence Zone and the

ocean over which they are generated, concentrating on the relationship between organised convection over the Indian Ocean and SST. They reported that if SST, is above 28°C it is no more an important factor in determining the variability of cloudiness and also that the correlation between Western Arabian sea surface temperature and monsoon cloudiness are positive and significant. Similar studies by Rasmusson (1984), showed that the eastward movement of the SST pattern over Eastern Pacific, convective regions and subsequent monsoon rainfall in India are connected. He had brought out, that the area with SST 28°C and above migrates from north to south from August to January and that areas with SST above 28°C are associated with large scale convective clouds which also migrate in the same fashion.

According to Goswami (1984), the monsoon circulation is a result of competition between two heat sources, one located over the Indian sub-continent and the other located near the equator associated with the SST maximum there. It was also found that July SST over the Arabian sea and July rainfall are significantly negatively correlated, over Central India.

Joseph et al (1984) found that along with the monsoon rainfall over India, SST over the North Indian Ocean was found to have a 3 year oscillation.

Sastry and Ramesh Babu (1985) examined the annual variation of SST over most of the Arabian Sea and found out that it showed an anomalous bimodal pattern with higher temperatures during May and October and lower temperatures during January or February and July or August. They looked into the reasons for summer cooling of the Arabian Sea in relation to the dynamic and thermodynamic processes, and found that the surface cooling during summer in the Northern Arabian sea is due to upwelling and advection of cold water, whereas in the Eastern Arabian sea, the entrainment of cold water into the surface layer and the subsequent turbulent mixing play a dominant role.

Shetye (1984) observed that SST along the zonal strip of 9-11°N goes through four phases (i) a warming phase from approximately February to May (ii) cooling from May to August (iii) Warming from September to Mid November and (iv) cooling from mid November to January. His results also suggested that during the two warming phases the mixed layer shallows are due to detrainment and the increase in SST is predominantly due to heat gained at the surface. Cooling occurs due to detrainment of the underlying waters.

In another study, Gopinathan and Sastry (1986) indicated that significant positive correlation existed between

the extent of coverage of the warm pool in the Bay of Bengal during May and the rainfall over India during the following summer period. Kershaw (1985) reported that the use of more realistic and warmer surface temperatures especially for the East Arabian sea in models, enables a better prediction of the development of a monsoon depression, than the climatological SST. Ramesh Babu et al (1985) also studied the SST over Arabian Sea in relation to the rainfall during the monsoon period and found that they are correlated.

Further studies by Joseph and Pillai (1986), have shown that poor monsoon is able to produce a warm SST anomaly over the North Indian Ocean due to factors such as (1) reduced wind mixing (2) evaporation over the area and (3) cloud cover. This spatially large warm SST anomaly created by the poor monsoon persisted during the following October to next May.

A recent study by Ramesh Kumar et al (1986) envisages the role of Arabian Sea surface temperature on the monsoon rainfall on the West coast of India. The study showed that somewhat high and positive correlations exist between the West coast rainfall and the 27°-28°C SST range in the Eastern (Central) Arabian Sea during a good monsoon season. It should be noted here that, they used the rainfall at Goa as representing the west coast region. The main

feature of the composited SST anomaly for heavy/deficient monsoon rainfall years by Shukla (1986a) is that the differences in SST anomalies between heavy rainfall years and deficient rainfall years for August, September and October are larger than those for April, May and June.

In similar investigations, Shukla (1986) and Goswami (1986) pointed out that the results of some of the above studies using SST anomalies should be viewed with caution because, SST anomalies during pre-monsoon months are within the range of observational errors. For the above study Shukla used 75 years data whereas Goswami used 100 years data and they also calculated the correlations of SST anomaly in the North Indian Ocean. Shukla pointed out that warm (cool) SST anomaly during April, May and June was not necessarily indicative of the above (below) average monsoon rainfall, though heavy rainfall is followed by negative SST anomalies, while Goswami reported that the July SST in the Arabian sea and the July rainfall were significantly negatively correlated. His studies showed that the composite SST anomalies in the Arabian Sea for heavy and deficient rainfall years did not show any significant anomaly during the post-monsoon months.

Most of the above studies were based on simple statistical methods. Suppiah (1988) in his study on the

relationships between Indian Ocean SST and the rainfall of Sri Lanka used the Empirical Orthogonal Function (EOF) analysis for finding the spatial and temporal variation of the SST. The analyses revealed that low (high) SSTs in the previous winter months could lead to a strong (weak) summer monsoon circulation that in turn leads to a strong (weak) contrast in wind speed between the two currents of the Arabian sea. As a consequence, a strong (weak) southern current of the Arabian sea branch could bring below (above) normal rainfall over Sri Lanka and above (below) normal to the Malabar coast.

1.3 PRESENT STUDY

Many of the aforementioned studies could not adequately provide, a diurnal and daily variation of the different energy budget parameters. They had either given monthly means or averages for a period. This situation had been partially overcome, with the successful documentation of the present study. Also, although many studies had been carried out to find the relation between Arabian sea surface temperature and Indian summer monsoon rainfall, few were interested in the Indian West coast rainfall in particular. It should also be noted that, Ramesh Babu et al (1981) in their similar study had taken the rainfall of a single station, Goa, as representing the whole of West coast. The present

study incorporates rainfall of six monsoon periods for thirteen Indian westcoast stations and satellite derived sea surface temperature data to find the same relation.

1.4 DATA USED IN THE PRESENT STUDY

The data used in the present study are aerological data taken during MONSOON-77 and MONEX-79 published by the India Meteorological Department and GOSST-Comp charts published by NOAA. The surface and upper air data used are those taken at intervals of 6 hours at 00, 06, 12 and 18 GMTs by ships that were stationed in the form of polygons as shown in figure 1.1 over the Arabian Sea, during the period mentioned against each phase below. The parameters collected were dry bulb temperature, sea surface temperature, dew point temperature, geopotential height, wind speed and direction from surface upto 200 mb, for every 50 mb interval from 1000 mb. The details of the four phases are given below.

Phase - I	(07.06.1977 to 20.06.1977)
(1) Priboy	(12.5°N, 63.9°E)
(2) Okean	(14.5°N, 66°E)
(3) Shirshov	(12.5°N, 68°E)
(4) Priliv	(10.5°N, 66°E)

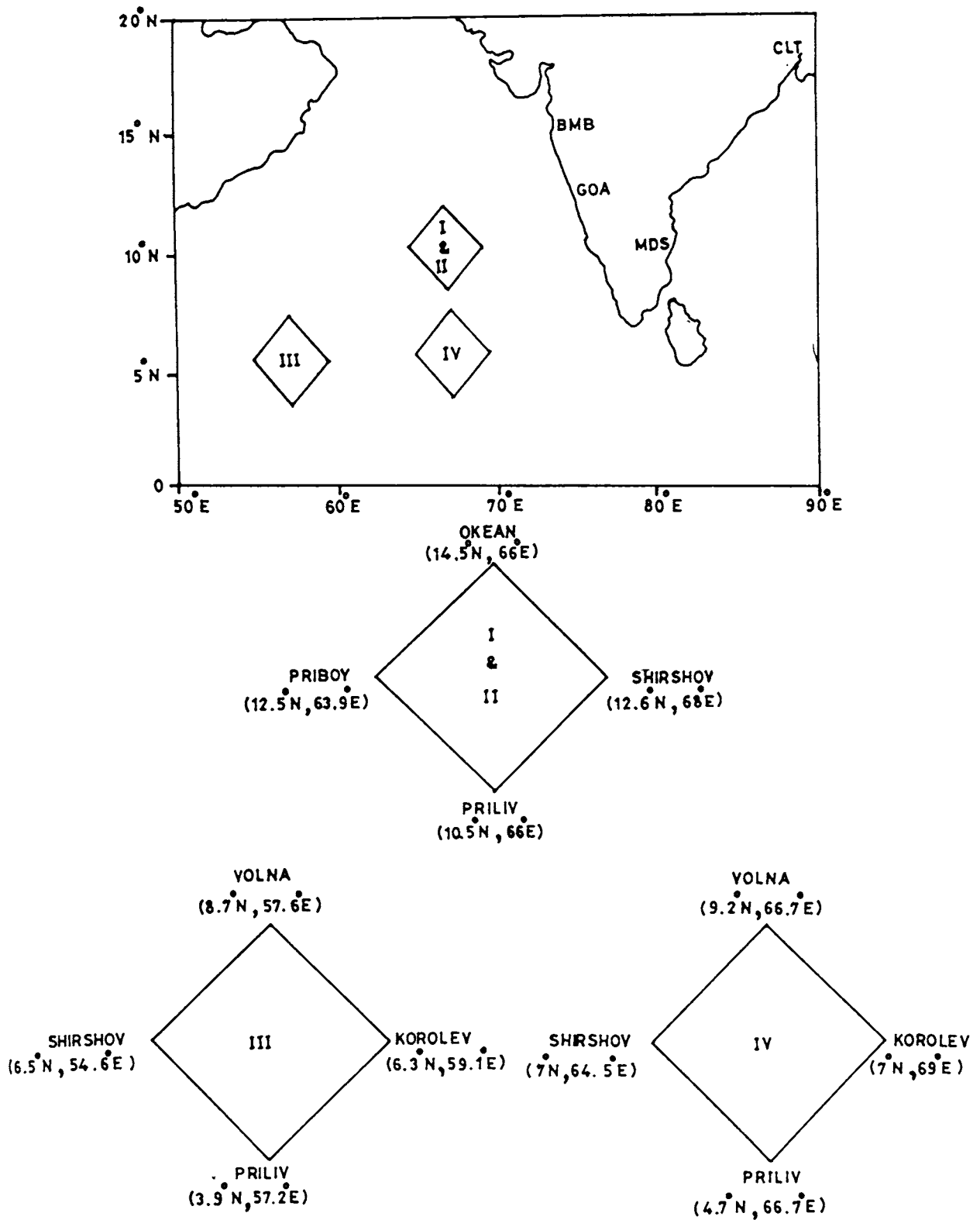


FIG.1 MAP SHOWING THE AREAS OF STUDY.

Phase - II (02.07.1977 to 15.07.1977)

Ships and positions same as that of Phase-I

Phase - III (17.05.1979 to 30.05.1979)

(1) Shirshov (6.5°N, 54.6°E)

(2) Volna (8.7°N, 57°E)

(3) Korolev (6.3°N, 59.1°E)

(4) Priliv (3.9°N, 57.3°E)

Phase - IV (02.06.1979 to 12.06.1979)

(1) Shirshov (7°N, 64.5°E)

(2) Volna (9.2°N, 66.7°E)

(3) Korolev (7°N, 69°E)

(4) Priliv (4.7°N, 66.7°E)

Hereafter in this thesis, whenever it is mentioned Phase-I it means the period 07.06.1977 to 20.06.1977; Phase-II means from 02.07.1977 to 15.07.1977; Phase-III means from 17.05.1979 to 30.05.1979 and Phase-IV is from 02.06.1979 to 12.06.1979, and Polygon-I, II, III and IV refer to the respective positions during the above four Phases in the Arabian Sea. Sea surface temperature values used are satellite-derived data for the months of June, July, August and September for the years 1977, 1979, 1981, 1982, 1983 and 1984. These SSTs were computed by NOAA once per day using an automated procedure known as Global Operational, SST computation (GOSST-Comp) as described by Brower

et al (1976). The procedure includes temperature retrievals from spectral radiance after applying statistical analysis and quality control checks to the data, correction for the effects of atmospheric attenuation by using time coincident measurements derived from Vertical Temperature Profile Radiometer (VTPR) and generation of contoured maps of the analysed SST field. They are the mean values computed for each block area of about 1° latitude and longitude. The global daily mean difference between satellite-derived SSTs and ship reports has been found to vary from 0.9°C to 0.4°C with RMS variation between 1.67°C and 2.23°C most of variance coming from ship observations. The daily rainfall for the monsoon months for the above mentioned six years were taken from the records of India Meteorological Department for the West coast stations of Trivandrum, Alleppey, Cochin, Kozhikode, Mangalore, Honavar, Panjim, Devagarh, Ratnagiri, Harnai, Bombay, Dahanu and Surat.

1.5 METHODOLOGY

The methods and the formulae used in the present study are given below. The atmospheric circulation parameters along with the budget parameters were computed for every 50 mb interval, for all the synoptic hours for which data were available.

1.5.1 Vorticity (Sec. ⁻¹)

The kinematic method was used to compute the vorticity with the help of finite difference technique.

$$\text{Vorticity} = \frac{\Delta v}{\Delta x} - \frac{\Delta u}{\Delta y}$$

$$\Delta v = v_E - v_W$$

$$\Delta u = u_N - u_S$$

Where v_E and v_W were the meridional components of wind at east and west walls respectively and u_N and u_S the zonal components at the north and south walls.

Δx is the length of the zonal wall and Δy is the length of the meridional wall.

1.5.2 Divergence (Sec. ⁻¹)

Divergence (D) also was computed using the kinematic method as follows.

$$\text{Divergence (D)} = \frac{\Delta u}{\Delta x} + \frac{\Delta v}{\Delta y}$$

Here, $\Delta u = u_E - u_W$

$$\Delta v = v_N - v_S$$

Symbols have the meanings explained above.

1.5.3 Vertical Velocity (mb sec.⁻¹)

The continuity equation in the isobaric co-ordinate system was used to compute the vertical velocity (ω) at the different pressure levels from 1000 to 200 mb level with a 50 mb interval.

$$\frac{\partial u}{\partial x} + \frac{\partial v}{\partial y} + \frac{\partial \omega}{\partial p} = 0$$

$$\frac{\partial \omega}{\partial p} = - \left[\frac{\partial u}{\partial x} + \frac{\partial v}{\partial y} \right] = -D$$

The divergence of the whole column of atmosphere was suitably adjusted to make the vertically integrated divergence vanish. The layer mean divergence was corrected following O'Brien's (1970) method.

where, the correction factor, =

$$C = \frac{\int_{P_t}^{P_b} D \partial p}{\int_{P_t}^{P_b} \partial p}$$

$D_c = D - \text{Correction}$

The assumed lower boundary condition $\omega_{1000} = 0$ and upper boundary condition $\omega_{200} = 0$, is achieved by making the sum total of corrected divergence (D_c) between 1000 and 200 mb zero

$$\text{i.e.} \quad \int_{P_{200}}^{P_{1000}} D_c \, dp = 0$$

The vertical velocity ω , at any level (ω_2) is the sum of this velocity at the level just below it (ω_1) and the product of corrected layer mean divergence and the pressure interval (Δp).

$$\text{i.e.} \quad \omega_2 = \omega_1 + D_c \times \Delta p$$

1.5.4 Kinetic Energy ($\text{m}^2 \text{sec.}^{-2}$)

The mean kinetic energy (K.E.) was computed using the following equation.

$$\text{K.E.} = 1/2 (\bar{u}^2 + \bar{v}^2)$$

The mean values of \bar{u} and \bar{v} at all the levels were calculated for each polygon and used to compute mean kinetic energy. Although the mean K.E. was computed for all the levels, only those at 1000 mb, 700 mb, 500 mb and 200 mb levels are presented.

1.5.5 Precipitable Water Vapour (Kg)

The amount of precipitable water vapour (PWV) at the four ships positions were computed as follows.

$$\text{PWV} = 1/g \int_{P_t}^{P_b} q \, dp$$

where,

The specific humidity q (Kg/Kg) was obtained using the following formula.

$$q = \frac{e}{p - (1 - \epsilon)e}$$

where $\epsilon = 0.6222$

p = Pressure in N/m

and e , the vapour pressure

is computed using Tetan's formula (Murray 1967) as given below.

$$e = e_0 \exp [a(T-273.16)/(T-b)]$$

where,

$$e = 6.1078$$

and T = Dew point temperature in degree kelvin

$$\text{For } T = 263^\circ\text{K, } a = 21.87 \text{ and } b = 7.66$$

and

$$\text{For } T = 263^\circ\text{K, } a = 17.26 \text{ and } b = 35.86$$

Making use of the precipitable water vapour value (PWV) at each ship position, the average for the polygon per unit area was found as follows,

$$APWV = \left(PWV_E + PWV_W + PWV_N + PWV_S \right) \times \frac{1}{4}$$

Here the suffixes E,W,N and S stand for east, west, north and south. Although PWV at all the different ships were calculated, only the total value (TPWV) for the entire

polygon area is presented which is equal to APWV x area of the polygon.

1.5.6 Moisture Budget

The moisture budget equation was taken as -

$$E - P - \text{NMFD} = 0$$

where,

$$\begin{aligned} E &= \text{Rate of Evaporation} && (\text{Kgm}^{-2} \text{ sec.}^{-1}) \\ P &= \text{Rate of Precipitation} && (\text{Kgm}^{-2} \text{ sec.}^{-1}) \\ \text{NMFD} &= \text{Net Moisture Flux Divergence} && (\text{Kgm}^{-2} \text{ sec.}^{-1}) \end{aligned}$$

The budget parameters were calculated using the following methods.

Evaporation (E) was estimated using the Bulk Aerodynamic method following Rao et al (1981) as,

$$E = C_d \rho_a (q_s - q_a) V_a$$

where,

$$\begin{aligned} C_d, \text{ the drag coefficient} &= 1.6 \times 10^{-3} \text{ for } V > 13 \text{m Sec}^{-1} \\ &\text{and} \\ &= 1.4 \times 10^{-3} \text{ for } V < 13 \text{m Sec}^{-1} \end{aligned}$$

and

$$\rho_a \text{ the density of air, } = 1.2 \text{ kgm}^{-3}$$

Specific humidity at the sea surface was computed with Tetan's formula using SST and that at ship deck level using dew point at ship level. V is the wind speed at ship deck level in $\text{m}\cdot\text{sec}^{-1}$. Evaporation was computed for the four ship positions at every synoptic hour for which data was available. Total Mean Evaporation (TME) for the whole polygon area was computed by multiplying the mean evaporation from the four ships with the area of the polygon

$$\text{i.e. } \text{TME} = (E_E + E_W + E_N + E_S) \times 0.25 \times l^2$$

where, l is the length of the boundary wall, of the polygon. Net Moisture Flux Divergence (NMFD) was computed as follows.

$$\text{NMFD} = \text{MF}_E - \text{MF}_W + \text{MF}_N - \text{MF}_S$$

where MF, the Moisture flux across the boundary wall was calculated through stepwise integration using the following equation as,

$$\text{MF} = 1/g \int_{p_t}^p \bar{V}_n \bar{q} dp$$

\bar{V}_n is the average of the normal component of the wind in a layer and the other symbols have meanings same as explained before. Thus, the Moisture flux (MF) acquires the sign of the normal component of wind (V_n). By convention V_n is positive for westerlies and southerlies. Hence if MF is positive (negative) at west and south walls and negative

(positive) at east and north walls net inflow (outflow) of moisture occurs through these walls into (out of) the polygon area. If the net moisture flux is positive (negative) it means divergence (convergence) of moisture flux from the polygon area.

Making use of the mean rate of evaporation and the net moisture flux the rate of precipitation was computed as residual. The budget parameters were computed for all the different synoptic hours of the four phases. The values of constants are those widely used in similar computations.

1.5.7 Heat Budget

The following equation was used to compute the heat budget.

$$SH + LP + NHFD + R = 0$$

where,

SH = Sensible heat flux from sea surface (watts)

LP = Lxp = Latent heat flux due to precipitation (watts)

NHFD = Net Heat Flux Divergence (watts)

R = Radiative Heating/Cooling rate (watts)

The method of calculations of the above parameters is discussed below in detail.

$$\text{Sensible Heat (SH)} = C_d \int_a^p C_p (T_s - T_a) V$$

where,

$$C_d, \text{ the Drag Coefficient, } = 1.4 \times 10^{-3}$$

$$C_p, \text{ the specific heat at constant pressure} = 1004 \text{ J/}^\circ\text{K/kg}$$

$$T_s = \text{SST in } ^\circ\text{K}$$

$$T_a = \text{Dry bulb temperature in } ^\circ\text{K}$$

Mean sensible heat was computed for all the synoptic hours as an average of the value from the four ships. Using the mean value, the total for the whole polygon area was also computed by multiplying it with the area of the polygon.

Net Heat Flux divergence (NHFD) was found from the Heat Flux at the four boundary walls as follows

$$\text{NHFD} = \text{HF}_E - \text{HF}_W + \text{HF}_N - \text{HF}_S$$

where, HF is calculated as,

$$\text{HF} = 1/g \int_{p_t}^{p_b} (C_p \bar{T} + \bar{\phi}) V_n dp$$

The above integral was evaluated stepwise for every 50mb interval in the vertical. $C_p \bar{T}$ is the mean enthalpy of the layer.

$$\text{Geopotential } \bar{\phi} = g \bar{z}$$

where, g is the acceleration due to gravity and \bar{z} is the average thickness of the layer.

Similar to that discussed in Section 1.5.6, if HF is positive (negative) at west and south walls and negative (positive) at east and north walls, it is inflow (outflow) of heat to (from) the polygon area. Also if NHFD is positive (negative) it is heat flux divergence (convergence). Radiational heating is computed as the residual term.

1.5.8 Relation between SST and rainfall

As shown in the figure, the Arabian sea between 58°E to 78°E and 22°N to 8°N was divided into four quadrants viz. North West (NW), North East (NE), South West (SW) and South East (SE) and named as 1,2,3 and 4 respectively. Each quadrant was further divided into four sections and the weekly SST values at each of them were interpolated from isobars on GOSST-COMP charts. SST over each quadrant was then taken as the average of these four values. The corresponding weekly total rainfalls for the following weather stations were obtained from the records of India Meteorological Department: Trivandrum (TRV), Alleppey (ALP), Cochin (CHN), Kozhikode (KZK), Mangalore (MNG), Honavar (HNV), Panjim (PNJ), Devagarh (DVG), Ratnagiri (RTN), Harnai (HRN), Bombay (BMB), Dahanu (DHN) and Surat (SRT).

The coefficients of correlation (r) between the SST (x) and rainfall (y) were then computed using the following equation. (Spiegel 1961).

$$r(x,y) = \text{Covariance}(x,y) / (\sigma_x \sigma_y)$$

$$= \frac{1/n \sum (x-\bar{x})(y-\bar{y})}{\sqrt{\sum (x-\bar{x})^2 \times \sum (y-\bar{y})^2}}$$

Where,

$$r(x,y) = \text{Coefficient of correlation between } x \text{ and } y$$

x = SST at the different quadrants

\bar{x} = mean x

y = weekly total rainfall at the different stations.

\bar{y} = mean y

n = number of weeks

The correlations were computed between -

- (a) SST and corresponding week's rainfall
- (b) SST and subsequent week's rainfall
- (c) SST anomaly and corresponding week's rainfall

SSTs at all the quadrants were related to the rainfall of all the selected stations separately. The SST anomalies were found by taking the difference between the actual and normal SST values. These normals were taken from the climatic atlas of Hastenrath and Lamb (1979). The regression equations for the above cases were also developed.

Analysis and discussion of the data has been carried out in relation to the synoptic situation that existed during the periods under study, which is described in the next chapter.

CHAPTER - II

2.1 INTRODUCTION

In this chapter the synoptic situation along with the circulation parameters for the period and area under consideration over the Arabian Sea are presented.

Earlier studies [Rao (1976), WMO (1975)] have reported the importance of both cross equatorial flow and evaporation from Arabian Sea, as sources of moisture for the Indian monsoon. Both these moisture sources are undoubtedly related to the strength of the low level southwesterly flow but the available water vapour has to be lifted upward for further development of weather. Here comes the importance of low level convergence and upper level divergence. The purpose of the study included in this chapter is to find out the characteristics of circulation, amount of water vapour and kinetic energy which prevailed during the four Phases.

The circulation parameters studied in detail are wind, vorticity, divergence and vertical velocity. The methods used for the computations of these parameters are given in the previous chapter, Section 1.5.

2.2 SYNOPTIC SITUATIONS

In this Section, the synoptic conditions prevailing

over the Arabian Sea and the West coast of India, during the period of study as revealed by the India Daily Weather Reports are broadly presented for each of the phases.

PHASE-1

The general synoptic features for the period 7 to 20 June 1977 can be summarised as follows: A well marked trough of low, off the West coast seen on the 7th developed into a marked low pressure area over East Central Arabian sea and by the 9th, it concentrated into a depression, with the upper air cyclonic circulation extending upto 7.6 Km above sea level. By tenth, it became a cyclonic storm centered at 18.5°N and 64.5°E . It then rapidly moved westwards and intensified into a severe cyclonic storm, and on the 11th reached 19.5°N and 64.5°E [Fig.2.1(a)]. The seasonal trough of low pressure lay over South East Bay and adjoining Andaman Sea. By 13th June the severe cyclonic storm moved westwards and the trough of low over East Central Arabian Sea off Goa coast persisted upto the 17th. On the 14th and 15th, the main feature was a depression in the West Central Bay, off Andhra coast. The trough of low moved north and ran through Dehra Dun to Aijal. By 16th June the monsoon advanced into North interior Karnataka and adjoining Maharashtra. From 18th to 19th June a well marked low pressure area over Gangetic West Bengal and a feeble trough of

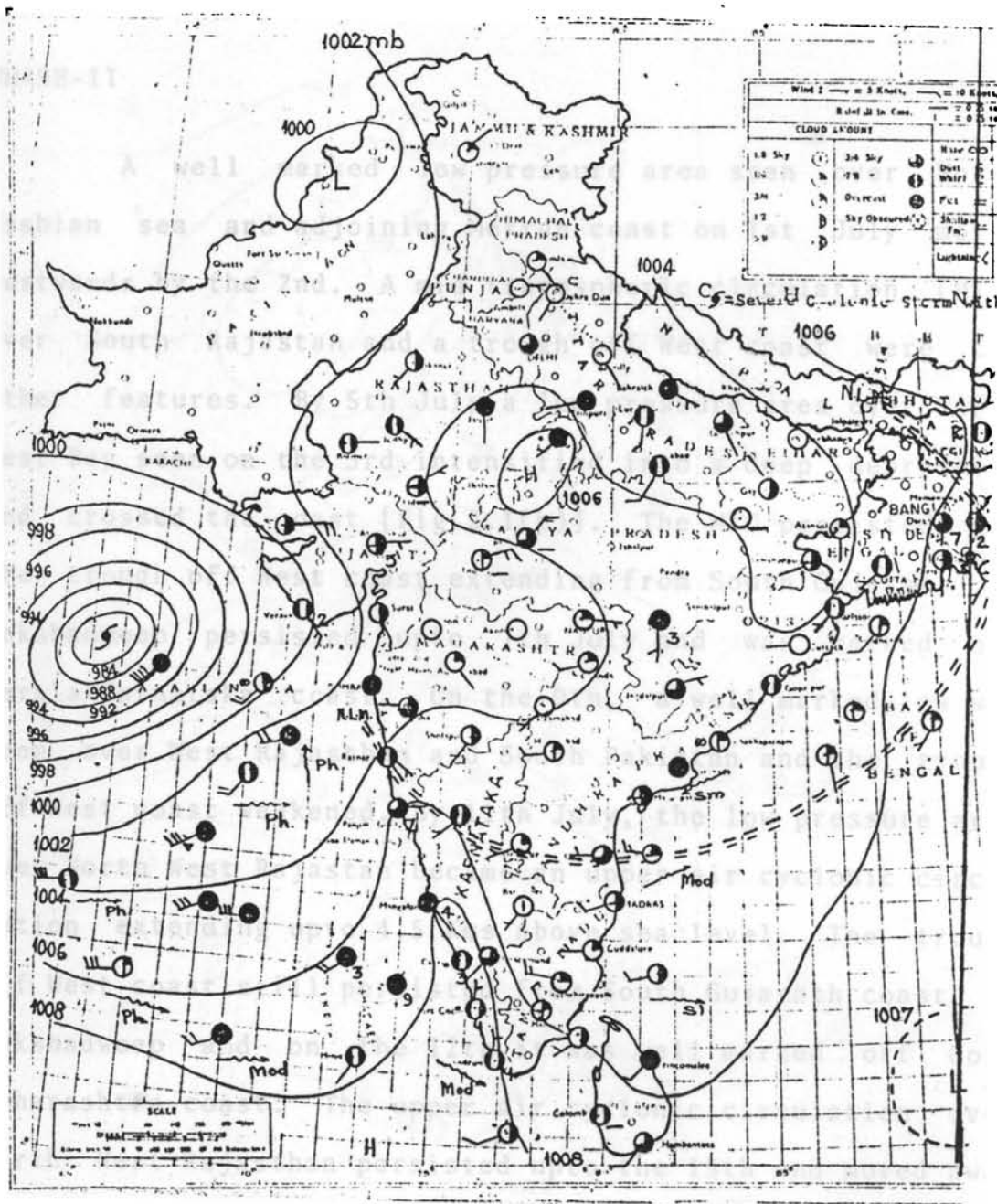


FIG.2.1(a) WEATHER MAP FOR 11TH JUNE 1977.

low on sea level chart off West coast were the main features. This trough off West coast persisted upto 20th June.

PHASE-II

A well marked low pressure area seen over North Arabian sea and adjoining Mekran coast on 1st July moved westwards by the 2nd. A mid tropospheric circulation (MTC) over South Rajasthan and a trough off West coast were the other features. By 5th July a low pressure area over North West Bay seen on the 3rd intensified into a deep depression and crossed the coast [Fig.2.1(b)]. The MTC persisted and the trough off West coast extending from South Gujarat to Lakshadweep persisted upto 7th July and was marked off Kerala-Karnataka coast. On the 9th, a well marked low was seen over West Rajasthan and South Pakistan and the trough off west coast weakened. By 11th July, the low pressure area over North West Rajasthan became an upper air cyclonic circulation extending upto 4.5 Kms above sea level. The trough off West coast still persisted from South Gujarath coast to Lakshadweep and on the 12th it was well marked off Goa-Maharashtra coast. The upper air cyclonic circulation over North West Rajasthan persisted upto the 13th and moved away by 14th July. The axis of seasonal trough during this period was almost always through Bikaner to North East Bay. Monsoon was weak in Konkan, Goa, Coastal Karnataka and Kerala. The

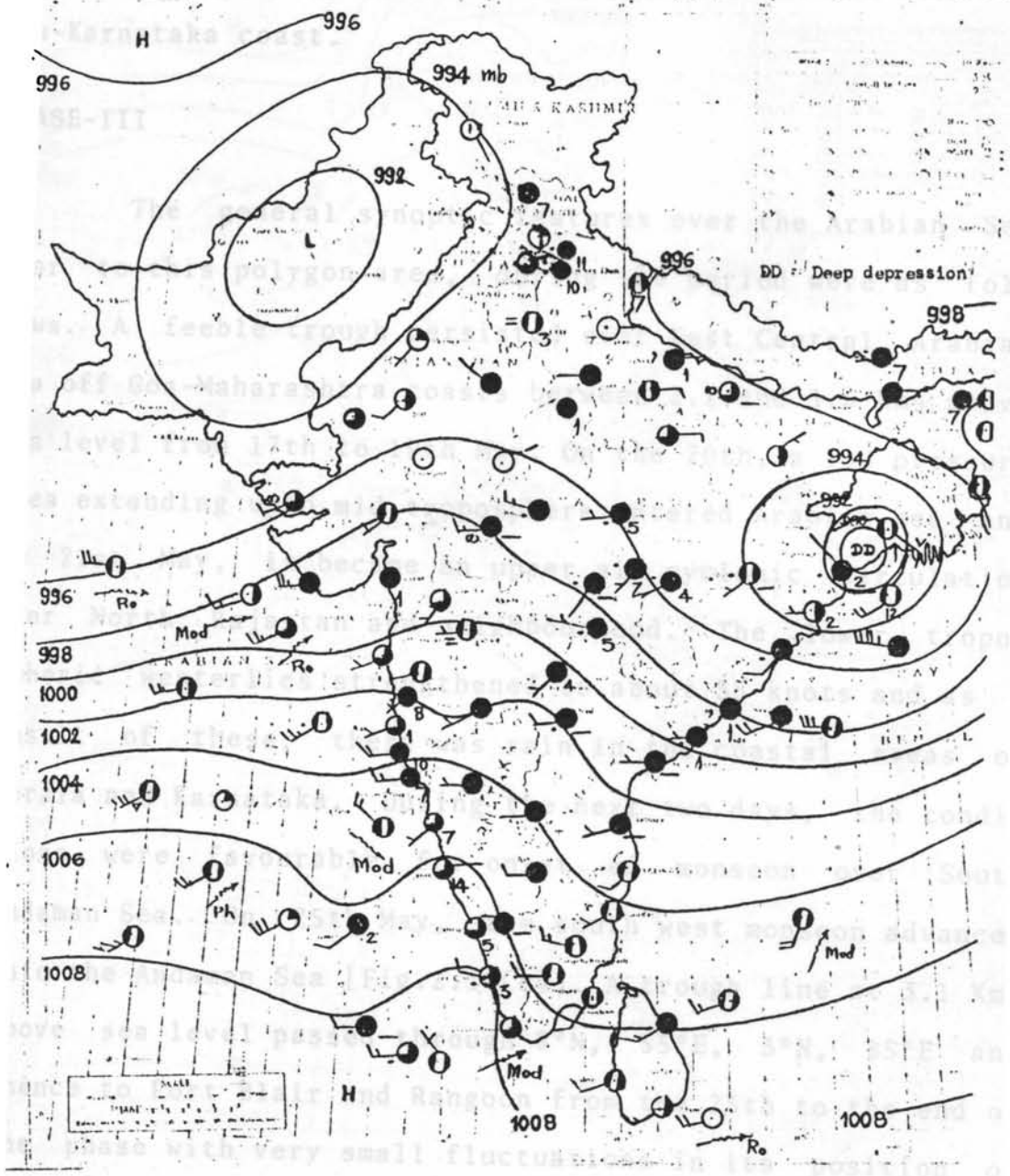


FIG.2.1(b) WEATHER MAP FOR 05TH JULY 1977.

trough off West coast extending from South Gujarat coast into North Lakshadweep persisted upto the 15th and by then a well marked off-shore vortex was seen embedded in it off Goa-Karnataka coast.

PHASE-III

The general synoptic features over the Arabian Sea near to this polygon area, during the period were as follows. A feeble trough persisted over East Central Arabian sea off Goa-Maharashtra coasts between 2.1 and 3.6 Kms above sea level from 17th to 19th May. On the 20th, a low pressure area extending upto mid troposphere entered Arabian sea and by 21st May, it became an upper air cyclonic circulation over North Rajasthan and neighbourhood. The lower tropospheric westerlies strengthened to about 35 knots and as a result of these, there was rain in the coastal areas of Kerala and Karnataka. During the next two days, the conditions were favourable for onset of monsoon over South Andaman Sea. On 25th May, the south west monsoon advanced into the Andaman Sea [Fig.2.1.(c)]. A trough line at 3.1 Kms above sea level passed through 8°N , 55°E , 3°N , 85°E and thence to Port Blair and Rangoon from the 25th to the end of the phase with very small fluctuations in its position on the different days. On the 26th and 27th May, a cyclonic circulation was seen embedded in this trough. Another upper

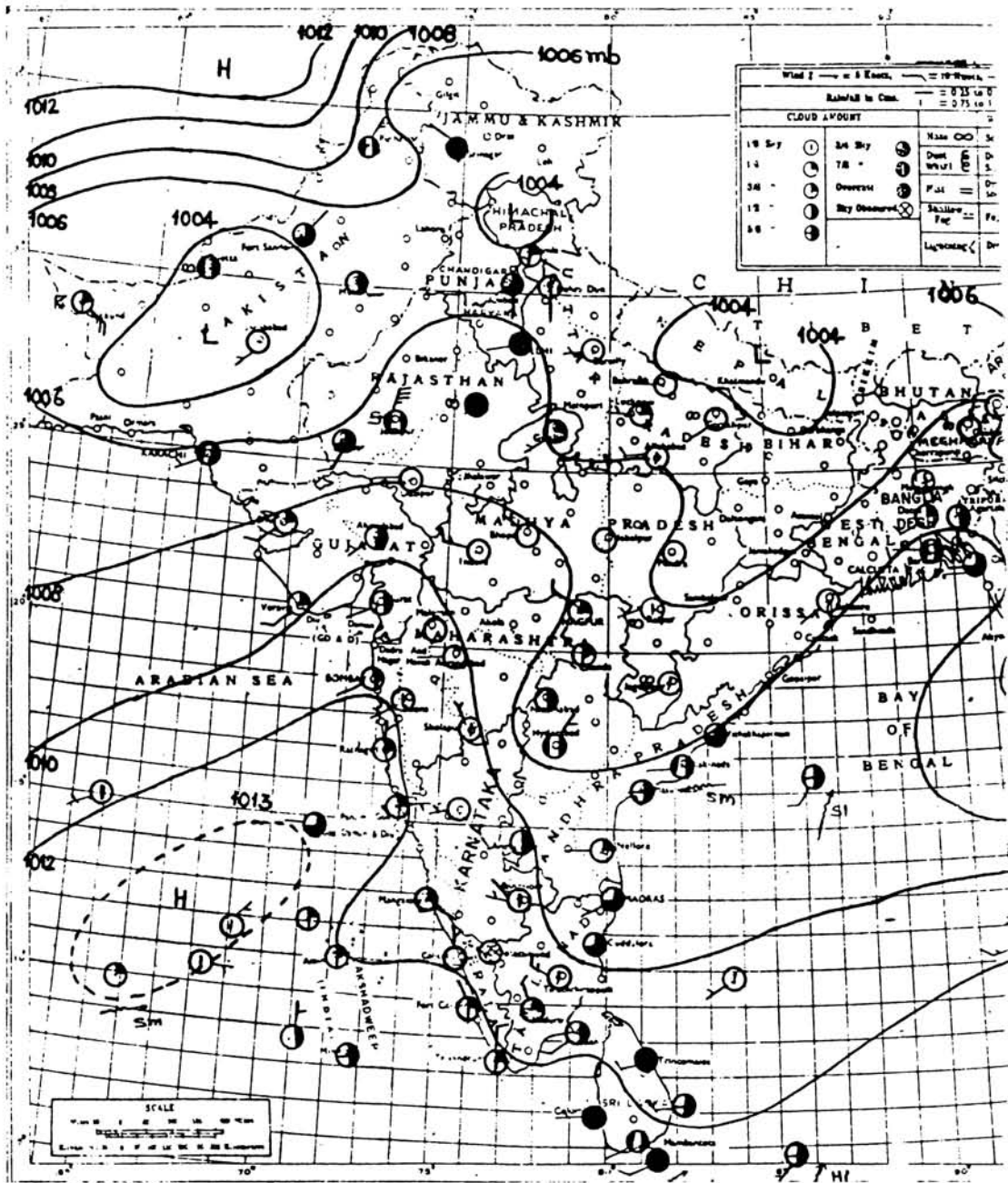


FIG.2.1(c) WEATHER MAP FOR 25TH MAY 1979.

air cyclonic circulation present over Comorin and Maldives area between 2.1 and 5.8 Kms above sea level on the 27th, moved to Kerala and adjoining Lakshadweep on the 28th and stayed there till 29th May. On the 30th, these systems moved eastwards and thereafter weakened.

PHASE-IV

The synoptic conditions that prevailed on 2nd and 3rd June were favourable for the onset of South West Monsoon over Lakshadweep and Kerala. But a trough of low pressure over Lakshadweep and adjoining Arabian Sea which persisted from 2nd to 4th June, moved westwards and hence by 4th, conditions became unfavourable for the onset. By the 5th a trough line present 3.1 kms above 6°N , 55°E and 4°N , 85°E on 2nd and 3rd moved northward and dry weather prevailed over Kerala. But on the 6th it came further down to 4°N , 55°E , Trivandrum and Port Blair and thereafter the lower tropospheric westerlies over Sri Lanka strengthened and another trough of low appeared over Lakshadweep. This trough which extended upto middle troposphere persisted upto the 14th. On 7th June a cyclonic circulation developed over South Tamil Nadu and by next day it had shifted to extreme South Peninsula. The trough of low pressure over Lakshadweep moved east by the 7th to the Kerala, South Karnataka coast, strengthened and under its influence, conditions became favou-

rable for the monsoon onset. On 10th and 11th the trough line at 3.1 Kms above sea level, ran roughly along 10°N over Arabian sea and 9°N , 85°E and onset of monsoon took place over Kerala [Fig.2.1(d)]. On 12th June a mid-tropospheric cyclonic circulation moved westwards across extreme South peninsula and by 13th reached Lakshadweep and remained there while monsoon strengthened over South Arabian Sea. By 14th, the trough at 3.1 Kms above sea level ran through Mangalore, (11°N , 78°E), and Trivandrum.

2.3 SPECIFIC HUMIDITY, WIND, PRECIPITABLE WATER VAPOUR, KINETIC ENERGY, VORTICITY, DIVERGENCE AND VERTICAL VELOCITY.

In this Section, the diurnal, the day-to-day and vertical variation of the above parameters are discussed one by one.

2.3.1 Specific Humidity

The vertical profiles of specific humidity at 00 and 12 GMTs are shown in Figs 2.2(a) to 2.2(h) respectively for Phases-I, II, III and IV.

PHASE-I

The specific humidity decreased with height consistently on all the days and at both the timings and, values

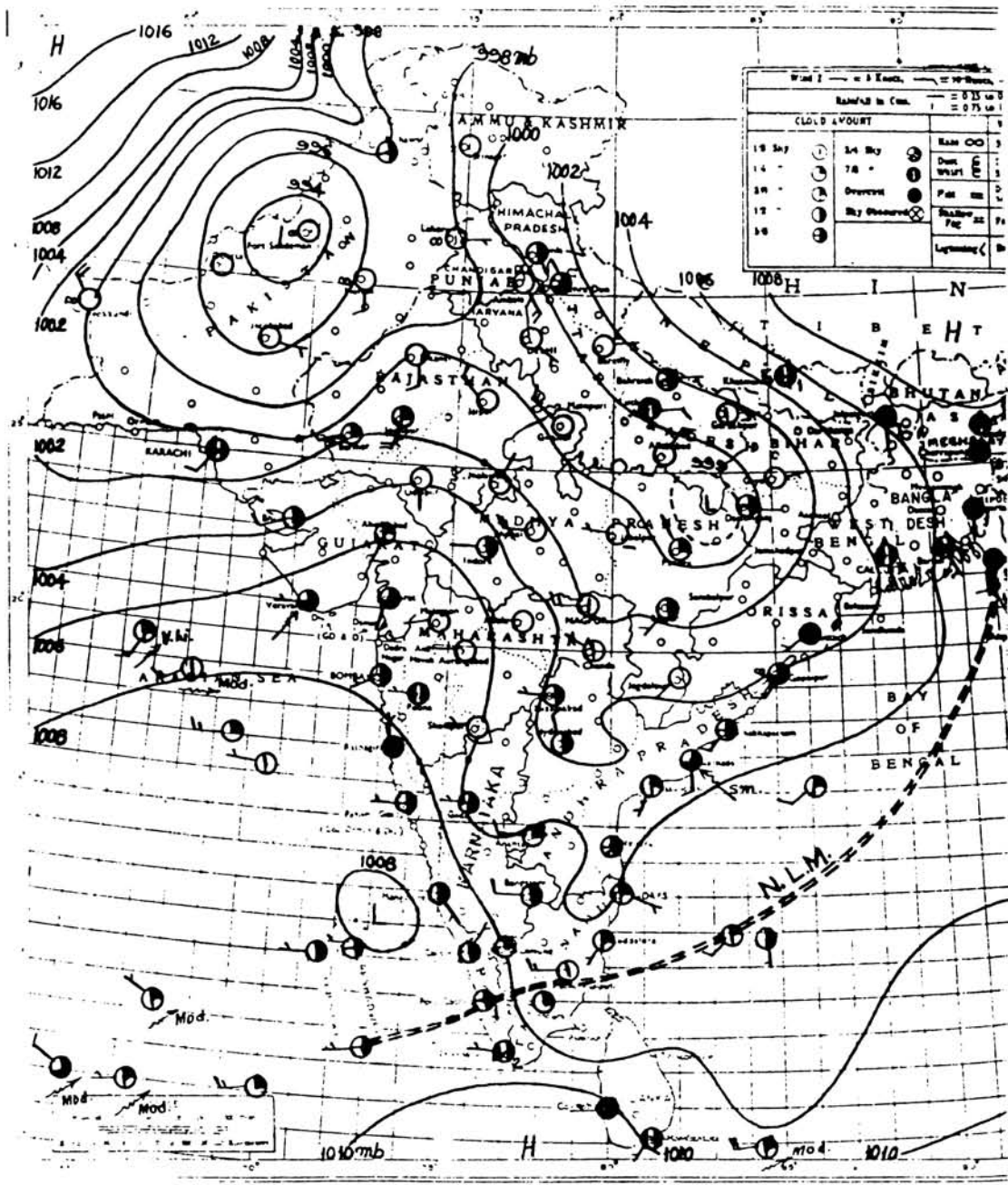


FIG.2.1(d) WEATHER MAP FOR 11TH JUNE 1979.

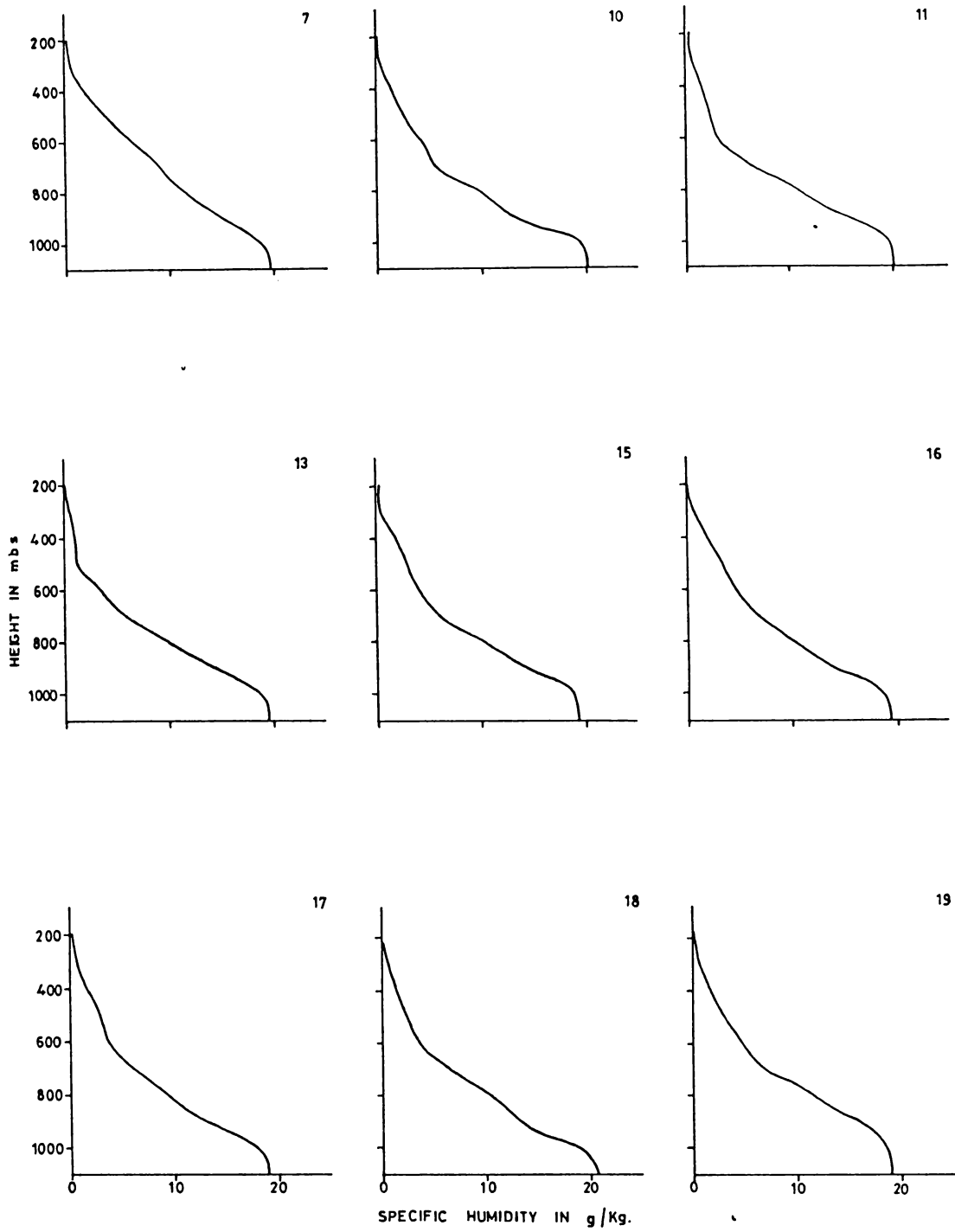


FIG.2.2(a) VERTICAL VARIATION OF SPECIFIC HUMIDITY AT 00 GMT DURING PHASE-I

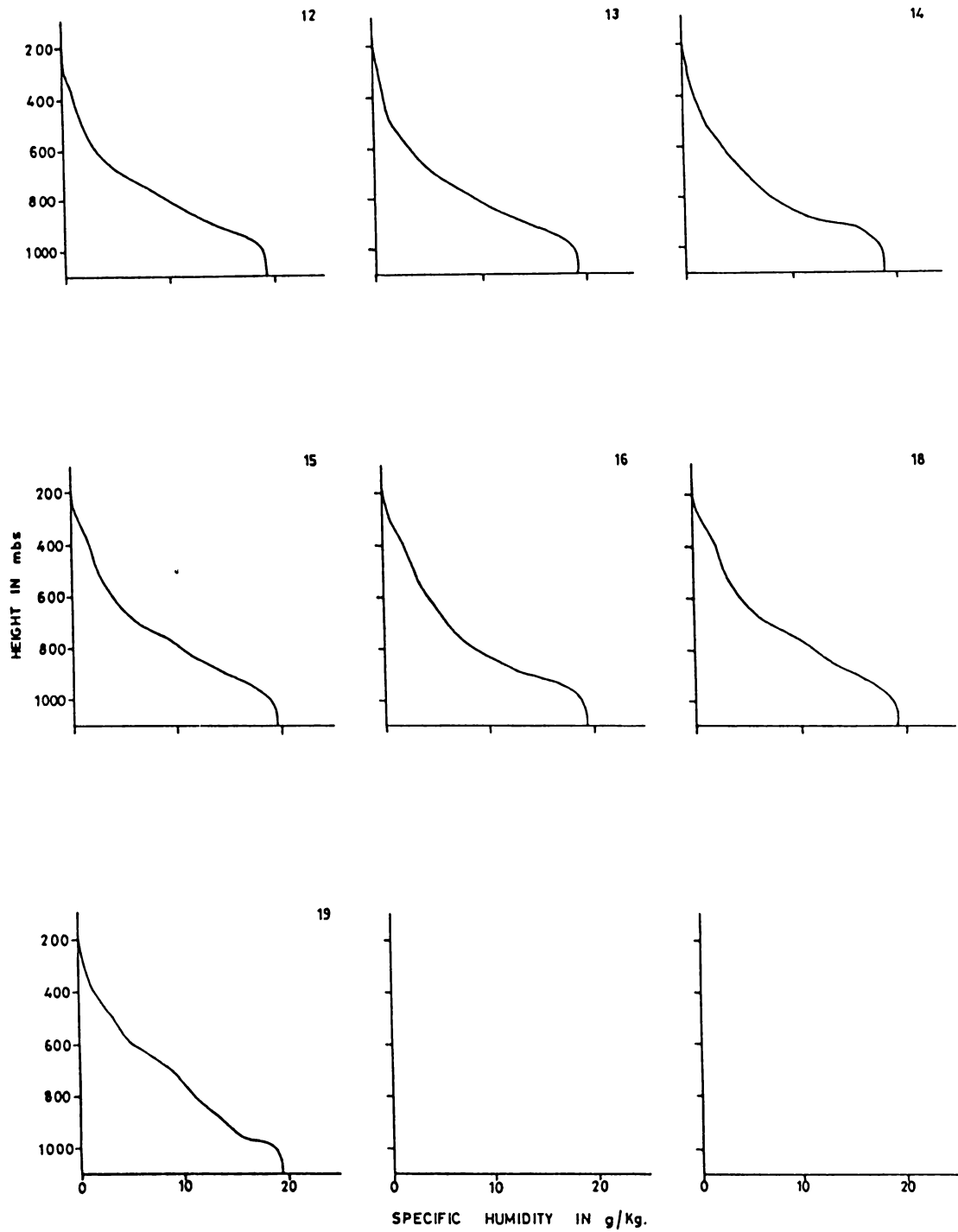


FIG.2.2(b) VERTICAL VARIATION OF SPECIFIC HUMIDITY AT 12 GMT DURING PHASE-I

reached zero by about 200 mb. The decrease was rather sharp upto middle troposphere and gradual thereafter. However, the variation beyond the mid-troposphere becomes less important in view of the very low humidities at these levels. Generally, the values varied between 20 gms/Kg at the surface to 3 gm/Kg at 500 mb.

PHASE-II

The specific humidity variations were almost similar to that of the previous phase with a consistent decrease with height. There were rare occasions of reversals at about 550 mb level. The values were generally lower at 00 GMT, than that at 12 GMT and also than that during Phase-I.

PHASE-III

No significant differences were noticed in the values when compared to the previous phase.

PHASE-IV

Although specific humidity showed similar vertical variations to that of the other phases, the surface values were slightly higher especially so during the latter part of this phase.

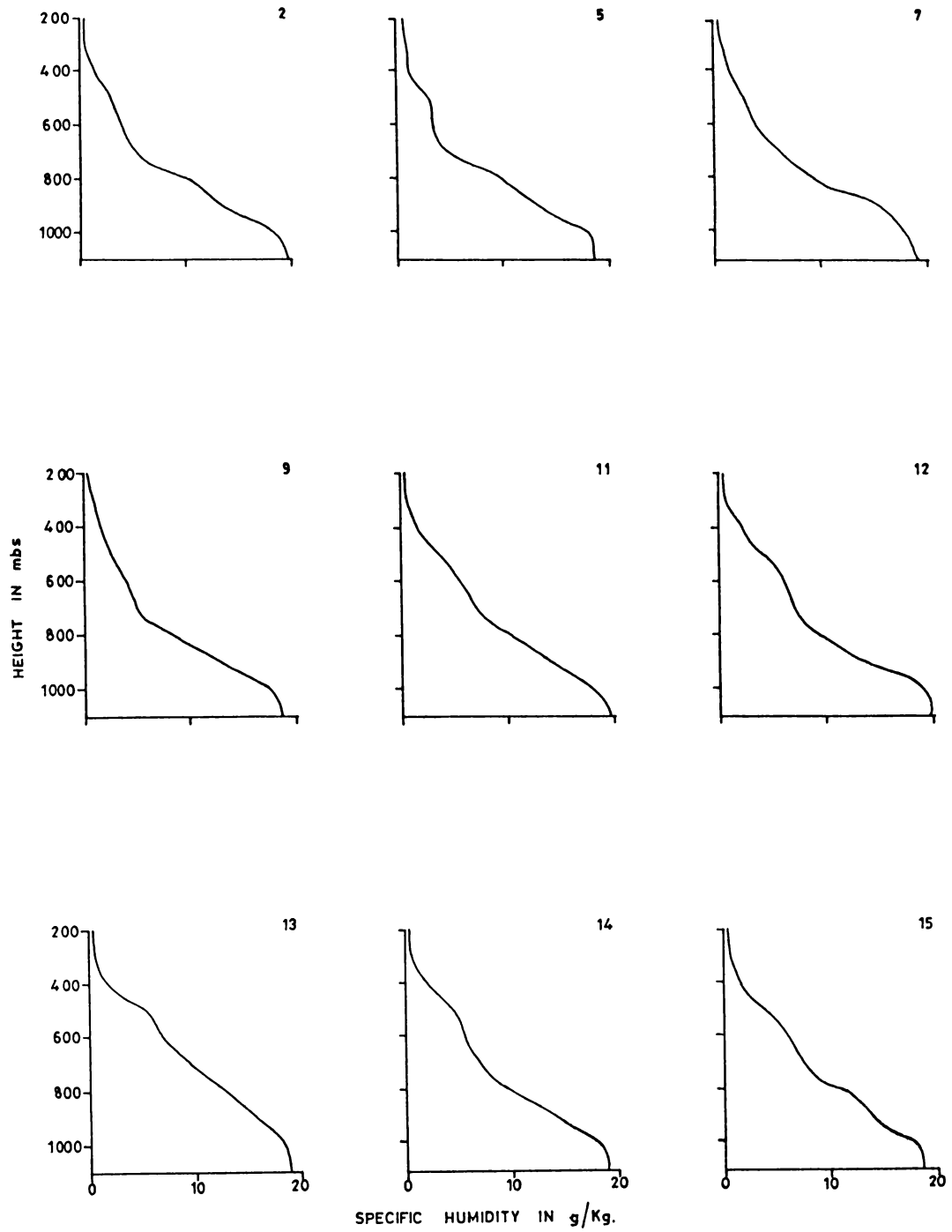


FIG.2.2(c) VERTICAL VARIATION OF SPECIFIC HUMIDITY
AT 00 GMT DURING PHASE-II

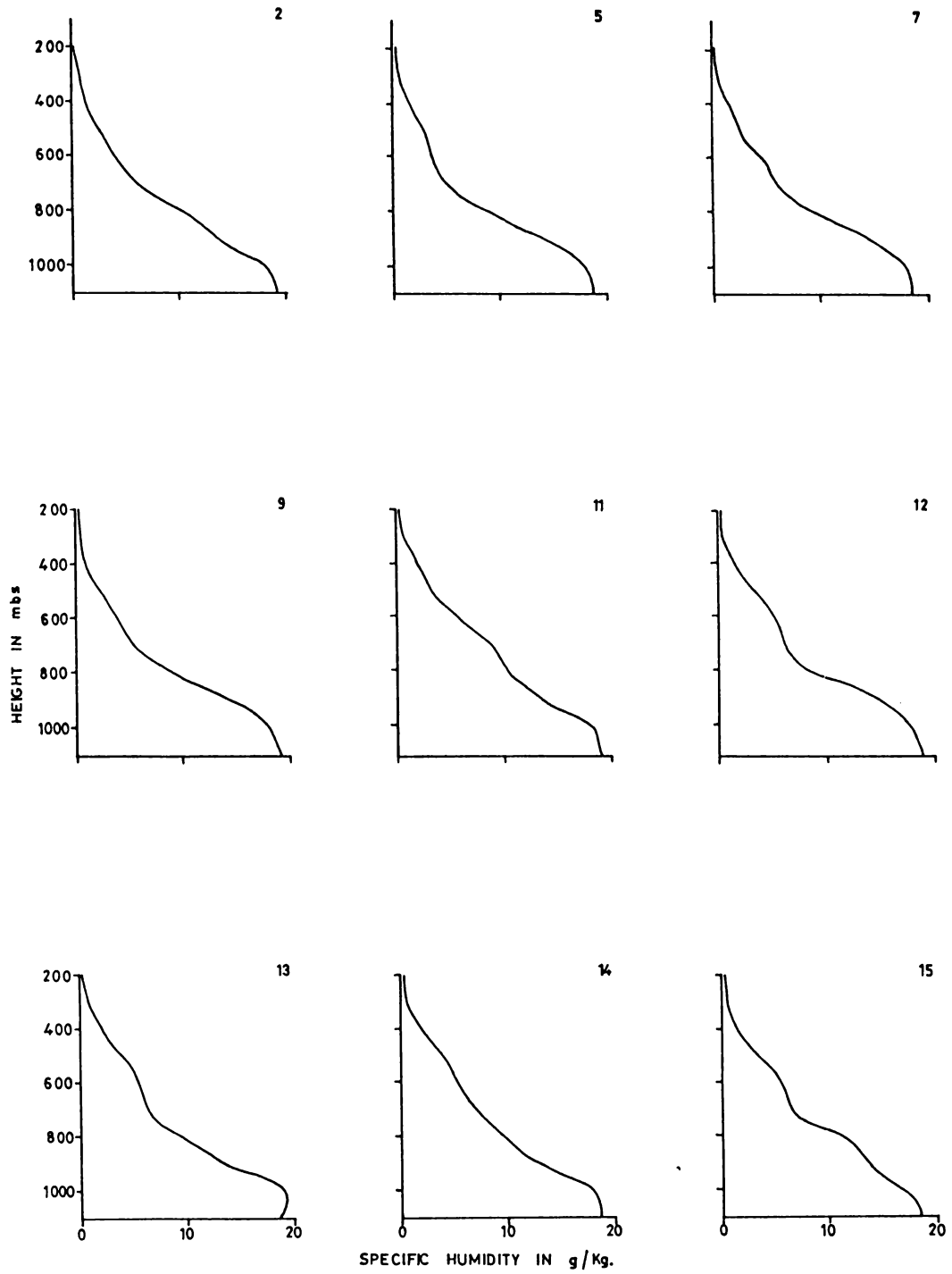


FIG.2.2(d) VERTICAL VARIATION OF SPECIFIC HUMIDITY AT 12 GMT DURING PHASE-II

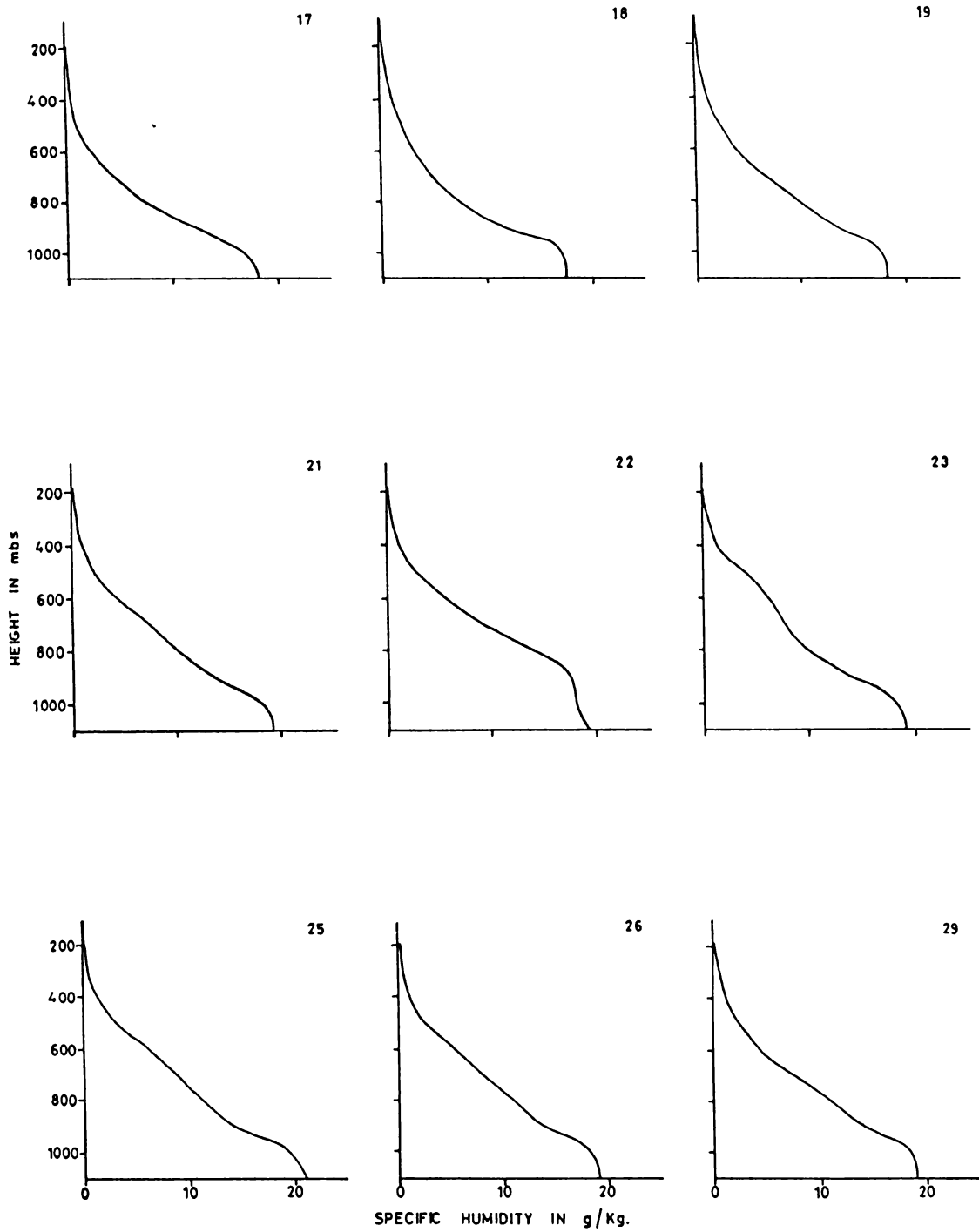


FIG.2.2(e) VERTICAL VARIATION OF SPECIFIC HUMIDITY AT 00 GMT DURING PHASE-III

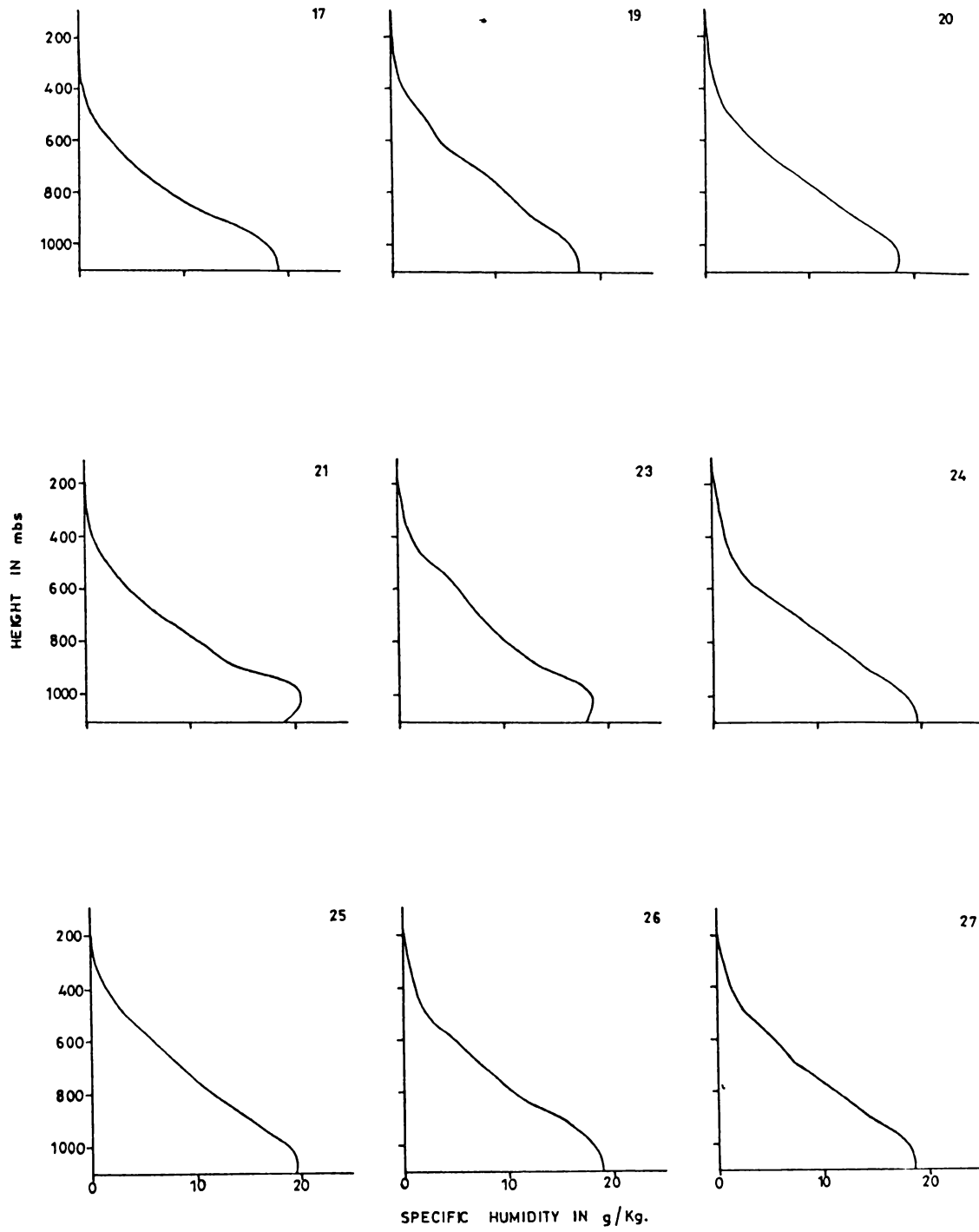


FIG.2.2(f) VERTICAL VARIATION OF SPECIFIC HUMIDITY
AT 12 GMT DURING PHASE-III

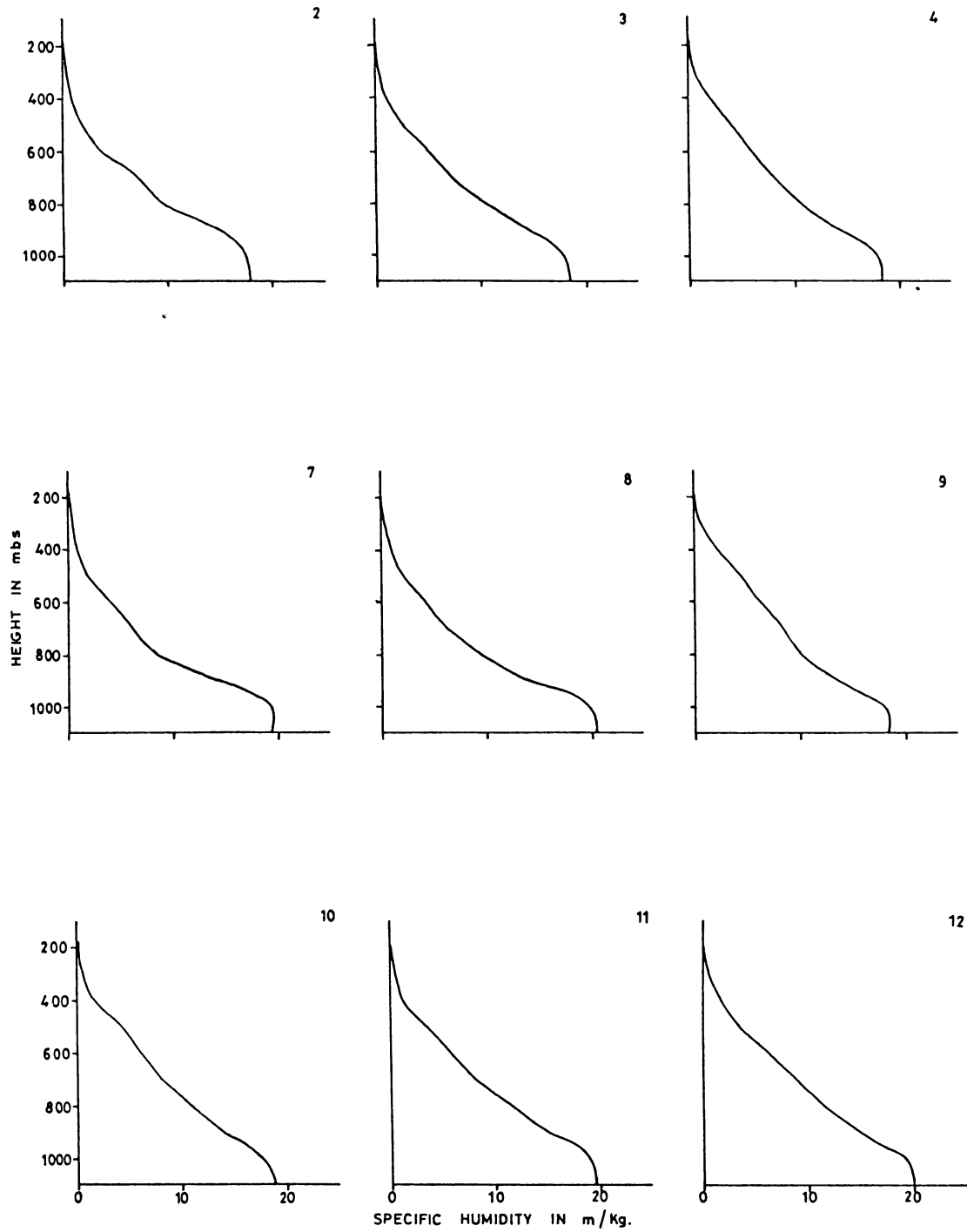


FIG.2.2(g) VERTICAL VARIATION OF SPECIFIC HUMIDITY AT 00 GMT DURING PHASE-IV

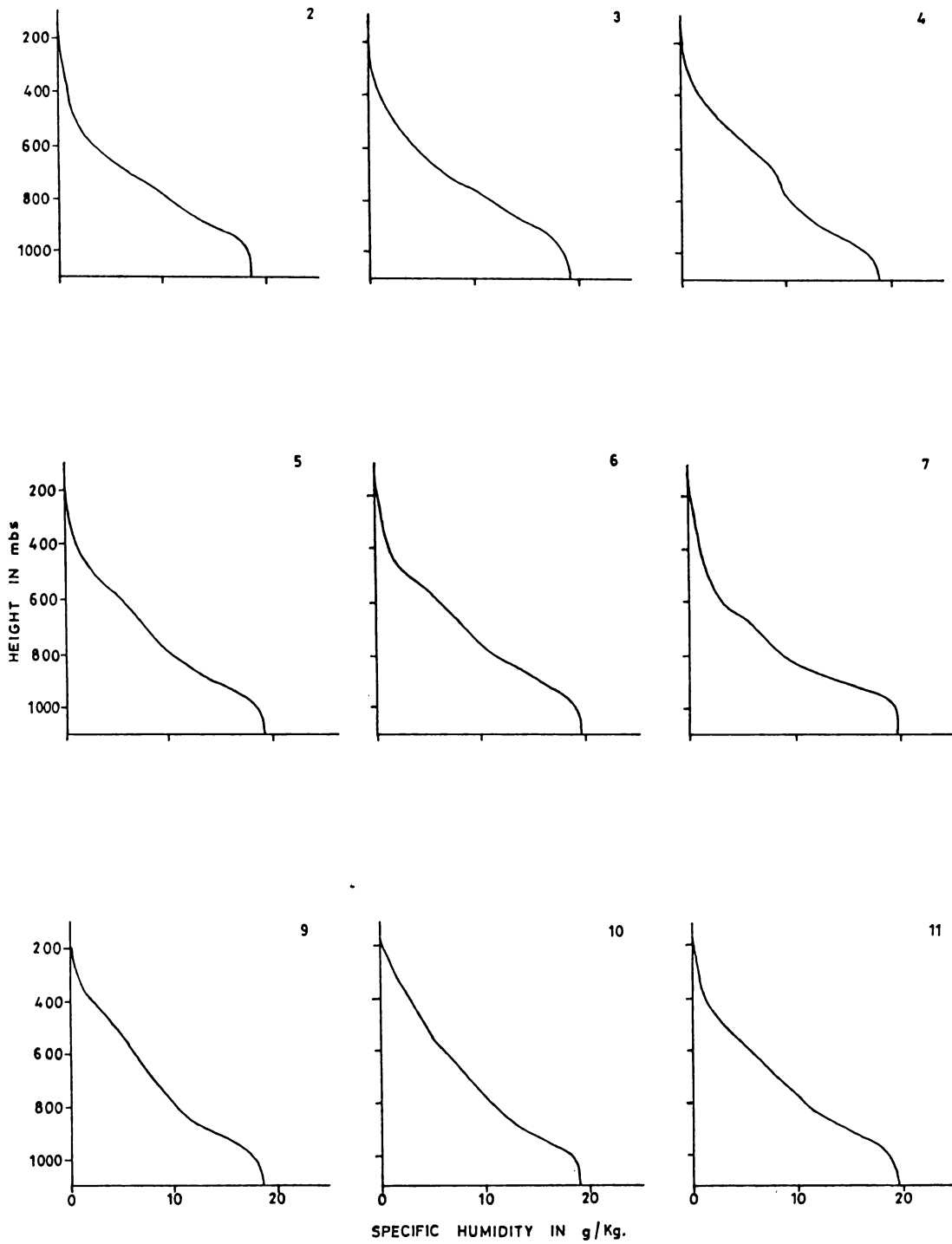


FIG.2.2(h) VERTICAL VARIATION OF SPECIFIC HUMIDITY
AT 12 GMT DURING PHASE-IV

2.3.2 Wind

Here (Fig.2.3(a) to Fig.2.3(h)) the variation of zonal and meridional components of wind at 00 and 12 GMTs, in the vertical for the four Phases-I, II, III and IV respectively are discussed.

PHASE-I

On all the days at 00 GMT, westerlies persisted almost upto 500 mbs and on some days penetrated upto 400 mbs. The westerly intensity maximum was found around 900 mb level, except on 17th June.

The meridional component did not vary much in the vertical, upto 400 mb. In fact many a time, the maximum was found at the surface itself. The change of direction from southerly to northerly took place mostly around 700 mb. There were rare occasions of changing directions twice.

At 12 GMT, the winds were slightly stronger. But the pattern of variation was almost similar. The change from westerly to easterly took place between 400 and 500 mb region and the meridional winds very rarely changed sign twice in the vertical. The westerly maximum was noticed around 800 mb region. It was also seen that, as in the case of 00 GMT, the meridional winds were weak.

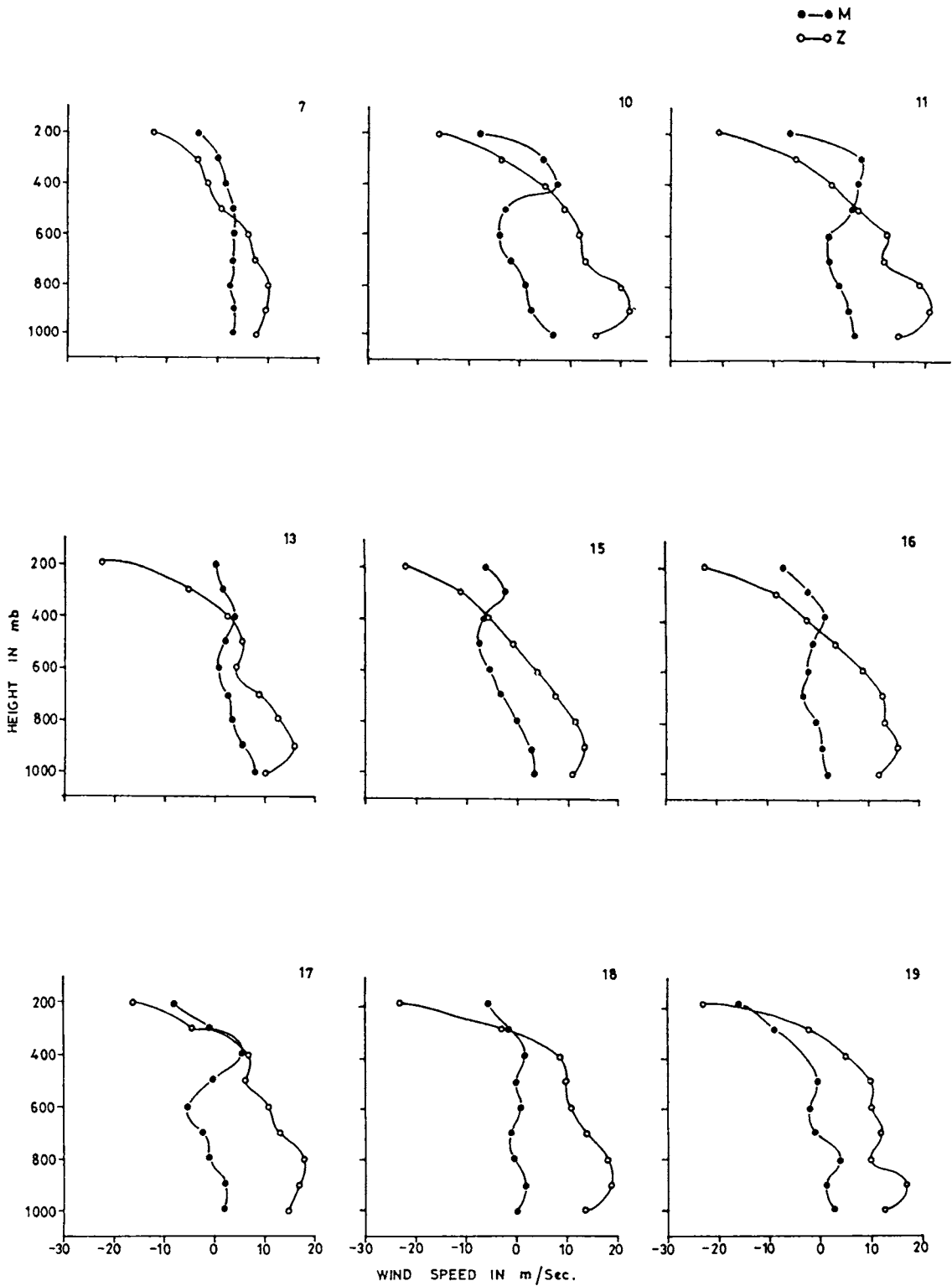


FIG.2.3(a) VERTICAL VARIATION OF ZONAL AND MERIDIONAL WIND AT 00 GMT DURING PHASE-I

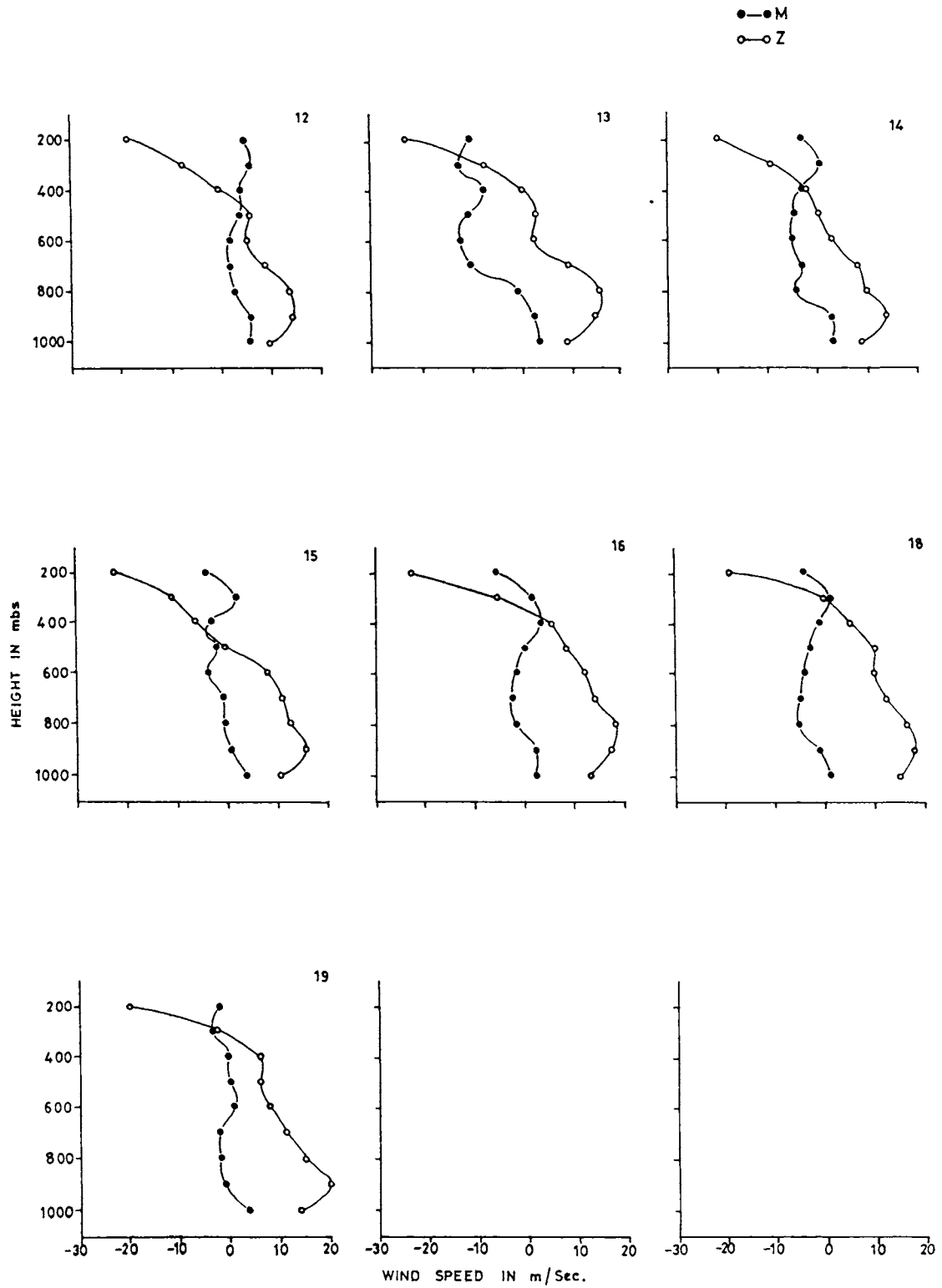


FIG.2.3(b) VERTICAL VARIATION OF ZONAL AND MERIDIONAL WIND AT 12 GMT DURING PHASE-I

Since the westerlies persisted upto middle levels, it could be inferred that the southwest monsoon was quite strong during this period. It should also be noted that the zonal wind maximum was around 200 mb level where the Easterly jet is normally located, during the monsoon period.

PHASE-II

In this phase too, westerlies existed well above 500 mb level and the changing over to easterlies took place at comparatively higher levels from 1st upto 8th July than rest of the period. The zonal wind maximum was at 200 mb while the westerly maximum was around 800 mb.

In this phase also, the meridional wind velocity as well as variations were much less. On many days, they changed direction more than once in the vertical. The domination of zonal to meridional winds could be easily seen. The variations were similar at both the synoptic hours.

PHASE-III

During this phase, the zonal winds were comparatively of lower velocities and the westerlies prevailed in a much shallow lower layer. In other words, surface westerlies changed to easterlies at around or below 650 mb level. The change of direction took place more than once and hence one finds strong westerlies in the higher levels too. From 17th

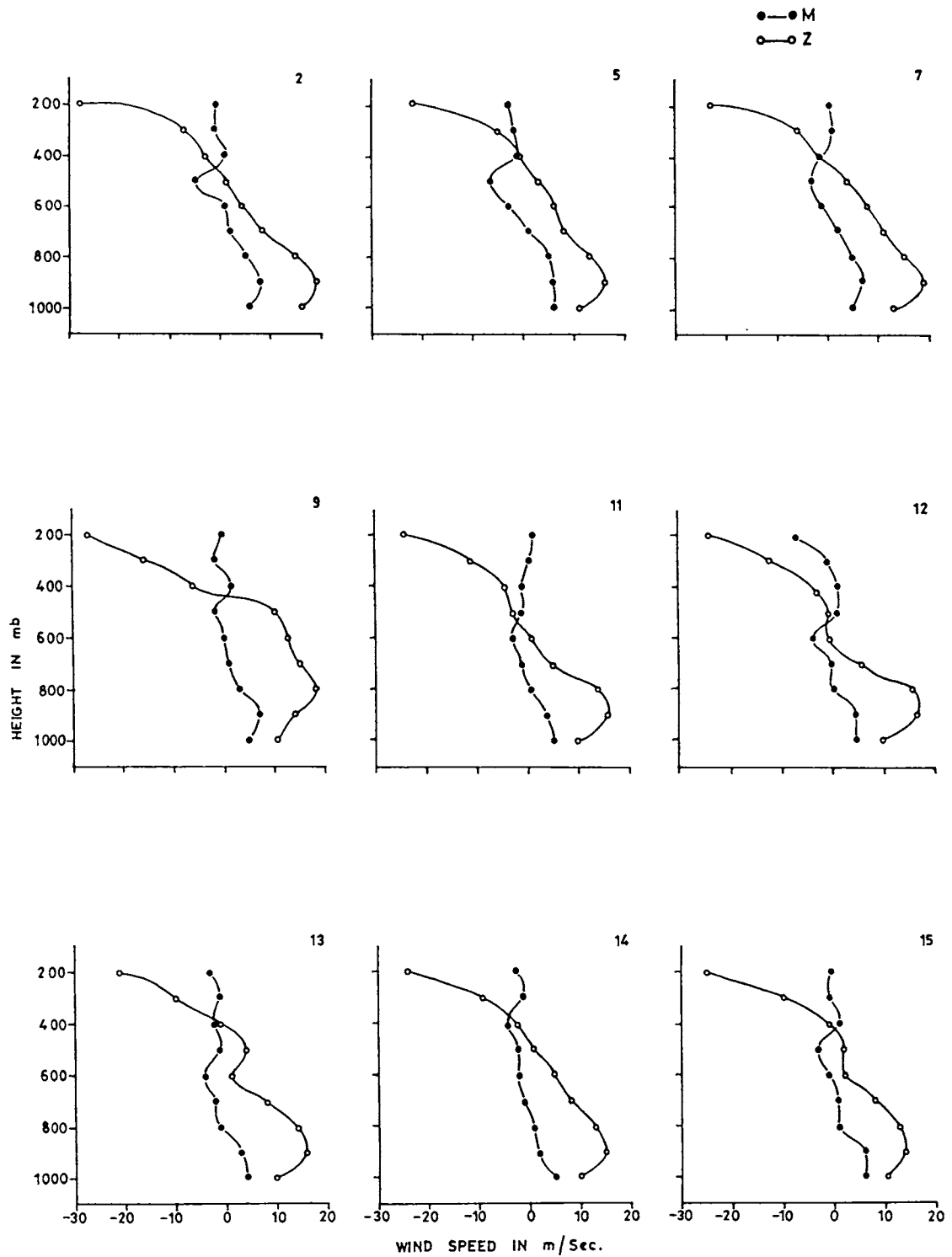


FIG.2.3(c) VERTICAL VARIATION OF ZONAL AND MERIDIONAL WIND AT 00 GMT DURING PHASE-II

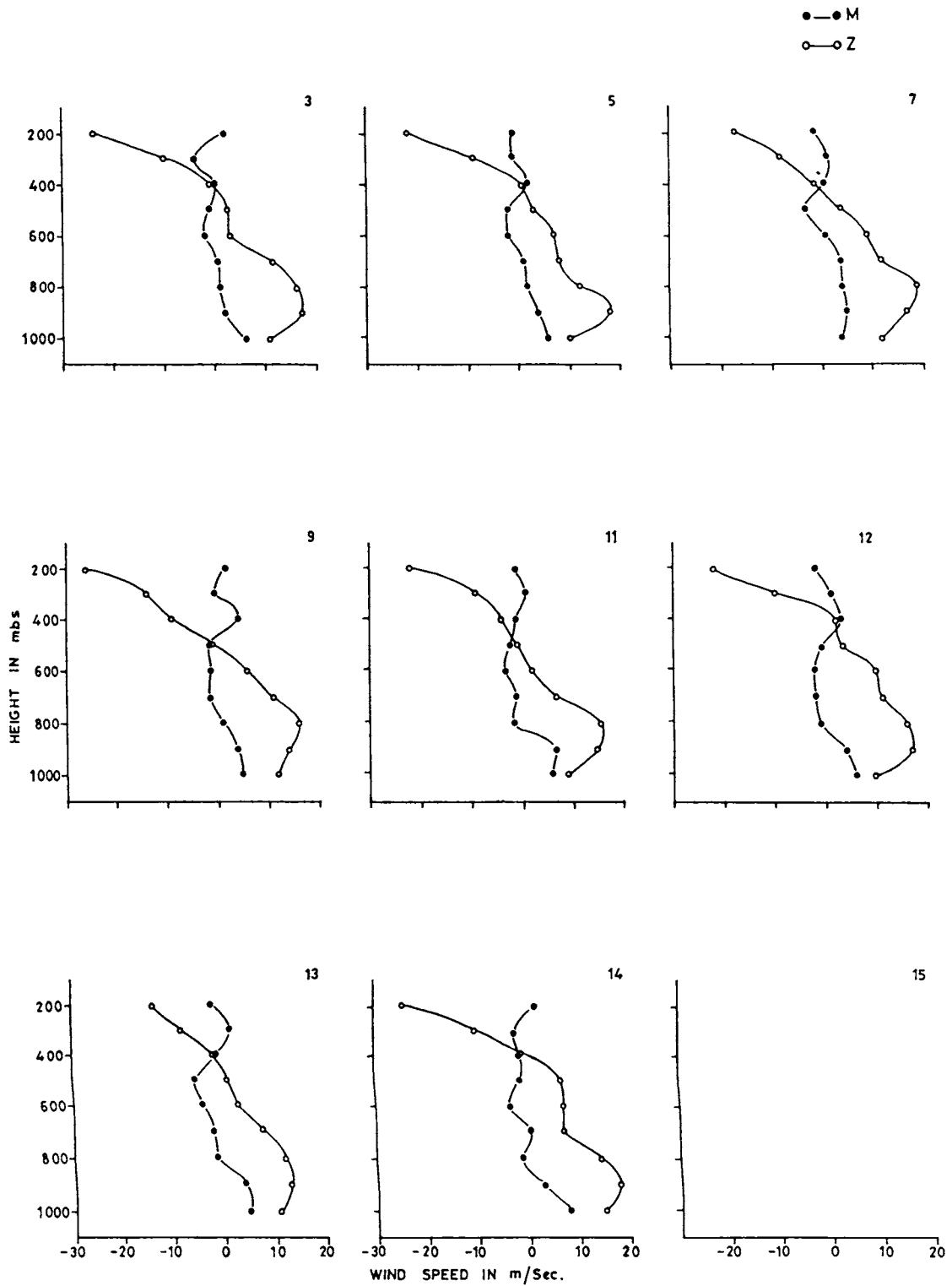


FIG.2.3(d) VERTICAL VARIATION OF ZONAL AND MERIDIONAL WIND AT 12 GMT DURING PHASE-II

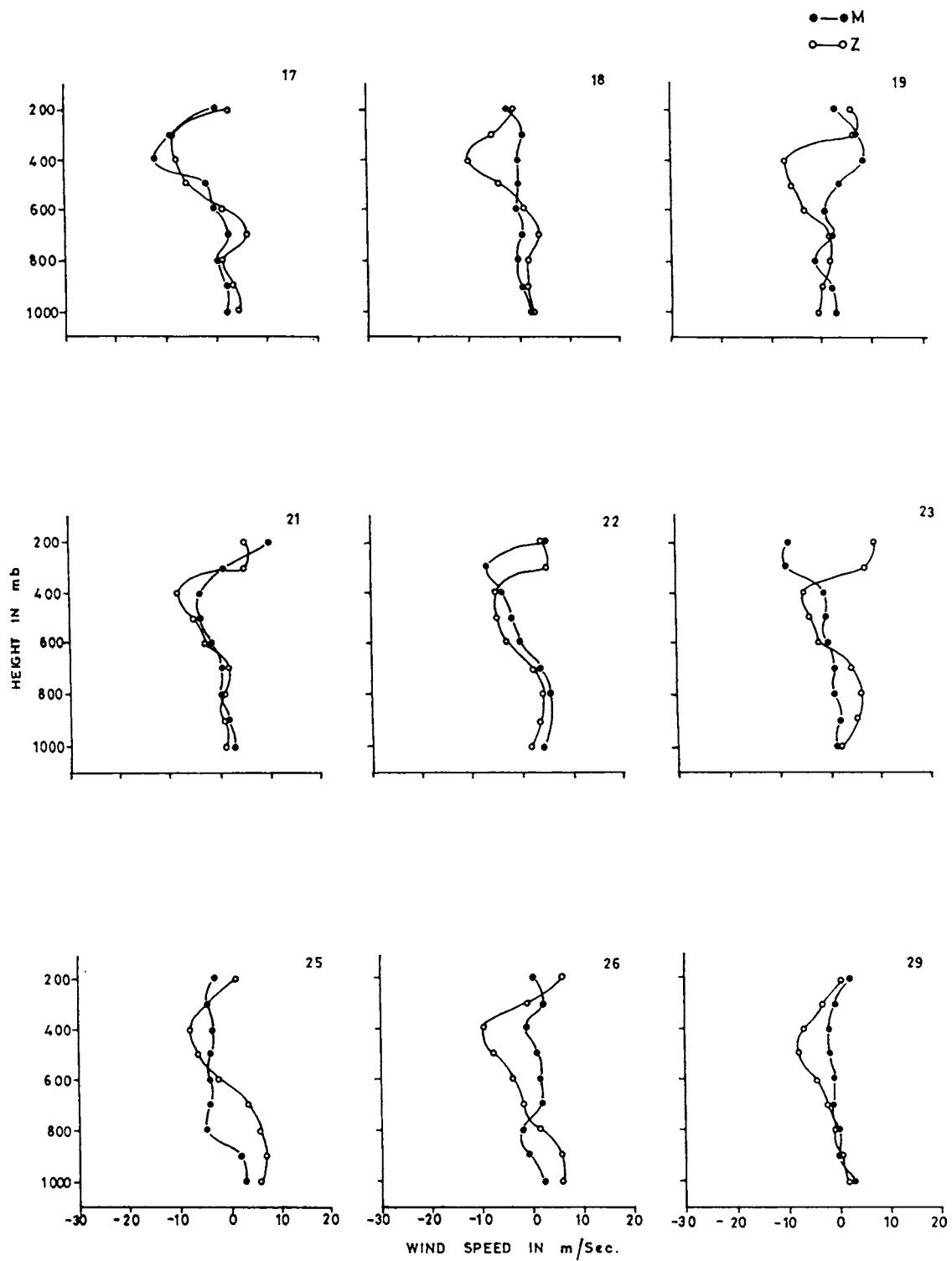


FIG.2.3(e) VERTICAL VARIATION OF ZONAL AND MERIDIONAL WIND AT 00 GMT DURING PHASE-III

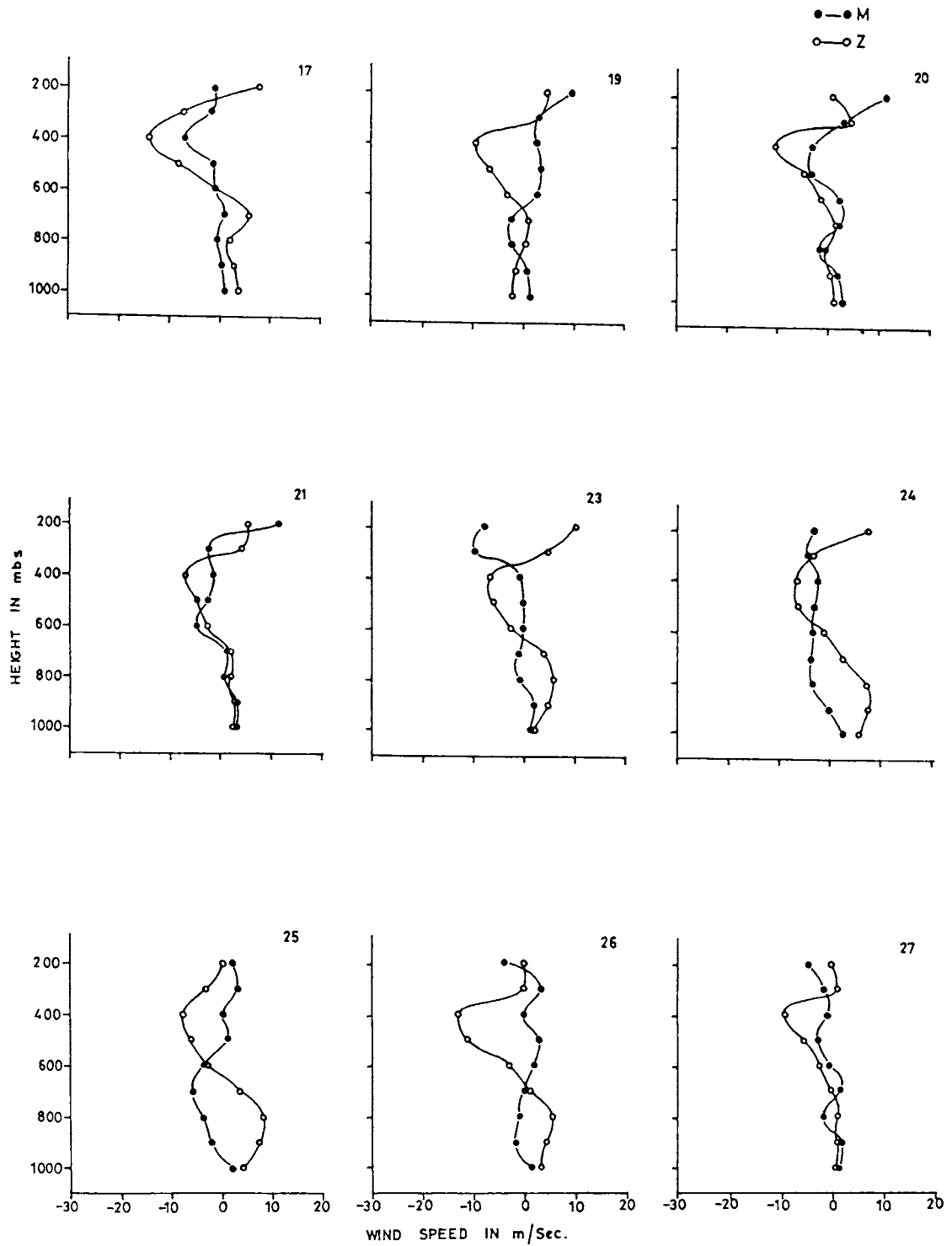


FIG.2.3(f) VERTICAL VARIATION OF ZONAL AND MERIDIONAL WIND AT 12 GMT DURING PHASE-III

to 24th May, there was a clear steep decrease in velocity of the easterlies in the upper levels and on some days it became westerlies by 300 mb level. After 24th this decrease was very gentle. On almost all the days the easterly maximum was noticed around 400 mb. Although the patterns were similar at 00 and 12 GMTs, the zonal wind velocity was higher at 12 GMT.

The meridional component was clearly insignificant and southerlies were observed in the lowest layers but the direction changed more than twice in the vertical.

PHASE-IV

From 2nd to 7th June, the zonal wind velocities and their vertical variations were insignificant and from 8th onwards, the pattern was similar to that during Phase-I. The westerly maximum was around 850 mb and the winds decreased in intensity and almost vanished at about 500 mb level. The easterlies were strongest around 200 mb and the zonal winds changed direction only once in the vertical.

An interesting feature is the dominance of northerlies in the lower layers from 7th to 11th June at both the synoptic hours and on many days these northerlies became southerlies only in the upper levels. During the rest of the period southerlies were present in the near surface layer.

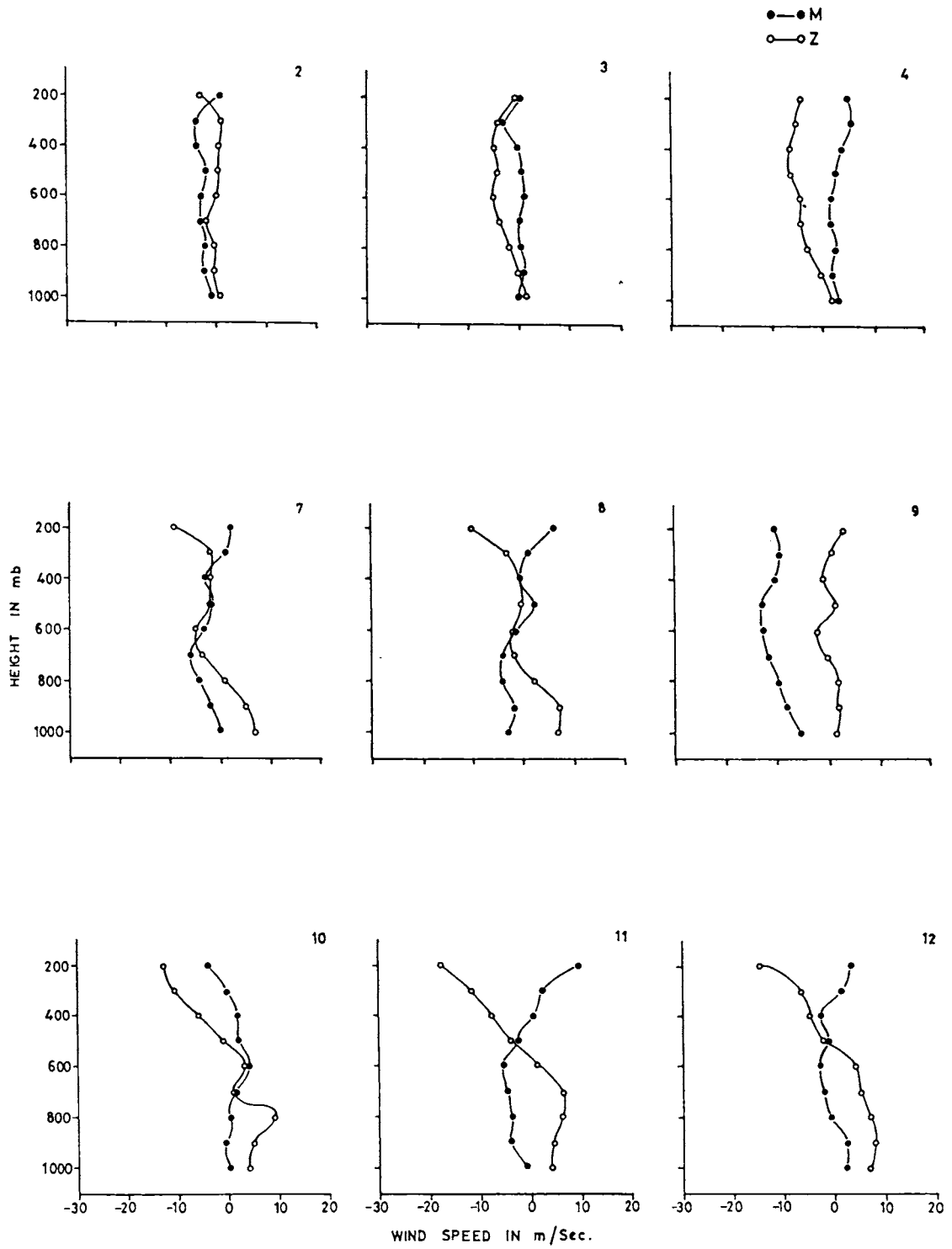


FIG.2.3(g) VERTICAL VARIATION OF ZONAL AND MERIDIONAL WIND AT 00 GMT DURING PHASE-IV

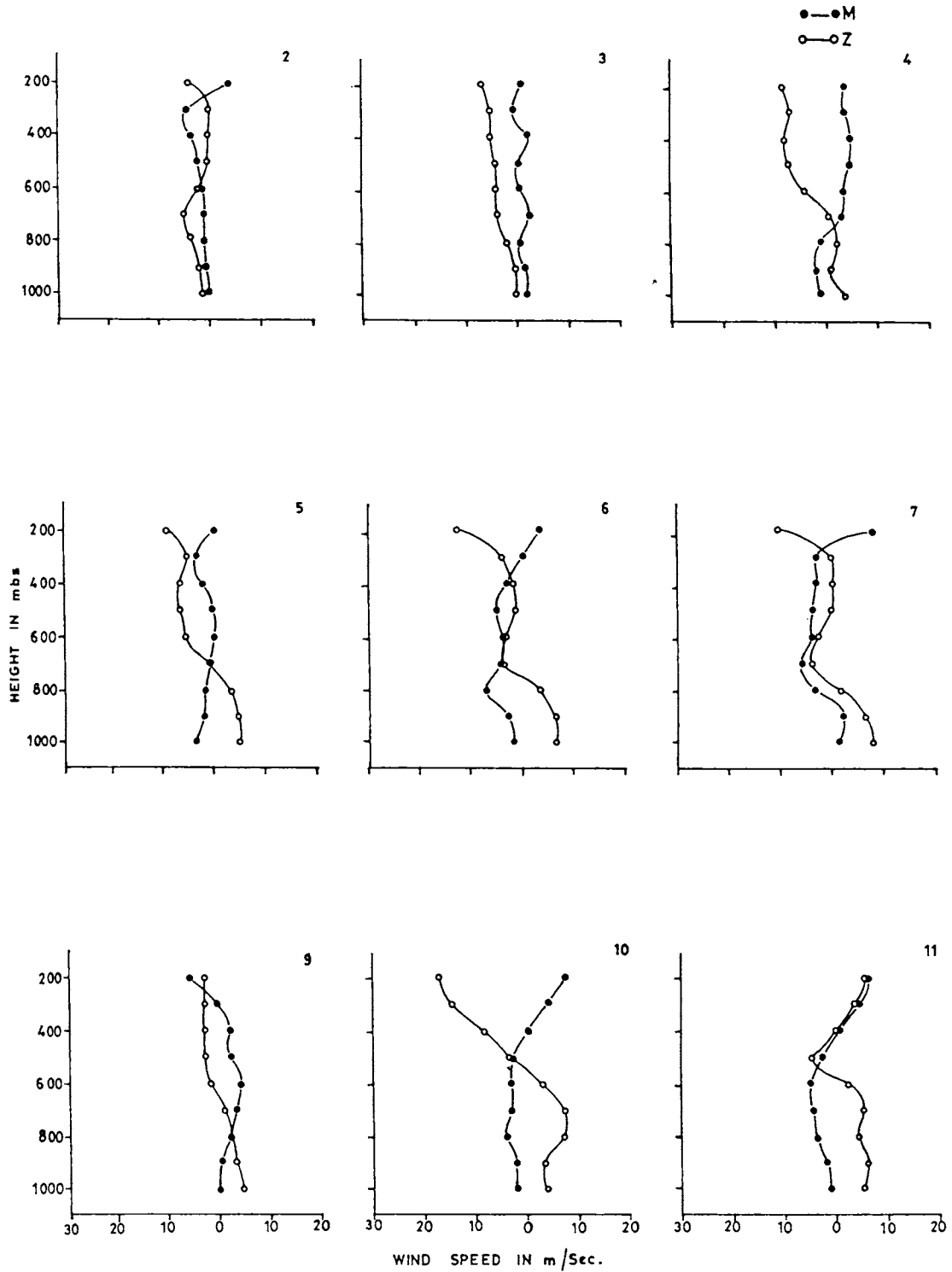


FIG.2.3(h) VERTICAL VARIATION OF ZONAL AND MERIDIONAL WIND AT 12 GMT DURING PHASE-IV

The above discussions have brought to light the following observations: There were no significant change in the specific humidity values, and the meridional components of wind also exhibited little variation. During the active phase of the monsoon, zonal winds changed direction only once in the vertical, and westerlies persisted to relatively higher levels and also there was an easterly wind maximum around 200 mb level. The diurnal variation of these parameters were insignificant.

2.3.3 Precipitable Water Vapour

Fig.2.4(a) to 2.4(d) give the day to day variations of precipitable water during the four phases. [One unit is 1×10^{12} Kg, which is equal to 4.92 kg/m^2 in phase I and II and 5.3 Kg/m^2 in Phase-III and IV]. The daily and diurnal variations of moisture in terms of amount of precipitable water vapour integrated from surface to 200 mb for the entire polygon area is discussed in this section.

PHASE-I

The diurnal variations were much less for this parameter and there was no regular pattern for the diurnal variation. From the 7th to 10th and on 19th and 20th of June the values were comparatively higher and above 10×10^{12} kg. The highest values were found to be on the 7th and lowest on 14th June.

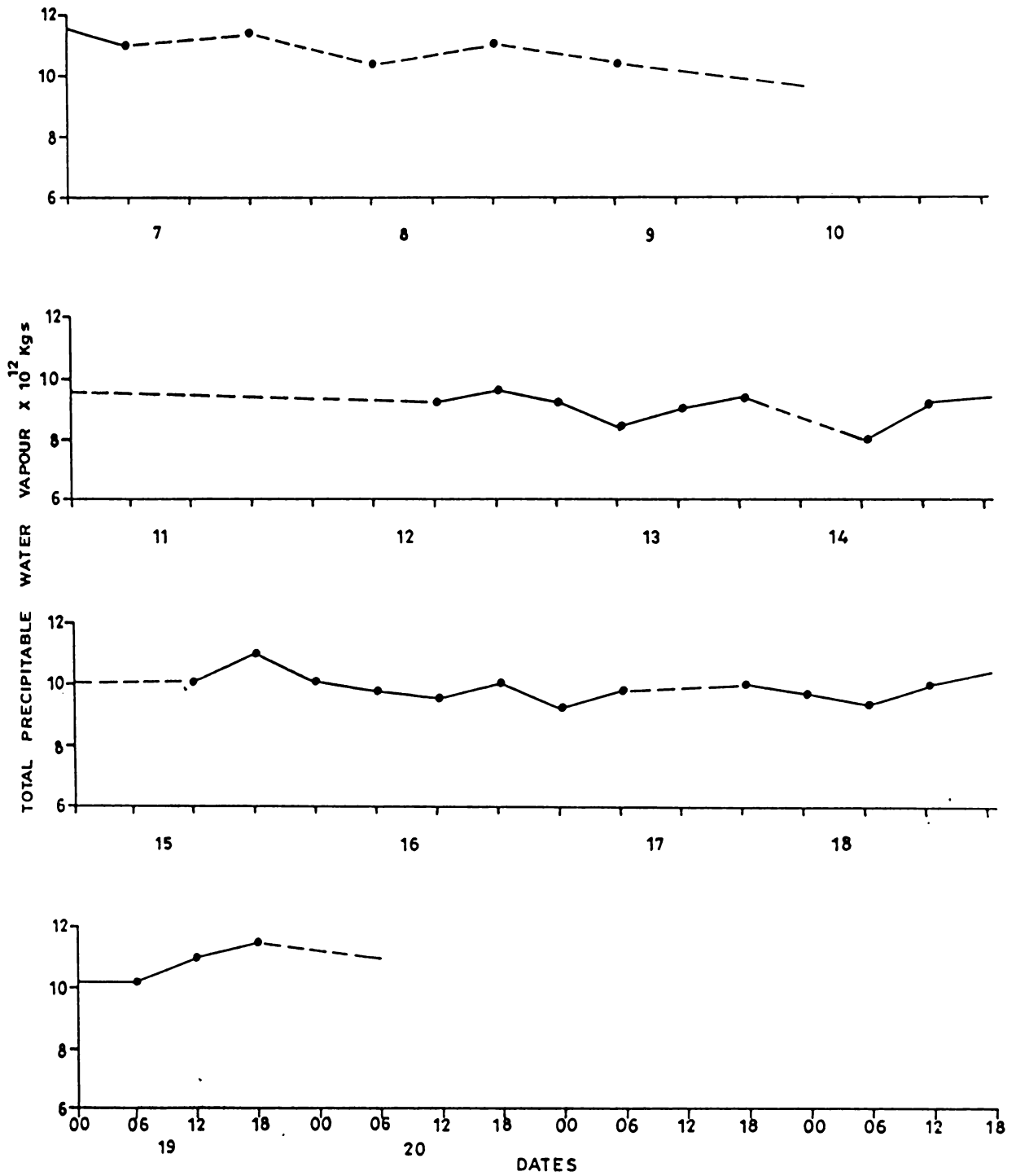


FIG.2.4(a) VARIATION OF PRECIPITABLE WATER VAPOUR DURING PHASE-I

PHASE-II

This phase was comparatively drier with the values being almost always less than 10 units. Higher values were observed between 10th and 15th July with a gradual increase in the water vapour content from the 9th to 11th. There were conspicuous or sudden variations on many days.

PHASE-III

During this period the values were almost always above ten units and there were significant day-to-day as well as diurnal variations too. For example, on 24th May between 00 and 06 GMT, the value decreased by 9 units. (From 26th to 29th there is lack of data). The exceptionally high values on 24th and 25th is a noteworthy feature. The maximum during this phase was observed at 00 GMT on 24th. There was a gradual increase in value from 9th to 22nd and from 28th to 30th and a decrease from 24th to 27th May.

PHASE-IV

During this period, the amount of precipitable water vapour is high almost always being above 11×10^{12} Kg. The value showed an increasing trend from the 2nd evening to the 5th and on some days such as 7th and 11th June. A prominent jump of about 3×10^{12} Kg. was noticed at 00 GMT on 12th.

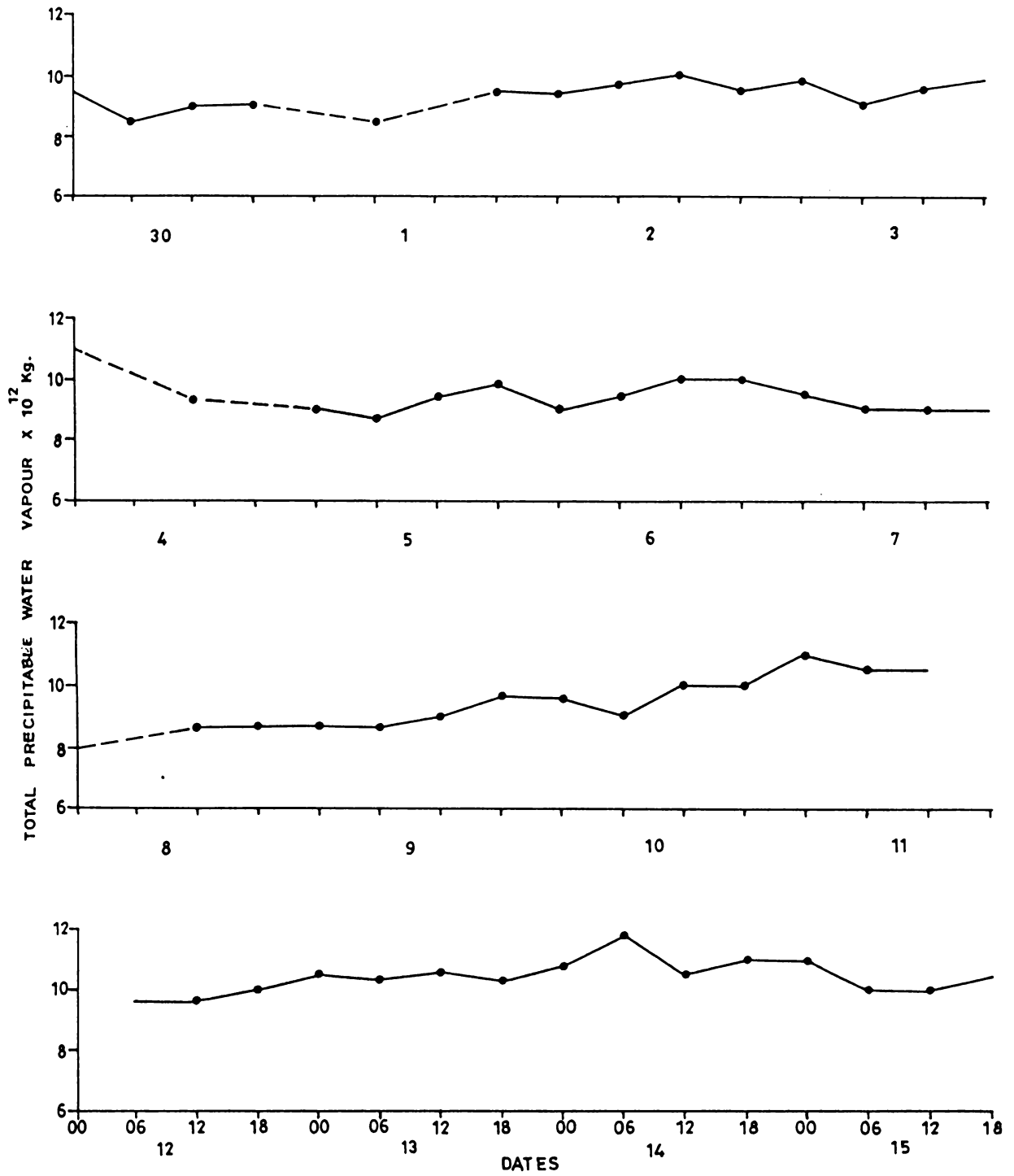


FIG.2.4(b) VARIATION OF PRECIPITABLE WATER VAPOUR DURING PHASE-II

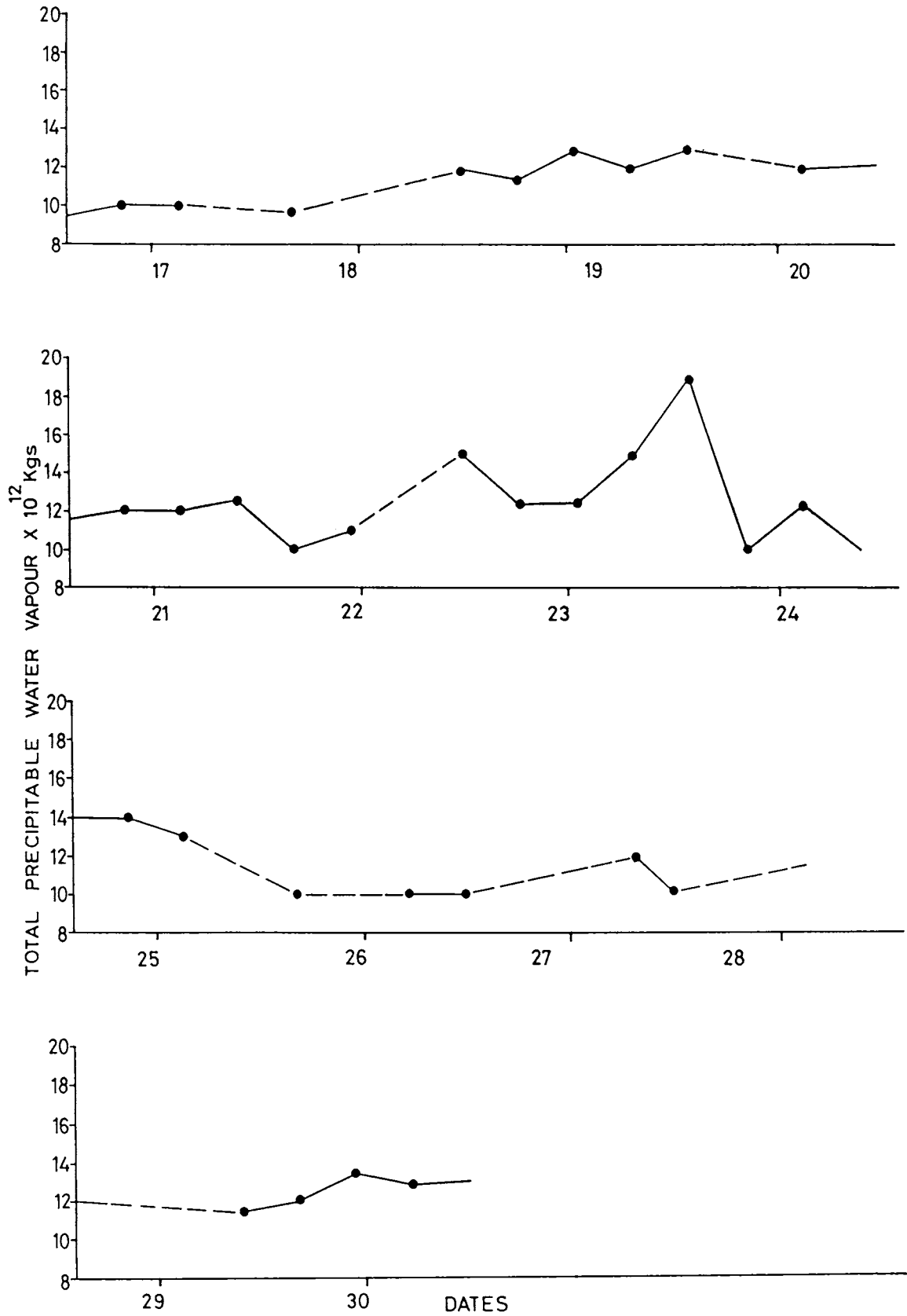


FIG.2.4(c) VARIATION OF PRECIPITABLE WATER VAPOUR DURING PHASE-III

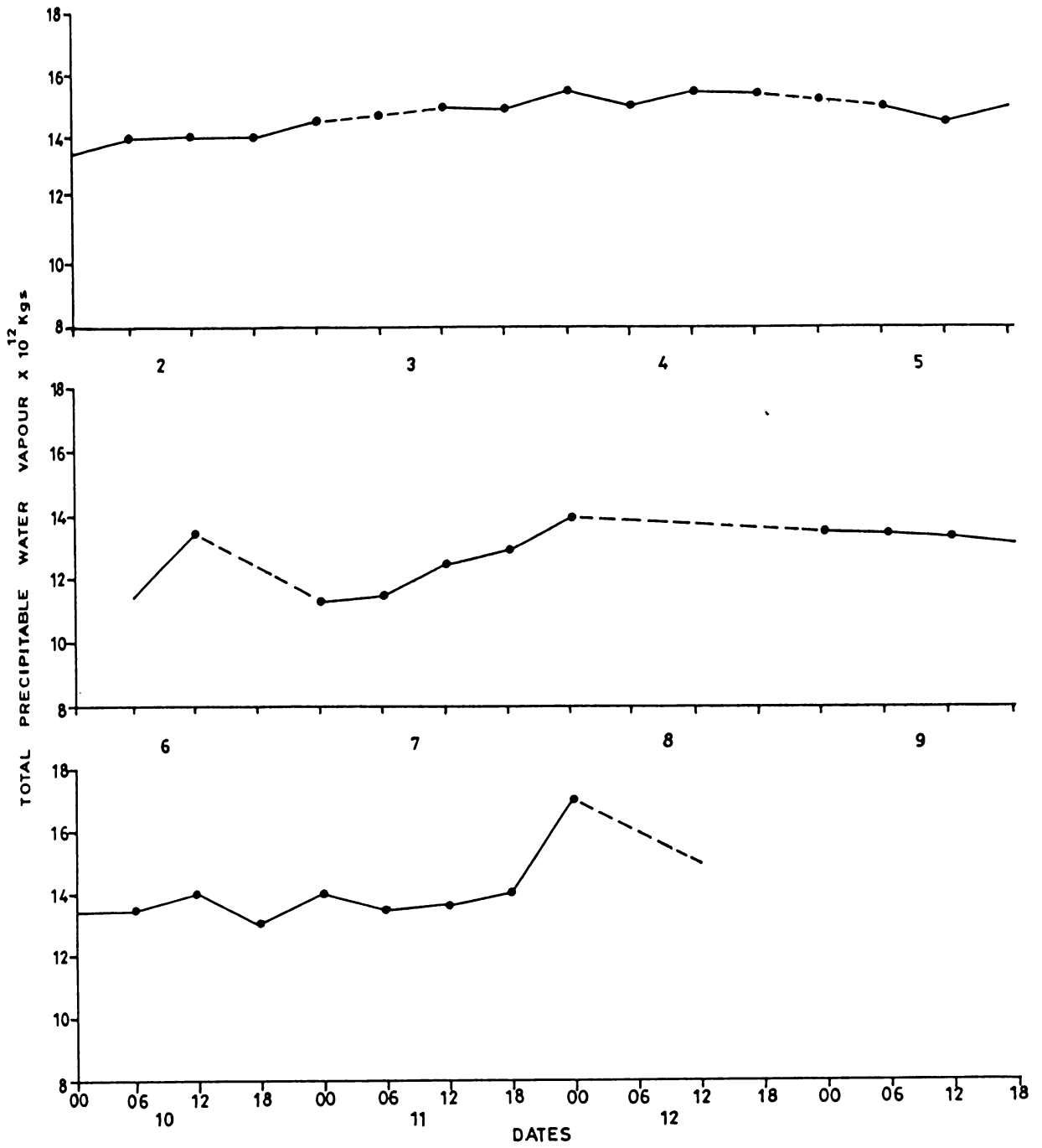


FIG.2.4(d) VARIATION OF PRECIPITABLE WATER VAPOUR DURING PHASE-IV

2.3.4 Kinetic Energy

Time section of kinetic energy at four levels, for the four phases are now discussed below. Fig.2.5(a) to 2.5(d) show the values for the Phases-I to IV respectively.

PHASE-I

It can be seen that kinetic energy showed a steady increase at all the levels from 7th to 10th June. This was followed by a slight decrease upto the 12th and thereafter remained almost unchanged till the end of the phase. Kinetic energy maximum was at 700 mb on a few days (7th, 8th and 9th) in the earlier part of the phase and at 200 mb level afterwards. The value was minimum at 500 mb level where the low level westerlies changed over to easterlies. The highest value was around $2.5 \times 10^2 \text{ m sec}^{-2}$.

PHASE-II

In general, the kinetic energy values were much higher than that in the previous phase, with the maximum values around 4×10^2 units. The day to day variations were significant at the 200 mb level with alternate high and low values. The values were highest at 200 mb level and it was the lowest at 500 mb. At the surface, the values were that between 700 mb and 500 mb levels.

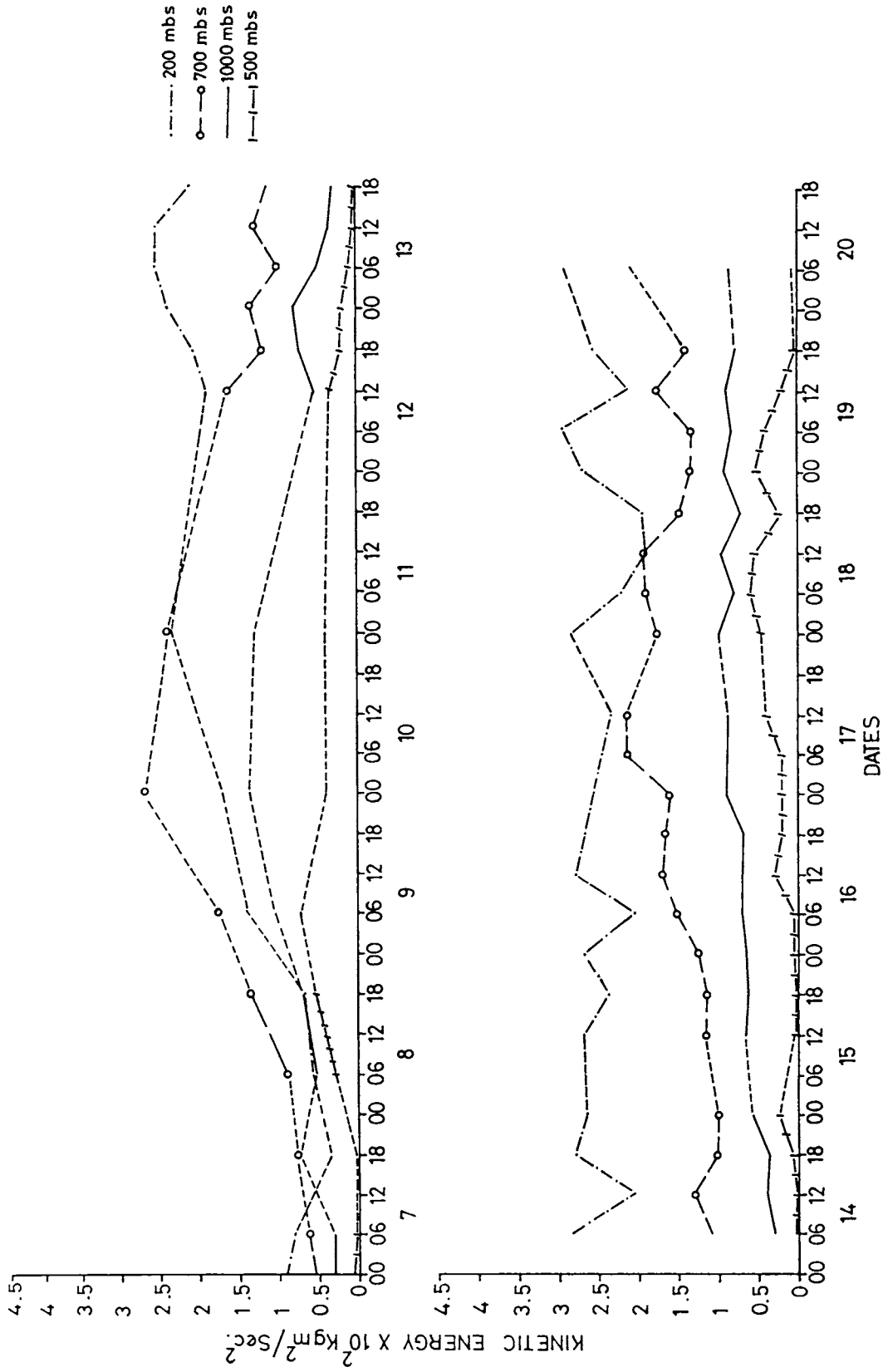


FIG.2.5(a) VARIATION OF KINETIC ENERGY DURING PHASE-I

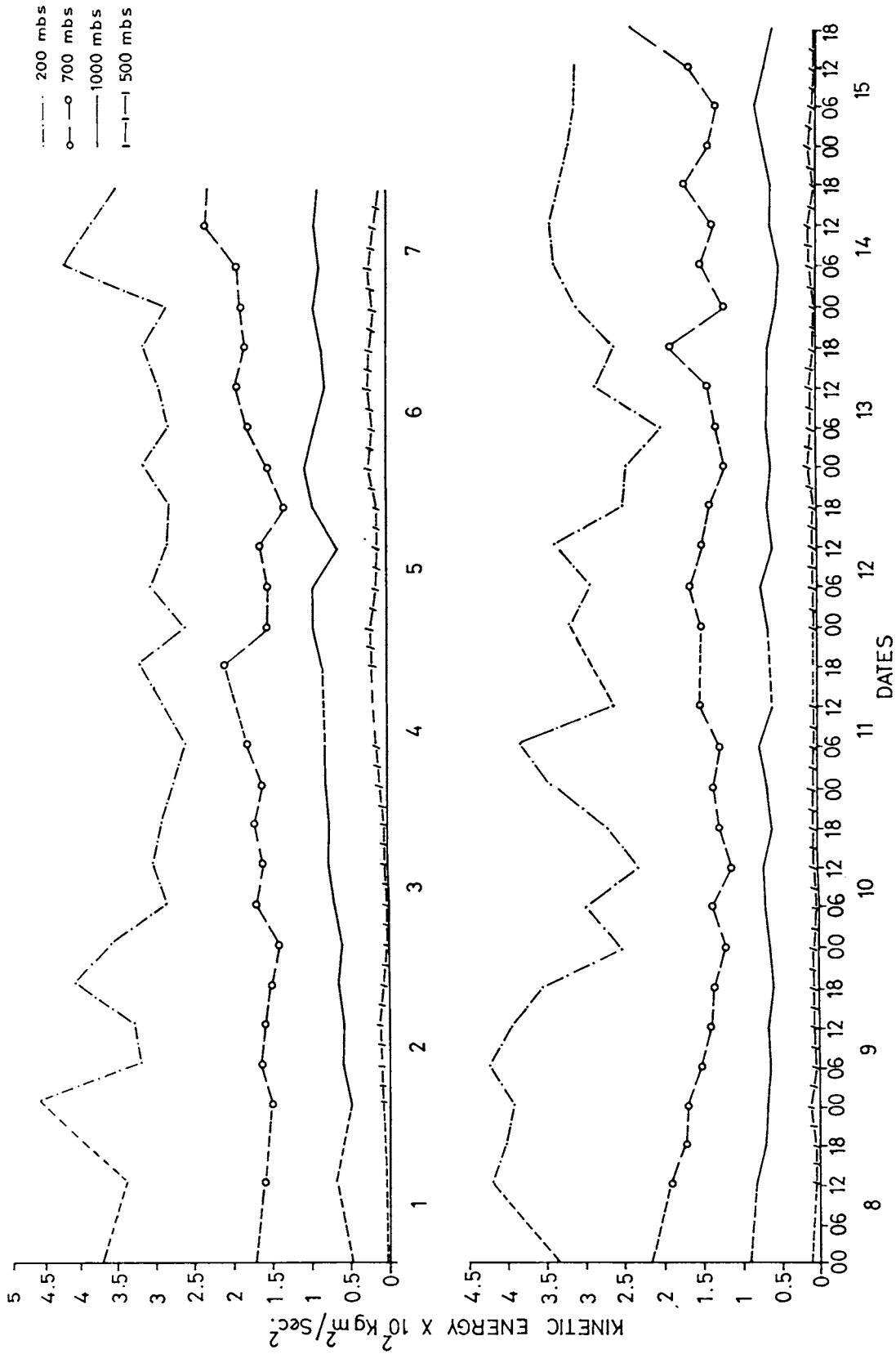


FIG.2.5(b) VARIATION OF KINETIC ENERGY DURING PHASE-II

PHASE-III

The values were much lower, almost one order lesser than that in the previous two phases. The maximum and minimum values differed considerably. Except during the period from 23rd-26th May, the lowest energy was observed at the 700 mb level. Kinetic energy was maximum at the 200 mb level from the 19th to 26th while on other days maximum was at 500 mb level. The variations at 200 mb and 500 mb levels were characterised by good fluctuations while it was less at the surface and 700 mb levels except on 25th May.

PHASE-IV

Except during the period from 4th to 7th June, the daily variations of kinetic energy at the levels other than 200 mb, were very low. There was generally an increasing trend from the 2nd to 7th and the 9th to 11th and decreasing on other days. In the latter part of the phase, the values were rather very high at the 200 mb level. The level of minimum energy was 700 mb upto 7th June and thereupon 500 mb.

The variation pattern of kinetic energy did not show a consistent decrease or increase with height. It followed the prevailing wind pattern.

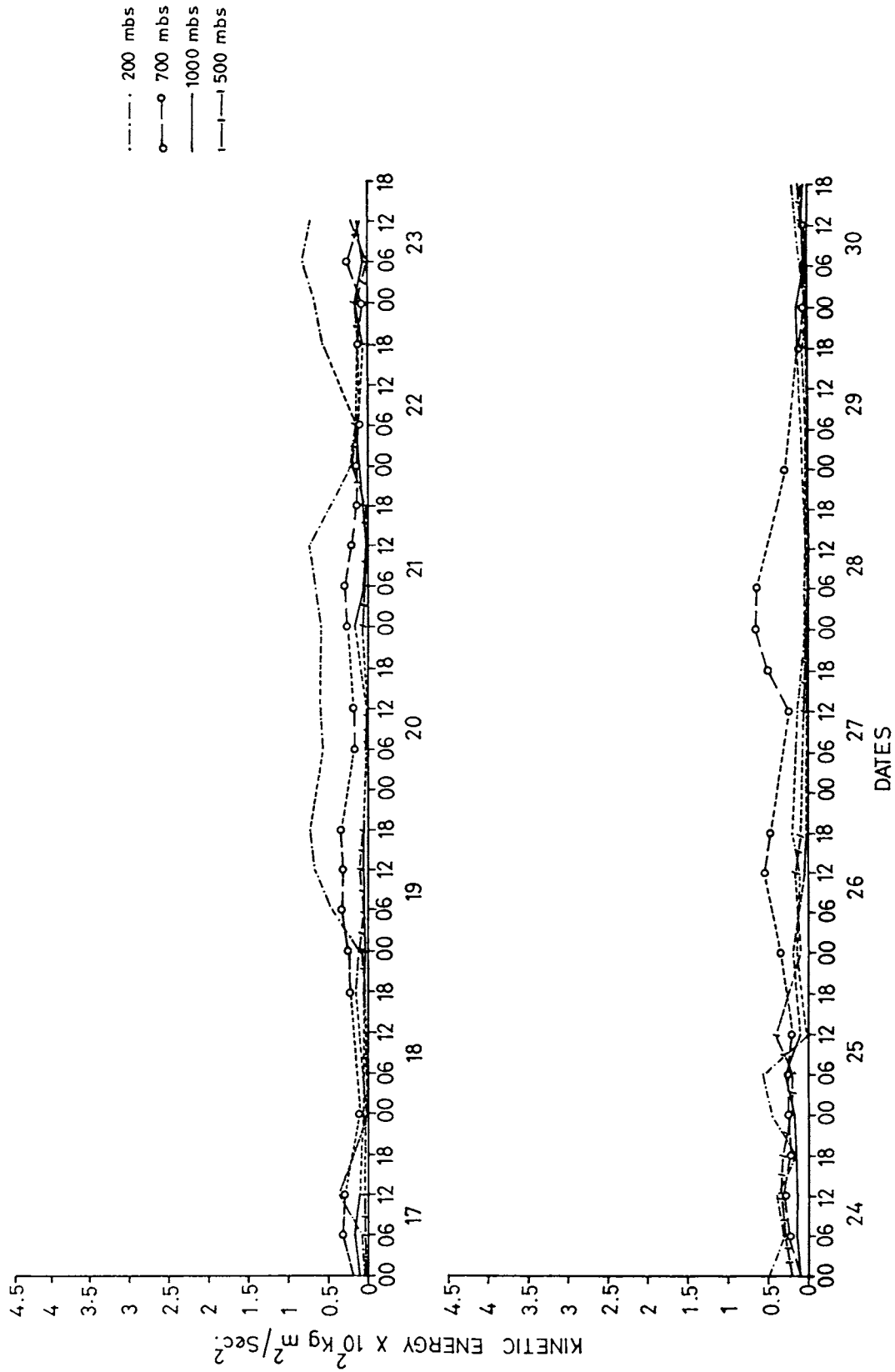


FIG.2.5(c) VARIATION OF KINETIC ENERGY DURING PHASE-III

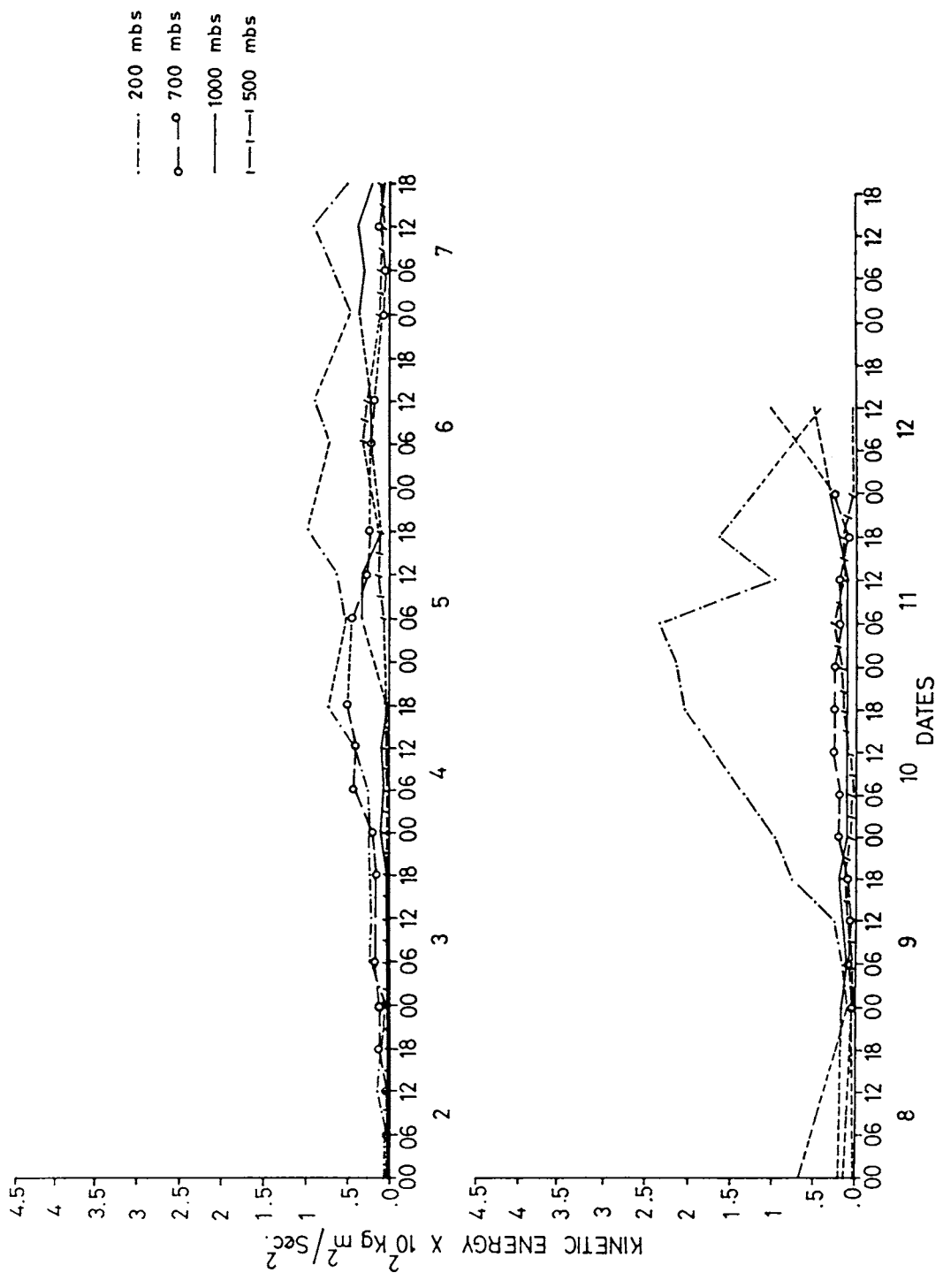


FIG.2.5(d) VARIATION OF KINETIC ENERGY DURING PHASE-IV

2.3.5 Vorticity, Divergence and Vertical Velocity

This section deals with the vorticity, divergence and vertical velocity during the four phases. The gaps in the figures are due to lack of data and the shaded areas represent anticyclonic vorticity, divergence and downward motion.

PHASE-I

Fig.2.6(a) shows the vorticity, divergence and vertical velocity respectively during this phase.

Vorticity

On 7th and 8th June (except at 18 GMT) the atmosphere had generally anticyclonic vorticity in the near surface layer and cyclonic vorticity from about 950 to 250 mb. From 18 GMT on the 8th, to 00 GMT on the 10th, it was very high cyclonic vorticity althrough. The period from 12th June onwards was characterised by anticyclonic vorticity from surface to about 850 mb and in the higher levels from 400 to 200 mbs. Anticyclonic vorticity was very strong at the higher levels throughout the period and in the lower layers from 12 GMT of 13th to 12 GMT of 16th June. The middle layer had intermittent days of cyclonic and anticyclonic vorticity.

▨ Anticyclone Vorticity, Divergence, Downward motion.

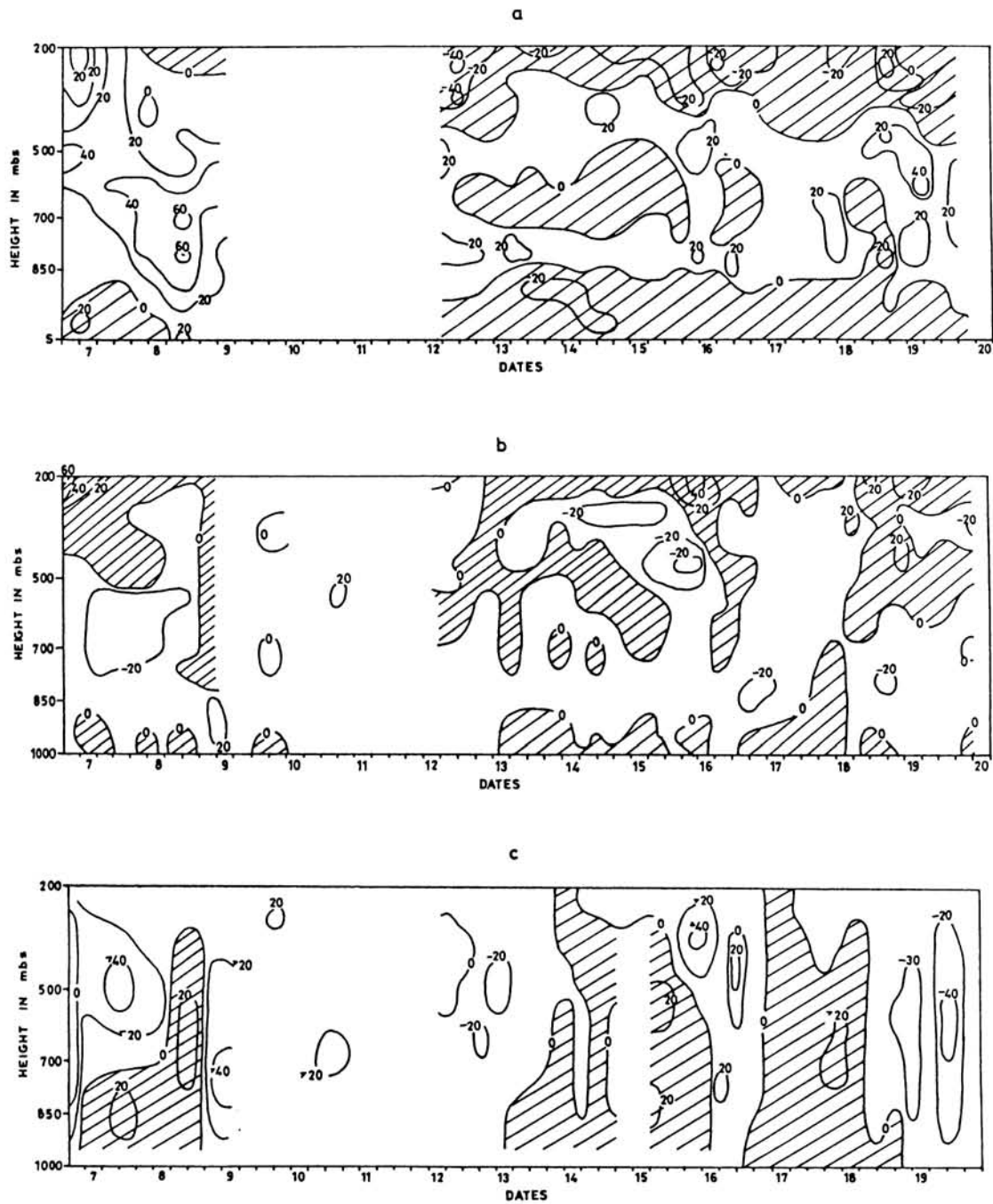


FIG.2.6(a) VERTICAL TIME SECTION OF (a) VORTICITY (b) DIVERGENCE and (c) VERTICAL VELOCITY DURING PHASE-I

Divergence

The period was characterised by divergence on almost all the days in the lower layers upto about 900 mb level except on 9th and 19th of June. The values were exceptionally high in lower levels at 00 GMT on 7th and 06 GMT on 9th. Above 900 mb it was mostly high convergence upto 500 mb on the 7th and 8th and only upto about 700 mb on the other days. Except on certain days like 8th, 17th and 18th June, where convergence prevailed even upto 250 mb, it was mostly upper level divergence on all the days with very high values like that on 7th, 16th and 19th June. From the 18th to the 20th, low level convergence and upper level divergence were noticed with the latter being of higher magnitudes.

Vertical Velocity

Downward motion prevailed in the lower atmosphere upto about 750 mb on almost all the days except from the 9th to 13th and 19th June. One could notice strong upward motion from surface to 200 mb, from the 9th to 13th with the core on 9th. This could be mainly because of the cyclonic storm that was formed in the Arabian Sea during this period. In general, positive vorticity coupled with convergence was the dominant feature during this period. However from the 13th to 18th, it was downward motion throughout the atmosphere, except on the 16th and the reverse was true from 18th to

▨ Anticyclone Vorticity, Divergence, Downward motion.

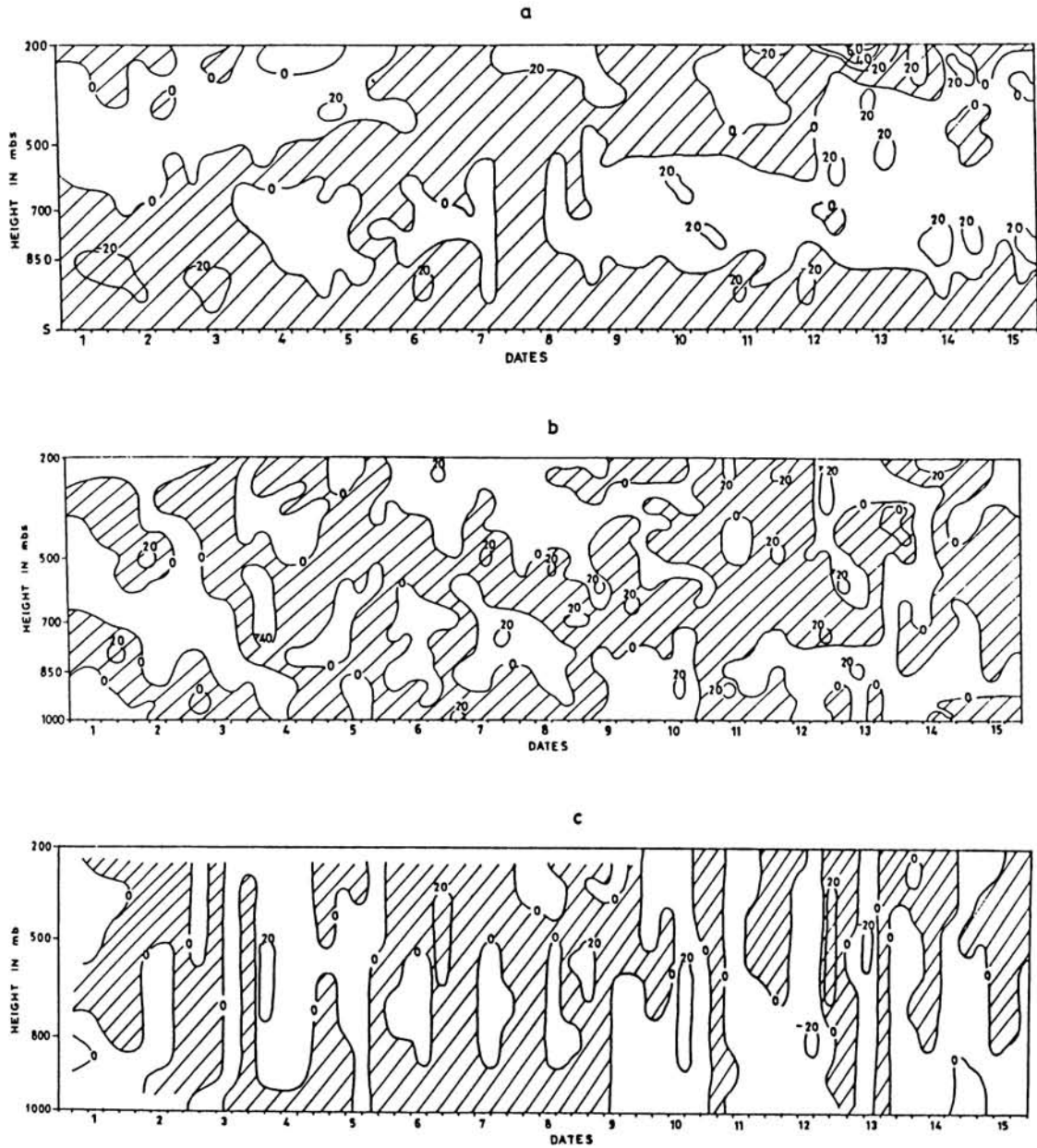


FIG.2.6(b) VERTICAL TIME SECTION OF (a) VORTICITY, (b) DIVERGENCE and (c) VERTICAL VELOCITY DURING PHASE-II

20th. If one recalls the divergence pattern during the 18th to 20th, it was low level convergence and upper level divergence which could also lead to upward motion.

During this phase, the variation of the above three parameters was in conformity to the synoptic situations which prevailed during that period, specially the vorticity pattern.

PHASE-II

Fig.2.6(b) shows the variation of above three parameters during the second phase.

Vorticity

Anticyclonic vorticity was predominant from surface to 450 mb from 1st to 8th July, while from the 8th to 15th, anticyclonic vorticity was confined to the layers from surface to 850 mb and that above 500 mb. The intermediate layer experienced cyclonic vorticity except during the latter half of this Phase (12th to 13th), where the middle layer cyclonic vorticity extended upto about 350 mb.

Divergence

It was mostly divergence in the lower levels almost upto 700 mb with exceptions on 1st, 9th and 13th July. Divergence dominated the whole atmosphere during this phase,

except in the middle levels from the 1st to 4th, 7th and 8th and in the upper levels on 4th, 7th, 13th and 14th July.

Vertical Velocity

Except for the downward motion in the lower layers from surface to 700 mb, from 1st to 3rd July at 12 GMT, it was upward motion elsewhere, on these three days. Very high values of downward motions were noticed throughout the whole atmosphere at 12 GMT on the 3rd and this suddenly changed to strong updrafts by 18 GMT. From the 3rd to 5th it was mostly upward motion and viceversa after that upto 9th. In general, from the 9th to 12th updrafts dominated the whole atmosphere and on the 10th it was updrafts allthrough with exceptionally high velocities at 12 GMT. A noteworthy feature is the sudden transition from high downward velocities at 12 GMT to very strong upward velocity at 18 GMT on 3rd and viceversa on 12th from 12 to 18 GMT, and again a reversal at 06 GMT on 13th. On 14th and 15th July, upward motion dominated the lower layers while it was the downward motion in the upper levels.

The circulation parameters especially vertical velocity pattern, clearly revealed the period to be an inactive phase of monsoon. It should be recalled that the synoptic charts also gave the same idea.

PHASE-III

Vertical time section of Vorticity, Divergence and Vertical Velocity for this phase are shown in Fig.2.6(c).

Vorticity

On 17th and 18th May it was almost all through cyclonic vorticity except from surface to 900 mb on 17th. From 19th to 21st May, cyclonic vorticity was observed from 900 to 600 mb and anticyclonic vorticity in the surface layers as well as upper levels. The situation was almost reversed from 21st to 23rd and anticyclonic vorticity dominated the whole atmosphere. From the 23rd to 28th, it was lower level (upto 800 mb) anticyclonic vorticity with cyclonic vorticity above that. Very strong cyclonic vorticity was found on 24th, above 300 mb and on the 25th and 26th around 400 mb level.

Divergence

Although there was an overall dominance of divergence during this period, convergence was seen in the lowest layers from 1000 to 900 mb on almost all the days with exceptionally high values on 25th May where it was convergence all through. In the middle layers also, convergence was seen on a few days while, it was divergence on all the days in the upper levels except on the 21st, 23rd and 24th.

▨ Anticyclone Vorticity, Divergence, Downward motion.

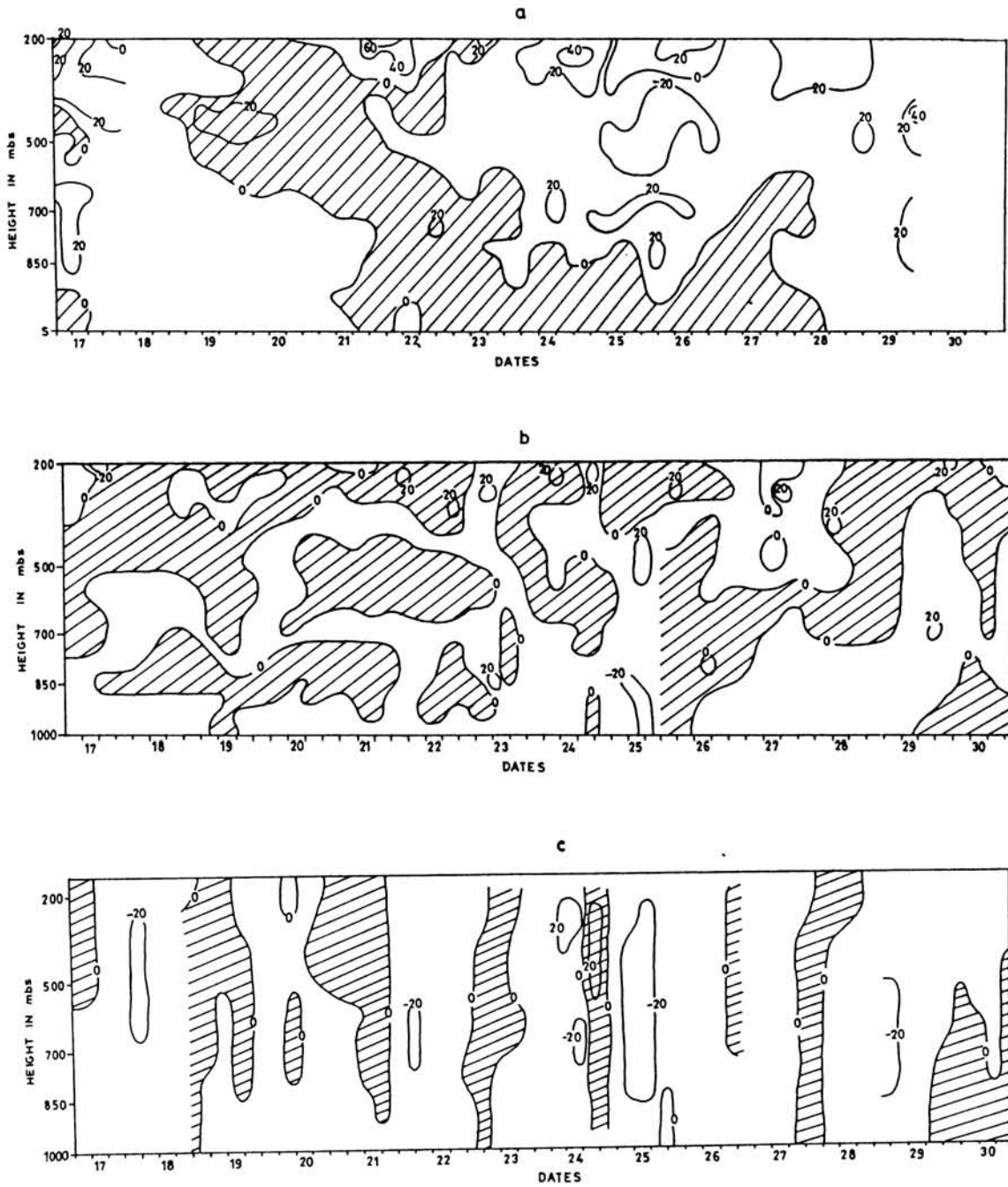


FIG.2.6(c) VERTICAL TIME SECTION OF (a) VORTICITY, (b) DIVERGENCE and (c) VERTICAL VELOCITY DURING PHASE-III

Upper level divergence were very high (more than 2×10^{-5} /sec) on all the days from 17th to 22nd and also on 24th May. The change from convergence to divergence took place within a span of 6 hours on many days like that on the 24th, at 18 GMT. In general, divergence values were higher than convergence.

Vertical Velocity

The figure 2.6(c) reveals alternate upward and downward motions with both being very strong on many days. For example, from 900 to 250 mb at 00 GMT on 18th, the atmosphere was characterised by strong upward motions of the order of $+2.5 \times 10^{-3}$ mb/sec. and at 18 GMT on 25th it was even higher 3×10^{-3} mb/sec downward motions. Sudden transitions from downward to upward motions were also noticed as can be seen on 25th May. There were synoptic hours on which only upward or downward motions were noticed. From the 17th to 25th in the lower layers and from the 25th to 29th 06 GMT, it was mostly upward motions, in the whole atmosphere.

The presence of strong cyclonic vorticity, low level convergence and strong upward motions on 17th and 18th May, may be due to the presence of a low in the vicinity of the polygon area, during that period. An examination of the synoptic charts on these days clearly reveal the presence of high pressure vortex over the Arabian Sea, near to the

polygon area, under study. Although the vertical velocity picture does not fully reveal the characteristics of the persistent anticyclone, the pattern of vorticity and divergence does suggest the presence of anticyclonic circulation during the latter part of the period.

PHASE-IV

Fig.2.6(d) gives the vertical and time to time variation of the three parameters for Phase-IV.

Vorticity

In general it was strong cyclonic vorticity in almost the whole layer of atmosphere on all the days except 5th June. The values were very high on the 3rd, 4th, 7th, 9th and 12th June. Anticyclonic vorticity prevailed in the higher levels from the 4th to 7th and early hours of the 11th with highest, values on the 4th, while on the 5th, it extended down to 650 mb level.

Divergence

On 2nd and 3rd June, it was convergence from 1000 mb to 900 mb and divergence from 900 to 200 mbs. From the 4th to 9th, although convergence dominated the whole atmosphere, divergence were also seen in the middle levels. During the period from 9th to 12th June, mostly strong convergence were

▨ Anticyclone Vorticity, Divergence, Downward motion.

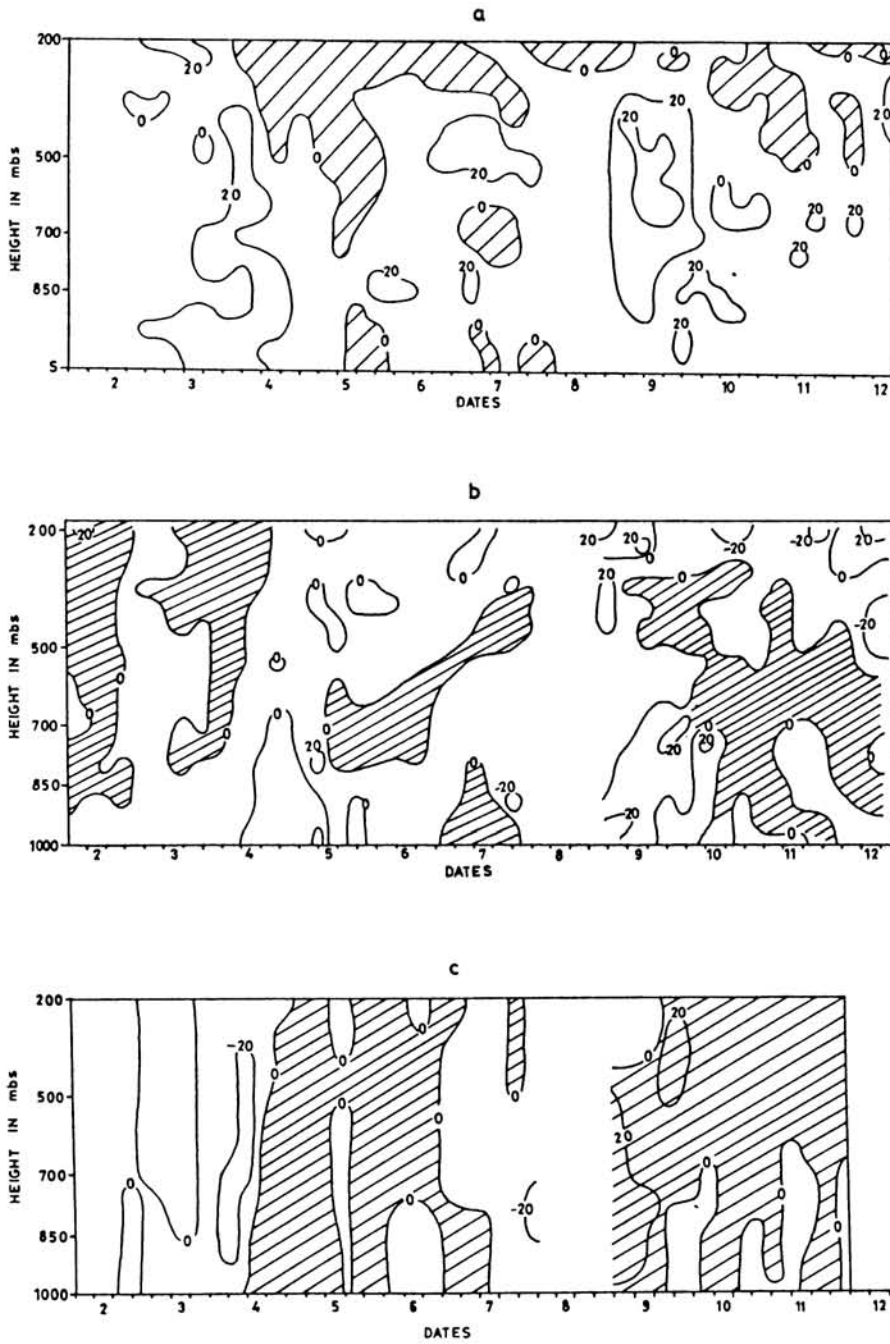


FIG.2.6(d) VERTICAL TIME SECTION OF (a) VORTICITY, (b) DIVERGENCE and (c) VERTICAL VELOCITY DURING PHASE-IV

noticed in the lower layers while it was divergence in the middle layer. It should be noted that, it was upper level convergence on all days except 2nd, 3rd and 4th June. Very high values of convergence were noticed at 00 GMT on the 9th from 650 to 300 mb level. In general one could not delineate the dominance of convergence or divergence during this phase.

Vertical Velocity

The whole phase was dominated by downward motion, except on 2nd, 3rd and 7th June and on these days upward motion was present almost all through the atmosphere. On certain days, like the 6th, 9th, 10th and 11th although not at all the synoptic hours, updrafts were present in the lower levels. On 3rd June at 18 GMT and on 4th at 00 and 06 GMTs, it was very high upward motions, from about 850 mb to 300 mb and within 12 hours, it suddenly changed to very high downward motions.

The synoptic situations reveal that this period was still a pre-onset phase. Although the vorticity pattern revealed good cyclonic conditions, this was not seen in the divergence and vertical velocity patterns.

A general comparison of the two years shows that 1977 was a better monsoon year than 1979. In June, when the

polygon positions were almost same, the synoptic situations were different. In 1977 June, the conditions were that of cyclonic situations, while in June 1979, there was predominance of downward motion, divergence, and low humidity. It should be remembered that, the period of study, during 1977, was monsoon onset time and that of 1979 was the pre-onset period. These conditions were more or less corroborated by the parameters discussed above.

CHAPTER - III

3.1 INTRODUCTION

Numerous investigators such as Sikka and Mathur (1965), Ananthakrishnan et al (1968), Findlater (1969a, 1969b), Krishnamurti and Bhalme (1969), Sikka (1980), Cadet (1981, 1983), Cadet and Reverdin (1981), have looked into the role of low level jet in transporting moisture from the Southern Hemisphere into the Arabian Sea and subsequently into the Indian subcontinent. It has been found (Howland and Sikdar 1983) that moisture flow over the Arabian Sea has a direct relationship with the deep convection over the sea and the spread of convective activity into the Indian continent during the south west monsoon.

A detailed knowledge of the changes in the three dimensional moisture field would be of extreme importance to monsoon forecasters. One way to examine this, is through the use of energy budget studies, which include heat and moisture budgets. The study of atmospheric moisture budget, which is dealt in this chapter, consist of sea surface evaporation and moisture divergence or convergence studies. Both these moisture mechanisms are related to the strength of the low level south-westerly flow over the west Indian Ocean area. Earlier studies [Pisharoty (1965), Saha (1970), Saha and Bavadekar (1973, 1977)] have been based on a

limited data sample and most of them excluded the flux of moisture above 400 mb level. Additionally many [Rao et al (1981), Sadharam (1987) and other] have computed moisture budgets over a monthly or weekly time scale. As already mentioned before, the purpose of this study is to have a look at the moisture budget estimates on a daily basis. The diurnal variation of the different parameters too have been studied.

3.2 EVAPORATION

The water vapour content of the atmosphere is maintained by evaporation from the oceans. Rao et al (1981), Ananthakrishnan et al (1984) and Sadharam and Rameshkumar (1988) are some of the many who have worked to find the role of evaporation from Indian Ocean on the Indian summer monsoon. As already described in the methodology section, the rate of evaporation from a water source exposed to the free air depends on the difference between the vapour pressures of the air and water. When cold dry air moves over a warmer water surface, evaporation becomes very large. The warm temperature of the water favours evaporation, while the air motions rapidly carry the water vapour aloft.

Distribution of evaporation diurnal and daily were studied and are presented in the next two sections. Evaporation values were positive indicating that the average sea

surface temperatures were always higher than the air temperatures and the rates were of the order of 10^7 Kg/Sec.

3.2.1 Day-to-day variations

Figs. 3.1(a) to 3.1(d) show the daily variations of rate of evaporation over the polygon areas at the four different synoptic hours during the Phases-I to IV respectively.

PHASE-I

The evaporation rates were highest in the first few days of this phase. This could have been due to the high wind associated with the low pressure system during this time. It was a minimum around the middle of the phase and a secondary maxima in the last part. The rates were highest on 9th June and lowest on 14th June at 06 GMT, and there was generally a decrease from the 9th to 14th and increase thereafter upto the 17th at all the timings. At 00 and 18 GMTs, it decreased from 17th to 18th and thereafter increased upto 19th. It was the reverse pattern at the other two timings. The variations were comparatively less at 12 GMT. The values in this phase ranged between 1.5 and 4.5×10^7 Kg/sec.

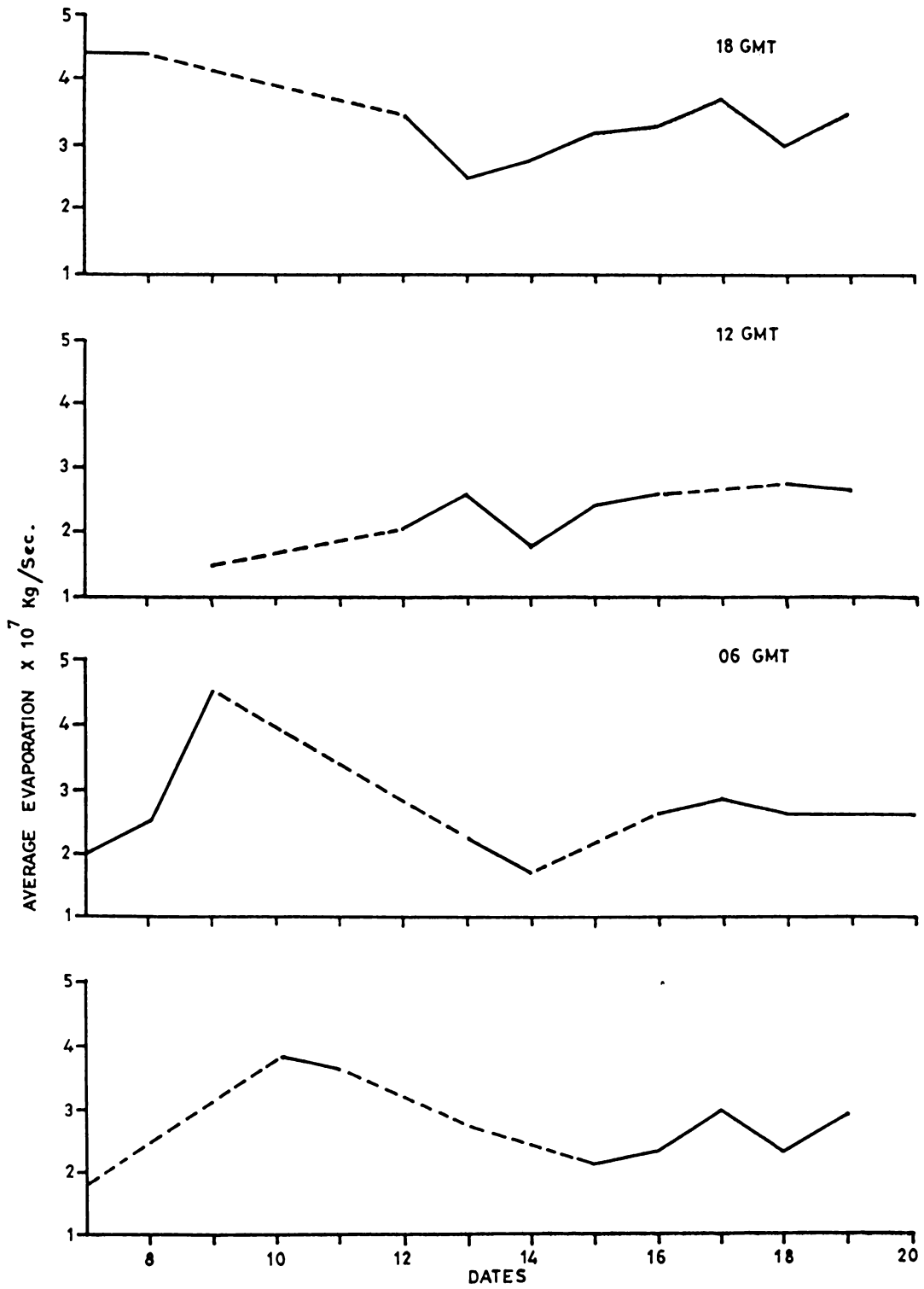


FIG.3.1(a) DAY TO DAY VARIATIONS OF RATE OF EVAPORATION FOR PHASE-I

PHASE-II

The day-to-day variations were insignificant and the values remained around 2×10^7 kg/sec during the whole phase. The values were slightly higher between 3rd and 10th July at 00, 06 and 12 GMTs, whereas at 18 GMT higher values were observed from 2nd to 8th. At all the timings evaporation was highest on 7th and lowest on 12th of July at 00 and 12 GMTs respectively.

PHASE-III

Evaporation values were lower than the previous two phases on almost all the days. At 00, 06 and 18 GMTs although the values did not differ significantly, it was an increase from 17th to 26th May and thereafter decrease upto the 29th at 00 GMT, while, at 18 GMT the increase was only upto 24th and at 06 GMT there were both decrease and increase during this period. At 12 GMT, evaporation rates decreased from 17th to 20th and 25th to 27th May. After the 27th, there was an increasing trend.

PHASE-IV

At 00 GMT, the evaporation increased from the 2nd to 9th and 10th to 12th of June and in between it decreased. At 06 and 12 GMTs, the variations were similar, with increase from the 2nd to 5th, and the 6th to 7th, while there was

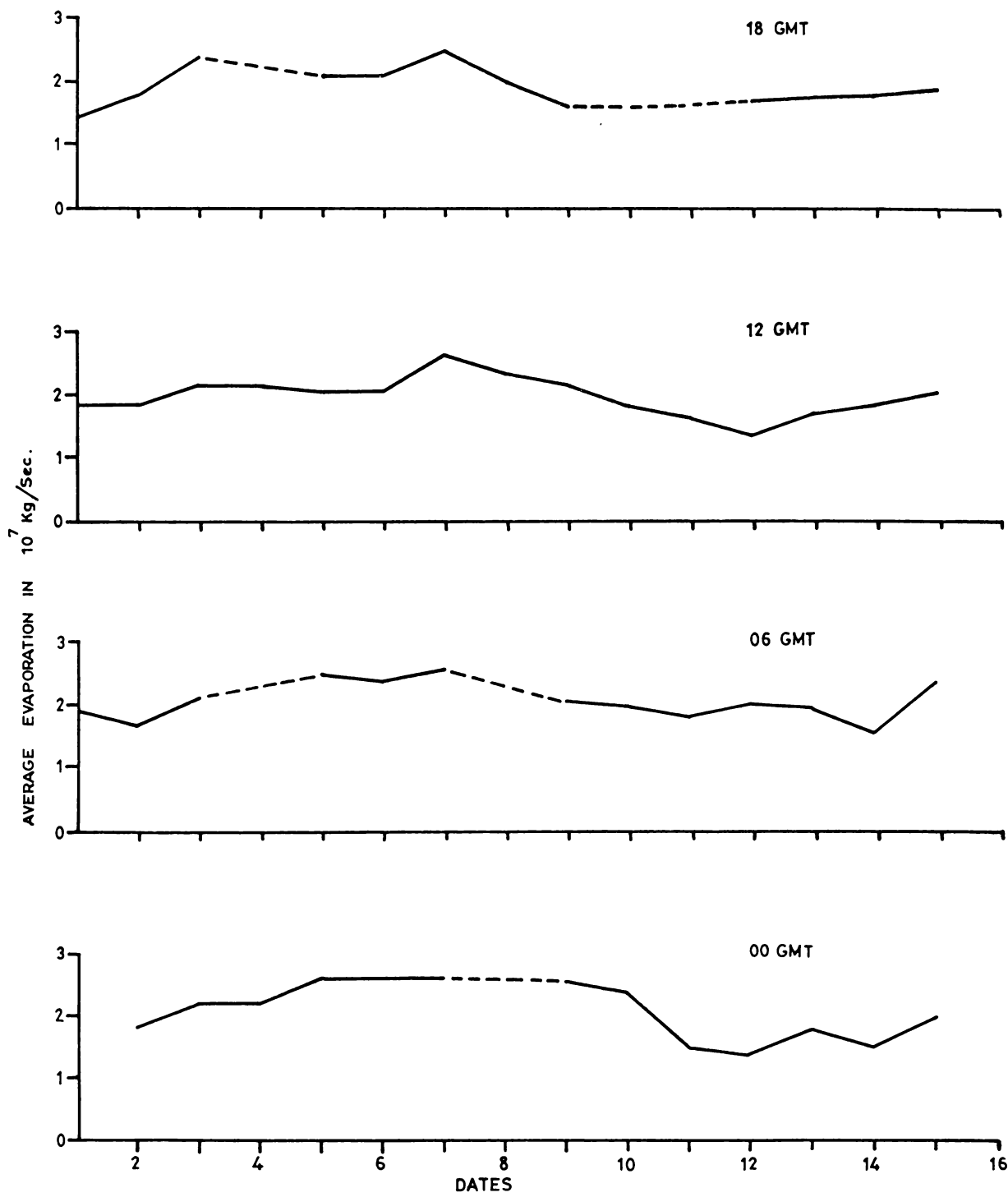


FIG.3.1(b) DAY TO DAY VARIATIONS OF RATE OF EVAPORATION FOR PHASE-II

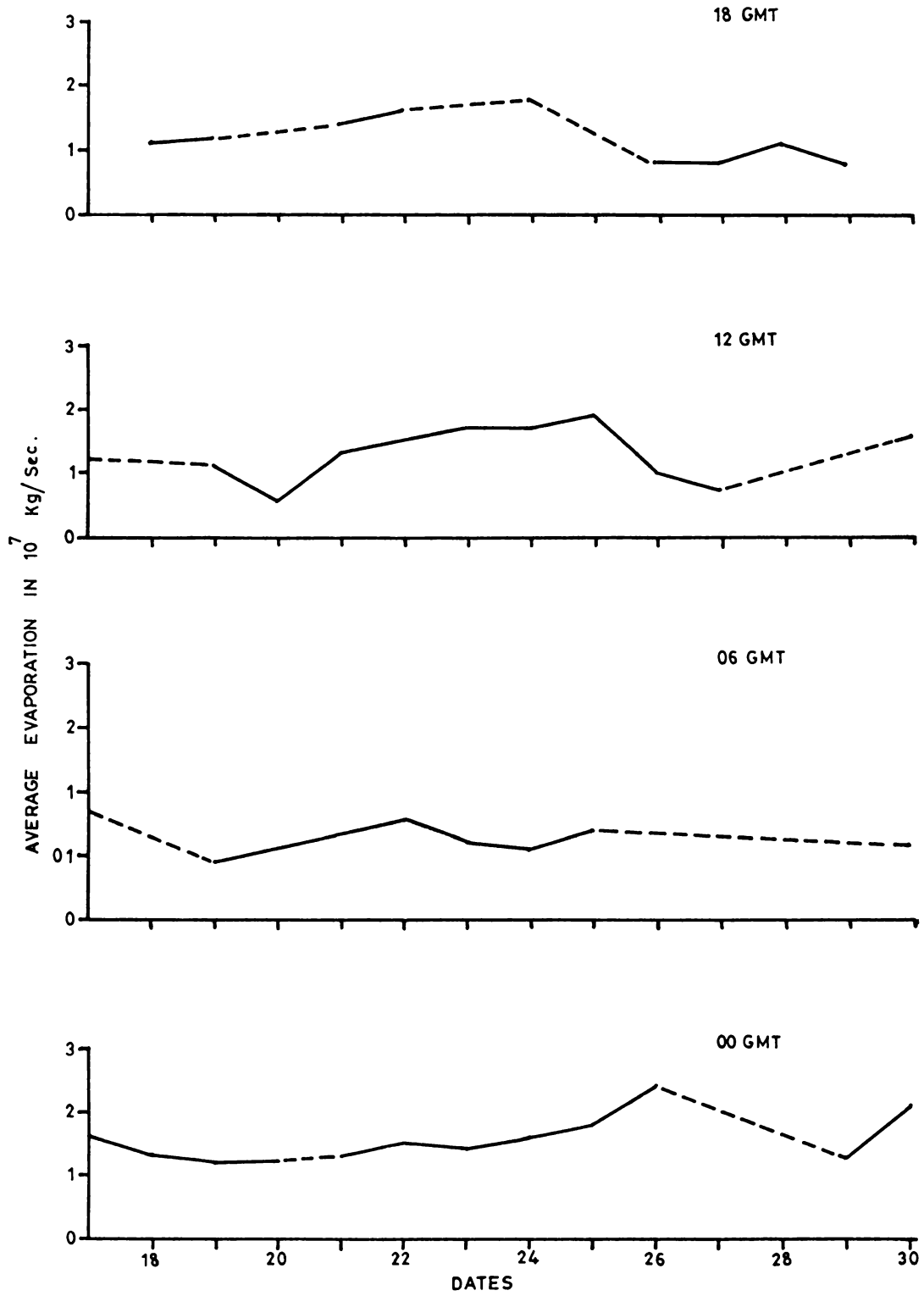


FIG.3.1(c) DAY TO DAY VARIATIONS OF RATE OF EVAPORATION FOR PHASE-III

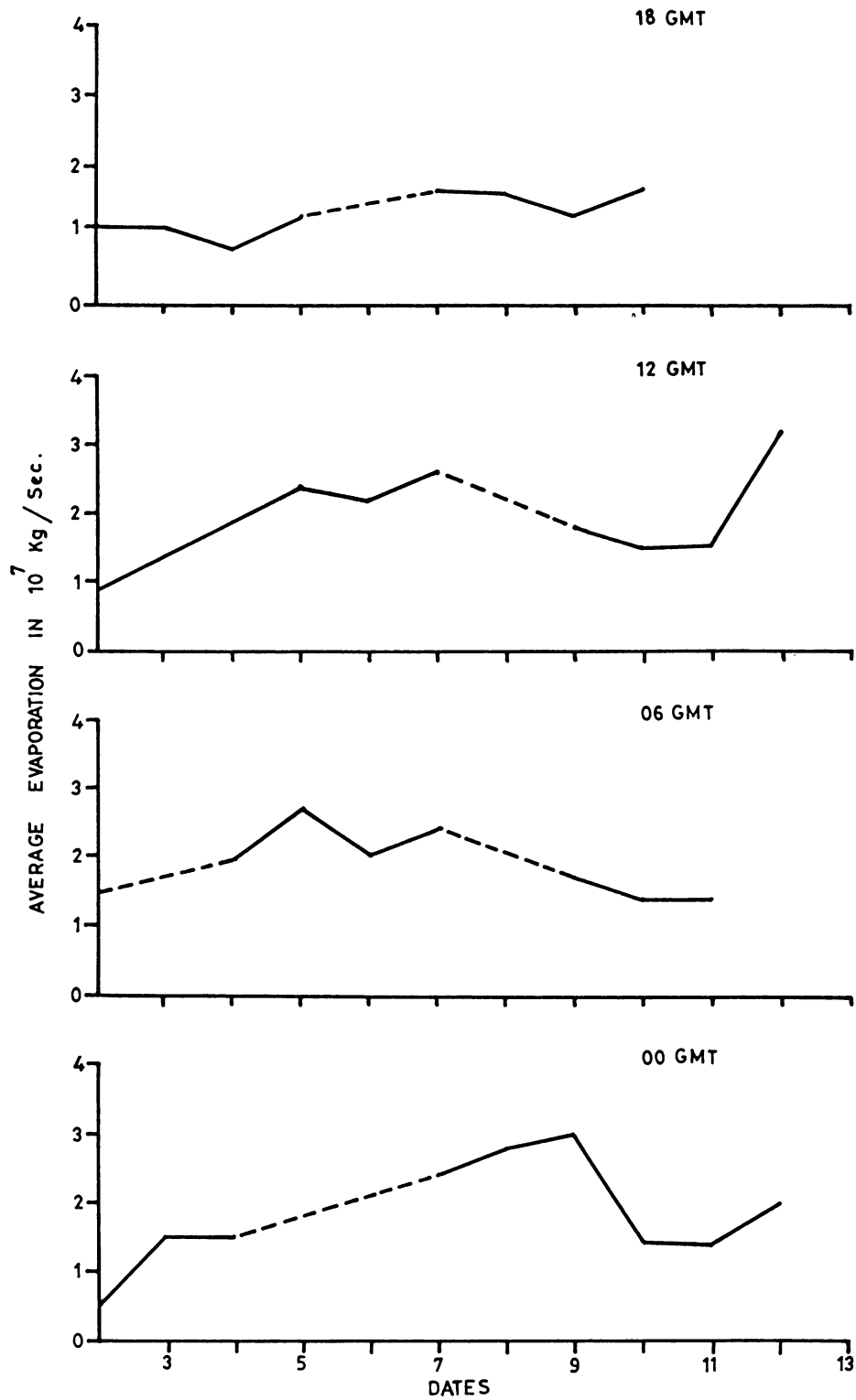


FIG.3.1(d) DAY TO DAY VARIATIONS OF RATE OF EVAPORATION FOR PHASE-IV

decrease from the 5th to 6th and from the 7th to the end of the phase. At 18 GMT, the variations were quite insignificant. The values were comparatively higher at 00 GMT on 9th, 06 GMT on 5th, and 12 GMT on 12th of June. At all the timings, except 18 GMT, the minimum value was on 2nd, and at 18 GMT when it was on 4th.

3.2.2 Diurnal Variation

Fig.3.2 gives some typical patterns of diurnal variations of evaporation over the four phases. Evaporation did not show a marked diurnal variation, although on certain days 13th June 77, 30th May 79 and 9th June 79, there were changes of around 1×10^7 Kg/Sec in a time period of six hours.

On a few days (nine out of thirty) the values showed alternate decrease and increase and on others it was a steady increase or decrease throughout. In Phase-I, except on 13th June, the variations were insignificant, but the values were generally higher than that in the other Phases. Particularly high values were obtained on 7th and 8th June 1977. This might have been due to the high winds prevailing during that period due to the low pressure system. During Phase-II generally it was decreasing from 00 to 18 GMT except on 3rd and 14th July. It was almost a reverse pattern

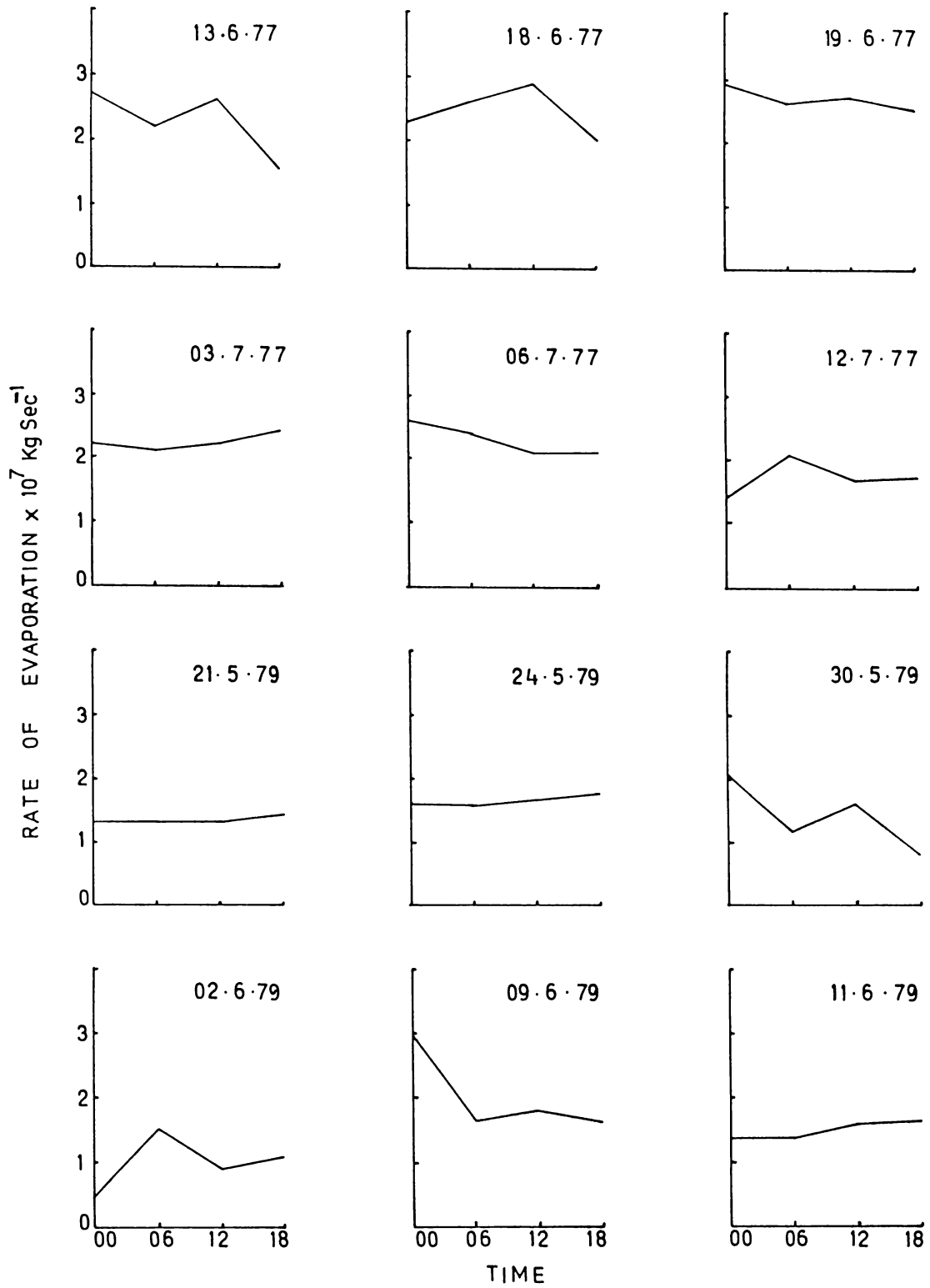


FIG.3.2 DIURNAL VARIATION OF RATE OF EVAPORATION FOR THE FOUR PHASES

in Phase-III with exceptions on 26th and 30th. Phase-IV was a period of good diurnal variation with alternate decrease and increase. The values were also higher in the latter part of the phase. It was seen that, on almost all the days of study, evaporation decreased from 12 to 18 GMT. Except in the second phase, the values at 12 GMT were higher than that at 00 GMT.

3.2.3 Average Surface evaporation

Average surface evaporation is obtained as the product of mean evaporation from the four synoptic hours and the area of the polygon. Fig. 3.3 shows the day-to-day variations of the same. During Phase-I, the values increased from 7th to 9th and decreased from 9th to 14th of June. From the 14th onwards it increased upto the 20th. Maximum evaporation was noted on 9th and minimum on 14th. In Phase-II also, there was alternate decrease and increase, but the values did not vary much in magnitude. The values were comparatively higher on 7th and 15th July. During Phase-III, there was a decrease from the 17th to 20th and 25th to 28th May. Evaporation was high on the 22nd, 25th and 29th with maximum on the 25th. Phase -IV was a period of good day to day variations. There was a remarkable increase in values from 2nd to 5th and 10th to 12th of June 1979. During the intermediate period, the values did not vary much.

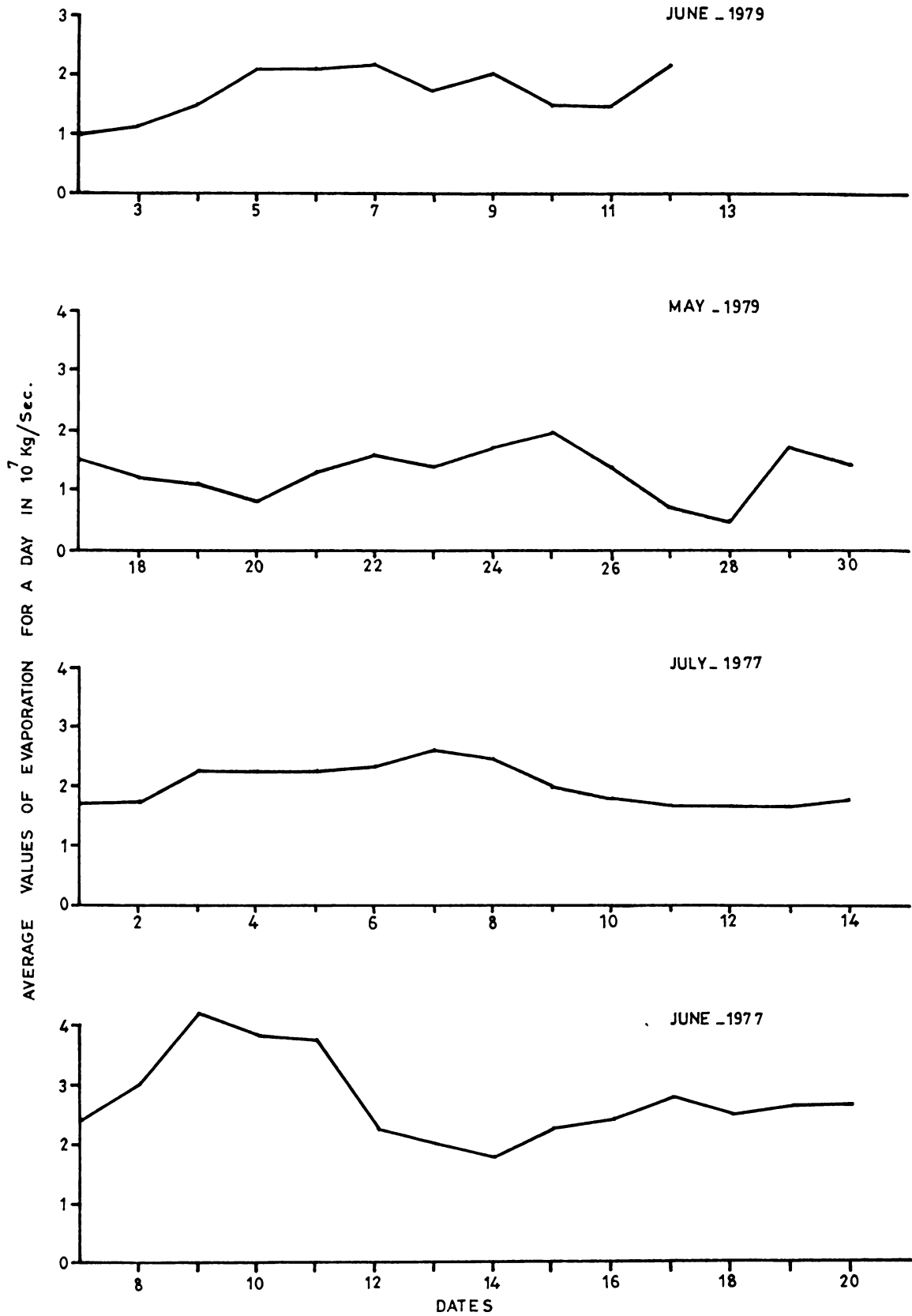


FIG.3.3 DAY TO DAY VARIATIONS OF AVERAGE EVAPORATION DURING THE FOUR PHASES

3.3 MOISTURE FLUX

As already explained in section 1.5, moisture flux for the entire column of atmosphere from surface to 200 mb above the ship positions were obtained by step wise integration of the product of the specific humidity and the normal component of wind at that point. This was then multiplied with the length of the wall (1) to get this value for the whole length of the wall and is discussed below.

3.3.1 Day-to-day variations

Figs. 3.4 (a) to 3.4 (d) show the daily variations of the sum of flux of moisture from surface to 200mb, for the four different timings at the four boundaries and at the polygon positions 1 to 4 respectively.

PHASE-I

During the first few days, (7th to 10th June) at 00, 06 and 18 GMTs the flux gradually increased, but from 10th June onwards, decreased upto the 14th at the west and east walls. It subsequently increased upto the 19th June. The Moisture flux variations at the west and east walls were almost opposite to that at the other two walls. Data was not available for 12 GMT upto 12th of June.

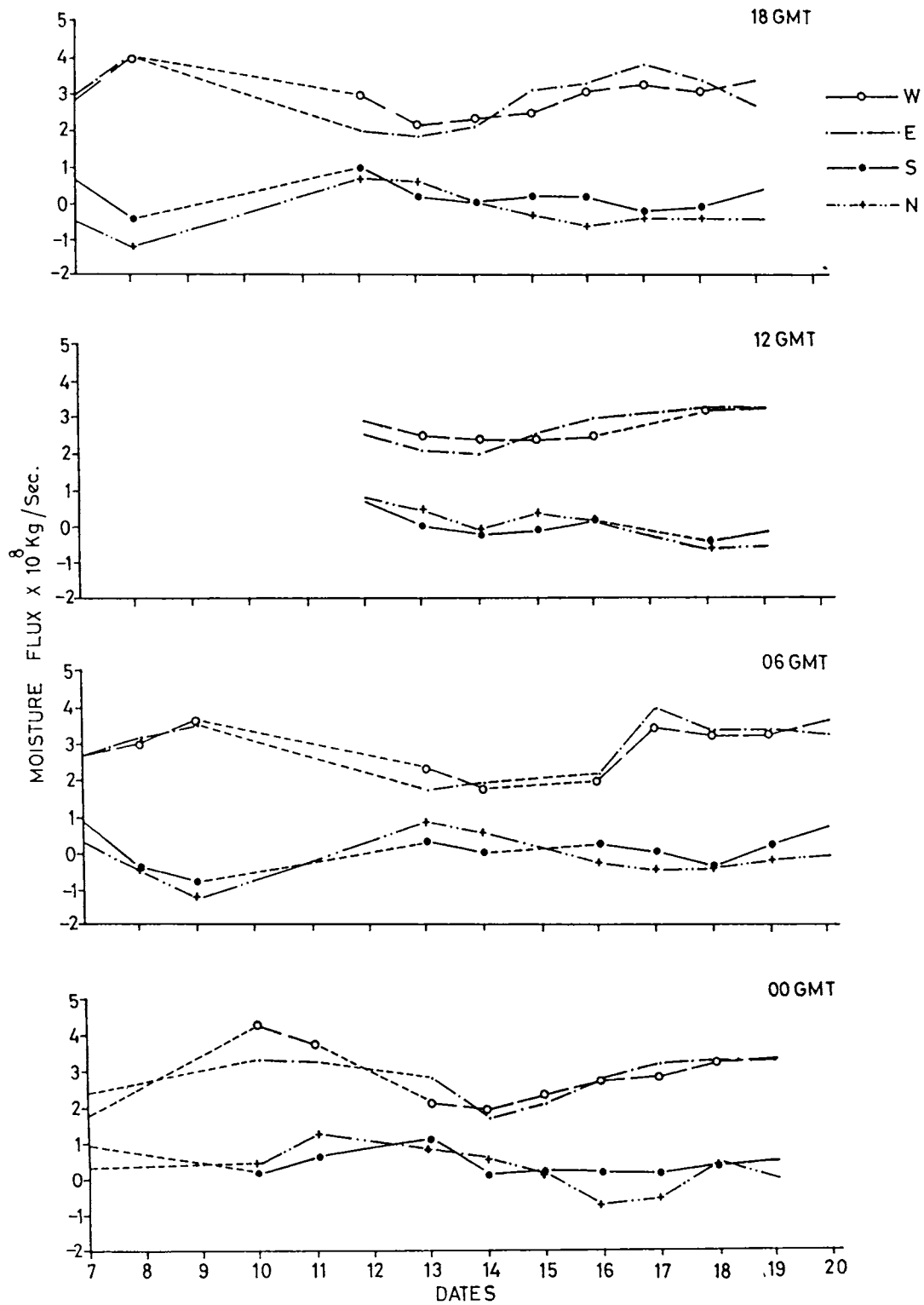


FIG.3.4(a) DAY TO DAY VARIATIONS OF SUM OF MOISTURE FLUX FROM SURFACE TO 200 mbs DURING PHASE-I

PHASE-II

In general, the daily variations were low at all the four walls but comparatively higher at the east and north walls. For all the synoptic hours, the moisture fluxes were higher at the zonal walls than that at the meridional walls. There were practically no negative values during the whole period. At the east and west walls at all the four synoptic hours, the values were high on 7th July.

PHASE-III

During this phase, the values as well as variations were significant only from 21st to 27th May at all the walls. The values were almost always negative at the north and south walls and positive at the other two. This would mean that the net moisture flux converged into the area is very less or would have been divergence. There were comparatively higher values at the south and west walls and the variations were opposite at the opposite walls.

PHASE-IV

This phase showed more variations at all the synoptic hours than the previous two periods and was characterised by alternate high and low values, with the largest variations at the southern wall. There were high negative as well as positive values during this Phase.

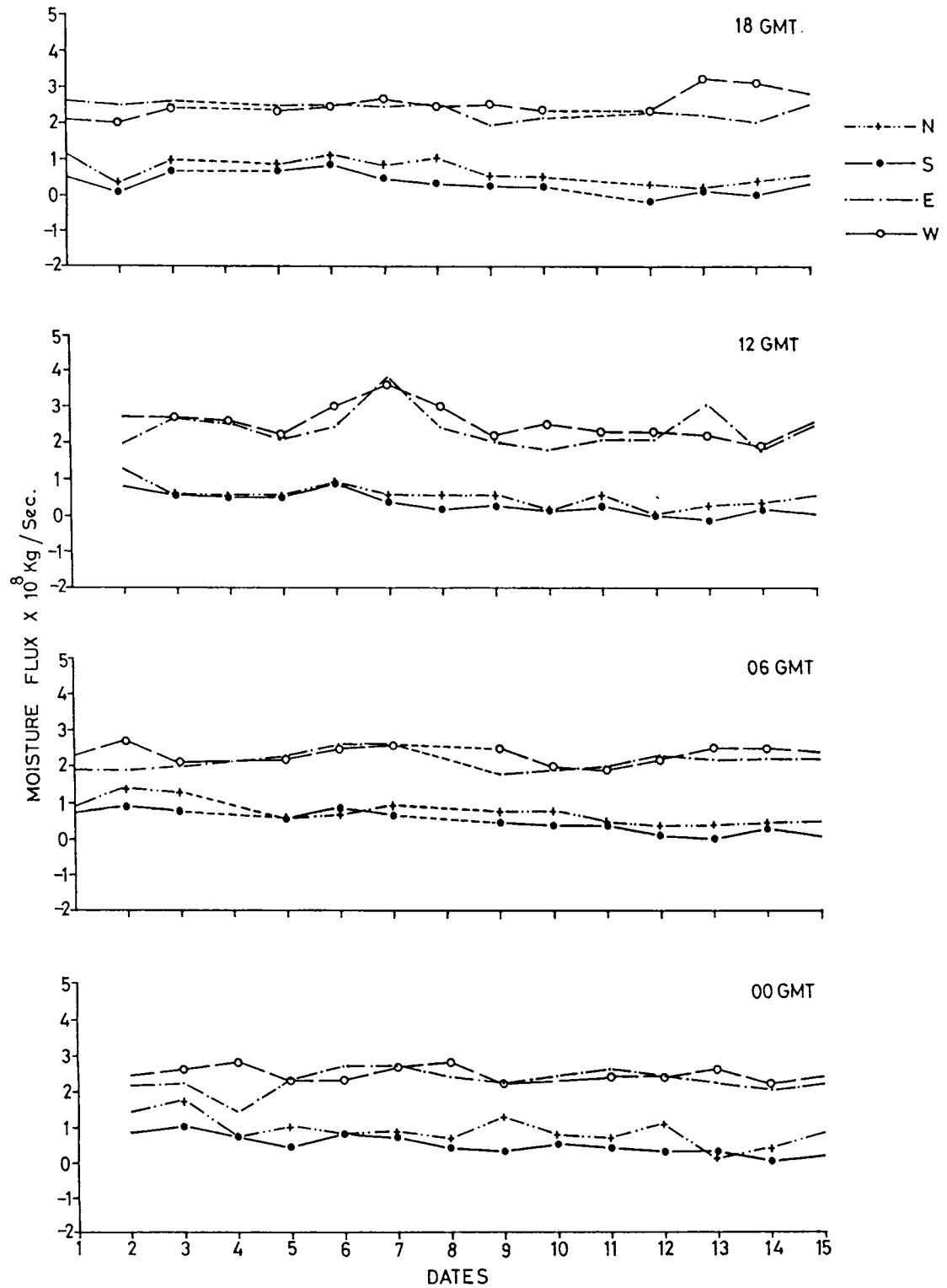


FIG.3.4.(b) DAY TO DAY VARIATIONS OF SUM OF MOISTURE FLUX FROM SURFACE TO 200 mbs DURING PHASE-II

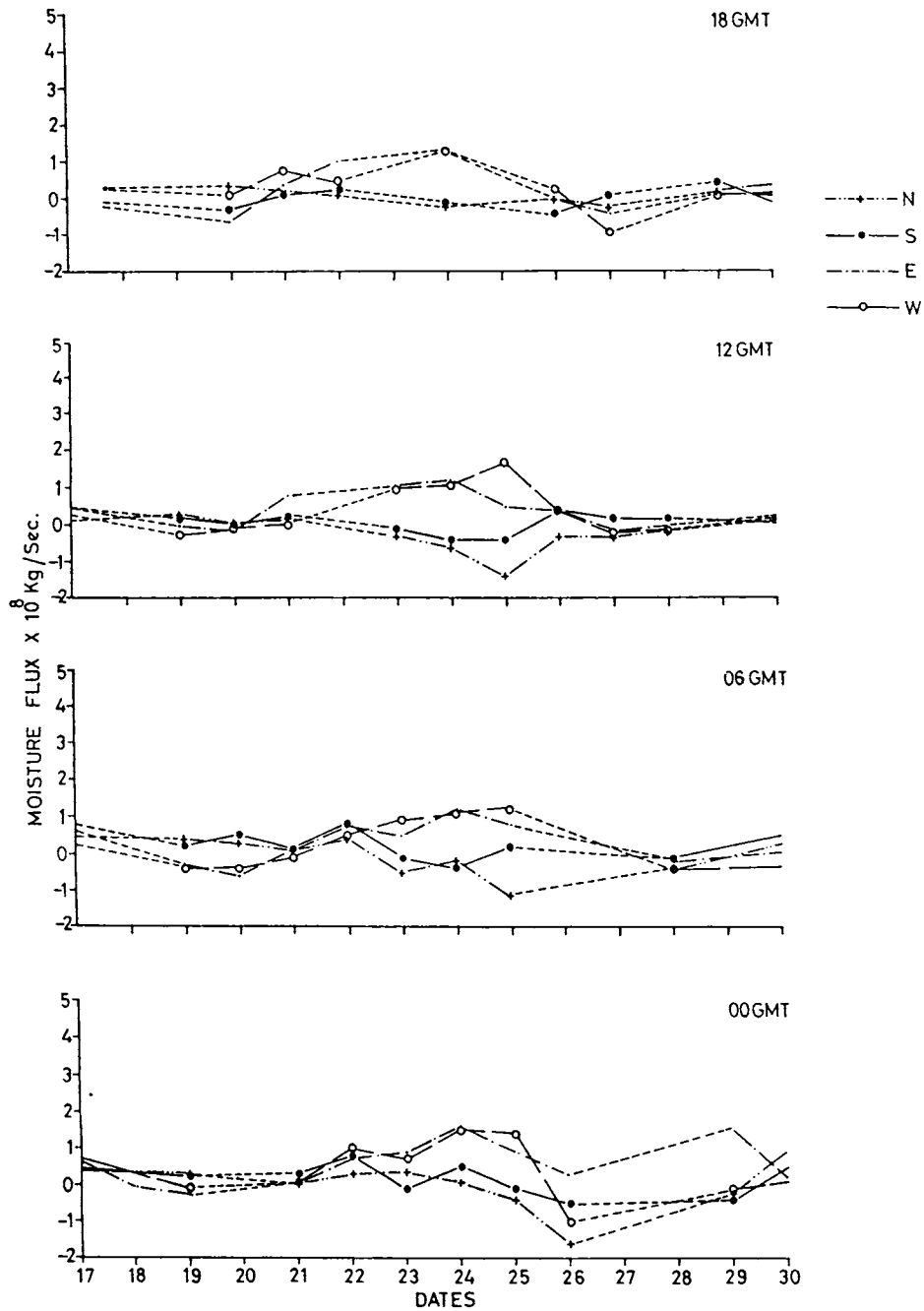


FIG.3.4.(c) DAY TO DAY VARIATIONS OF SUM OF MOISTURE FLUX FROM SURFACE TO 200 mbs DURING PHASE-III

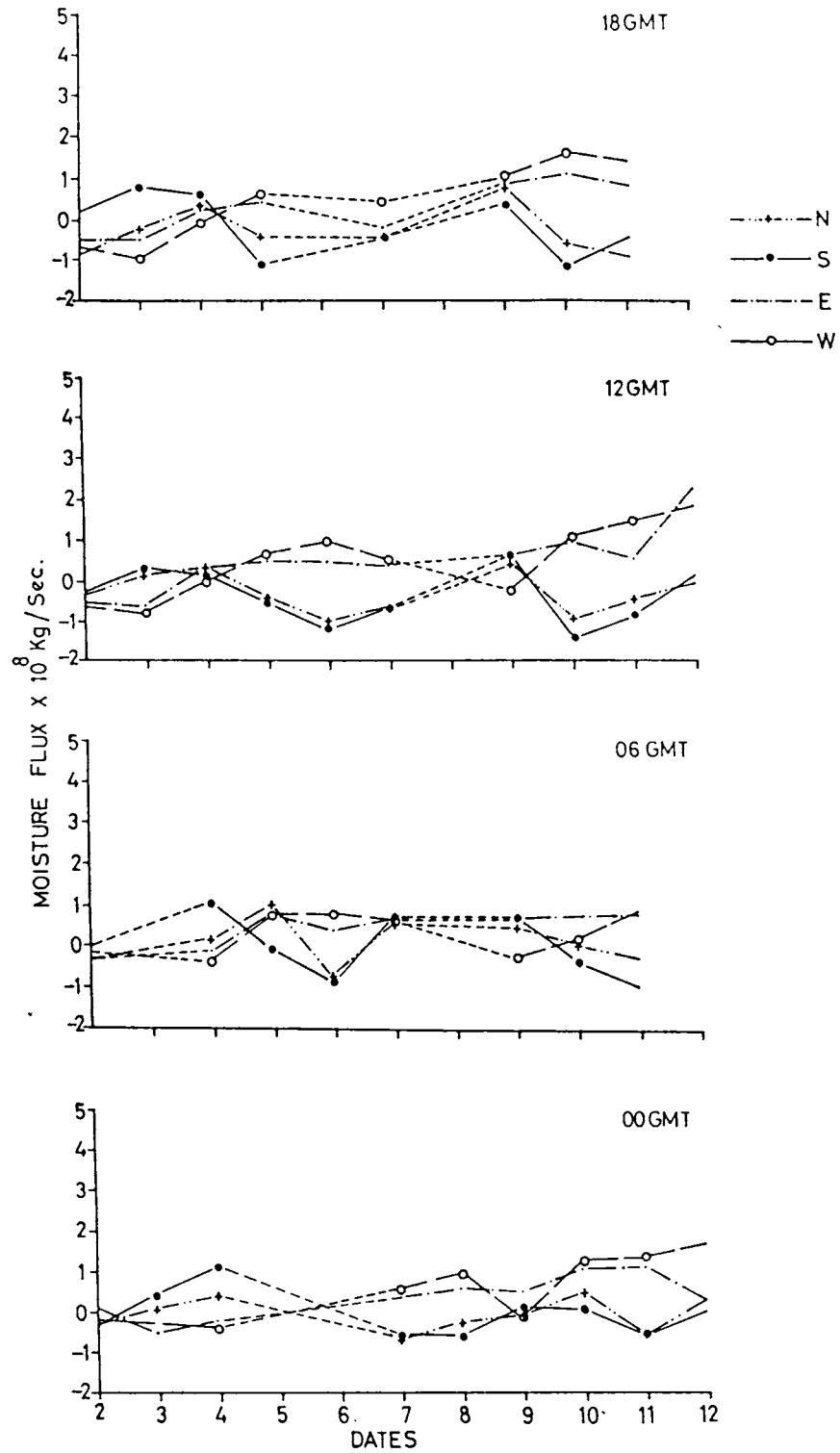


FIG.3.4(d) DAY TO DAY VARIATIONS OF SUM OF MOISTURE FLUX FROM SURFACE TO 200 mbs DURING PHASE-IV

In all the periods discussed above, the variations were opposite at the meridional walls and zonal walls. It was almost always positive flux at the meridional walls, while it fluctuated from positive to negative at the other two. It should be remembered here that the signs of these fluxes are determined by the direction of the wind prevailing during that time. To have a better insight into the vertical variation of these fluxes, the daily means of moisture fluxes were computed from surface to 700 mb (3.1 Kms) and from 700 to 200 mb separately.

Figs.3.5(a) to 3.5(d) exhibit the pattern of variation of sum of Moisture flux from surface to 700mb for the four periods. The values although lower in magnitude, were of the same order as that above.

PHASE-I

It can be seen that the variations were more in the first part of this phase. The variations were similar to the vertical variations computed from surface to 200 mb at the opposite walls. But the daily values were rather high at the eastern wall, which means that, there was net moisture influx through the zonal walls. Moisture flux increased from the 7th to 11th and from 14th to 17th June at the zonal walls. It decreased from 11th to 14th June and from 17th to the end of the period at the east wall while it was the

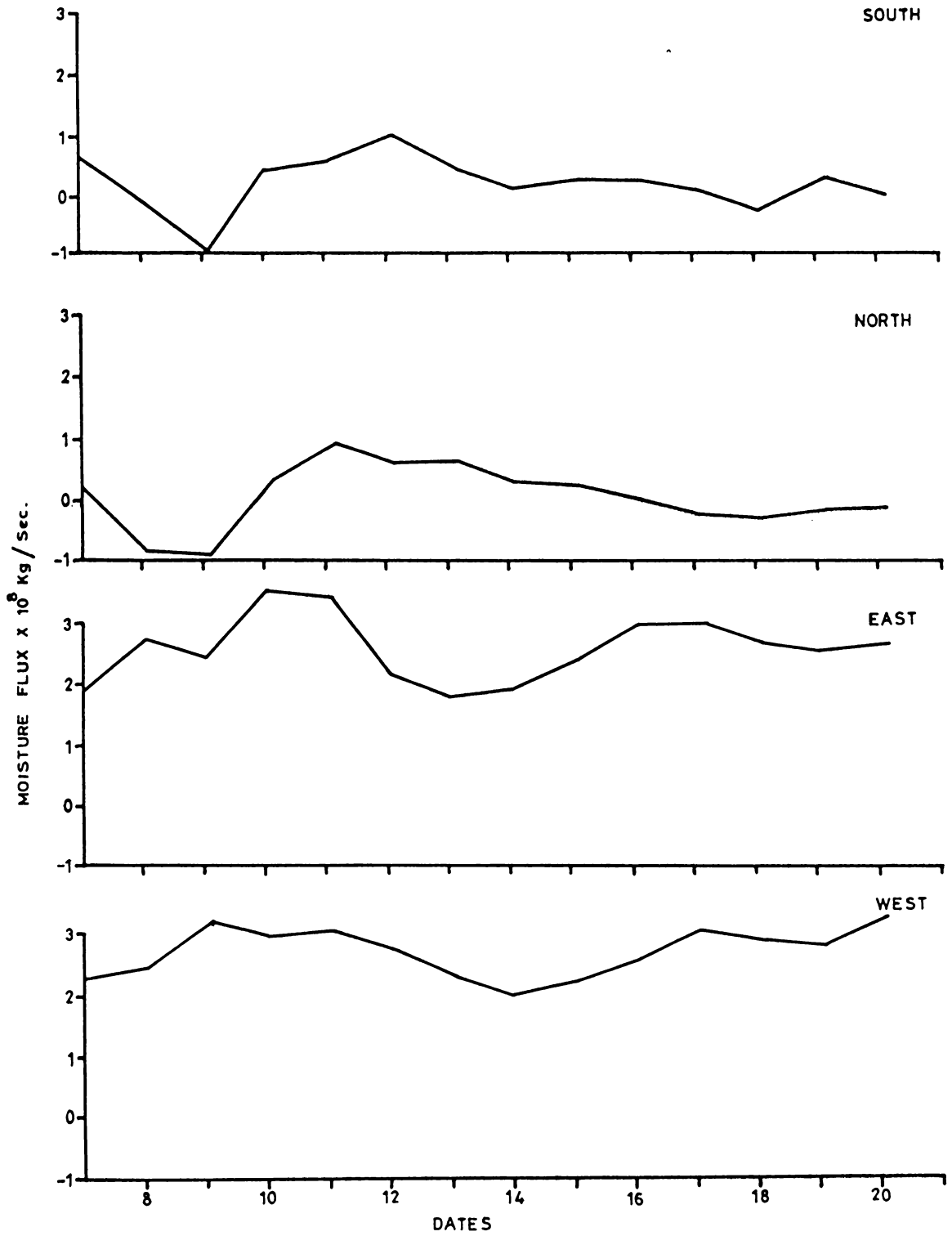


FIG.3.5(a) DAY TO DAY VARIATIONS OF SUM OF MOISTURE FLUX FROM SURFACE TO 700 mbs DURING PHASE-I

reverse at the west. The values were always positive at the zonal walls and both positive and negative at the meridionals.

PHASE-II

During this period, moisture flux variations were less and the values always positive at all the four walls. This would mean that the winds were southwesterlies. Most of the time, the values at the meridional walls were higher than that at the zonal walls.

PHASE-III

Except at the southern wall, (with always positive values) moisture flux variations were significant at all the other three walls with the values swinging from positive to negative and viceversa. Flux decreased from 17th to 20th May at the zonal and southern walls, while it remained almost constant at the north wall. At the zonal walls, it then increased upto the 25th and thereafter showed a decreasing trend. At the north wall, it decreased from the 22nd to 25th and thereafter increased upto 30th May.

PHASE-IV

At the west and east walls, there was an initial decrease followed by a slow increase almost upto the end of

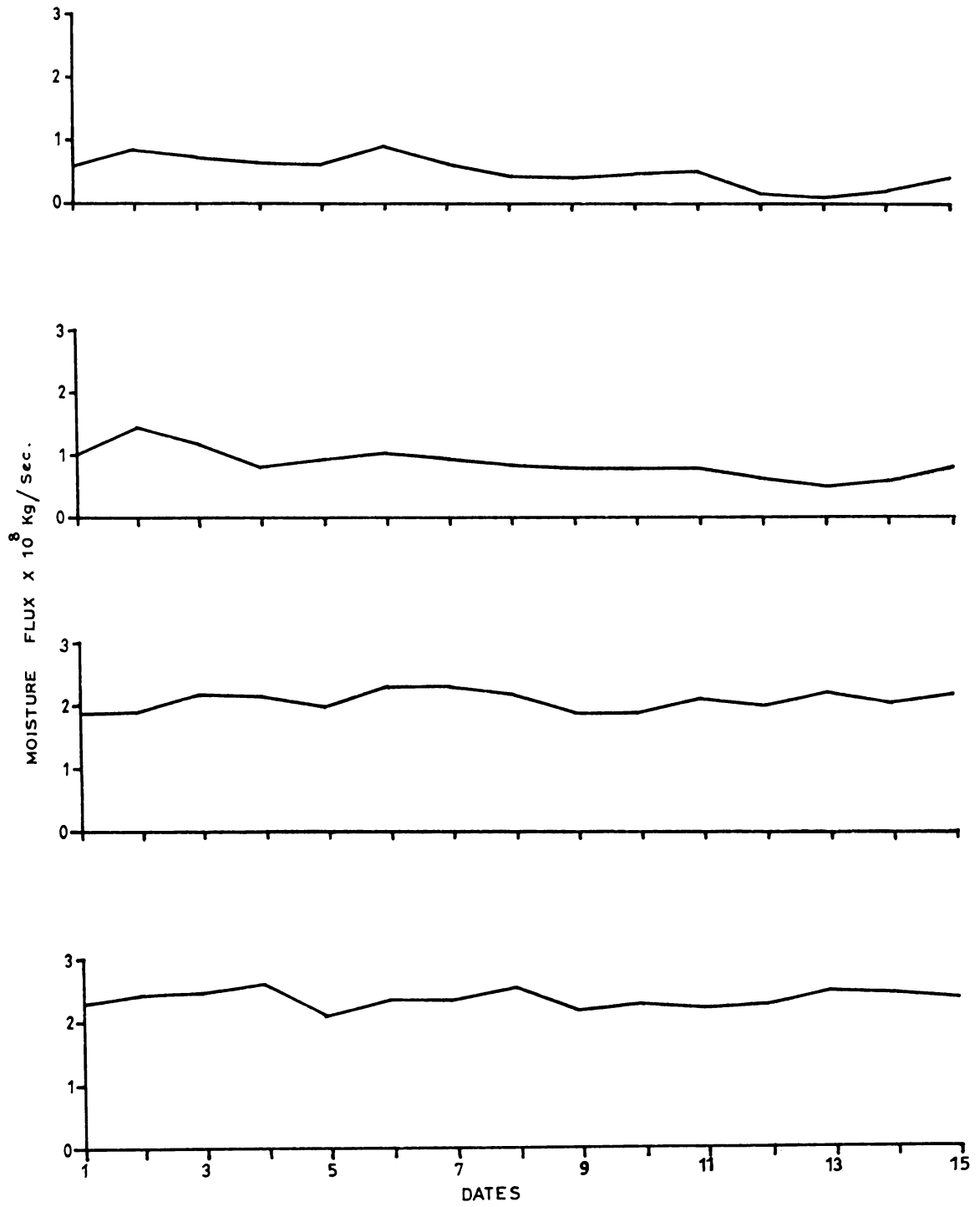


FIG.3.5(b) DAY TO DAY VARIATIONS OF SUM OF MOISTURE FLUX FROM SURFACE TO 700 mbs DURING PHASE-II

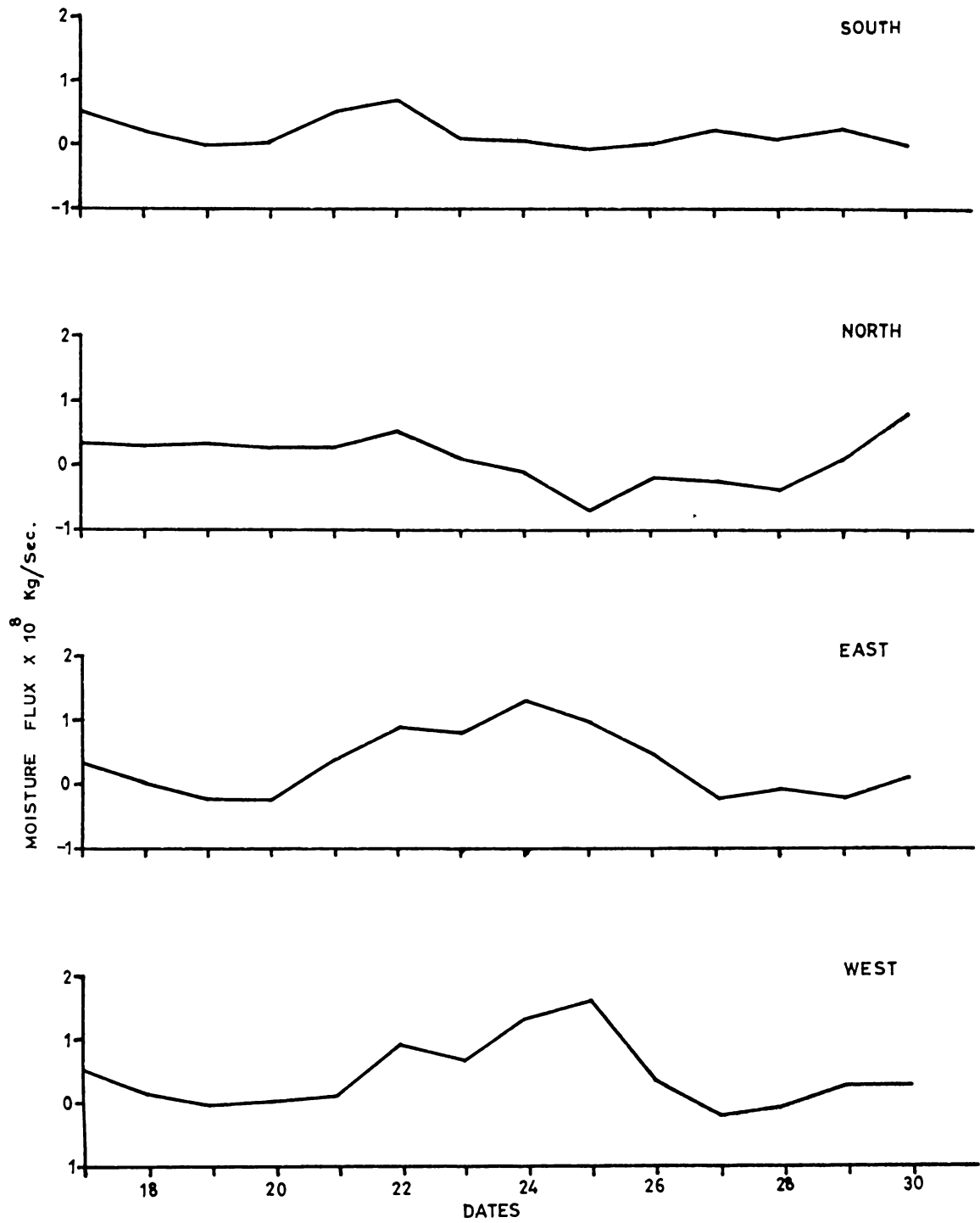


FIG.3.5(c) DAY TO DAY VARIATIONS OF SUM OF MOISTURE FLUX FROM SURFACE TO 700 mbs DURING PHASE-III

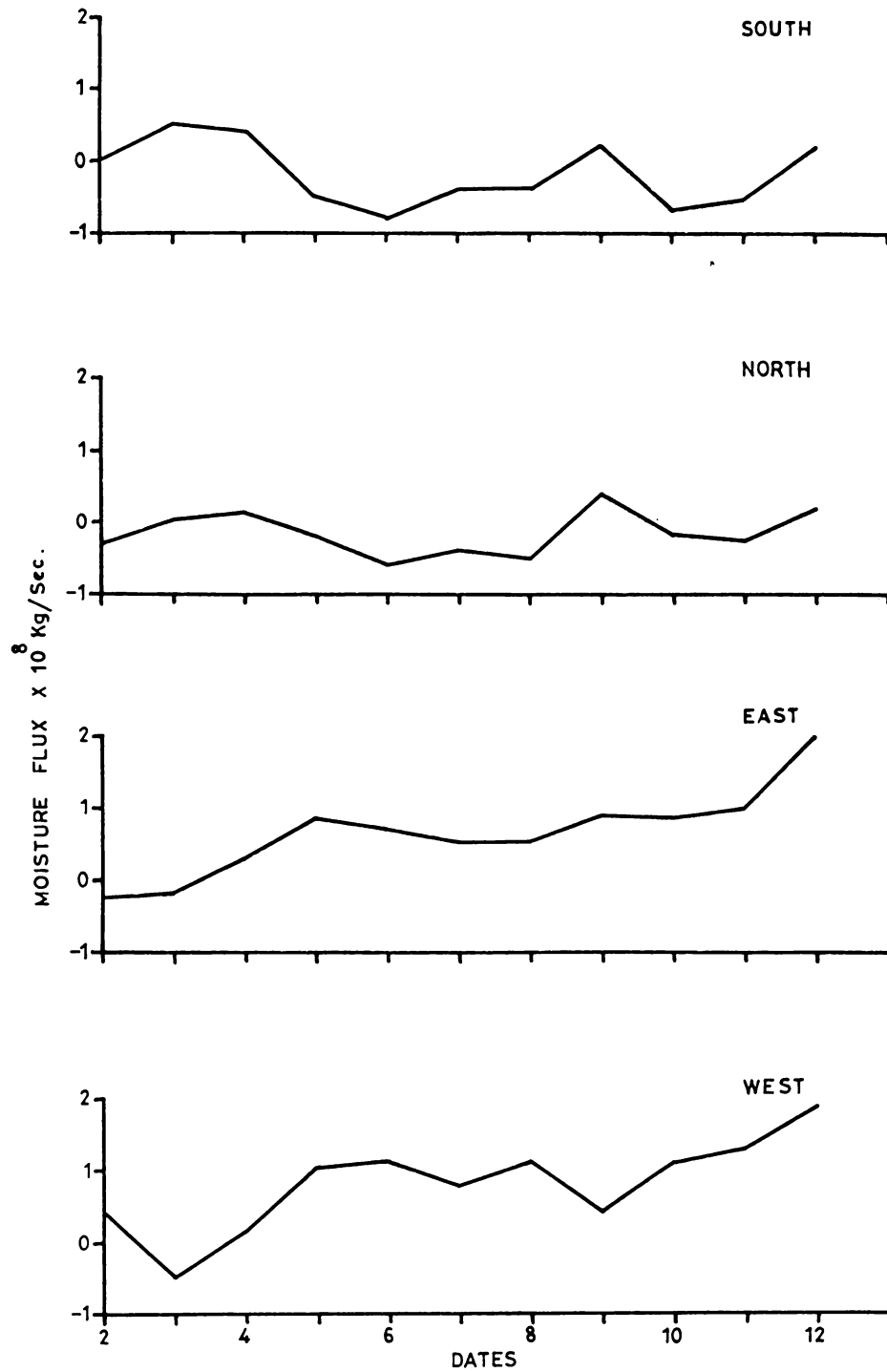


FIG.3.5(d) DAY TO DAY VARIATIONS OF SUM OF MOISTURE FLUX FROM SURFACE TO 700 mbs DURING PHASE-IV

the period and the values were always positive after 3rd June. Unlike the zonal walls, meridional walls showed a wavy pattern with the flux values fluctuating from positive to negative values.

The Figs. 3.6(a) to 3.6(d) show the daily variation of the sum of moisture flux from 700 to 200 mb. at the different walls for the Phases-I to IV respectively. It should be noted that the values are almost always one order less than that of sum from surface to 200 mb except in Phase-I. Hence, it is inferred that the maximum moisture transport was confined to the first three kilometers of the atmosphere. The variations also were very insignificant.

PHASE-I

Variations of the fluxes during this period were almost similar to that observed in the lower layer but with less magnitudes. At the zonal walls, the flux values were positive as well as negative. The moisture flux was higher at the beginning and end of the phase, especially at the zonal walls. This could be due to the high winds and lot of mixing because of the low pressure system present during that period.

PHASE-II

At all the four walls, the moisture fluxes were very

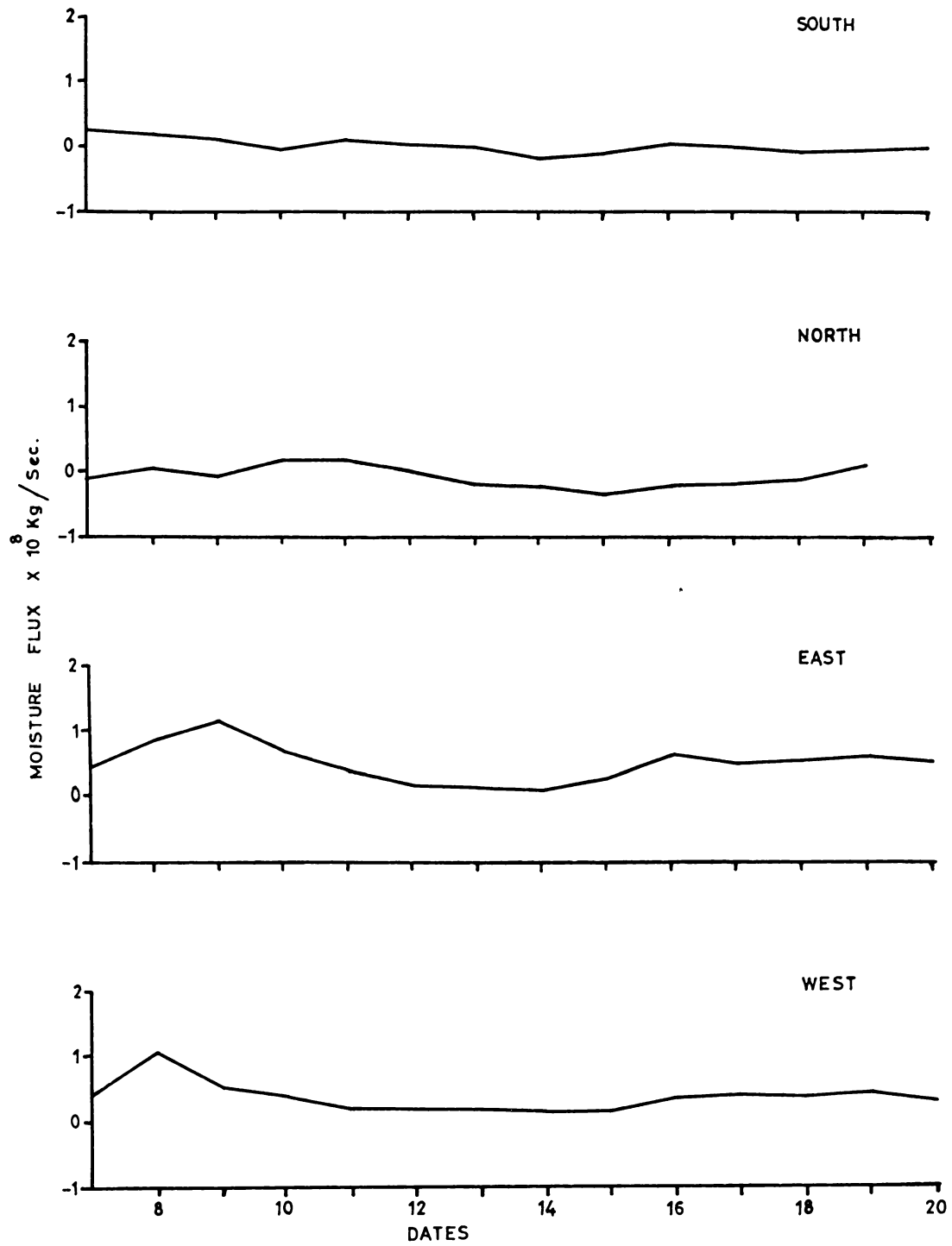


FIG.3.6(a) DAY TO DAY VARIATIONS OF SUM OF MOISTURE FLUX FROM 700 TO 200 mbs DURING PHASE-I

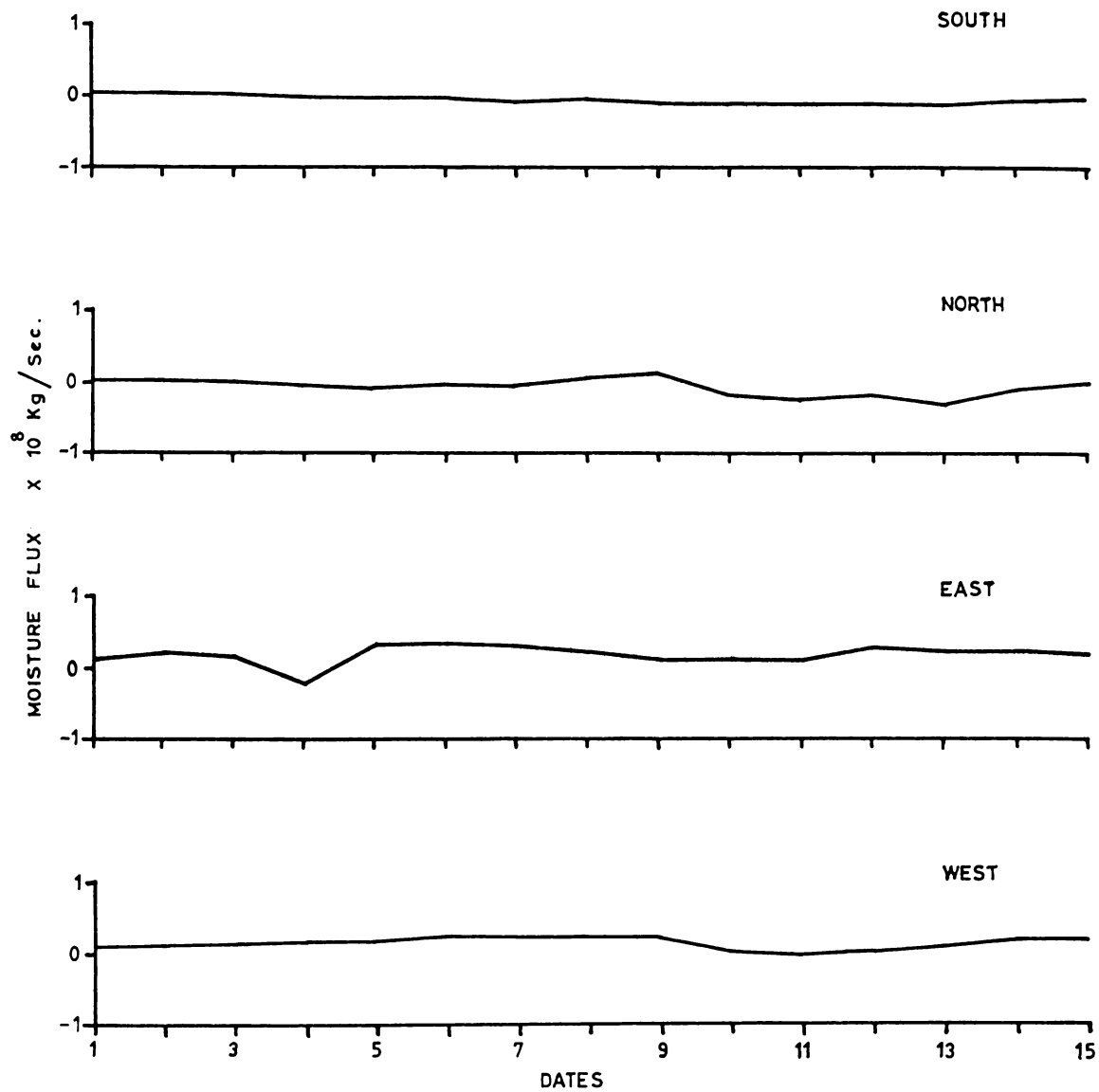


FIG.3.6(b) DAY TO DAY VARIATIONS OF SUM OF MOISTURE FLUX FROM 700 TO 200 mbs DURING PHASE-II

low. There were more negative values than positive at all the four walls and at the west wall, it was always negative.

PHASE-III

In this phase also the values were very low and there were more negative values at all the four walls and at the west wall, it was always negative.

PHASE-IV

The flux was almost always negative at the four walls, during the first part of this phase. From the 2nd upto about 8th June and thereafter it was positive at the western wall. At the eastern wall, except on 10th, it was inflow (negative) all through and at the north and south walls, both outflow and inflow of moisture flux were observed.

To get an actual picture of the accumulation (convergence) or depletion (divergence) of moisture into or from the area of study, the net moisture flux was studied and is presented in the section 3.4.

3.3.2 Diurnal Variation

Diurnal variation of moisture flux at all the four walls on all the days had been studied but figures for typical variations are only presented. It did not exhibit

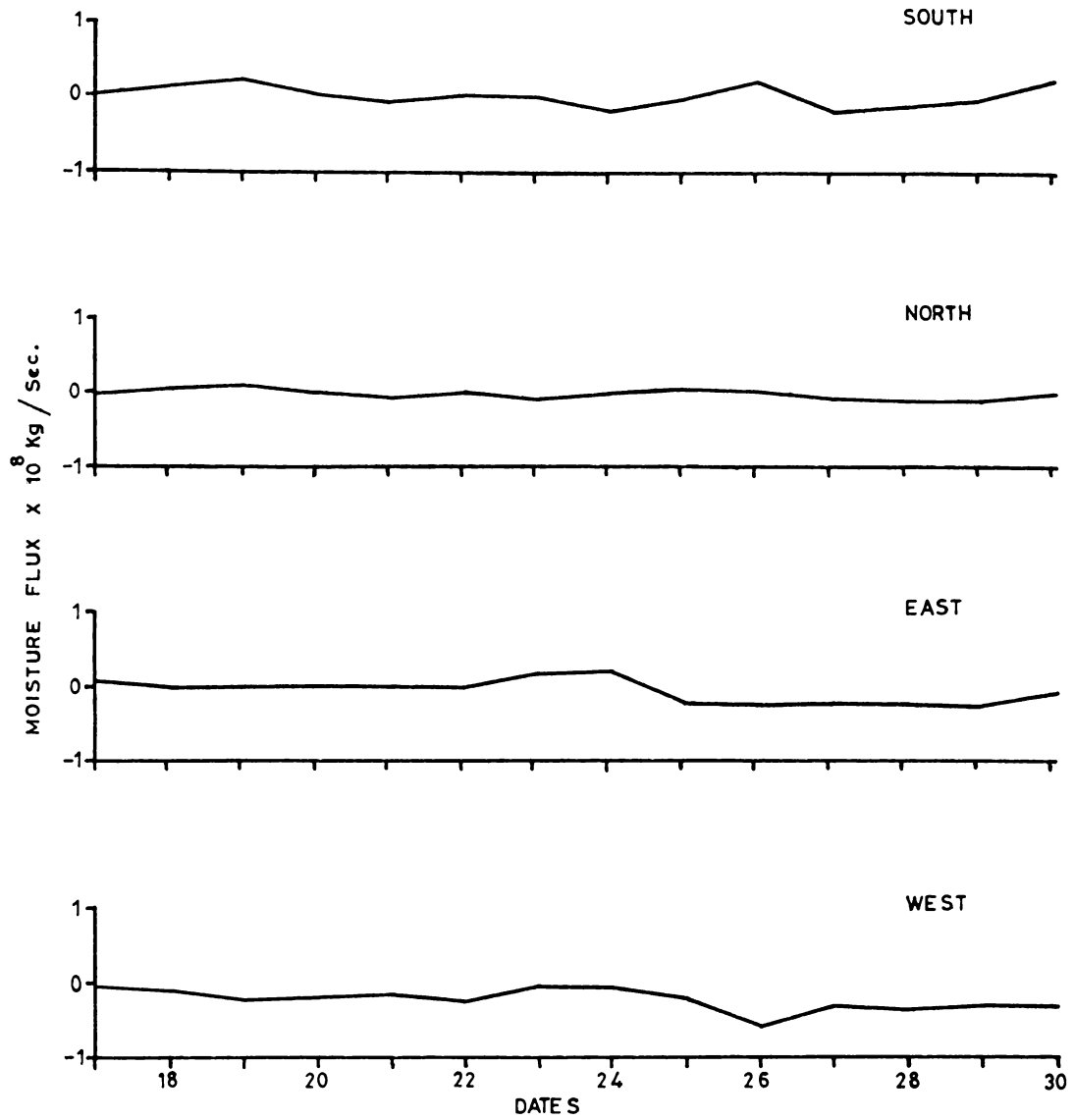


FIG.3.6(c) DAY TO DAY VARIATIONS OF SUM OF MOISTURE FLUX FROM 700 TO 200 mbs DURING PHASE-III

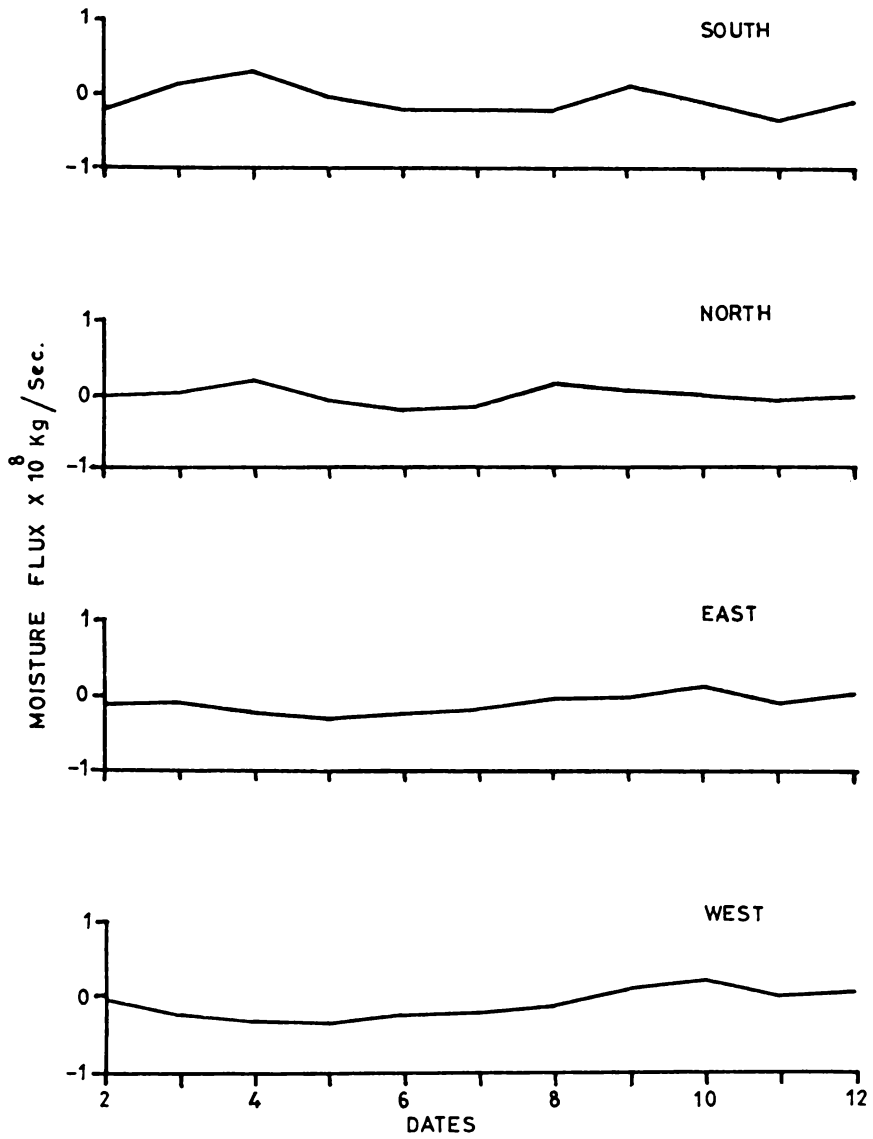


FIG.3.6(d) DAY TO DAY VARIATIONS OF SUM OF MOISTURE FLUX FROM 700 TO 200 mbs DURING PHASE-IV

any specific pattern. Figures 3.7(a) to 3.7(d) give the same for the Phases-I, II, III and IV respectively.

PHASE-I

In this phase, similar to the day to day variations, the diurnal variations were also alike at opposite walls. From 7th to 15th June, when it was positive and increasing from 00 to 18 GMT, at the zonal walls, it was both positive and negative, and also decreasing at the meridional walls. The rest of the period showed no significant variation except at the northern wall on the 16th and eastern wall on the 17th. The values were higher and positive at the zonal walls while both positive and negative at the other two. This brings out that mostly divergence or convergence of net moisture was due to meridional winds rather than the zonal winds.

PHASE-II

In the second phase, the diurnal variations were less significant and almost alike at all the four walls and the values were always positive but comparatively lower at the meridionals. There were practically no variation at all the walls on 2nd, 5th, 9th and 11th July. On the 3rd, it decreased from 00 to 06 GMT and then, after an increase upto 12 GMT remained the same upto 18 GMT. On 10th, the above

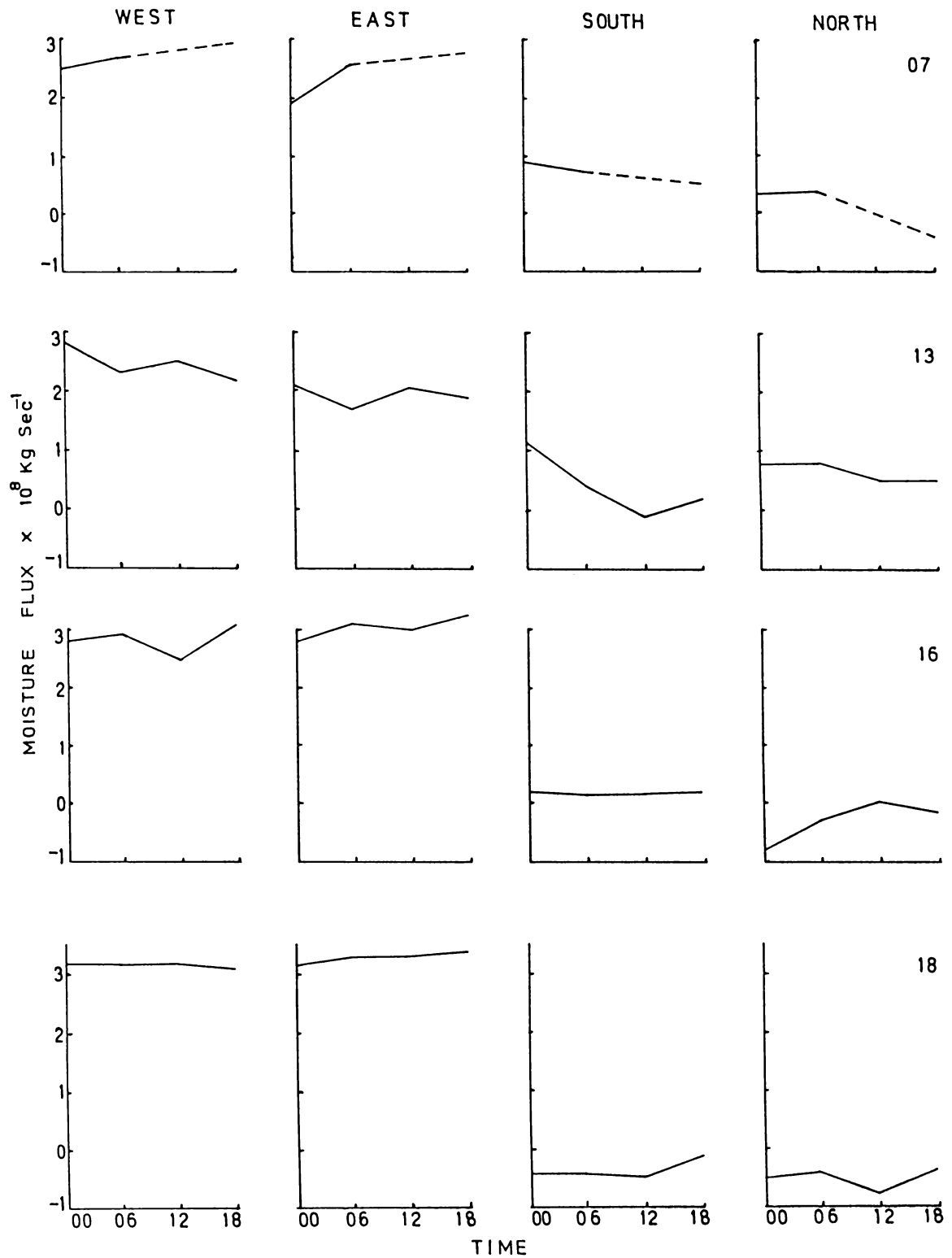


FIG.3.7(a) DIURNAL VARIATION OF SUM OF MOISTURE FLUX FROM SURFACE TO 200 mb DURING PHASE-I

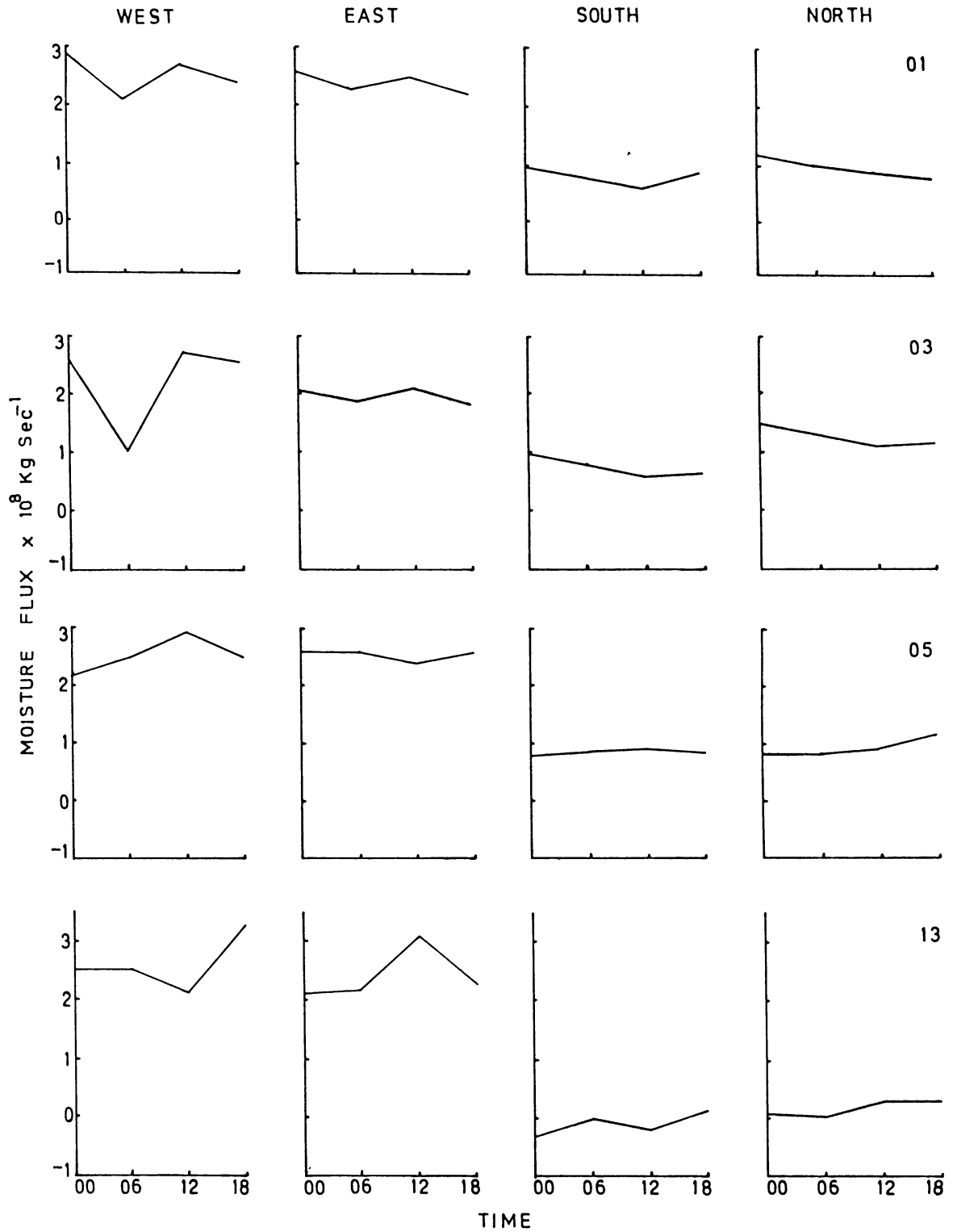


FIG.3.7(b) DIURNAL VARIATION OF SUM OF MOISTURE FLUX FROM SURFACE TO 200 mb DURING PHASE-II

pattern repeated itself at all the walls except the eastern wall. The variation pattern was opposite at the west and east walls on the 13th. It could also be inferred that, the net influx or outflow of moisture would be much less because, the values were always positive, at all the four walls.

PHASE-III

As seen from Fig.3.7(c) the values were much lower when compared with that in the first and second phases. On some days like that on 18th May, the values were steadily decreasing and on some others like that on 21st it was increasing. On all the other days, it was alternate hours of high and low positive and negative values with the flux decreasing from 00 to 12 GMT and increasing thereafter on many days. Except for a few days like 25th, with negative values at all the walls, one finds both positive and negative values on a given day.

PHASE-IV

During this phase, variations were similar to that of the IIIrd phase and they were more conspicuous at the north and south walls. The values were higher than that of the previous phase and comparable with that of the other two. In the earlier part of this phase, on days like 2nd June gave negative values of flux showing that the winds

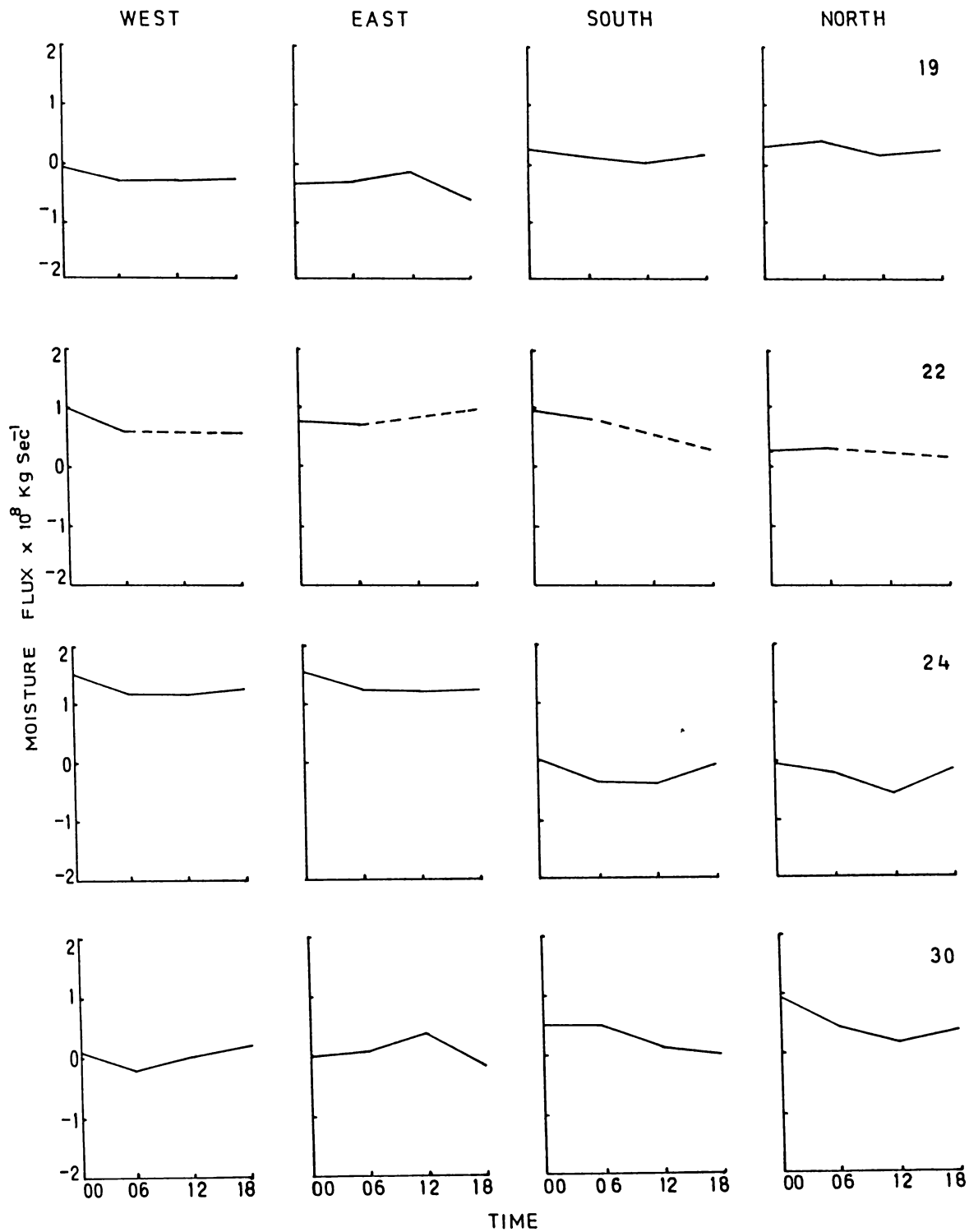


FIG.3.7(c) DIURNAL VARIATION OF SUM OF MOISTURE FLUX FROM SURFACE TO 200 mb DURING PHASE-III

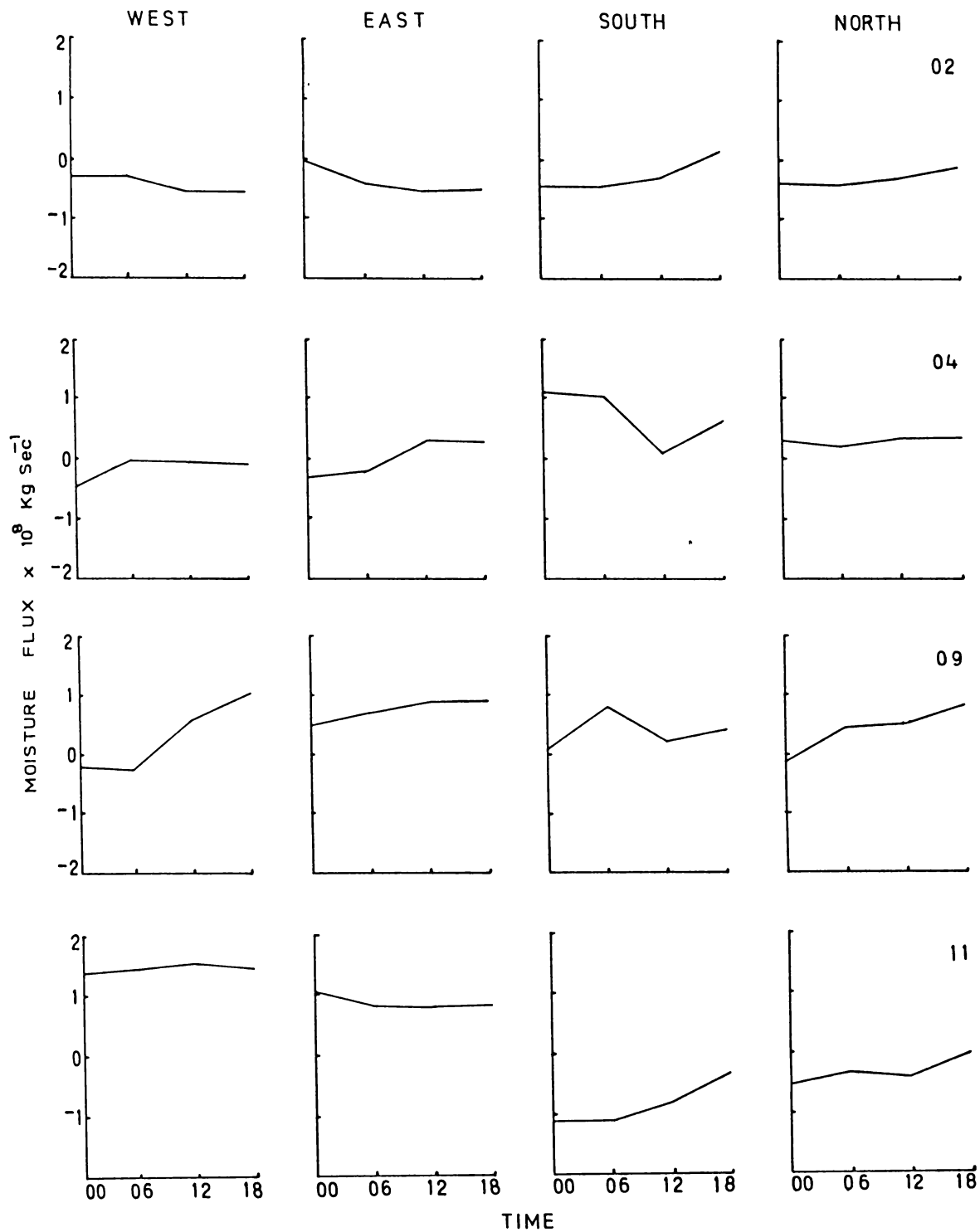


FIG.3.7(d) DIURNAL VARIATION OF SUM OF MOISTURE FLUX FROM SURFACE TO 200 mb DURING PHASE-IV

were north easterlies. Certain days like the 9th and 10th, showed good diurnal variations and especially so at the west and north walls, where the values increased from around zero to 1.8×10^8 kg/sec at the west boundary and 8.6×10^8 kg/sec at the north boundary on the 9th. But on some days like 11th June, the variations were negligible.

In general, on most of the days, the moisture flux values were positive at the western wall during all the phases. This would mean that, moisture was being brought into the polygon area through this wall. All the other walls gave both positive and negative values.

3.4 NET MOISTURE FLUX DIVERGENCE

The method of calculating the net moisture flux had already been described in the section 1.5. It is the sum of the differences of the fluxes at the west wall from east wall and that of the southern wall from northern wall (E-W+N-S). It is convergence of moisture if the value is negative and divergence if positive.

3.4.1 Day-to-day variations

Figs. 3.8(a) to 3.8(d) show the variations at the four synoptic hours for the four phases respectively. The highest values were obtained during the first phase.

PHASE-I

Moisture convergence was noticed during most of the days at all the timings. The variations were highly significant at 00 GMT where the change in values were as high as 2×10^8 Kg/Sec and it was much less at other hours. The moisture convergence during most of the days could have been due to the presence of low pressure system prevailed in the Arabian Sea during that period.

PHASE-II

In this Phase, it was net moisture divergence all through at 00 GMT. At the other timings, both convergence and divergence were noticed on different days.

PHASE-III

There were good daily variations in the amount of moisture flux converged and diverged into the area, especially so from 21st to 25th May, when it was high convergence. This is a noticeable feature of this phase.

PHASE-IV

The variations were not much considerable and the values were also low, with an exemption on 12th June. On the 12th, it was high convergence in the early hours of the

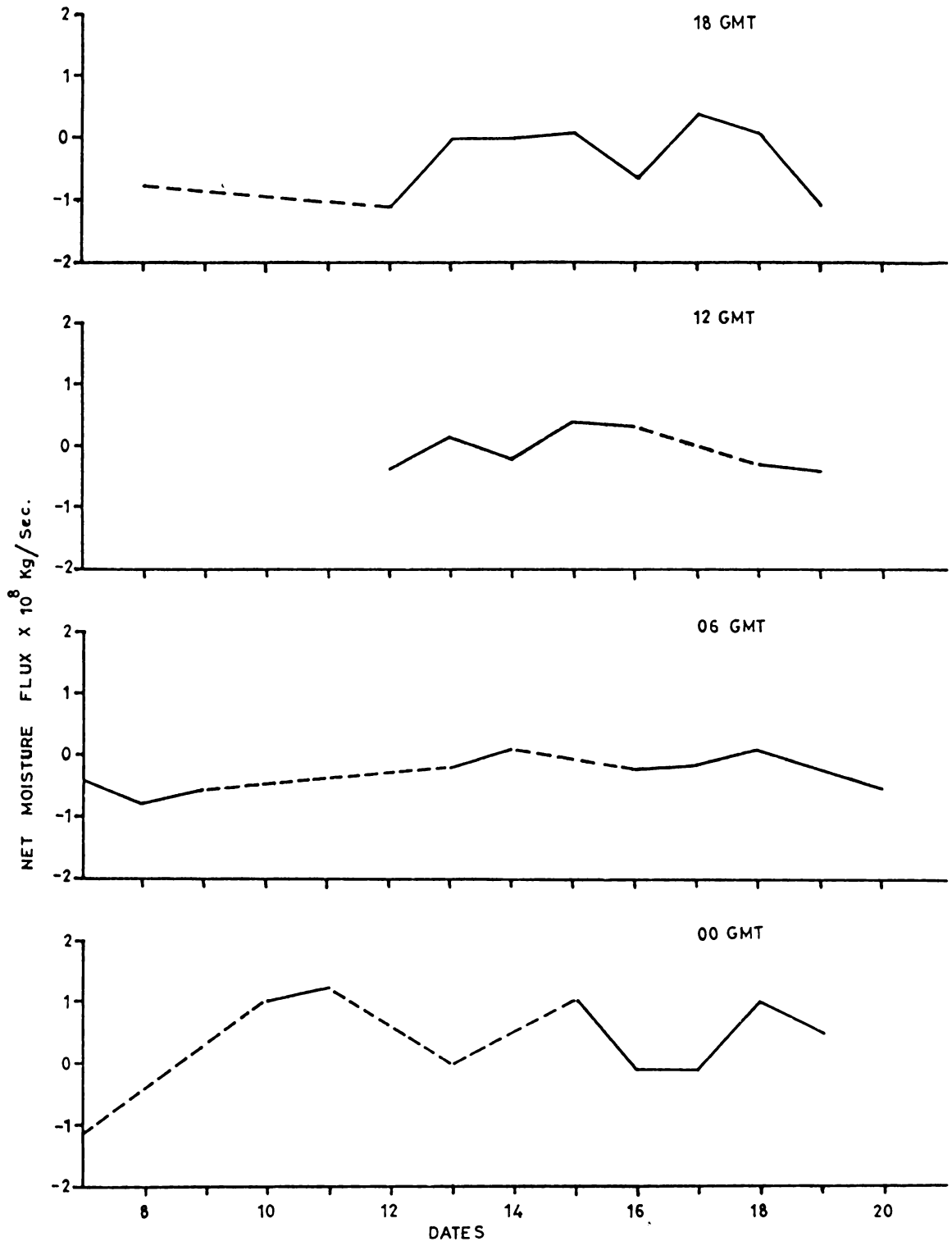


FIG.3.8(a) DAY TO DAY VARIATIONS OF NET MOISTURE FLUX DIVERGENCE DURING PHASE -I

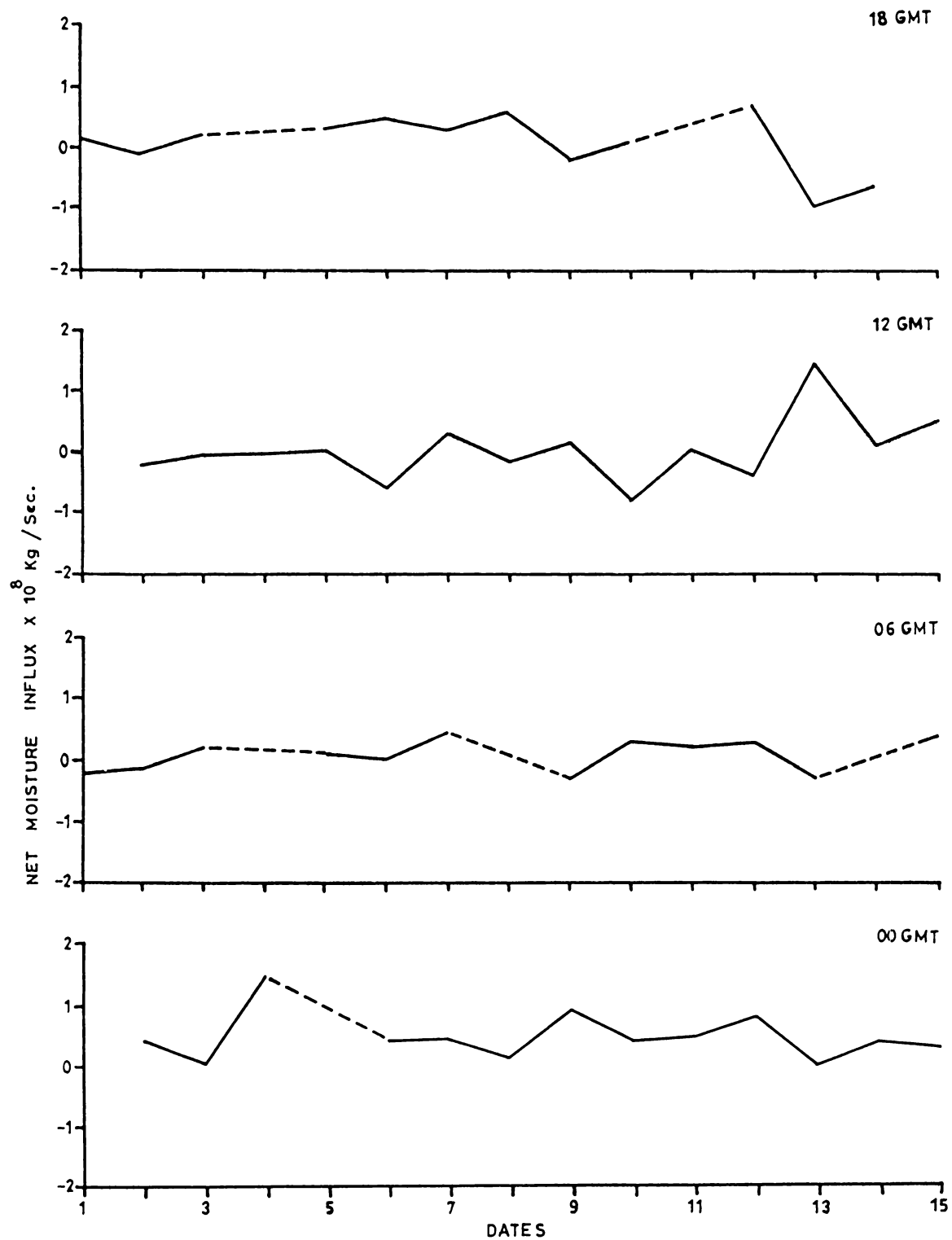


FIG.3.8(b) DAY TO DAY VARIATIONS OF NET MOISTURE FLUX DIVERGENCE DURING PHASE-II

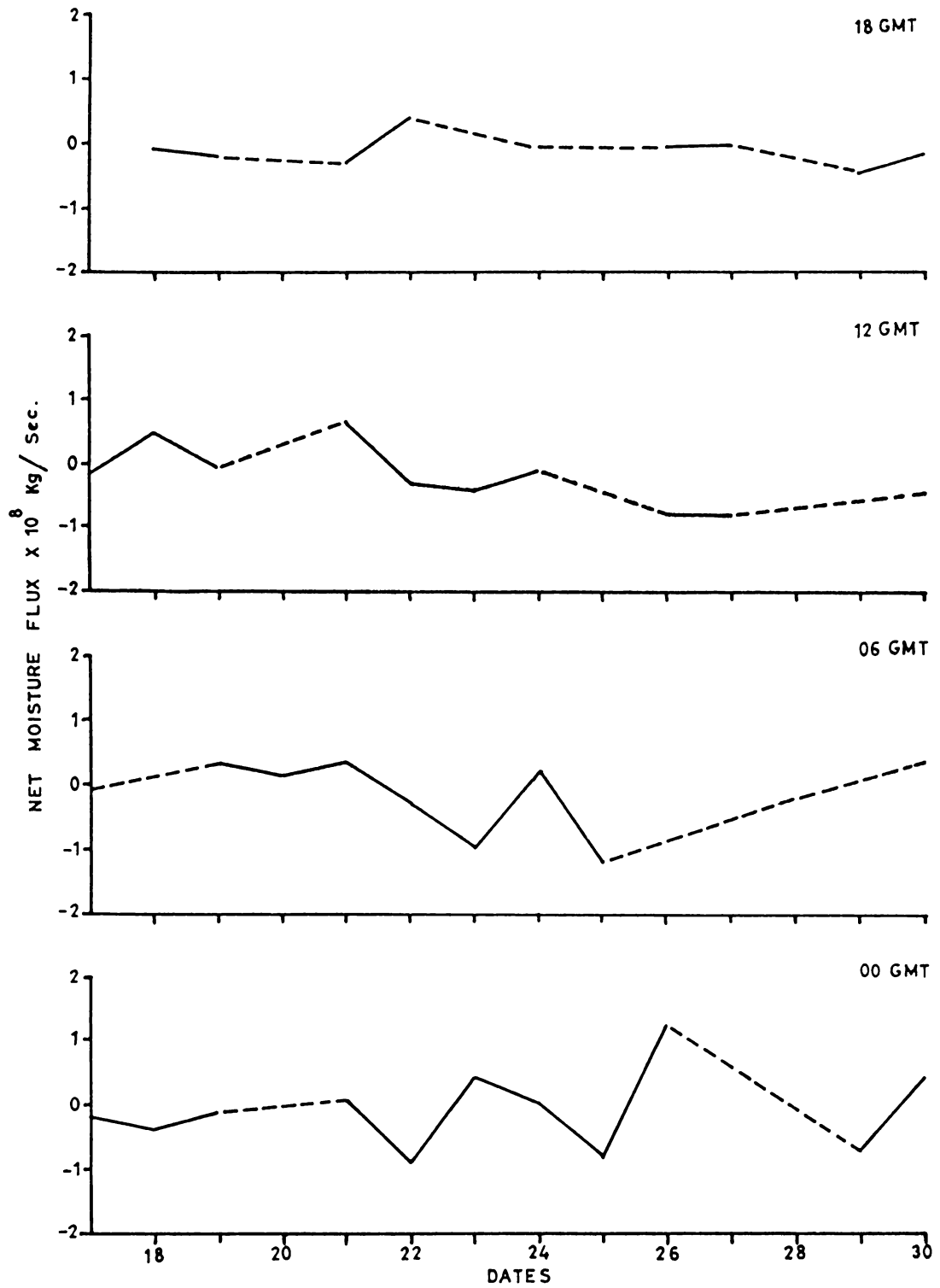


FIG.3.8(c) DAY TO DAY VARIATIONS OF NET MOISTURE FLUX DIVERGENCE DURING PHASE-III

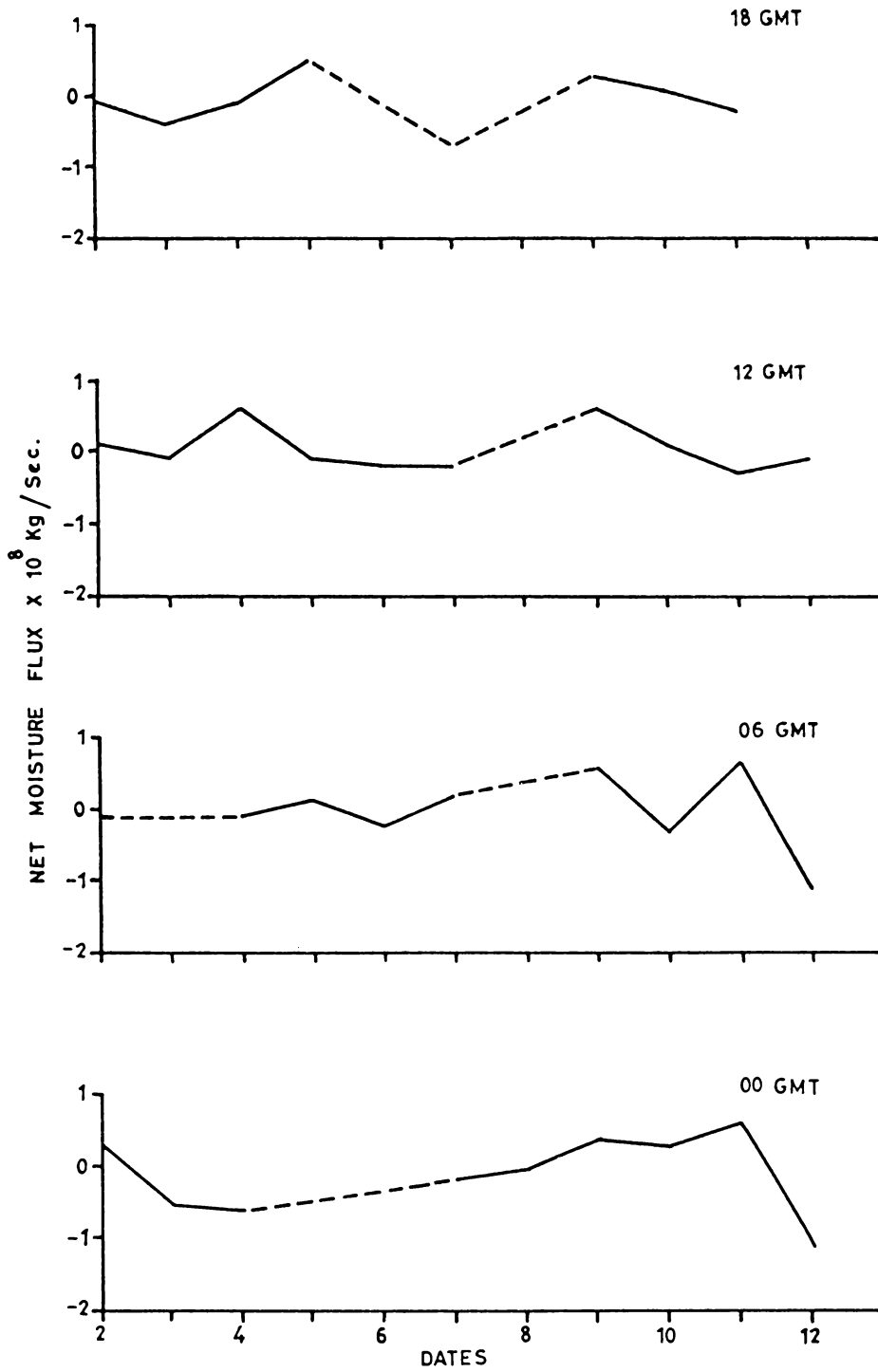


FIG.3.8(d) DAY TO DAY VARIATIONS OF NET MOISTURE FLUX DIVERGENCE DURING PHASE-IV

day. Incidentally, on this day the monsoon onset took place over Kerala Coast.

3.4.2 Diurnal Variation

Figs. 3.9(a) to 3.9(b) give the diurnal variation of the net moisture flux divergence during the four Phases-I, II, III and IV respectively. It showed no regular pattern of variation.

PHASE-I

It was moisture convergence on the 8th and 12th June during the whole day. Convergence were high at 00 and 18 GMTs and low in between. On 12th, convergence increased with time while on 13th it decreased upto 12 GMT and became divergence. The other days, experienced both convergence and divergence on the same day, with convergence at 00 GMT becoming divergence by about 18 GMT, on most of them. Rare occasions of convergence of moisture flux increasing from 12 to 18 GMTs as on 19th June were also found.

PHASE-II

During this phase, it was divergence on more number of days and especially so at 00 GMT, with exceptions on the 4th, 13th and 14th July. On the 3rd, 6th, 8th, 9th, 10th, 12th and 13th of July, the variation pattern was zigzag,

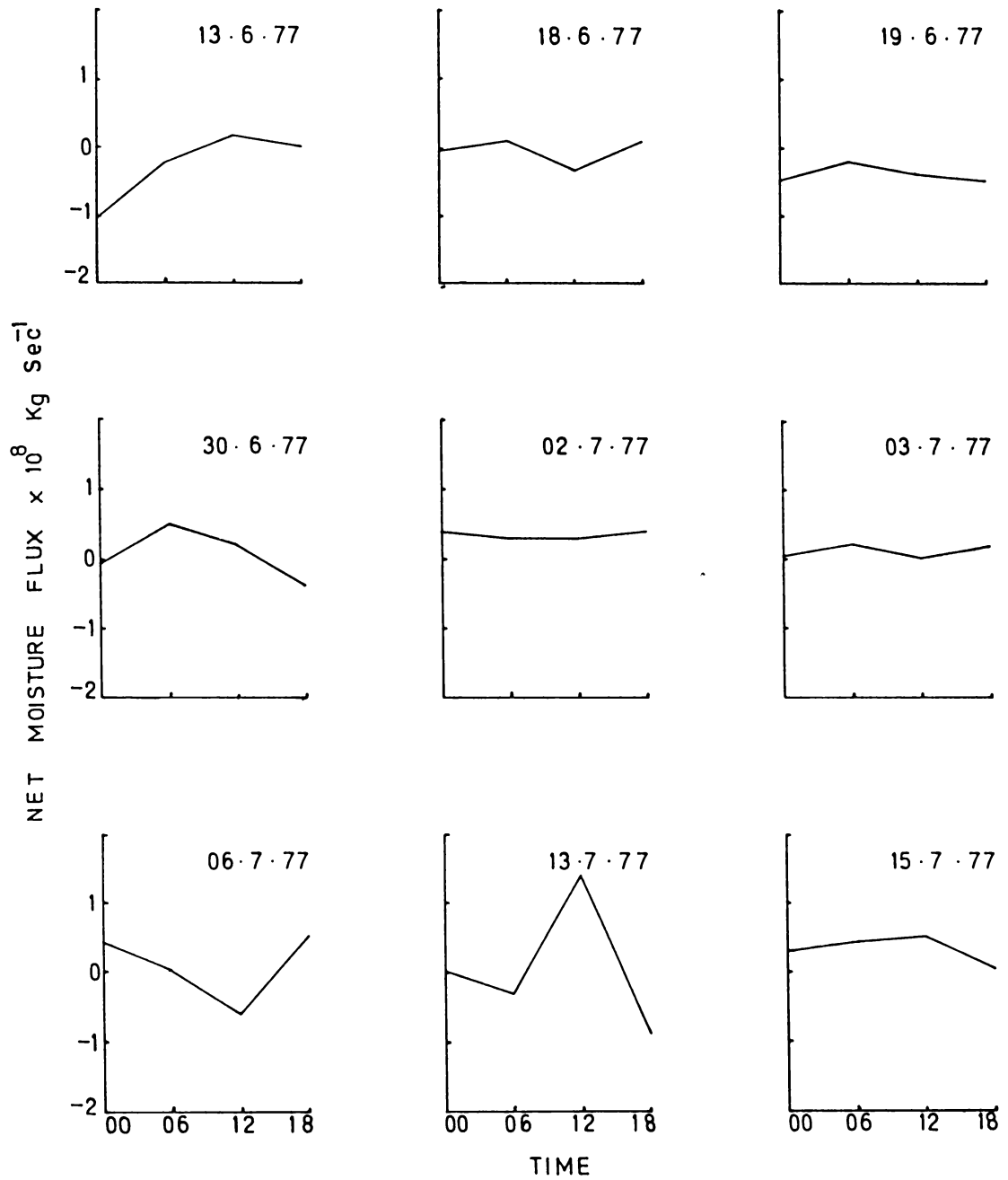


FIG.3.9(a) DIURNAL VARIATION OF NET MOISTURE FLUX DURING PHASES-I & II

with alternate hours of divergence and convergence or the same increasing and decreasing. On the 14th it was convergence through out while on the 15th, it was only divergence and the remaining days experienced both divergence and convergence at different synoptic hours.

PHASE-III

In this phase also, both convergence and divergence of moisture fluxes were obtained on the same day, with the changes taking place even within six hours. The diurnal variation was negligibly small on the 17th, 20th, and after 27th of May. On many days it was convergence at 00 GMT, which increased to high values as on 25th or decreased and became divergence as on 22nd May. But on 26th May divergence at 00 GMT became convergence by 18 GMT.

PHASE-IV

The fourth phase also showed good diurnal variation. On 2nd, 4th, 5th, 7th and 10th of June there was moisture convergence and divergence alternately, from 00 to 18 GMT, with remarkably high variations on the 4th. On the 3rd it was convergence decreasing from 00 to 12 GMT and thereafter increasing. On 9th, it was always divergence, with the value initially increasing and decreasing thereafter.

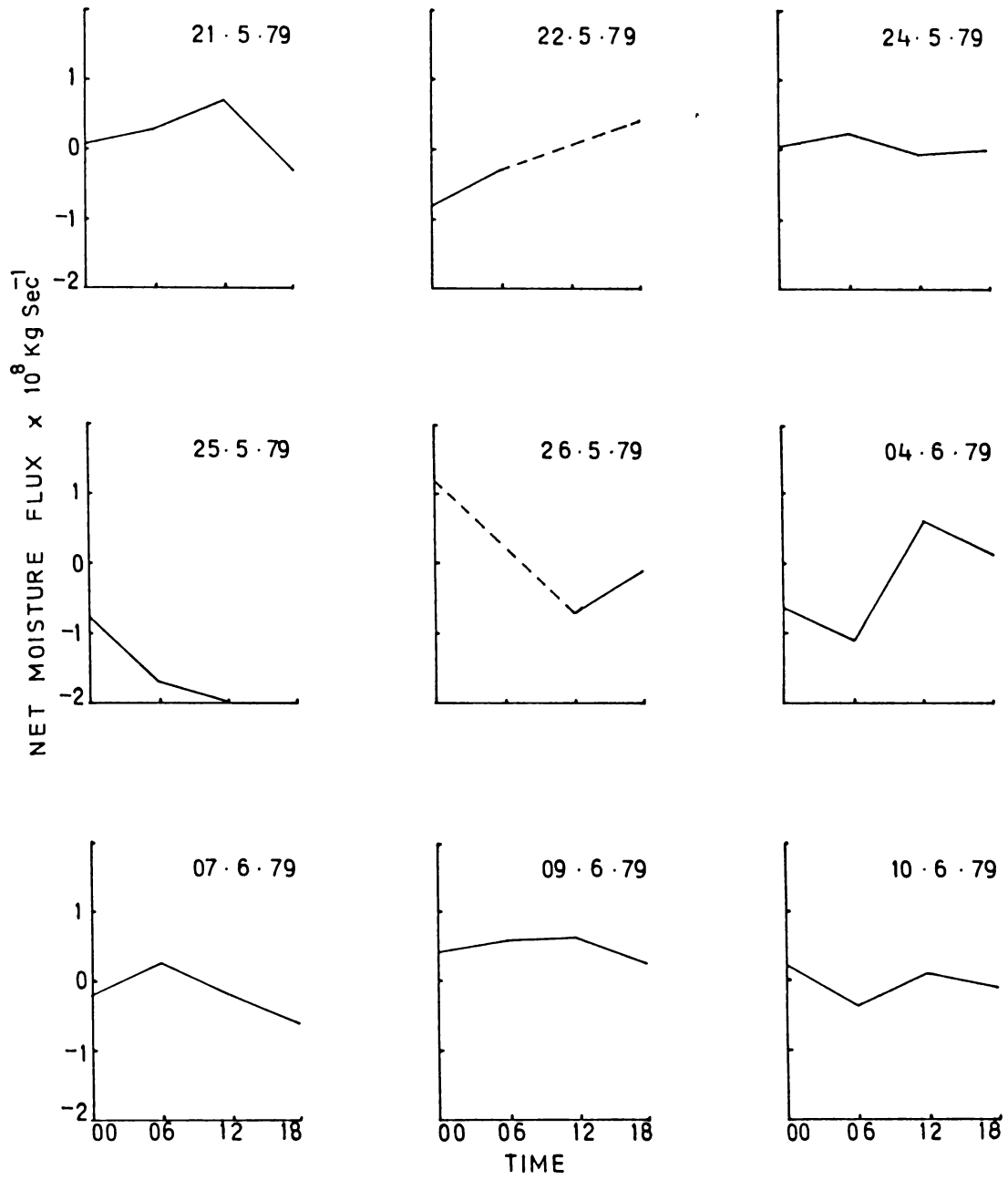


FIG.3.9(b) DIURNAL VARIATION OF NET MOISTURE FLUX DURING PHASES-III & IV

Although the above patterns differed for the different timings it is worthwhile to look at the mean daily variations also.

3.5 MEAN NET MOISTURE FLUX

This was obtained as an average for a day the net moisture flux from that at the four synoptic hour.

3.5.1 Day-to-day Variations

The Fig.3.10 exhibits the day-to-day variations of the same for the four phases.

There was significant variation in the Phases-I and III with convergence on more number of days. It was very low divergence during Phase-II and in the Phase-IV, but the values often changed sign which may due to the sudden changes in the weather. Convergence maximum was noticed on 25th May 1979.

So far, the moisture contribution through evaporation from the sea surface and the moisture diverged/converged by the winds had been discussed. The difference between these two, which gives the amount of moisture available for condensation is discussed in the following section and is referred to as precipitation.

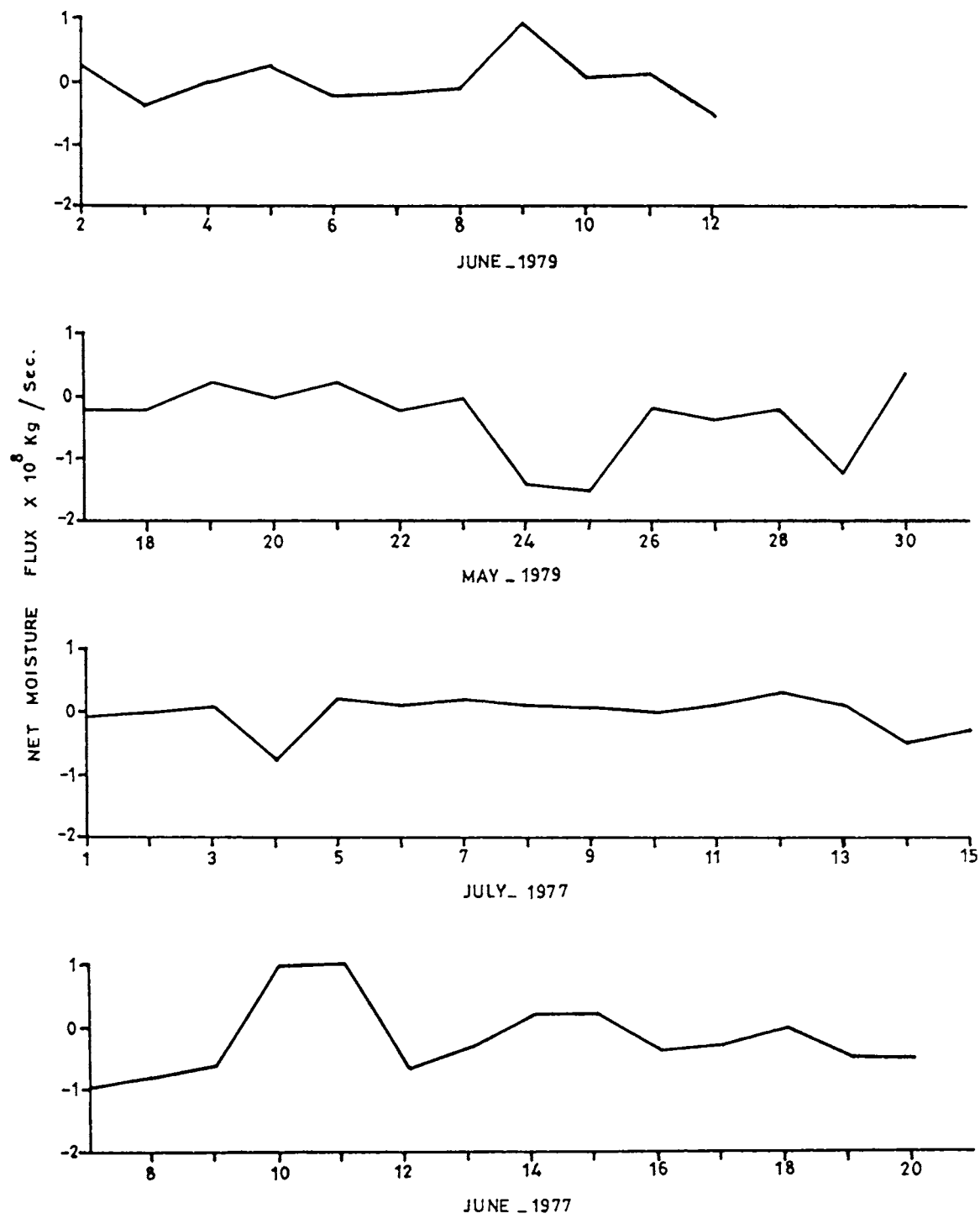


FIG.3.10 DAY TO DAY VARIATIONS OF AVERAGE NET MOISTURE FLUX DURING THE FOUR PHASES

3.6 PRECIPITATION

Although the daily values of precipitation of the four synoptic hours were computed, only the daily means are presented. This being a residual term it is felt that this would suffice.

Fig.3.11 shows the daily variation of average rate of precipitation for the four phases. When compared with the previous figures, it could be seen that, most of the time, the net moisture convergence coincided with high precipitation rates. In Polygon-I except on 10th and 11th, there was considerably high precipitation on most of the days. During Phase-II, the rate of precipitation was very low with exceptions on 4th and 14th July. During Phase-III, a prominent peak was observed on 25th. In Phase-IV, alternating positive and negative values of precipitation were also found.

The high precipitation rates most of the time coincided with high moisture convergence and presence of low pressure systems. The negative precipitation rates, observed on quite few occasions could be interpreted as due to the predominance of divergence of moisture flux over evaporation.

The energy budget studies would be incomplete if the sources and sinks of heat energy are not studied. The mois-

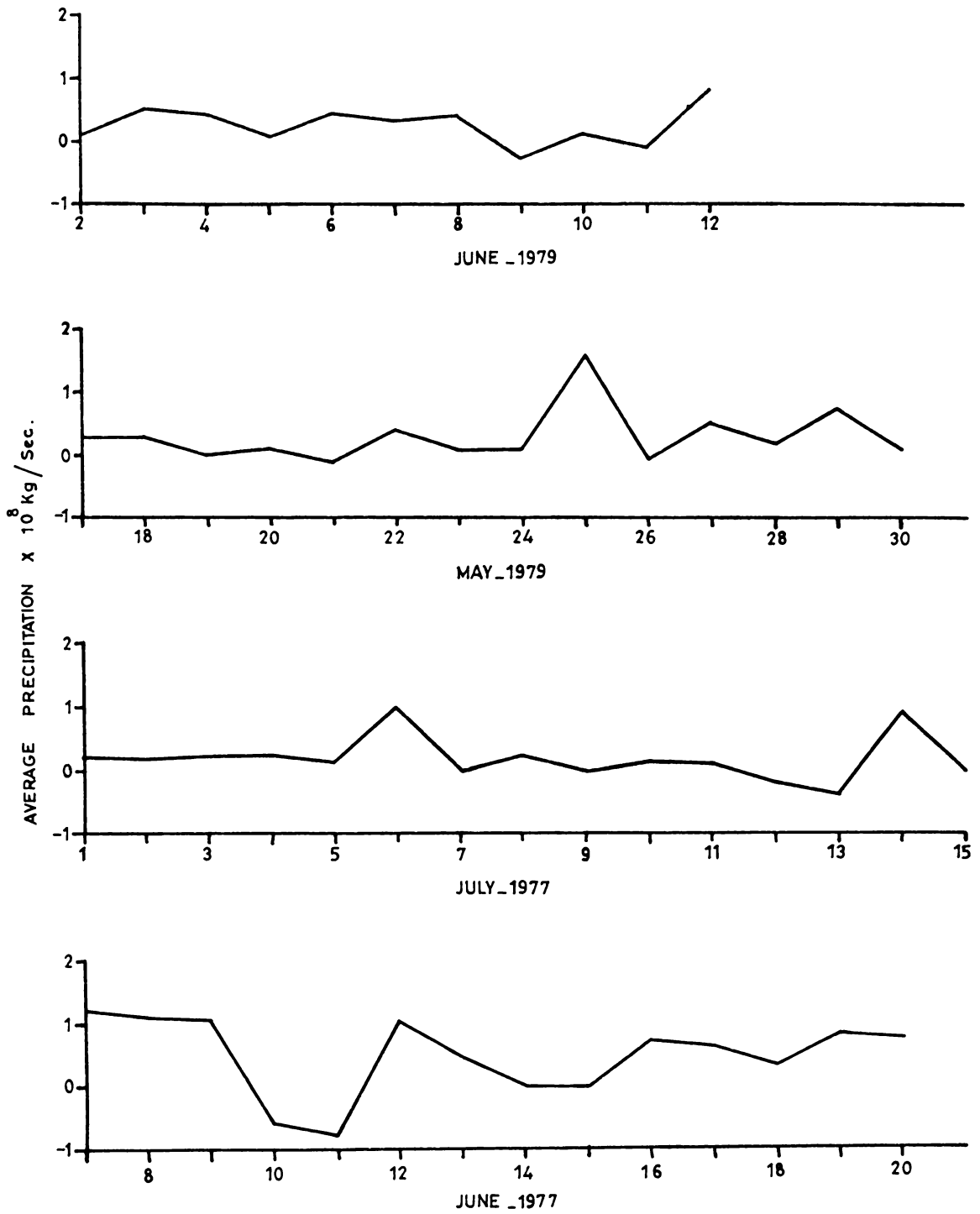


FIG.3.11 DAY TO DAY VARIATIONS OF RATE OF PRECIPITATION DURING THE FOUR PHASES

ture budget studies gave an insight into the amount of heat liberated due to condensation. The forthcoming chapter gives the details of the heat budget studies.

CHAPTER - IV

4.1 INTRODUCTION

This Chapter deals with the heat budget of the Arabian Sea area under study. Over the oceans as a whole, interaction at the air-water interface importantly affect both the atmosphere and the oceans. The amount of heat abstracted from the sea in terms of sensible heat, latent heat due to condensation and heat diverged away or converged into the area by wind, was studied to determine the heat budget of the column of the atmosphere with the sea surface over the polygon area as the lower boundary and 200 mb level as the upper boundary. The sensible heat is directly related to the wind speed and the air-sea temperature difference while the latent heat is determined by the wind speed and the vertical gradient of vapour pressure. Understanding the heat content variations in the Indian Ocean is an integral component of monsoon studies. Michael (1975), Rao et al (1977), Hastenrath (1980) had studied the heat budget of the tropical oceans.

4.2 SENSIBLE HEAT

As already discussed in section 1.5, the sensible heat flux at the four ship positions were estimated using the Bulk Aerodynamic formula and the average of these four

values has been used to calculate the rate of total sensible heat exchanged at the air-sea interface over the whole polygon area.

The diurnal and day to day variation of this parameter has been studied and is discussed here.

4.2.1 Day-to-day Variations

Figure 4.1(a) to 4.1(d) exhibit the same variations for the four Phases-I, II, III and IV respectively. Phases-I and IV showed good day-to-day variations, indirectly meaning that, they were periods of active weather.

PHASE-I

Although data is not available at all synoptic hours on the 8th, 9th and 10th June one could see that, there is a decrease in the values from the 7th to 11th. Except at 00 GMT, the fluxes were very low, from the 12th to 17th, and the daily variations were very insignificant. After 18th June, to the end of the phase, there was an increase in the sensible heat values at all the four timings.

PHASE-II

The day-to-day variations were most of the time insignificant at all the timings other than 12 GMT. Except at 00 GMT, the values were mostly negative in this phase,

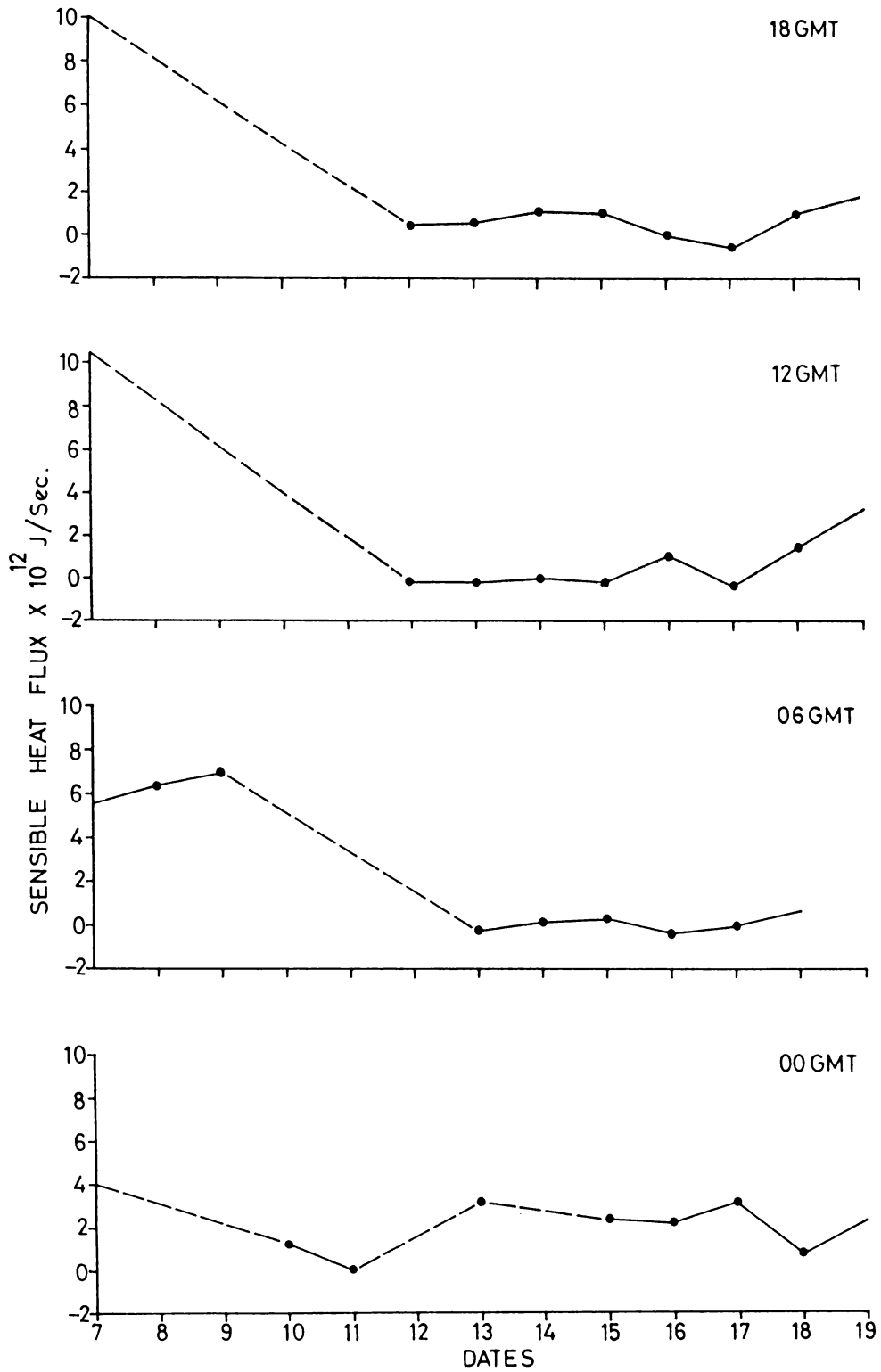


FIG.4.1(a) DAY TO DAY VARIATIONS OF RATE OF SENSIBLE HEAT DURING PHASE-I

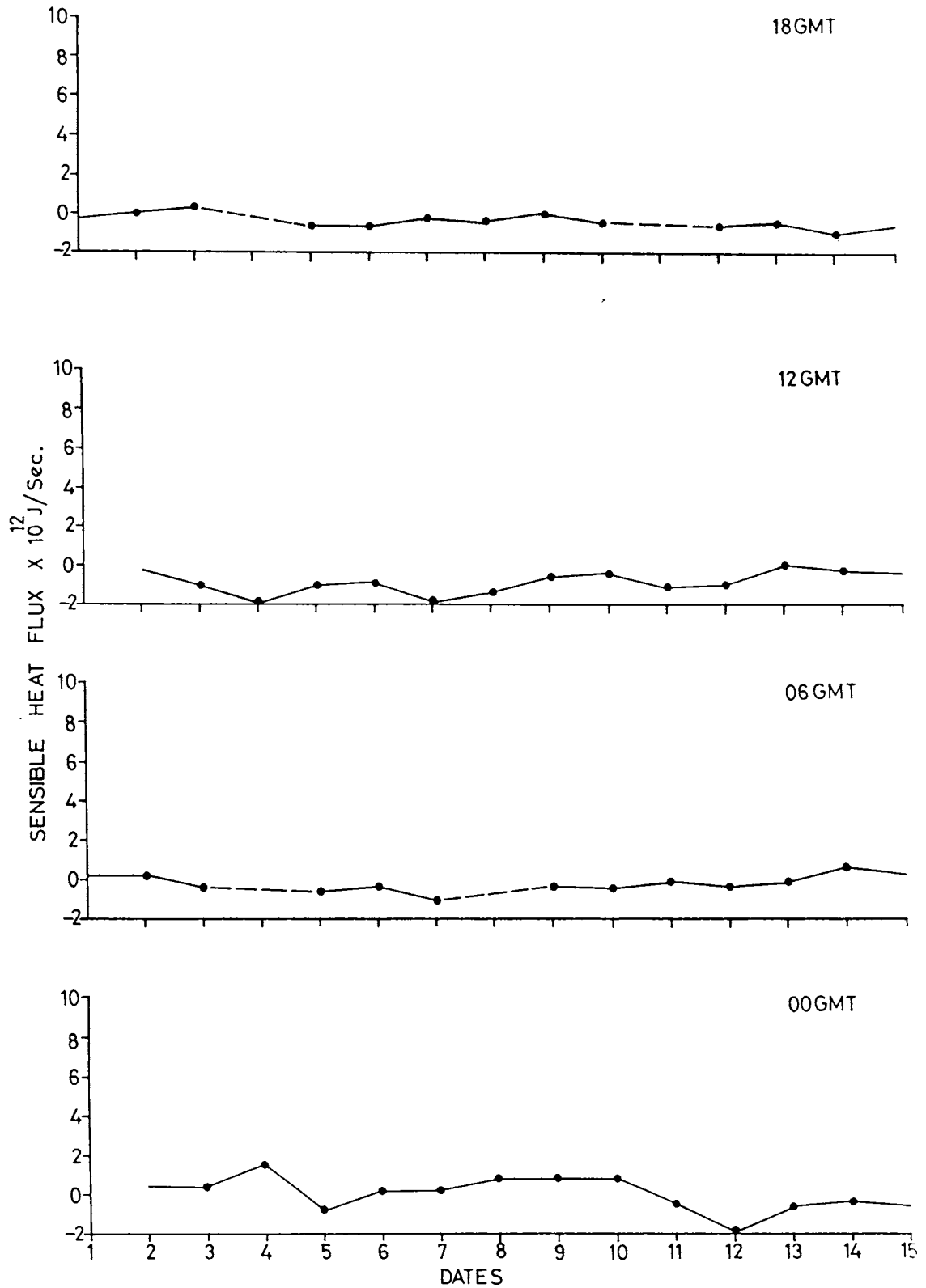


FIG.4.1(b) DAY TO DAY VARIATIONS OF THE RATE OF SENSIBLE HEAT DURING PHASE-II

showing that there was net heat loss. At 00 and 18 GMTs, the sensible heat flux increased from 1st to 4th July, while it was the reverse at the other two hours. From the 5th to 10th, there was an increasing trend, and after that a mild decrease upto the end of the phase. At 12 GMT, the value, was low on 4th and 7th July.

PHASE-III

The values were always positive and above 2×10^{15} J/Sec at all the timings during this phase, except at 06 GMT. From 17th to 22nd May, it was more or less invariant at 00, 12 and 18 GMTs, while at 06 GMT, it increased and decreased twice in between, with two peaks one on 20th and the other on 22nd May. From the 22nd, an increase was observed upto 26th at all the timings. 26th May showed the highest value of this phase. From 26th May, except at 18 GMT it decreased till the 29th and thereafter remained constant till the 30th at 06 and 12 GMTs. But at 00 GMT, it was higher on 30th it was the reverse at 18 GMT.

PHASE-IV

High positive values with considerable day-to-day variations was the feature of this phase. Sensible heat flux increased from the 2nd to 3rd and 7th to 9th of June at all the four synoptic hours. The variations were exactly similar

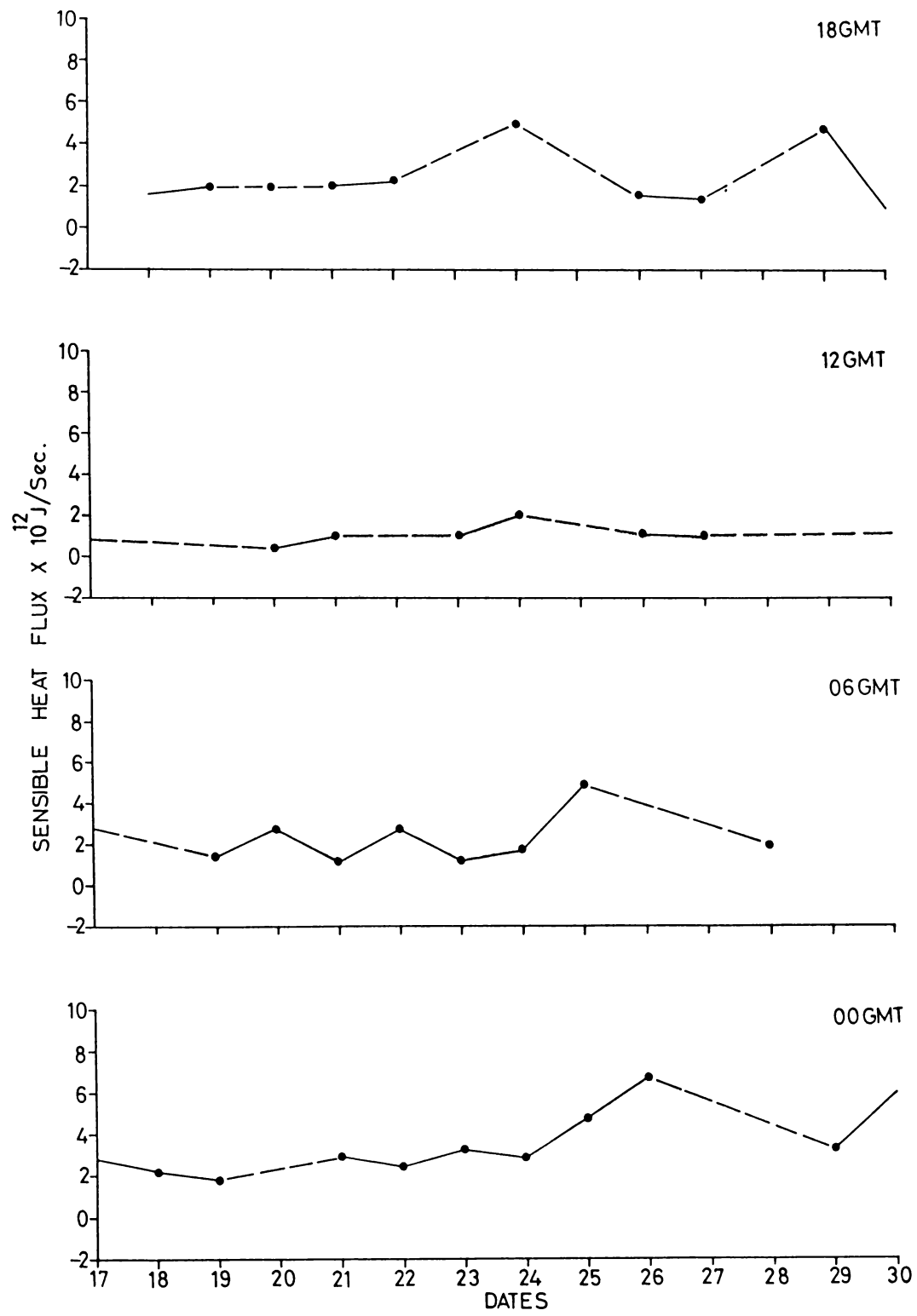


FIG.4.1(c) DAY TO DAY VARIATIONS OF THE RATE OF SENSIBLE HEAT DURING PHASE-III

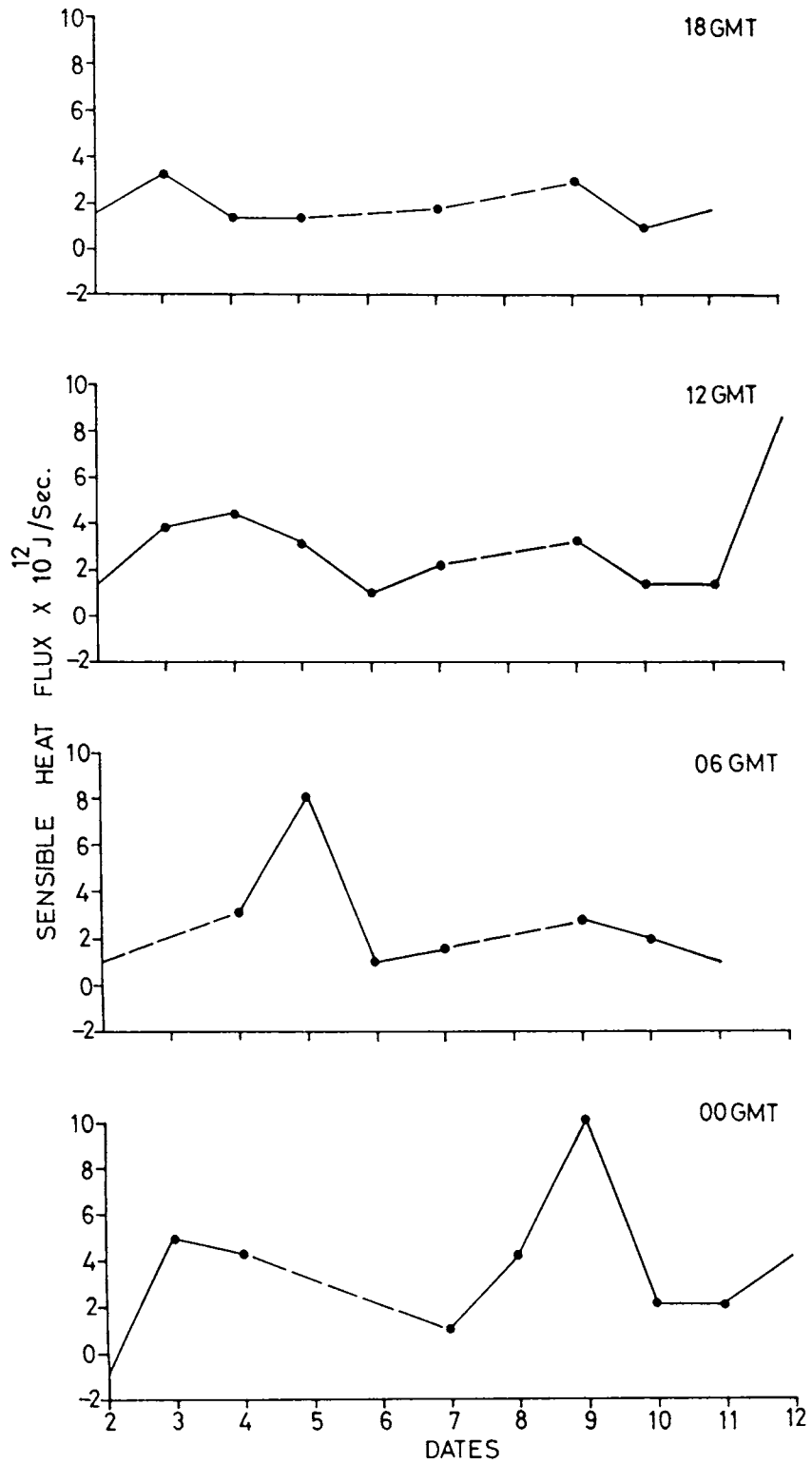


FIG.4.1(d) DAY TO DAY VARIATIONS OF RATE OF SENSIBLE HEAT DURING PHASE-III

at 00 GMT, with a primary peak on the 9th and a secondary on the 3rd. There was a decrease from the 3rd to 7th and 9th to 11th June at the 00 and 18 GMTs and almost a reverse at the other two timings.

4.2.2 Diurnal Variation

Figures 4.2(a) to 4.2(d) represent the diurnal variation of the sensible heat flux. It was noticed that there was not much diurnal variation although on many days the values were higher at 00 and 18 GMTs.

PHASE-I

On 7th and 8th June, it was very high positive values increasing with time. From the 13th to 17th, it showed an initial decrease from 00 to 06 GMT and thereafter remained almost the same although the value changed from positive to negative and viceversa twice on that day. On the 18th, it remained almost constant while on 19th, it decreased from 00 to 06 GMT, and 12 to 18 GMT while at increased in between.

PHASE-II

In this phase, the diurnal variations were most insignificant and the values were very low. But on most of the days, especially from 1st to 12th July, the heat gain

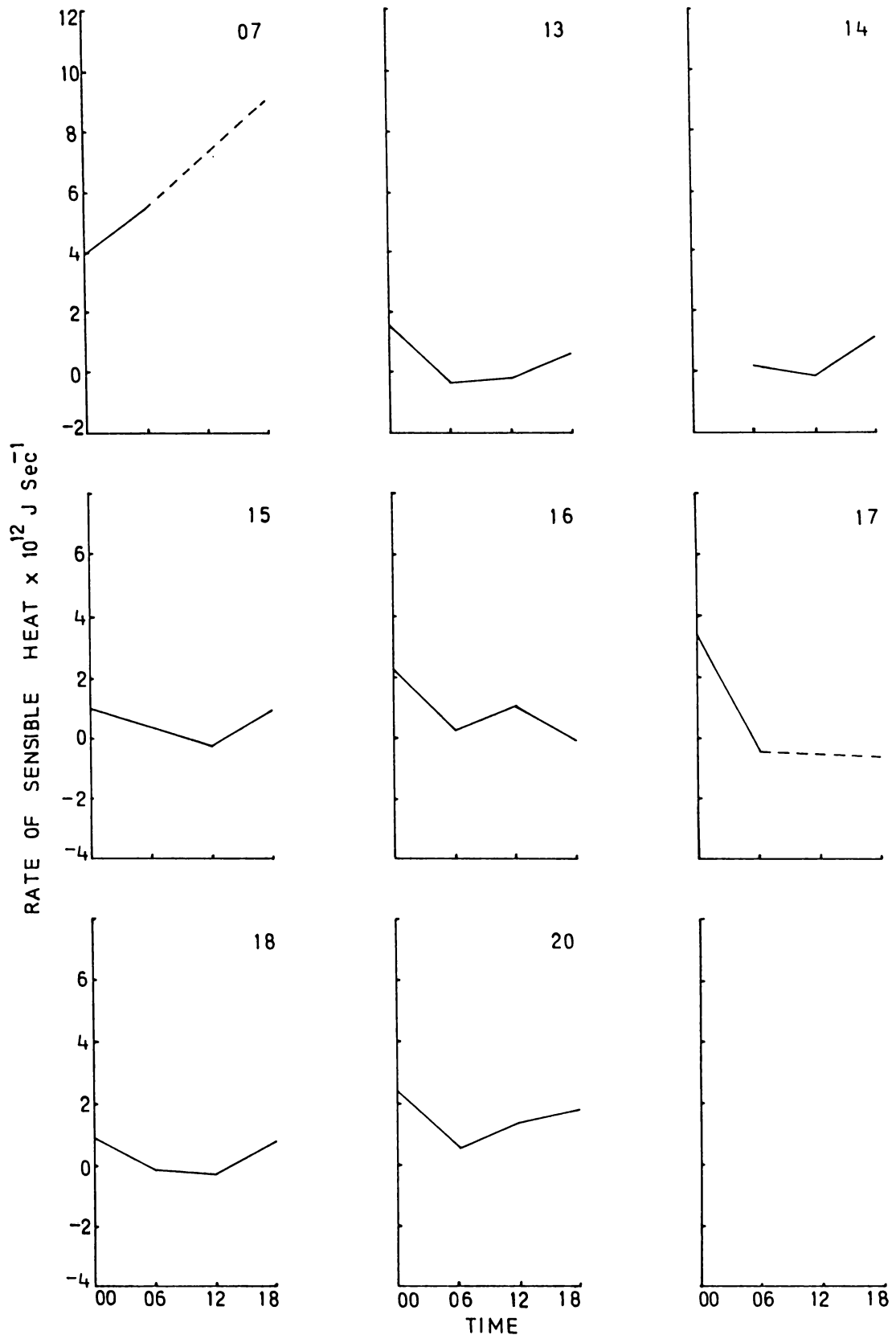


FIG.4.2(a) DIURNAL VARIATION OF RATE OF SENSIBLE HEAT DURING PHASE-I

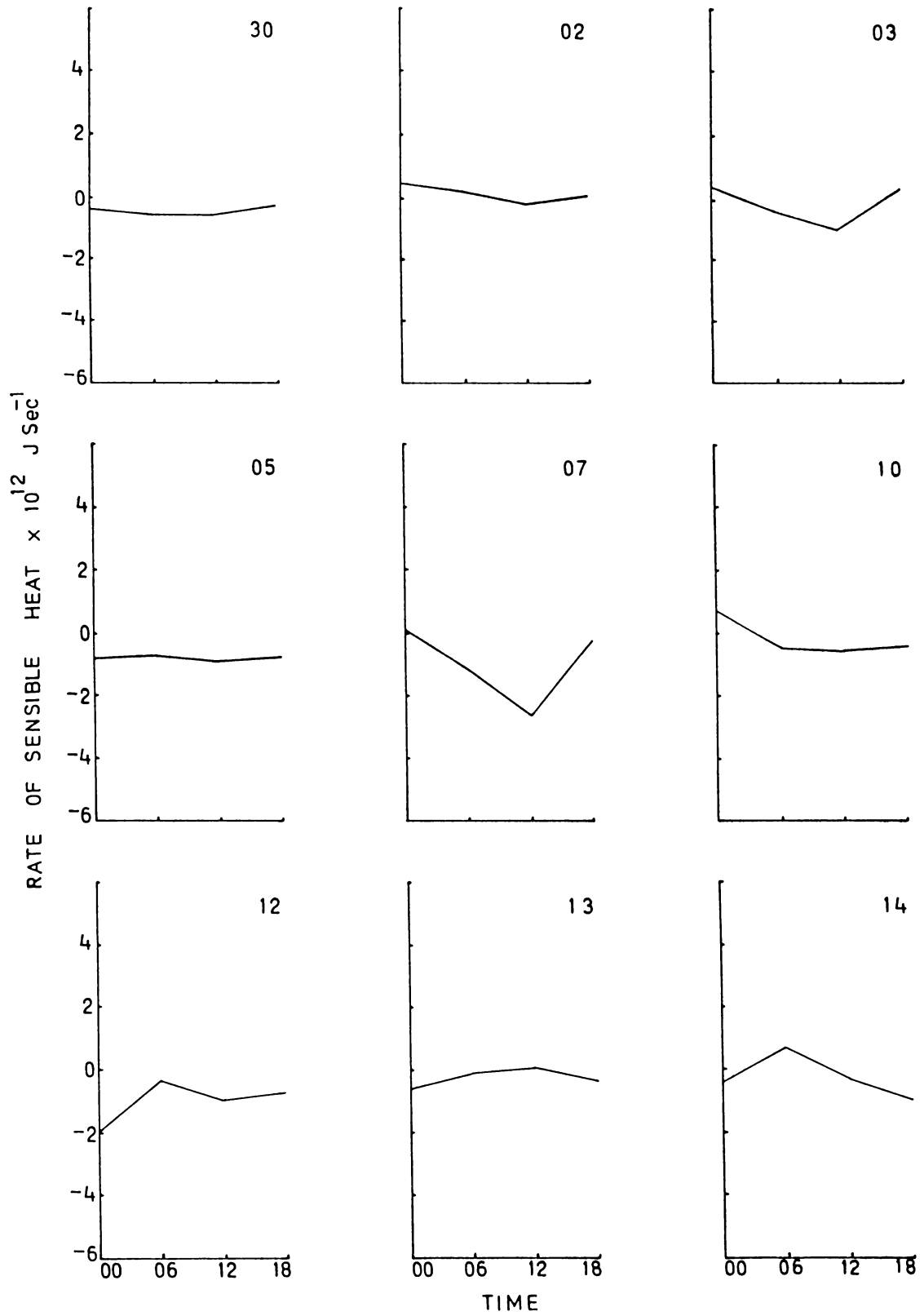


FIG.4.2(b) DIURNAL VARIATION OF RATE OF SENSIBLE HEAT DURING PHASE-II

observed at 00 GMT turned to a heat loss by 06 GMT and its magnitude increased by 12 GMT. The values were lowest at 18 GMT or in other words, the heat loss decreased from 12 to 18 GMT.

PHASE-III

During this phase, although there was not much diurnal variation, from 17th to 24th and on 26th May, the values were comparatively higher at the 00 and 18 GMTs while the lowest was at 12 GMT. This would mean that the sensible heat flux decreased from 00 to 12 GMT and thereafter increased to 18 GMT. On the 25th, it was almost the reverse pattern with highest at 12 GMT. While on the 29th, the highest values were at 18 GMT. 30th May showed a steady decrease from 00 to 18 GMT.

PHASE-IV

From the 2nd to 4th June, the diurnal variation was very low and on 4th, it decreased from 00 to 06 GMT and 12 to 18 GMT with an increase in between. On the 5th, the value decreased from a high positive value from 06 GMT to 18 GMT. During the period from the 6th to 11th, sensible heat flux remained almost unchanged although on the 11th it did show a decreasing trend from 06 to 18 GMT. On 12th June, the values at 12 GMT were higher than that at 00 GMT and hence the pattern was wavy.

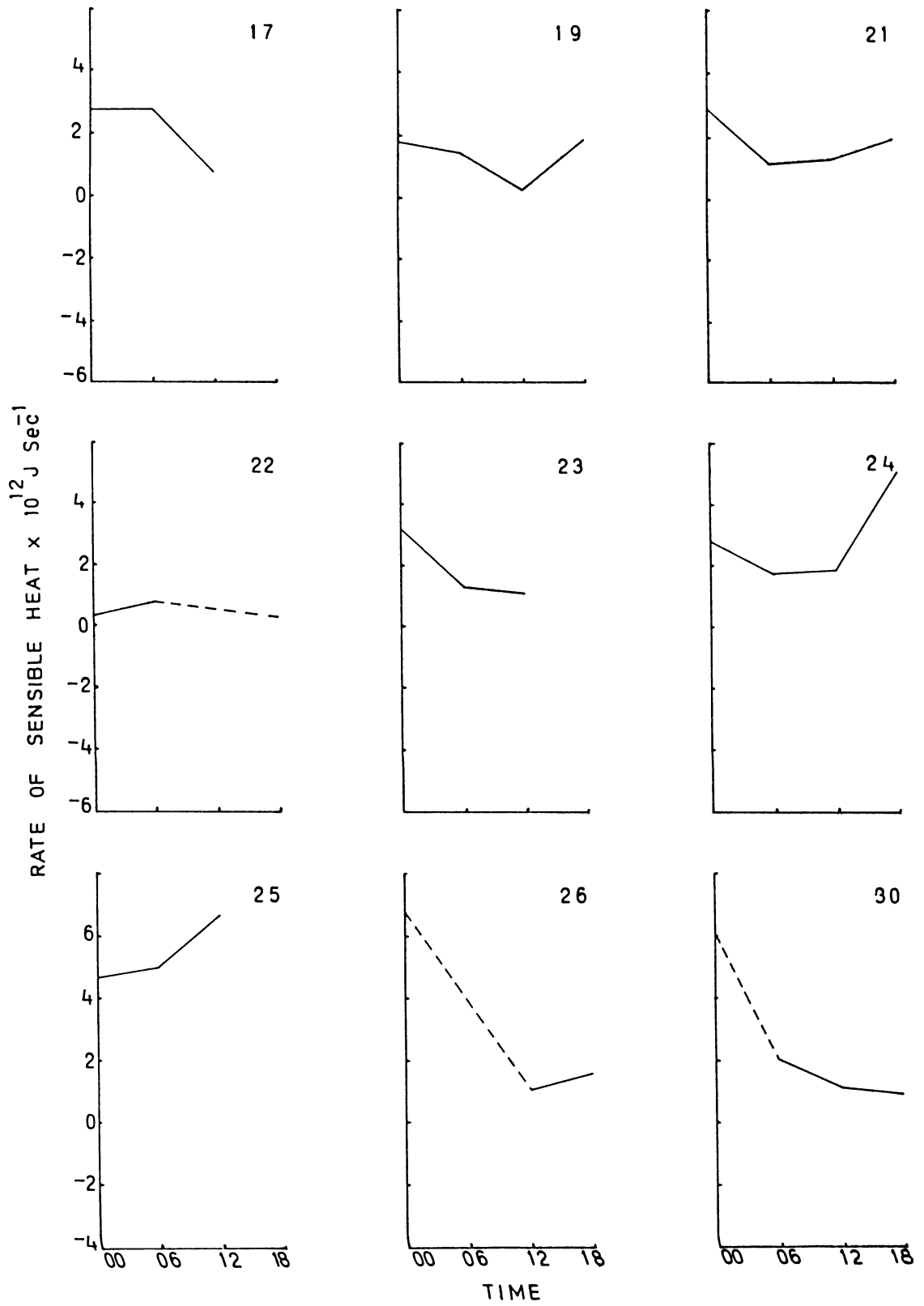


FIG.4.2(c) DIURNAL VARIATION OF RATE OF SENSIBLE HEAT DURING PHASE-III

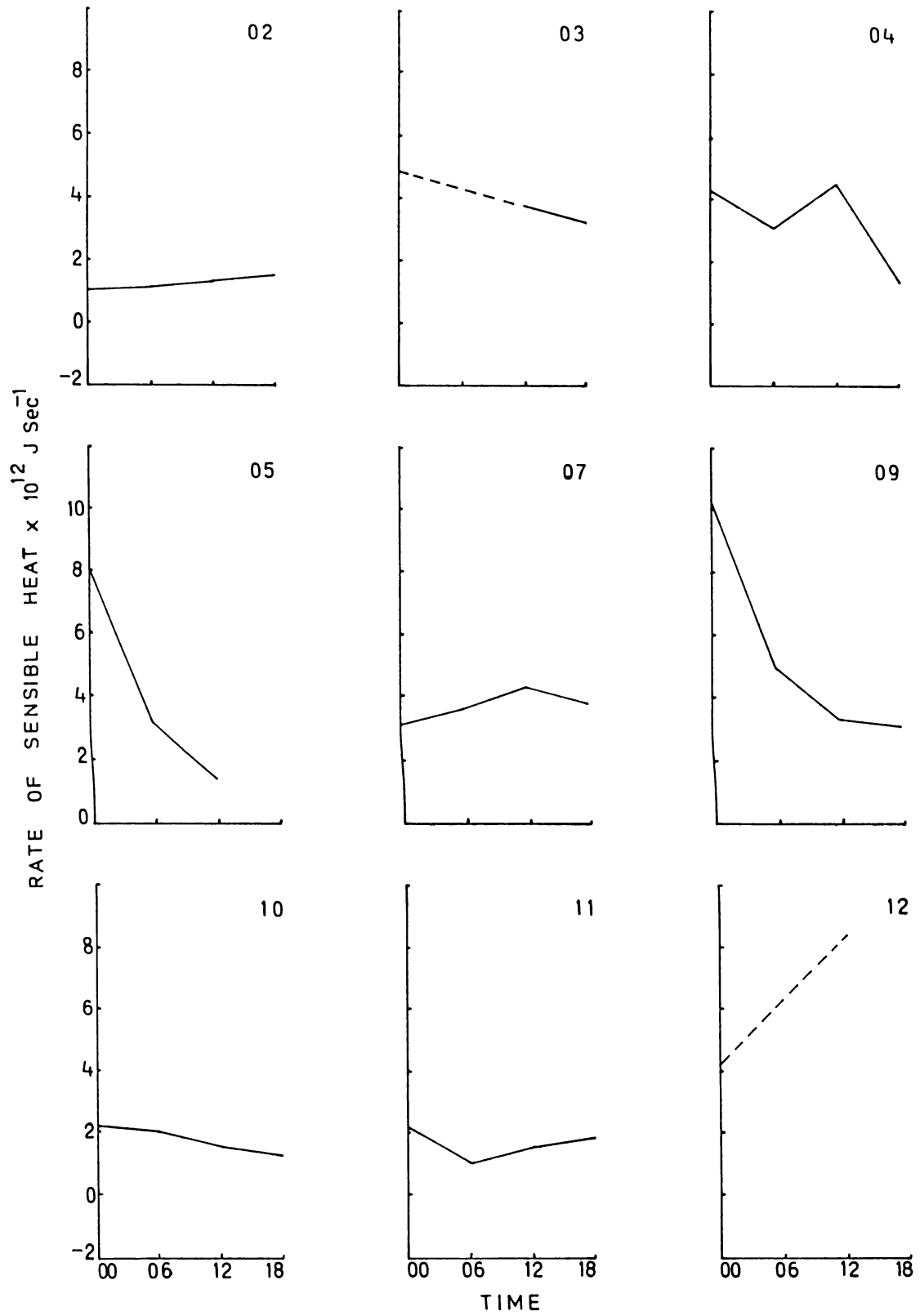


FIG.4.2(d) DIURNAL VARIATION OF RATE OF SENSIBLE HEAT DURING PHASE-IV

4.3 HEAT FLUX

This section discusses the variations of heat flux in terms of dry static energy. As already discussed in the methodology section, the total flux at individual locations (ships) were computed by integrating at 50 mb interval from 1000 mb upwards to the 200 mb level. In the lowest layer, the actual difference between the surface pressure and 1000 mb was considered. The lateral flux across each boundary is then obtained by multiplying individual station flux with the length of the wall. The diurnal and day to day variations of this parameter are discussed in detail below. The values were of the order of 10^{15} J/sec.

4.3.1 Day-to-day Variations

Figures 4.3(a) to 4.3(d) give the same for the heat flux at the four boundaries for the four synoptic hours, during the Phases-I to IV respectively.

PHASE-I

The day-to-day variations of heat flux showed a sinusoidal wave pattern with the crests around 10th and 17th June and troughs on 12th and 13th June through the zonal walls. The meridional walls showed a reversal in the position of the peaks. In other words, there was a decrease in value during the initial period of the phase and an increase

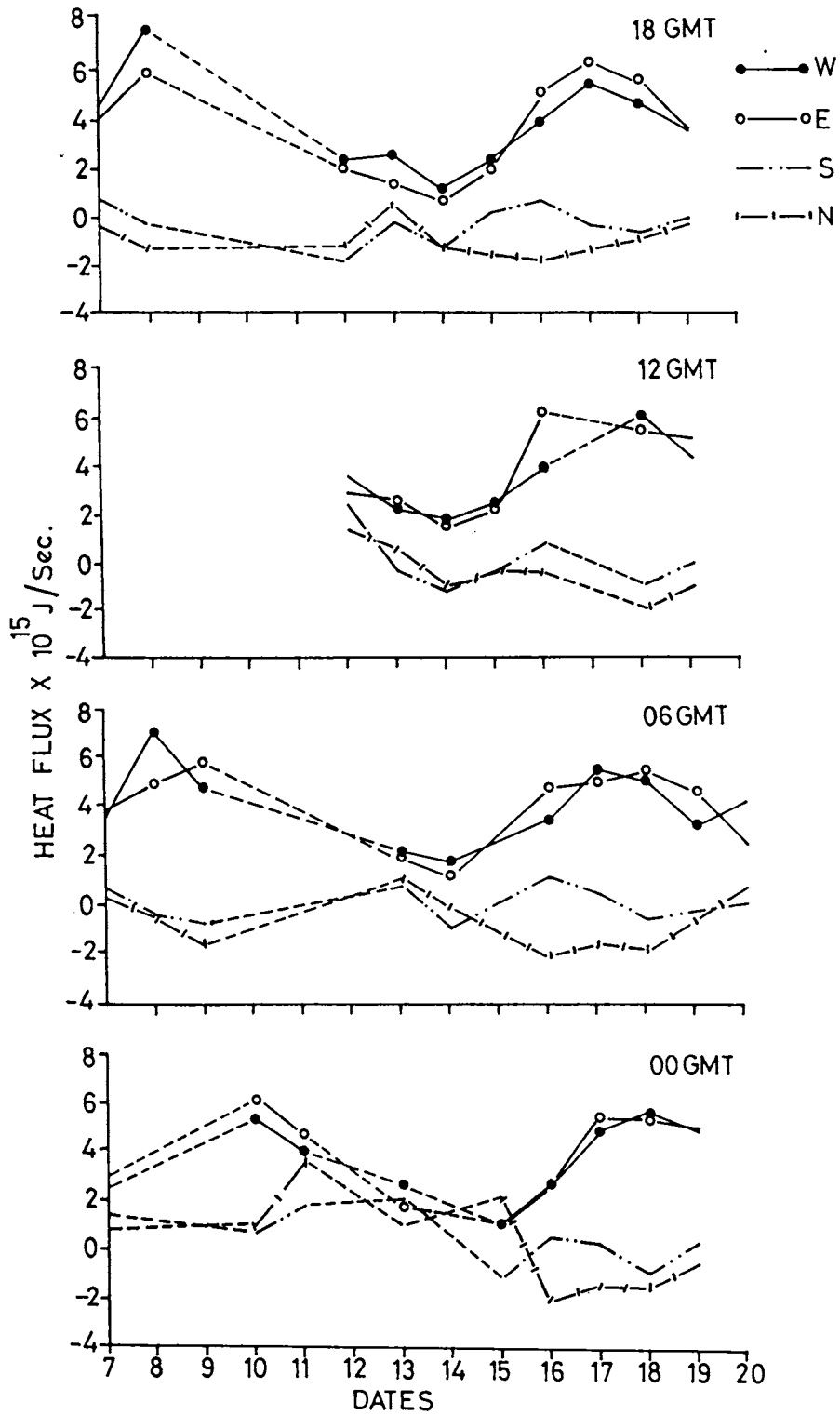


FIG.4.3(a) DAY TO DAY VARIATIONS OF HEAT FLUX DURING PHASE-I

—64907—

99

551.513 (267.34)
MEF

from 17th to 19th at the north and south walls. The 16th, 17th, 18th and 19th June were characterised by very high positive values at the zonal walls, low negative values at the north wall and low positive values at the south. The occasions of increase in the distance between the curves of fluxes of meridional and zonal walls coincided with the presence of either a cyclonic storm as on 10th or a trough of low pressure as on 18th, while the narrowing down coincided with high pressure belts. The pattern of variations were similar at opposite walls. In this phase, fluxes were positive at the zonal walls and almost always negative at the meridional walls excepting at 00 GMT.

PHASE-II

As it can be seen from Figure 4.3(b) values were very low all through the phase and especially so at the meridional walls. The pattern of variations were almost the same at all the synoptic hours. The values were relatively higher from the 3rd to 9th and the 12th to 14th at the zonal walls and decreasing from 1st to 3rd and 9th to 11th of July. At all the synoptic hours, lowest values of the phase were observed on 5th at the meridional walls. The flux values remained without much variation around 1×10^{15} J/sec at the north and south walls.

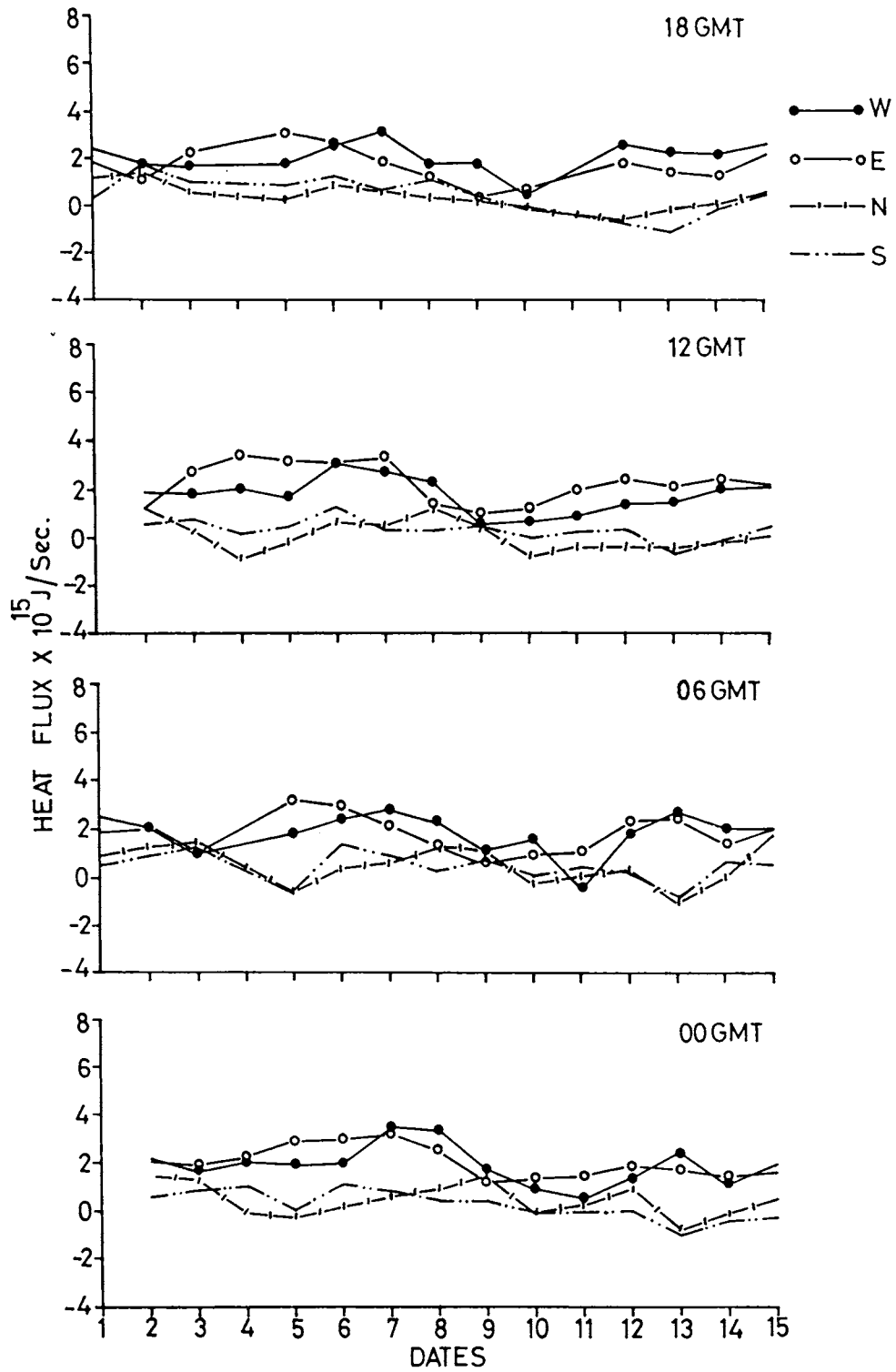


FIG.4.3(b) DAY TO DAY VARIATIONS OF HEAT FLUX DURING PHASE-II

PHASE-III

Unlike the other two phases, in this phase, there were alternate spells of negative and positive values at all the four walls and the variations were very conspicuous. An interesting feature of this period was that, except on 22nd, 23rd and 24th of May the fluxes at the zonal boundaries, were negative and relatively lesser than that at meridional walls where it was mostly positive which is contrary to that of the previous phases. At the meridional walls, except at 18 GMT, there was an increase in values from the 17th to 19th followed by a decrease upto the 24th and again an increase from 24th to 26th May. From the 26th, after a decrease upto the 28th, it increased upto the end of the phase. At 18 GMT, the pattern at the north and south walls was observed as a continuous decrease from the 18th to 24th. This pattern was almost reversed at the zonal walls upto the 26th and thereafter increased at both.

PHASE-IV

Except during the period from 2nd to 5th June, the day-to-day variations of heat flux was low. The values were mostly negative at the zonal walls at all the four timings and both positive and negative at the other two. In general, there was a peak in the positive value (divergence) on the 4th and 10th and a negative peak on the 7th at the meri-

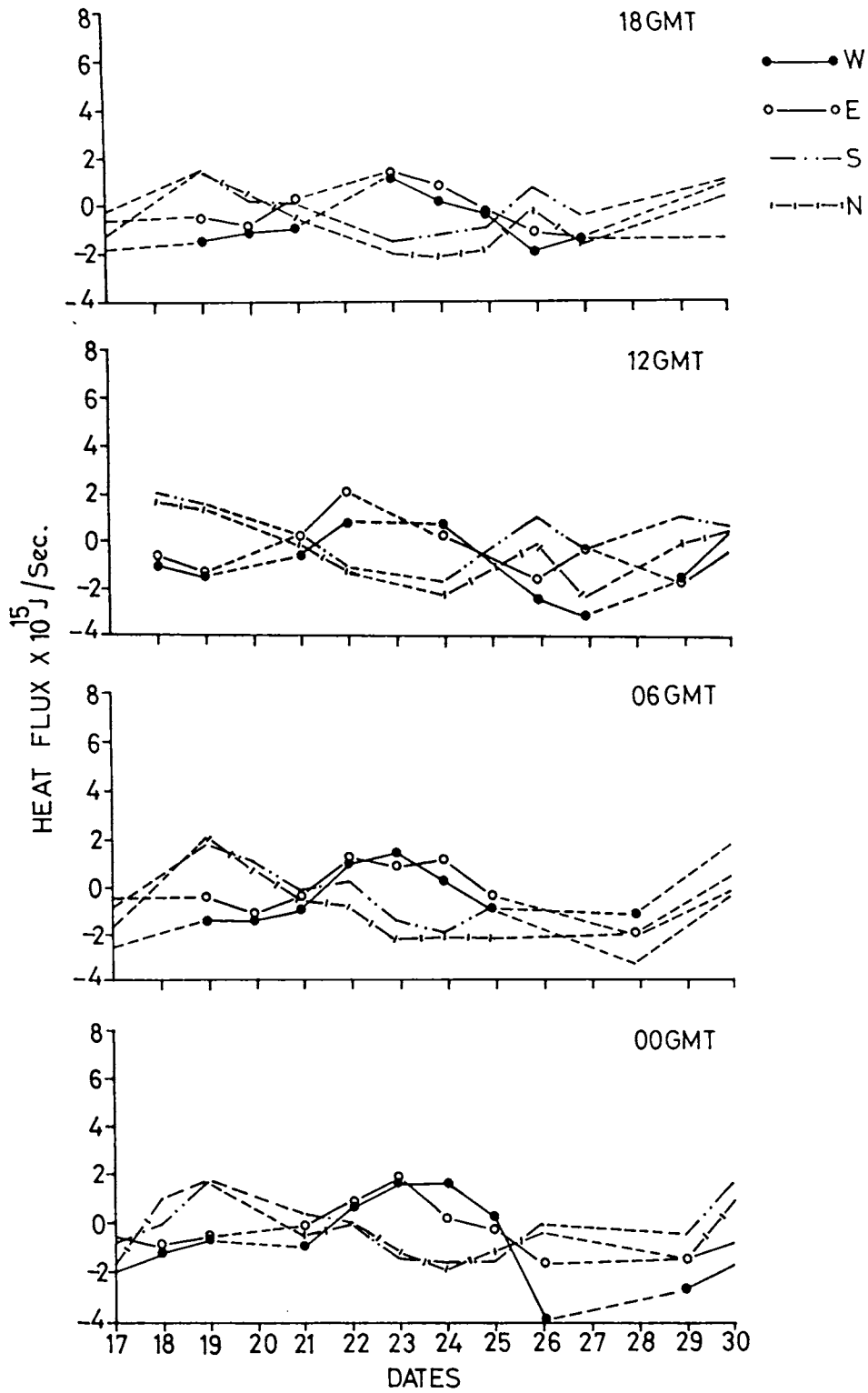


FIG.4.3(c) DAY TO DAY VARIATIONS OF HEAT FLUX DURING PHASE-III

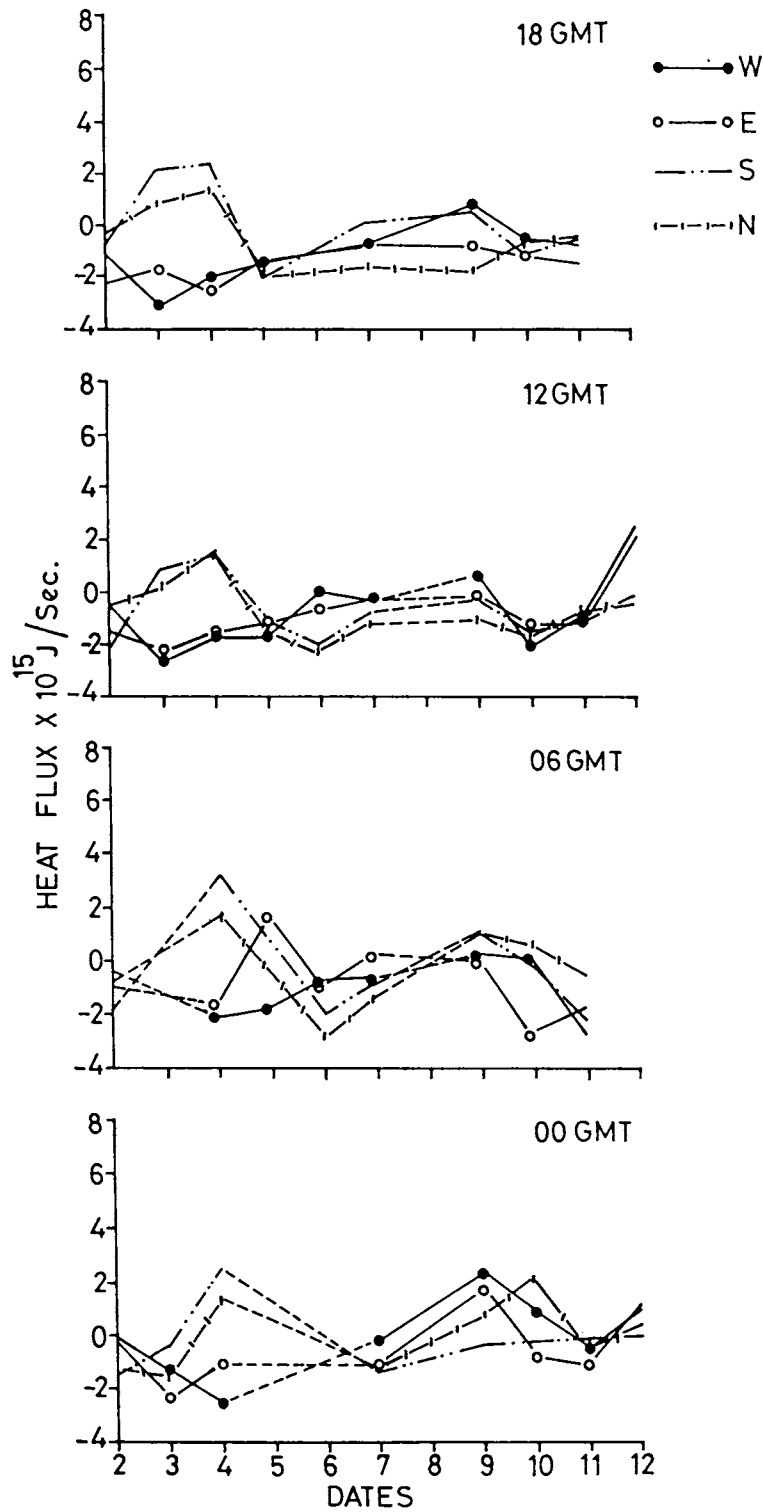


FIG.4.3(d) DAY TO DAY VARIATIONS OF HEAT FLUX DURING PHASE-IV

dional walls while the negative lowest value was on the 4th at the zonal walls. There was an increase in the heat flux divergence from 11th to 12th June at all the walls.

4.3.2 Diurnal Variation

The diurnal variation of heat flux was studied for all the days on which data was available for at least 3 synoptic hours. Figures 4.4(a) to 4.4(d) give the same for the four periods.

PHASE-I

The heat flux on the 7th, 8th and 12th of this phase, showed an increasing trend at the east and west walls and a decrease at the other two. Comparatively very high values were noted from 7th to 11th June at the zonal walls. On the 13th and 14th at 00 and 06 GMTs, it decreased at all the walls and after that increased to 12 GMT at the zonal walls and decreased at the meridionals. On both the days, except at the west wall, it decreased from 12 to 18 GMT, while on the 15th, the flux showed an increasing trend from 00 to 18 GMT at the south and zonal walls. On the 16th June, the variations were striking at all the walls and at the western wall, it increased from 00 to 18 GMT and at the other three, after increasing from 00 to 12 GMT decreased upto 18 GMT. From the 17th onwards the values more or less

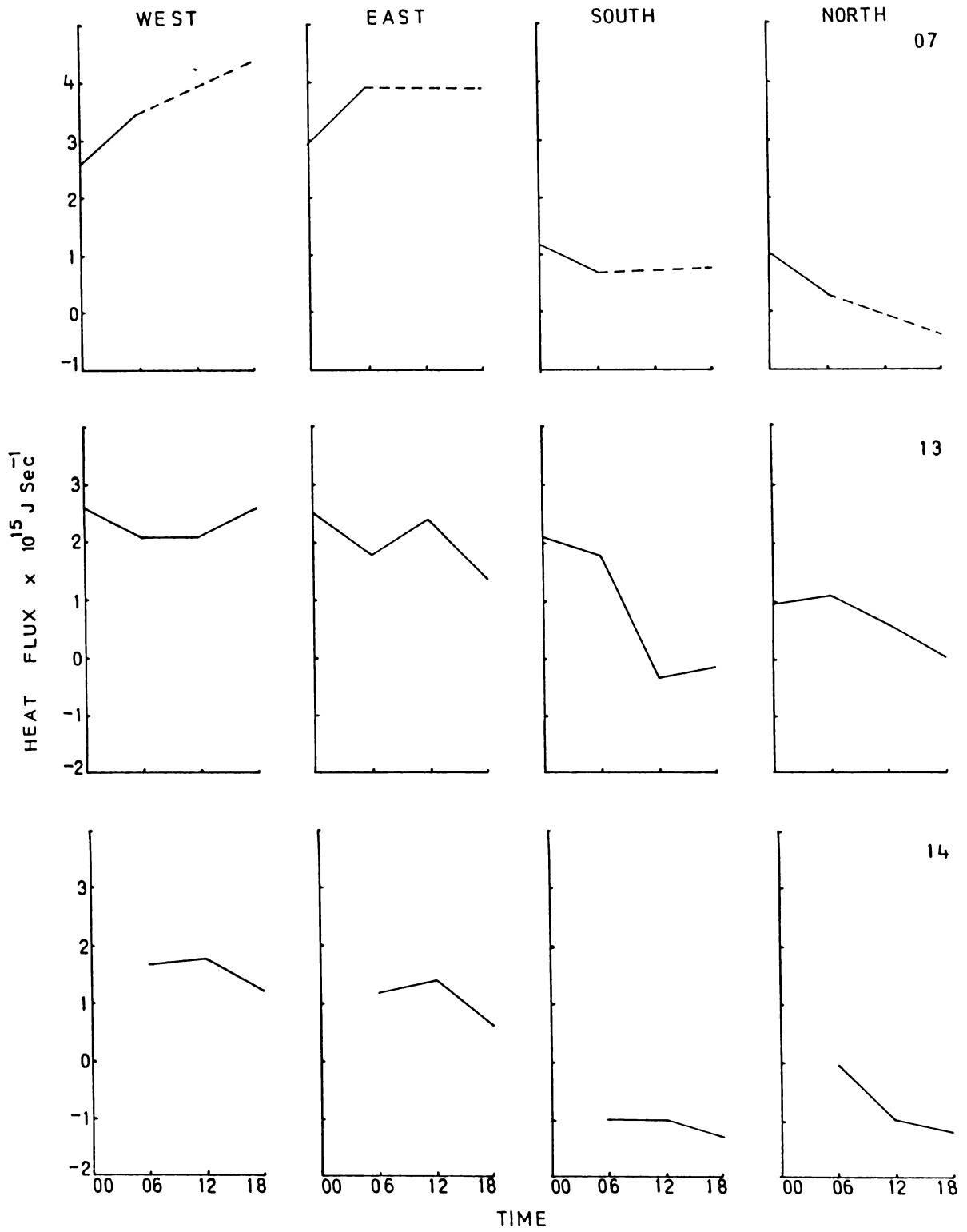


FIG.4.4(a) DIURNAL VARIATION OF HEAT FLUX DURING PHASE-I

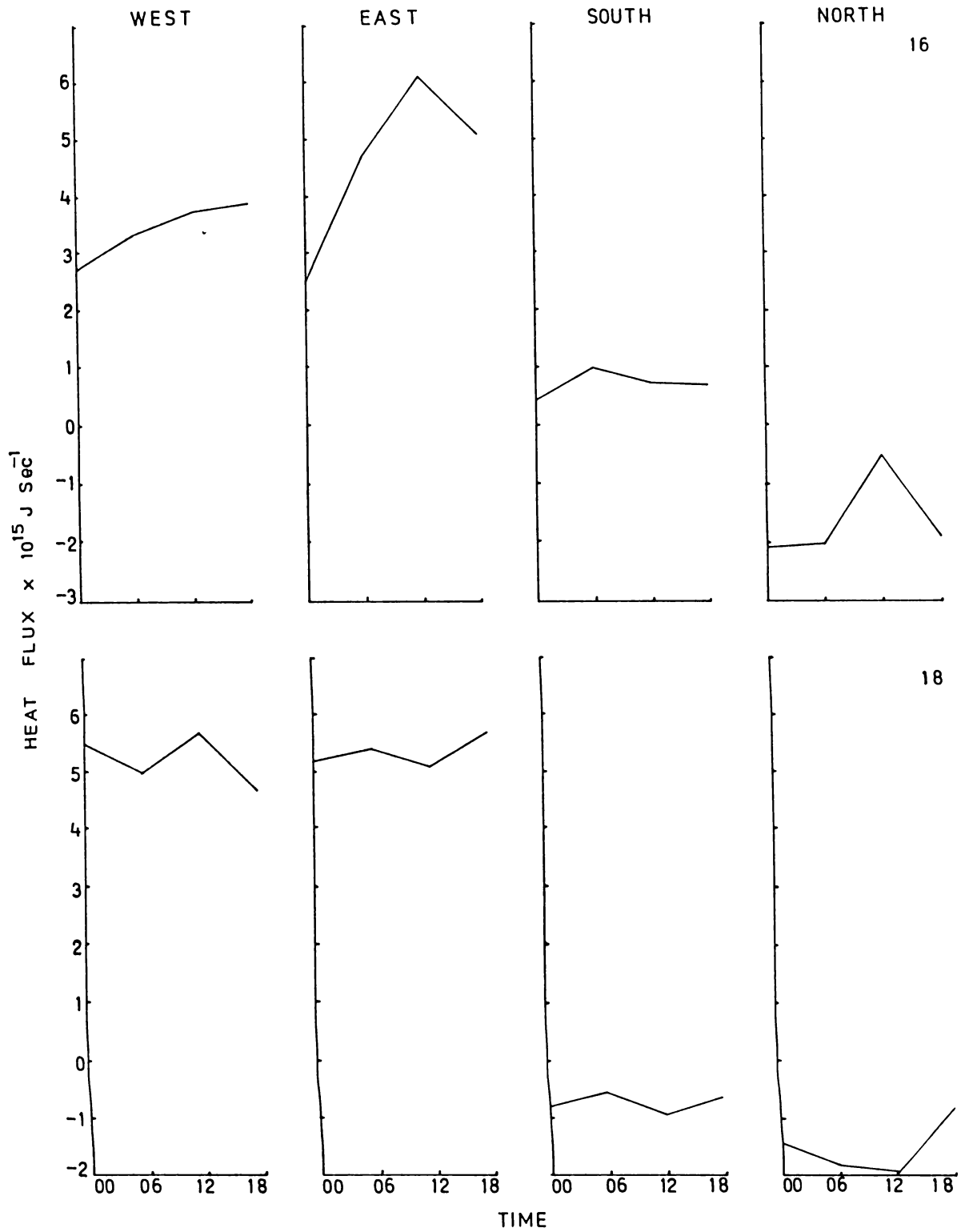


FIG.4.4(b) DIURNAL VARIATION OF HEAT FLUX DURING PHASE-I

remained near 5×10^{15} J/Secs at the zonal walls and below 2×10^{15} J/secs at the meridional walls with the variation pattern resembling sinusoidal waves. In general, the heat flux was always positive at the zonal walls and mostly negative at the meridional walls.

PHASE-II

During this Phase, the variations were much less from 1st to 8th May except on 3rd and the values were mostly positive at all the boundaries with higher values at the zonal walls. It was noted that on almost all the days, heat flux value showed an increase at the meridional walls, and it was especially so from 12 to 18 GMT, with a reverse at the zonal walls. On 3rd May the variations were more striking with a decrease from 00 to 06 and 12 to 18 GMTs and an increase in between at the zonal and southern walls while the pattern was reversed at the northern wall. On the 4th and 5th May although the variations were not prominent, the values showed an increasing trend at the meridional walls. The values were higher at the eastern wall than the western and only negative at the northern wall. This could lead us to the conclusion that, there was heat flux convergence into the area through the walls. The time of occurrence of peak values differed on all the days. On 6th July the values showed an increasing tendency while on the 8th, 9th and 10th

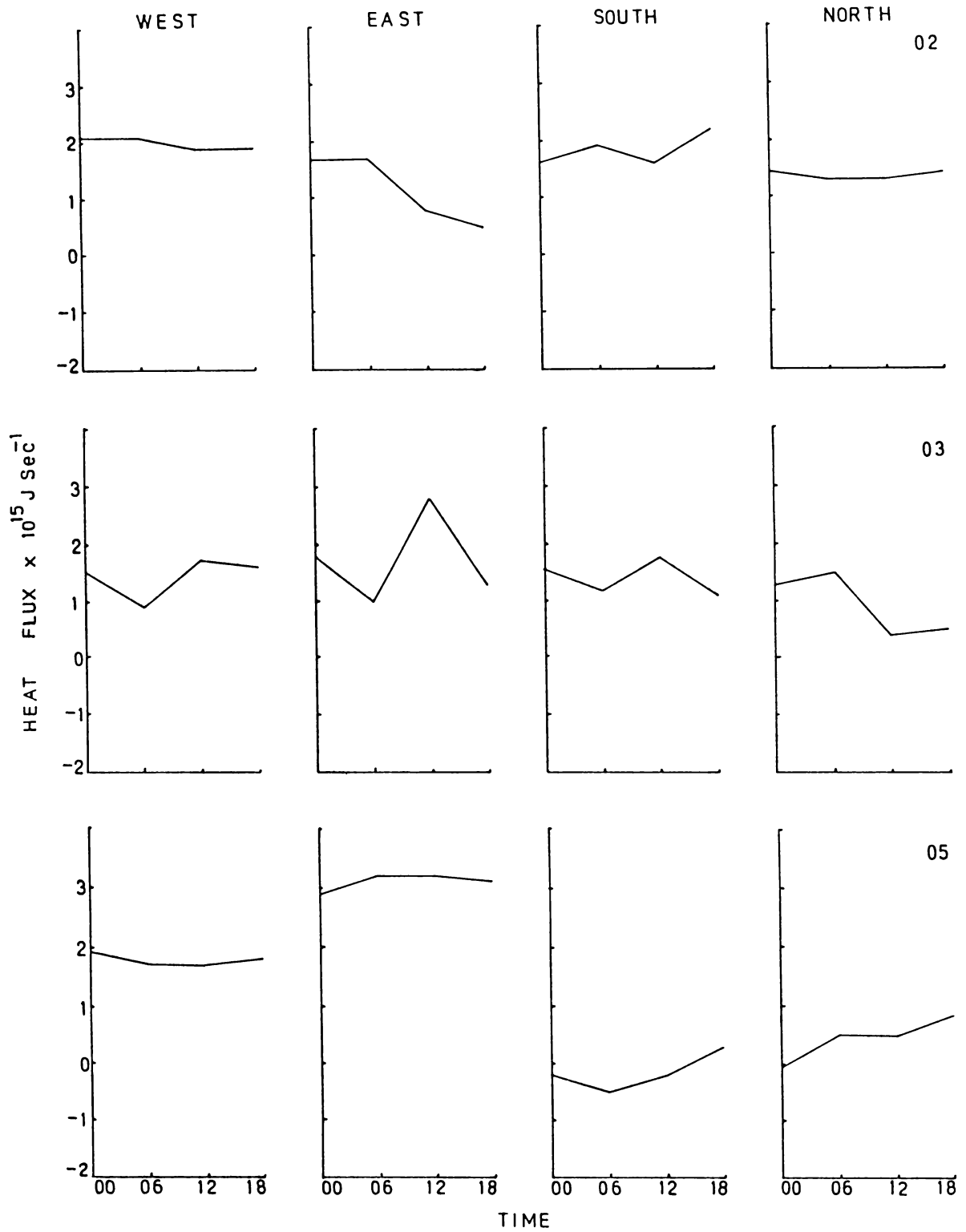


FIG.4.4(c) DIURNAL VARIATION OF HEAT FLUX DURING PHASE-II

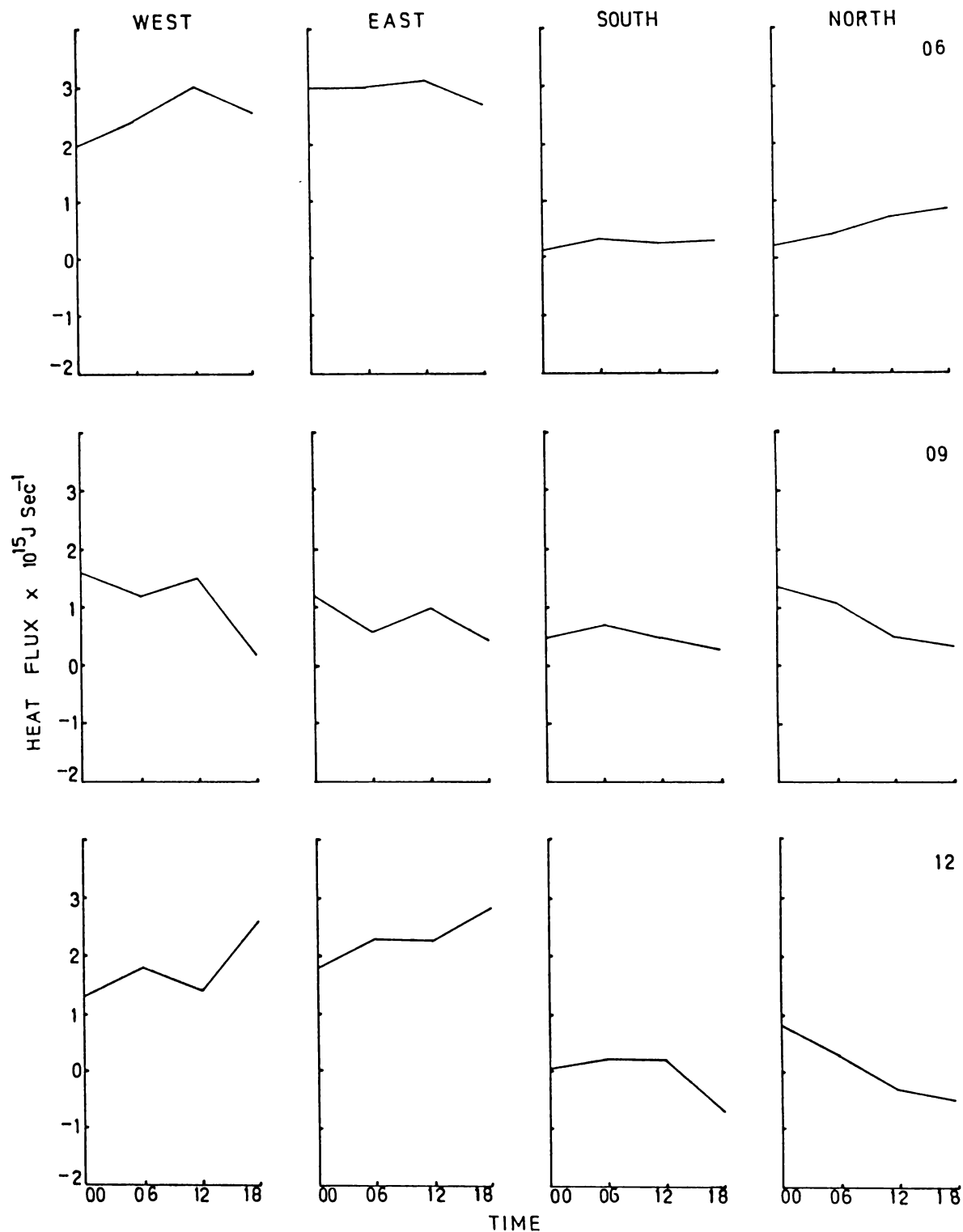


FIG.4.4(d) DIURNAL VARIATION OF HEAT FLUX DURING PHASE-II

they decreased. On the 11th the variations were exactly similar at the west and south walls with the values decreasing from 00 to 12 GMT and increasing thereafter while at the east and north walls it increased more than once during the day. The pattern of variations on the 12th at the meridional walls were exactly similar to that on 9th July and that at the zonal walls, it was reverse or in other words, values at 18 GMT were higher than that at 00 GMT. From the 13th to 15th, there were significant variations and the values remained near 2 units, (1 unit = 10^{15} J/Sec) at the zonal walls and were mostly around 1 unit at the meridional walls. On these days, there were sharp changes of around 1×10^{15} J/sec within 6 hours as can be seen at the west wall on the 13th, west, east and south walls on 14th and also at the north wall on 15th July.

In general, during this phase too, the values were only positive at the zonal walls, while at the meridional walls, there were a few days with negative values. This indicates that, while there was mostly inflow of energy at the west wall, it was outflow at the east wall and there were both inflow and outflow of energy at the other two walls.

PHASE-III

During this phase, considerable diurnal variations

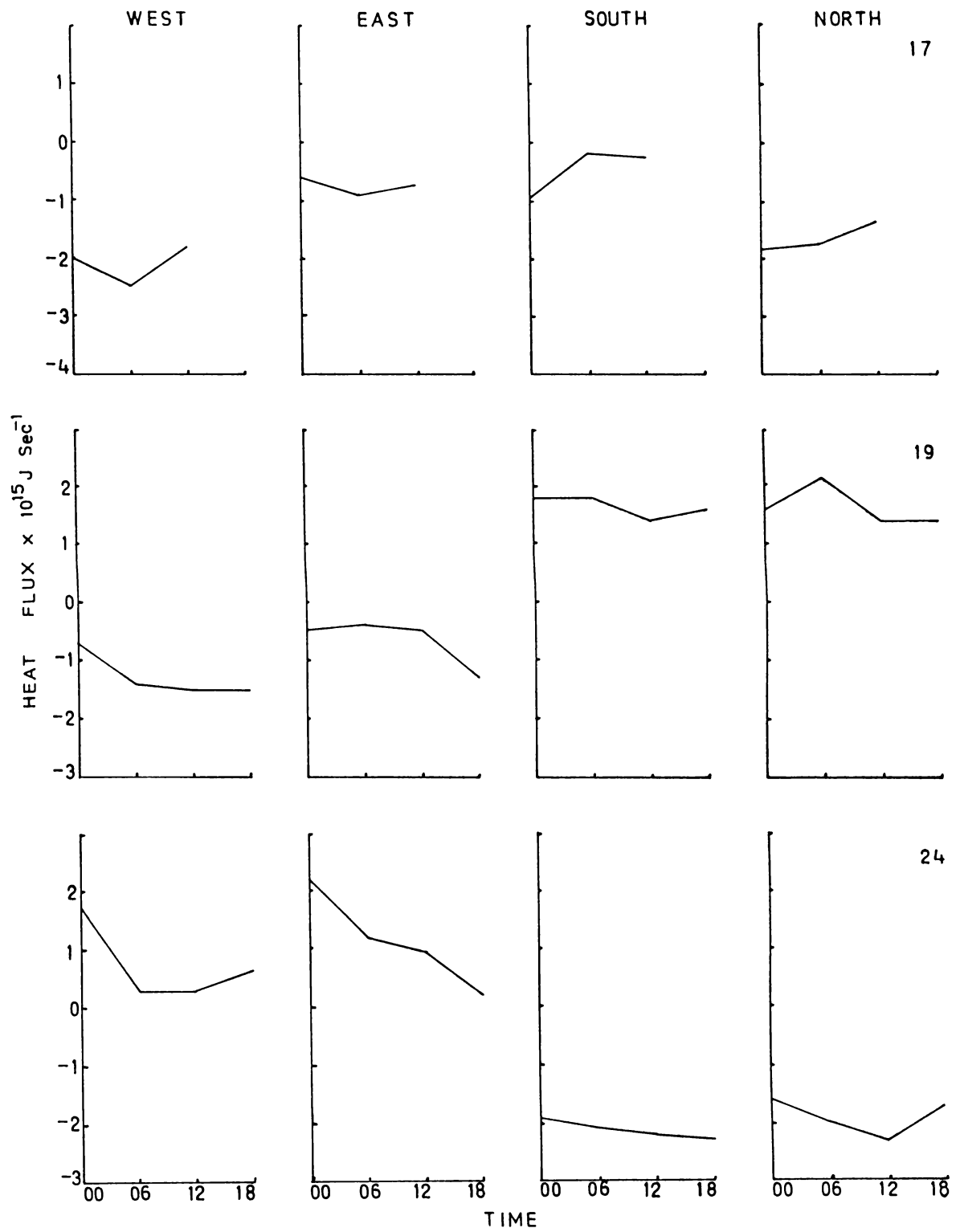


FIG.4.4(e) DIURNAL VARIATION OF HEAT FLUX DURING PHASE-III

were noticed on many days. On the 17th May, the values at 00 GMT were lesser than that at 12 GMT. It was the opposite pattern on the 19th, while on 21st May, except at the western wall, the fluxes were low, and there was an increasing tendency. On the 22nd and 30th of May, there were good variations, and it showed increasing tendency almost throughout at the zonal walls and decreasing tendency at the other two. On the 24th at all the four walls, the heat flux decreased from 00 to 18 GMT while on the 26th, except at the eastern wall, it increased throughout. The days 25th and 29th May were characterised by negative values at all the walls from 00 to 12 GMT, with highest at the northern wall. On the 25th it decreased from 00 to 06 and then increased to 12 GMT at the west and north walls while it increased throughout at a constant rate at the eastern boundary.

PHASE-IV

In Phase-IV, heat flux was mostly negative at all the walls with some exceptions at the meridional walls. Although the values showed good diurnal variation, the pattern was rather simple with either an decreasing trend like that at the zonal walls or an increasing tendency as that at the meridional walls on the 2nd, 3rd, 4th and 12th June. On the 7th and 9th at the western wall, it decreased from 00 to 06 GMT and 12 to 18 GMT and increased in between.

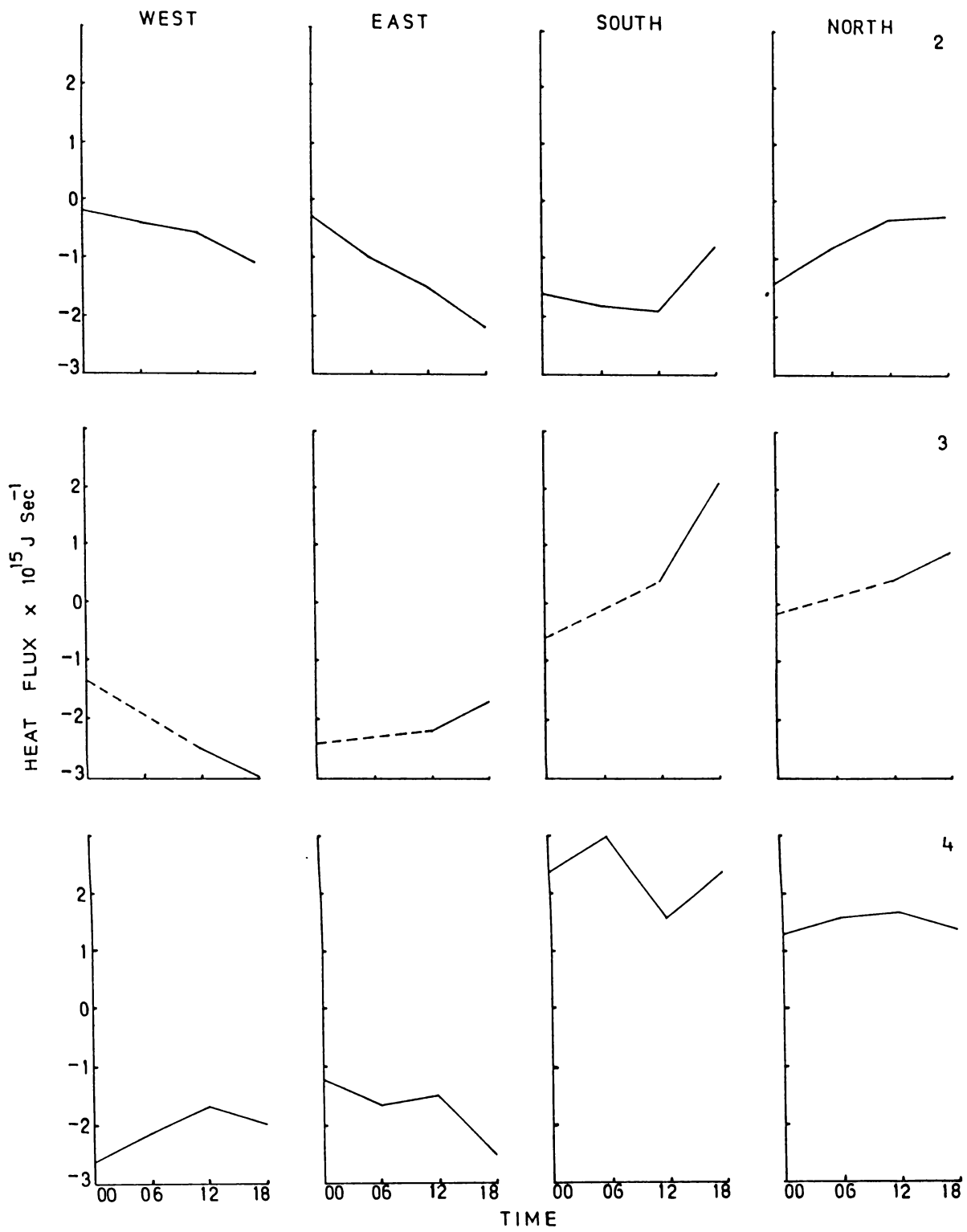


FIG.4.4(f) DIURNAL VARIATION OF HEAT FLUX DURING PHASE-IV

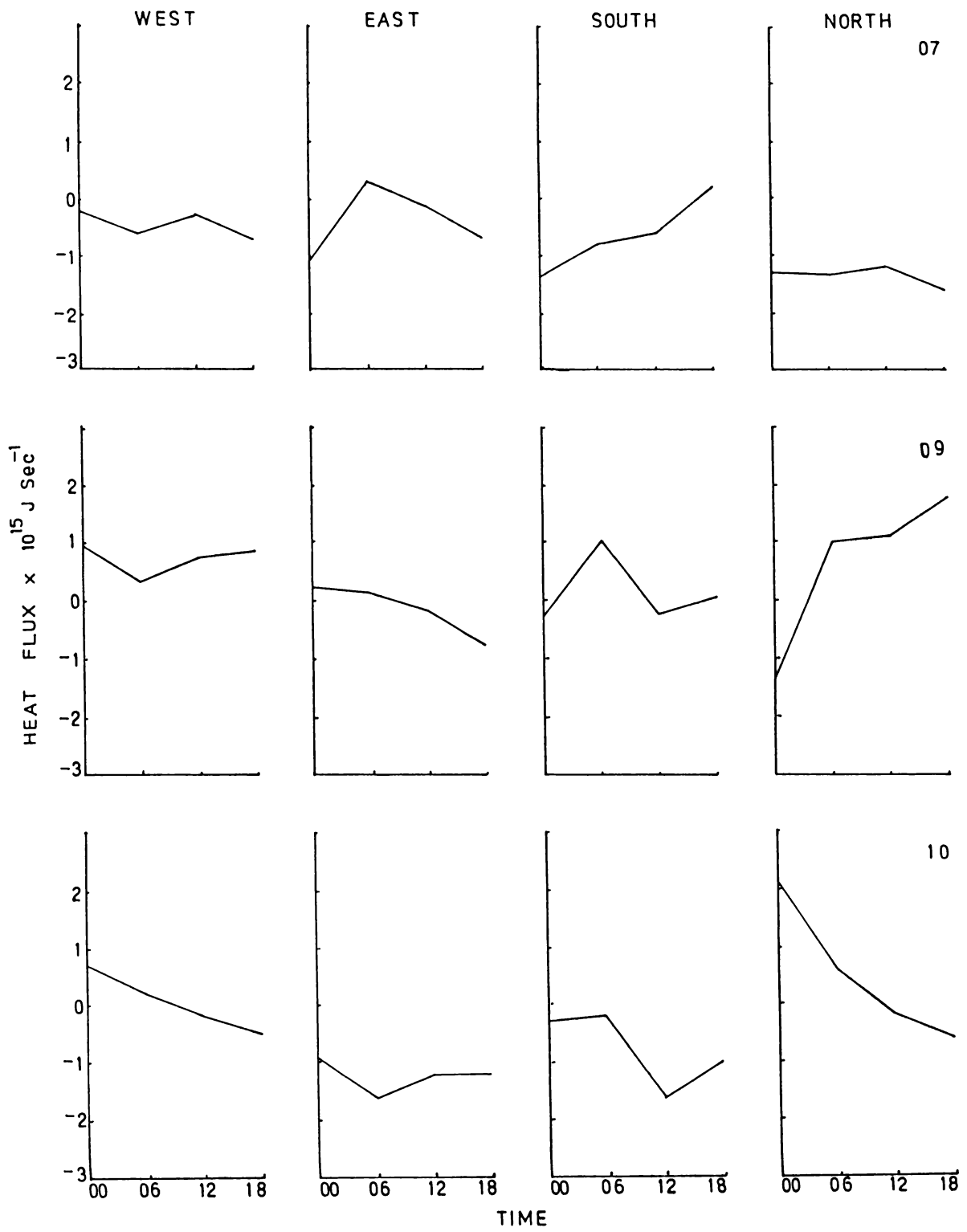


FIG.4.4(g) DIURNAL VARIATION OF HEAT FLUX DURING PHASE-IV

At the eastern wall on 7th June heat flux initially increased upto 06 GMT and thereafter decreased, while it kept on increasing from 00 to 18 GMT at the southern wall and there was not much variation at the west and north walls. Heat flux, decreased from 00 to 18 GMT through the eastern wall and changed from negative to positive value at the northern wall on 9th. At the respective southern wall it was an increase from 00 to 06 and 12 to 18 GMT while it was the reverse at the western wall. Heat flux decreased all through at all the walls on the 10th. On 11th June, it increased at the meridional walls and decreased at the zonal walls from 00 to 06 GMT and 12 to 18 GMT, while on 12th, it increased at the zonal and south walls.

4.4 HEAT FLUX DIVERGENCE

The parameter discussed in this section gives the actual rate of dry static energy being brought into or out of the polygon area. As explained in the section 3.3, for net moisture flux, this too was obtained as the sum of the differences between the heat flux at the opposite walls. Hence if it is of the same sign at the opposite walls, the value comes down or in other words, if there is influx at the west and south walls and outflow at the other two, the amount of heat converged or diverged into the area would be much less and vice versa.

4.4.1 Day-to-day Variations

Figure 4.5(a) to 4.5(d) show the daily variations of the divergence of net heat flux at the four polygon positions for individual synoptic hours.

PHASE-I

At 00 GMT, it was heat divergence from 7th to 11th June and convergence after the 15th upto the 20th. At the other three synoptic hours, it was the reverse of the above condition upto the 13th and thereafter peaks of convergence as well as divergence were noticed. It was convergence on the 7th, 8th and 9th at 06 GMT and from 7th to 13th at 18 GMT. In general, convergence of heat flux predominated this phase. The presence of a cyclonic circulation in the vicinity of the polygon area could have been the reason for this.

PHASE-II

In this phase, the heat flux values were almost always less than 1×10^{15} J/sec. In general, neither convergence nor divergence dominated except at 12 GMT when it was mostly divergence. The values were lower at all the synoptic hours especially in the period from the 6th to 10th July. The highest amount (-1.3×10^{15} J/Sec) of heat converged at

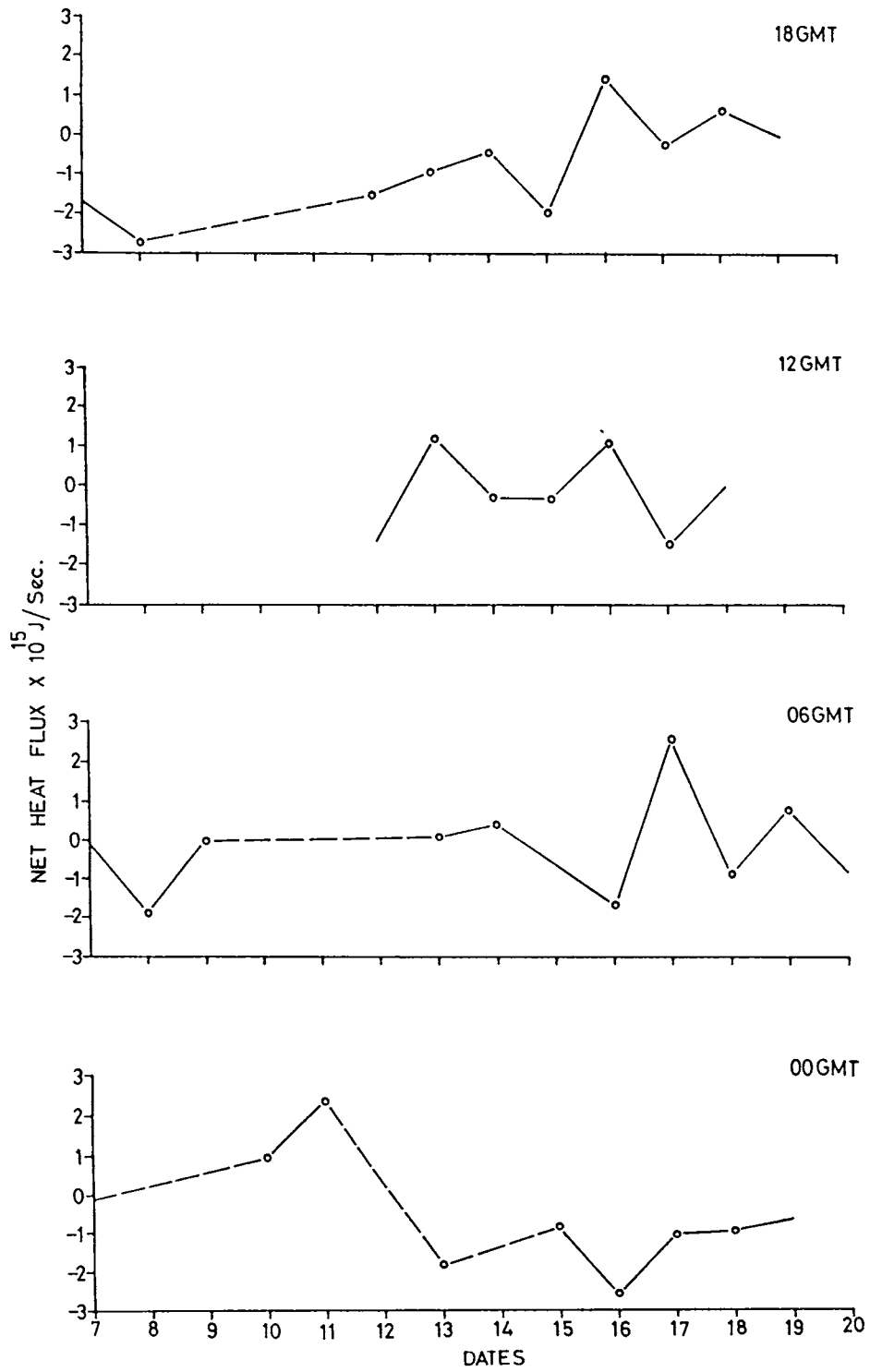


FIG.4.5(a) DAY TO DAY VARIATIONS OF NET HEAT FLUX DIVERGENCE DURING PHASE-I

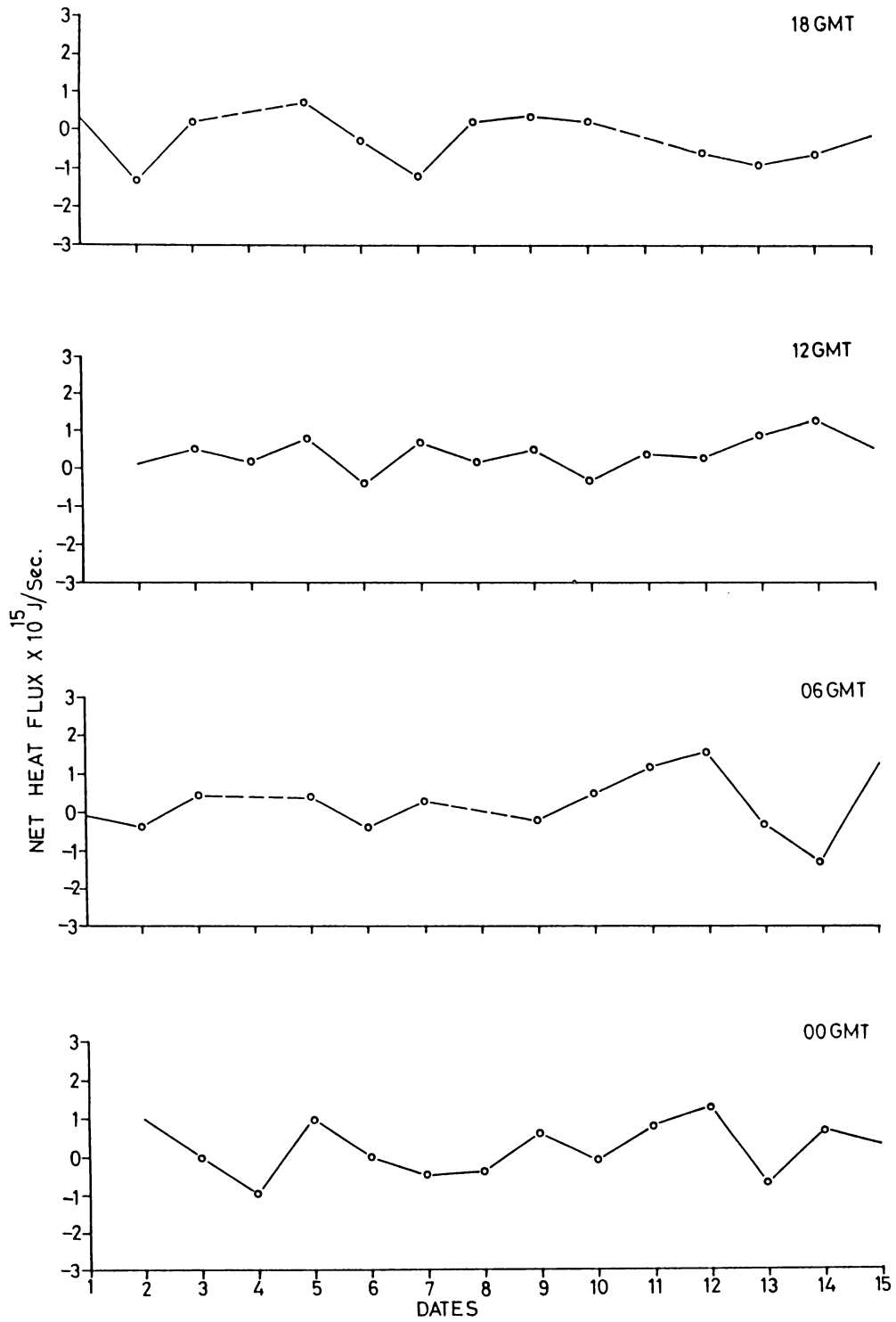


FIG.4.5(b) DAY TO DAY VARIATIONS OF NET HEAT FLUX DIVERGENCE DURING PHASE-II

18 GMT on the 2nd and 7th July and diverged ($1.6 \times 10^5 \text{ J/Sec}$) at 06 GMT on 12th July.

PHASE-III

It was seen that, during this phase heat flux divergence dominated at all the synoptic hours except 18 GMT. At 00 GMT, heat flux diverged from the polygon area on all the days other than 19th and 25th May, when it was marginal convergence. There were steep rises in the total net heat flux divergence on many days, like that on 25th, when the value increased from $-0.15 \times 10^{15} \text{ J/Sec}$ to $2.6 \times 10^{15} \text{ J/Sec}$ and on 26th at 00 GMT. From 17th to 21st May it was heat flux divergence from the polygon area, with varying magnitudes, at all the synoptic hours except 18 GMT. At 06 and 12 GMTs the net flux convergence increased from the 21st to 23rd. On 24th May it was divergence while on the 25th it was characterised by good convergence of heat at 06 and 12 GMTs. From 23rd to 26th May, there were large day-to-day variations with the values changing from positive to negative more than once in this period. After the 26th, the values increased upto the 30th at the 06, 12 and 18 GMTs.

PHASE-IV

The day-to-day variations in the amount of heat flux diverged from the polygon area was well marked in this

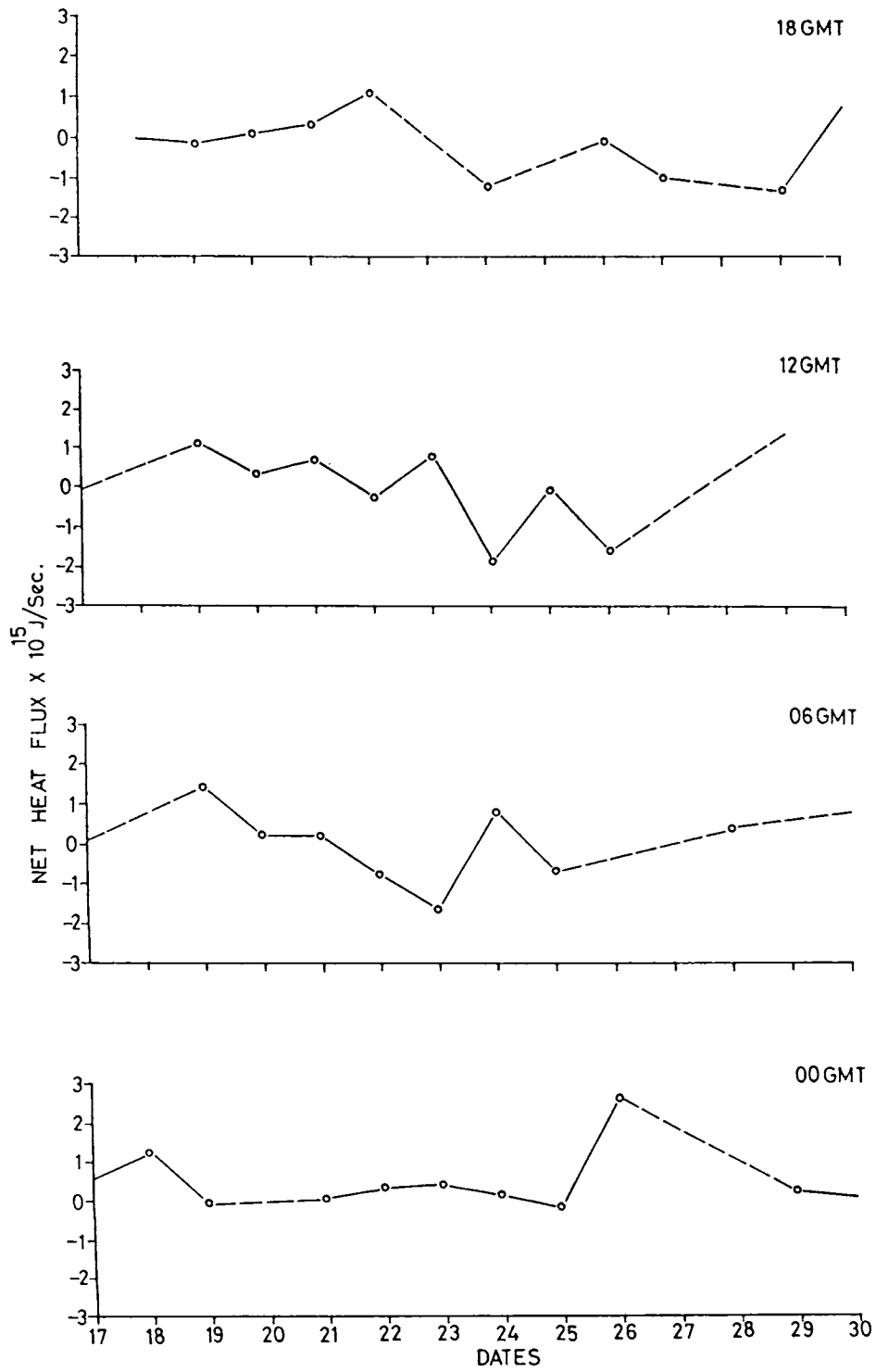


FIG.4.5(c) DAY TO DAY VARIATIONS OF NET HEAT FLUX DIVERGENCE DURING PHASE-III

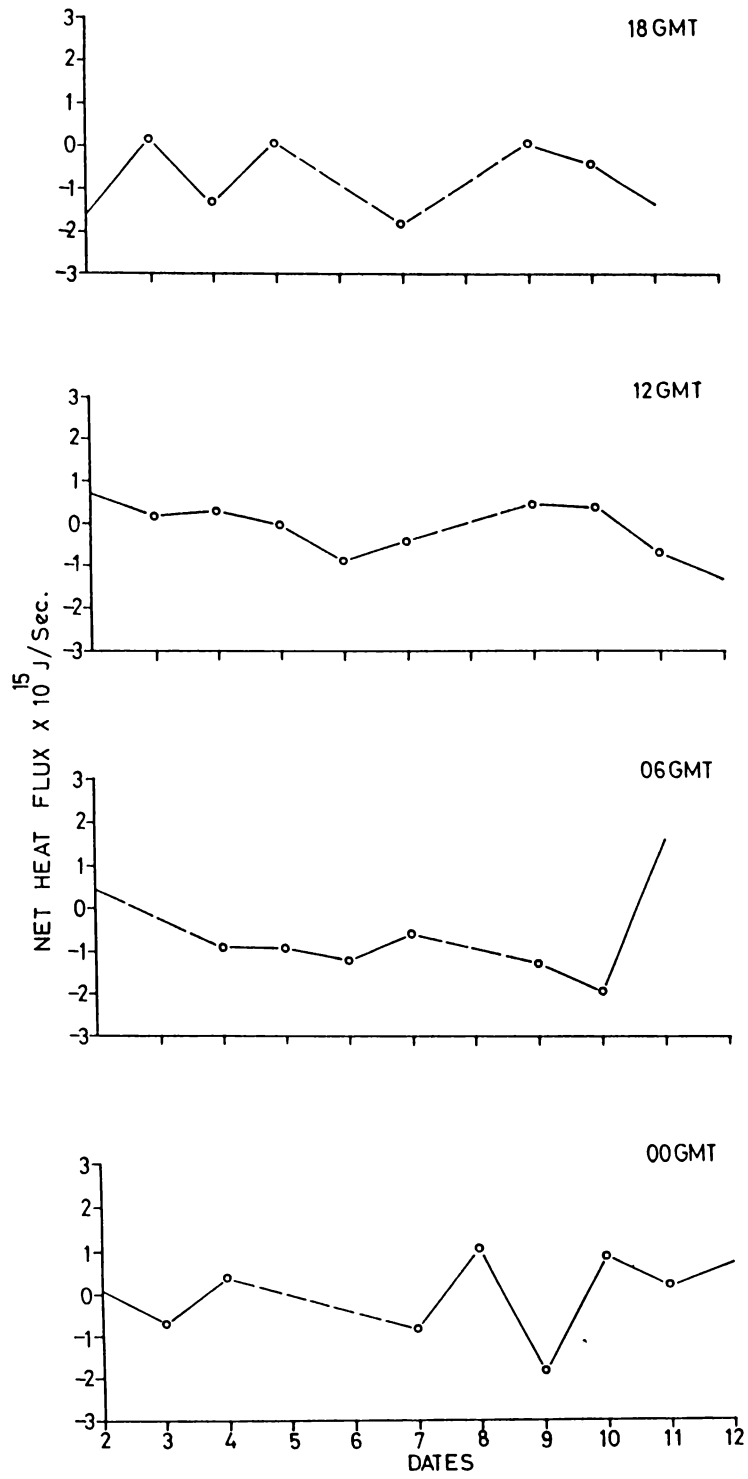


FIG.4.5(d) DAY TO DAY VARIATIONS OF NET HEAT FLUX DIVERGENCE DURING PHASE-IV

phase. Almost always, the values changed from positive at 00 GMT to negative at 18 GMT. At 06 GMT, it was convergence on more number of days with exception on the 2nd, 11th and 7th June and at 12 GMT, it was spells of divergence and convergence. At 18 GMT, however, it was good convergence and marginal divergence on alternate days starting with convergence on the 2nd.

4.4.2 Diurnal Variation

Figures 4.6(a) to 4.6(d) exhibit the diurnal variation of net heat flux divergence at the four polygon positions during the respective phases.

PHASE-I

The diurnal variation of total heat flux was quite marked during this phase. On 7th and 14th of June it decreased from 00 to 18 GMT while on the 19th it was the reverse. The variations were similar on the 13th, 15th and 16th June showing an increasing trend from 00 to 12 GMT and decreasing thereafter. On the 18th this pattern was reversed while on the 17th the decrease was only upto 06 GMT and it increased after that. On most of the days, convergence of heat in varying magnitudes were observed, with exceptions on 13th and 16th. There are only single peaks in the values on many of the days.

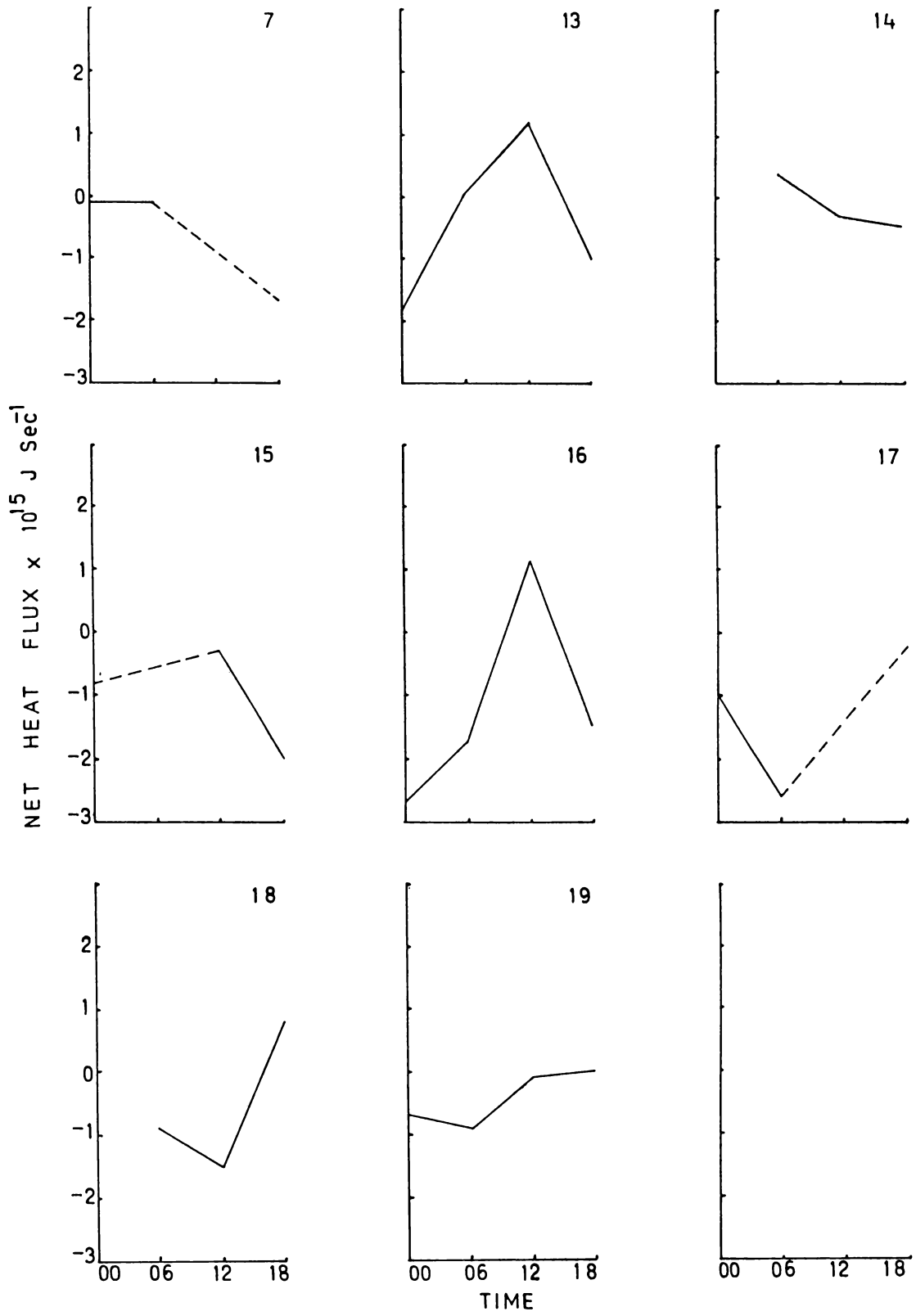


FIG.4.6(a) DIURNAL VARIATION OF NET HEAT FLUX DIVERGENCE DURING PHASE-I

PHASE-II

During this phase, although the values were lower than that of the previous period, the variations were well marked. Most of the days showed variations with two peaks, but there were few days with steady decrease, as on 12th July. Sudden transitions from convergence to divergence and viceversa in between two synoptic hours were also noticed on many days like the 2nd, 7th, 9th, 10th, 13th, 14th and 15th of July. Both heat convergence as well as divergence were present on all the days, except the 5th, on which the values were always positive and the 6th on which the values were only negative. The highest value observed in this phase was 1.4×10^{15} and -1.4×10^{15} J/Sec.

PHASE-III

In this phase, heat flux values exhibited good diurnal variations and the values were much higher, above 10^{15} J/Sec on many occasions. From 17th to 22nd May, it was mostly heat flux divergence during the four synoptic hours. The extremely high value of 2.6×10^{15} J/Sec observed at 00 GMT on 26th is noticeable. The sudden transitions from positive to negative were also noticed on certain days such as the 22nd, 23rd, 24th and 30th of May. On quite a few days, the heat flux changed from convergence to divergence or vice versa more than once during a day.

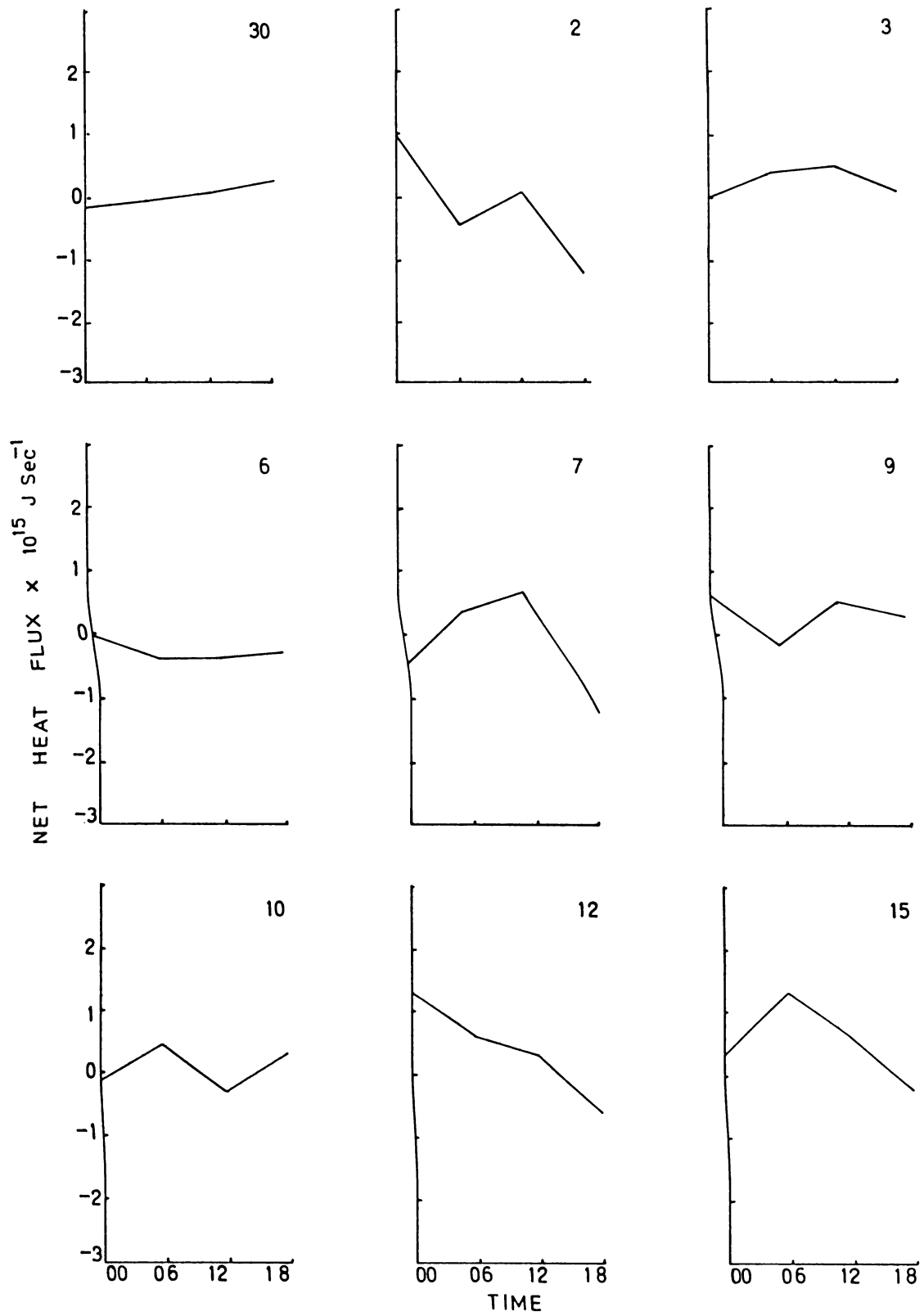


FIG.4.6(b) DIURNAL VARIATION OF NET HEAT FLUX DIVERGENCE DURING PHASE-II

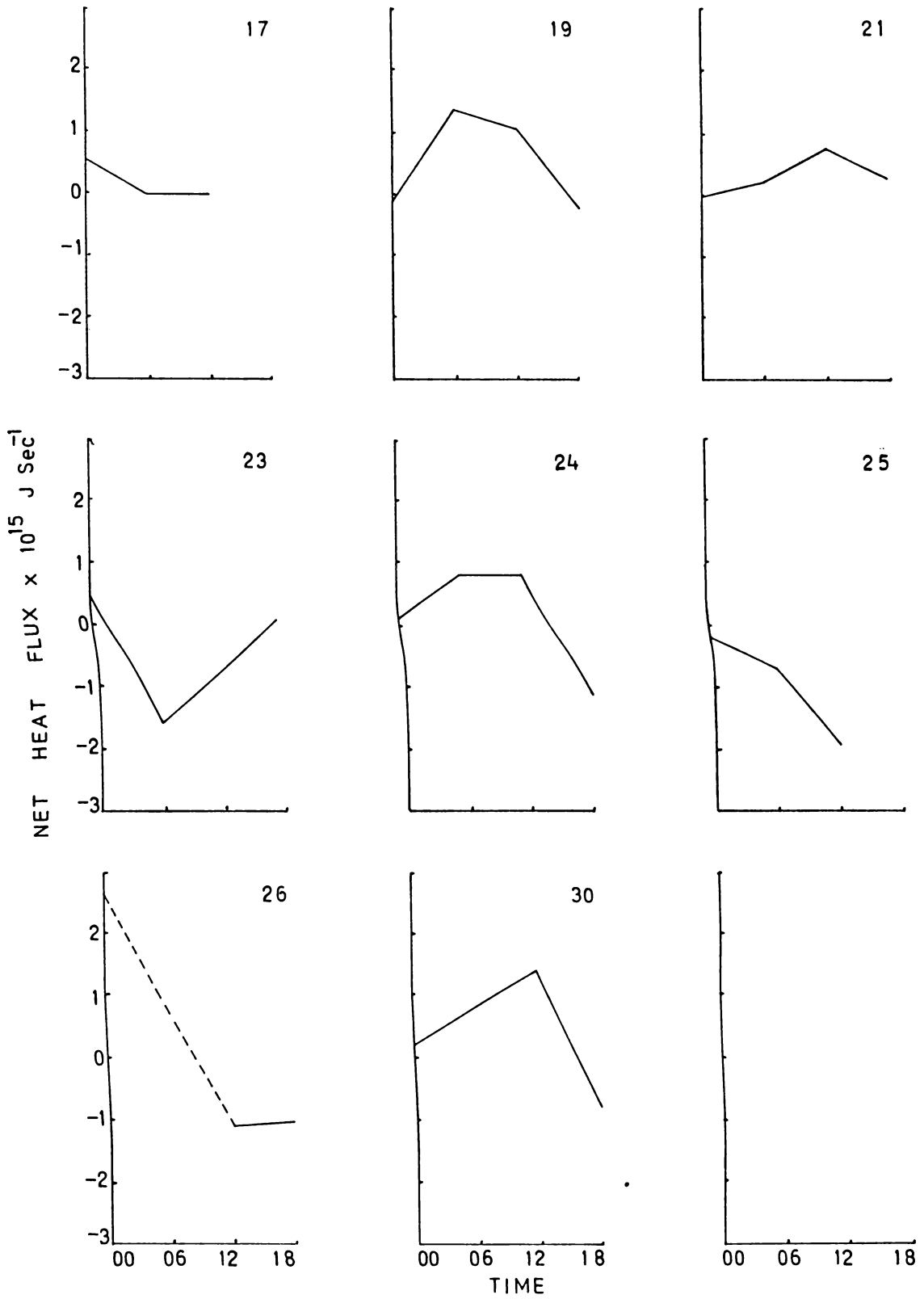


FIG.4.6(c) DIURNAL VARIATION OF NET HEAT FLUX DIVERGENCE DURING PHASE-III

PHASE-IV

The variations were similar to that in the IInd phase. On almost all the days in this phase, one could find the transition from divergence to convergence or vice versa, between 06 and 12 GMT hours. The divergence values were of lesser magnitudes than the convergence values. On the 2nd and 9th June there was an increasing trend in the magnitude of divergence from 00 GMT upto 12 GMT and thereafter a decrease. While on the 7th and 11th, the increase was only upto 06 GMT. Some days like the 4th and 10th June, showed two peaks of divergence at 00 and 12 GMTs. The above discussions are pertained to the diurnal variation of the total heat flux as a combined effect of the four walls.

4.5 AVERAGE NET HEAT FLUX DIVERGENCE

Figure 4.7 shows the daily variation of average total heat flux diverging from the Polygon areas I to IV. This was obtained as an average of the total net heat flux at the four synoptic hours. It was found that, the signs of this flux is exclusively determined by the wind directions. As such, these heat fluxes do not strictly follow the temperature pattern. It should be noted here, that this parameter refers to the average rate of accumulation or depletion of dry static energy into the polygon area.

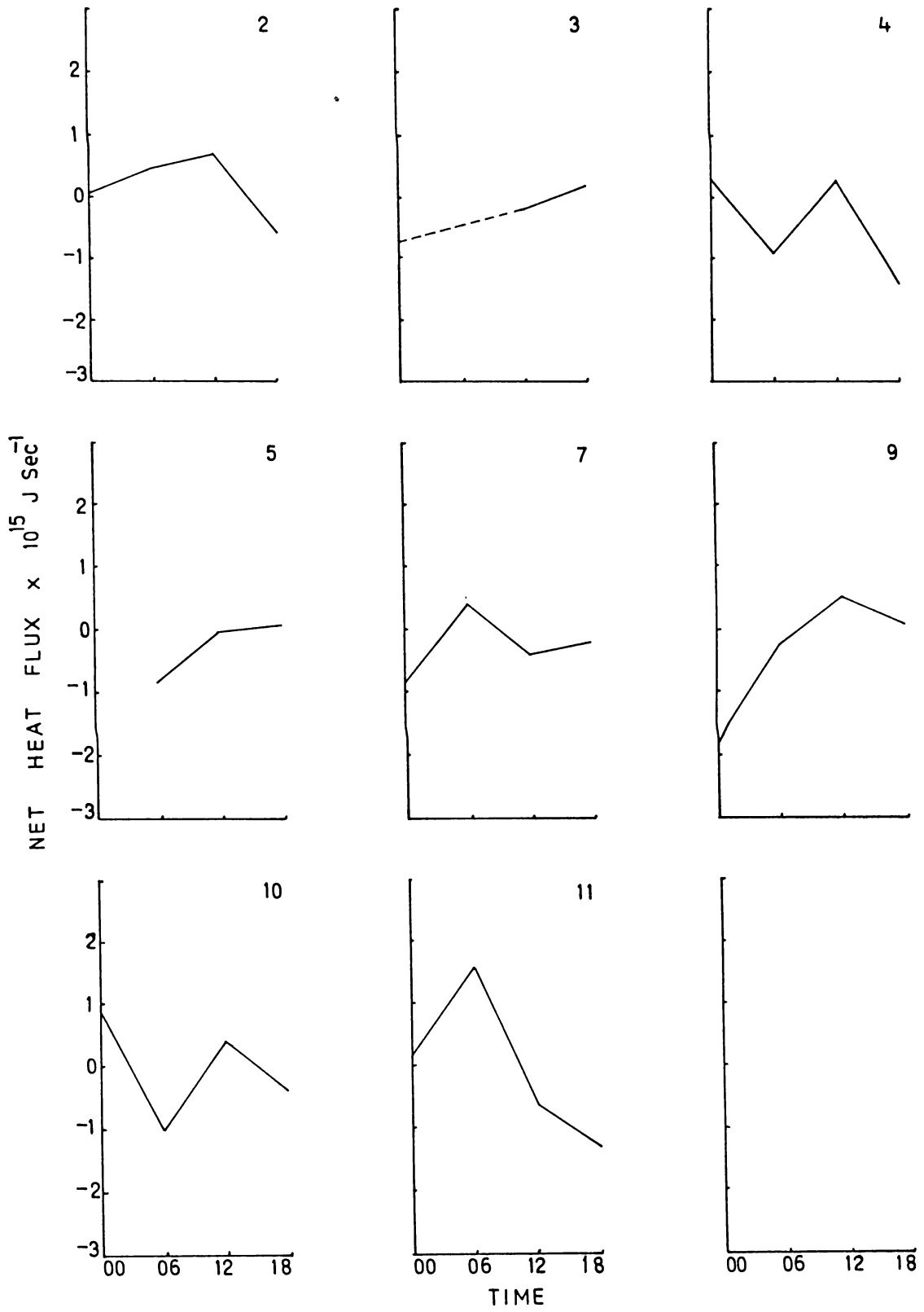


FIG.4.6(d) DIURNAL VARIATION OF NET HEAT FLUX DIVERGENCE DURING PHASE-IV

PHASE-I

An average picture showed that, it was net convergence of total heat flux at the first polygon area except on the 10th and 11th June. It could be seen that the values are much higher in this period with the highest positive values, of 2.4×10^{15} J/Sec on 11th and negative of 2.3×10^{15} J/Sec, on 8th June. The divergence increased from the 8th to 11th June and after that fell steeply to good convergence to the 12th. After the 12th, it was a wavy pattern with convergence decreasing and increasing alternately.

PHASE-II

The average heat flux divergence and convergence values were much lower and less than 10^{15} J/Sec. The highest value of heat divergence was observed on 12th July with 0.8×10^{15} J/Sec and that of convergence was on 5th with 0.4×10^{15} J/Sec. In this phase, divergence was present on more number of days.

PHASE-III

From the initial part of this period, it was divergence upto 23rd May. The net heat flux divergence after an increase from the 17th to 18th, decreased upto 23rd May. From the 23rd upto 30th it was alternately, convergence and divergence respectively.

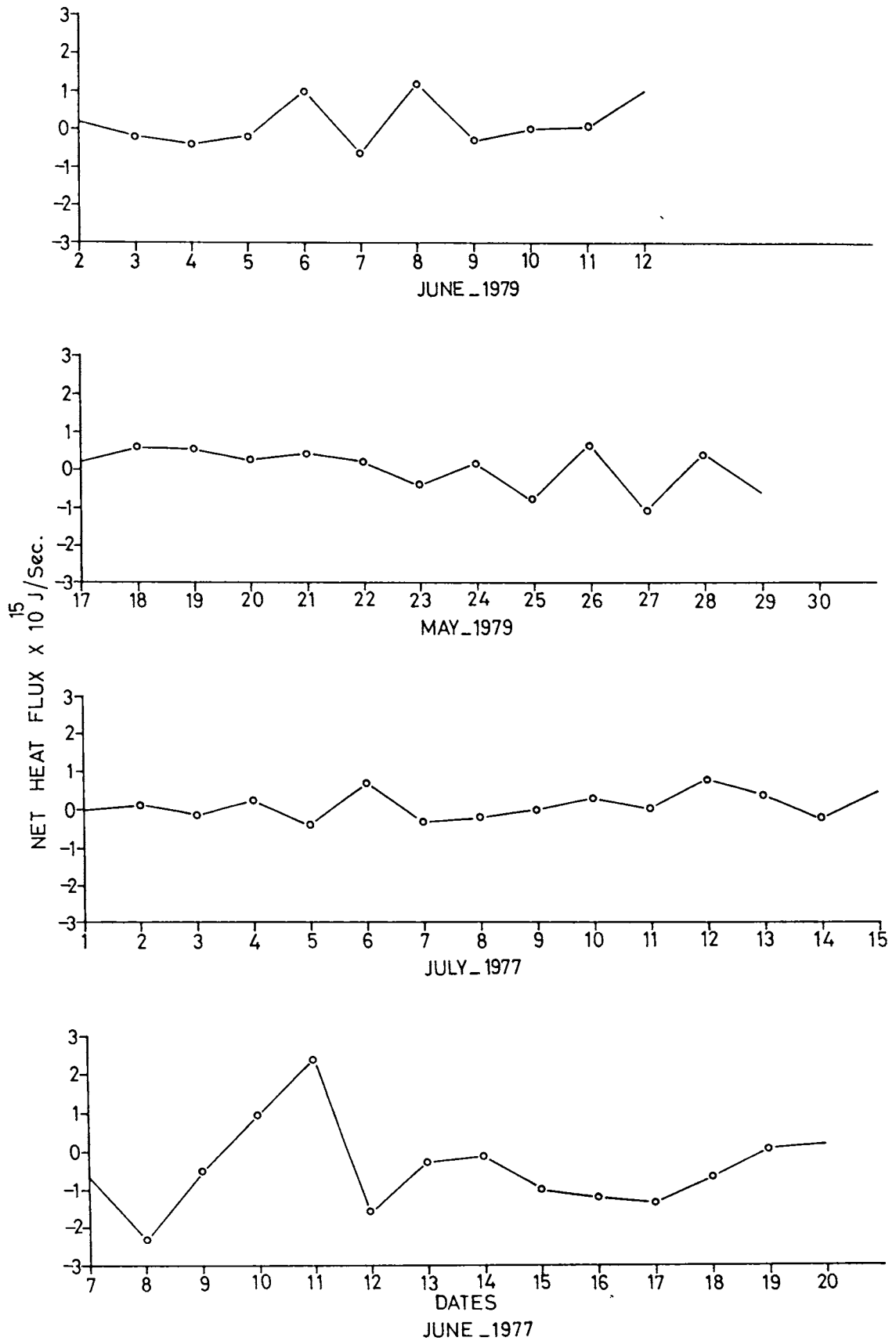


FIG.4.7 DAY TO DAY VARIATIONS OF AVERAGE OF NET HEAT FLUX DIVERGENCE DURING THE FOUR PHASES

PHASE-IV

Unlike Phase-III, it was convergence in the former part of this phase and later on, convergence and divergence alternated.

4.5 RADIATIVE HEATING

This term is obtained as a residue of the heat budget computations. As described in section 1.5, it is the difference between the sum of the sensible heat, heat flux divergence, and the heat of condensation. Radiative heating at all the four timings are combined to give the mean values for a given day. Negative values indicate cooling.

4.5.1 Day to day Variations

Figure 4.8 project the day-to-day variations of above parameter for all the phases. During the Phase-I it was seen that the pattern was almost the reverse of that of the average total heat flux divergence discussed in the previous section. On most of the days, it was radiative heating. The variation was most prominent between the 8th and 12th June, when it changed from maximum cooling (-2.2×10^{15} J/Sec) on the 11th secondary heating maximum on 12th. After 12th, it decreased upto the 14th and then increased to 17th June. From the 17th, it decreased to the 19th and again increased.

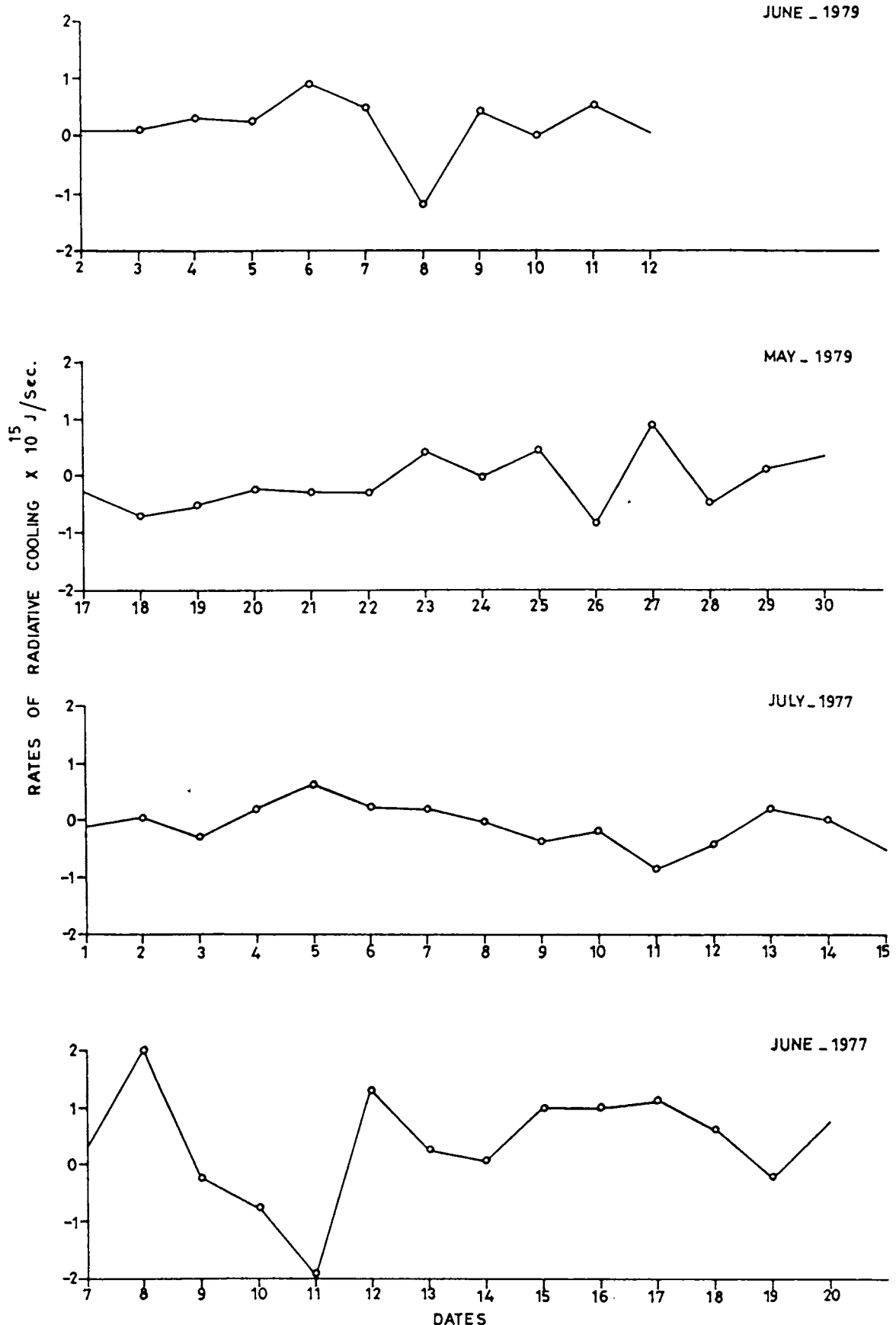


FIG.4.8 DAY TO DAY VARIATION OF RATE OF RADIATIVE COOLING

In the second phase, except on the 5th and 11th July the values were much lower than that of the previous phase and on many days less than 0.5×10^{15} J/Sec. Except from the 4th to 8th, it was mostly radiative cooling during this phase. The highest value (0.7×10^{15} J/Sec) was observed on the 5th and the lowest of -0.8×10^{15} J/Sec on 11th July.

Cooling was observed on more number of days during the third period. From 17th to 22nd of May, it was radiative cooling with not much difference in magnitudes. From 23rd onwards, it was alternately days of heating and cooling. The highest rate of heating was obtained on the 27th and the lowest on 26th May.

Unlike in the IIIrd phase, in this phase it was heating on all the days except 8th and 10th June although on the 2nd, 3rd and 12th it was only marginal. The values were almost always around 0.25×10^{15} J/Sec with exceptions on the 6th with 0.8×10^{15} J/Sec and on the 8th where it was -1.15×10^{15} J/Sec. The highest values of heating or cooling were observed during the first phase when compared to those at the others. On an average also, values were higher during this period (June 1977).

Hitherto studies were confined to find out the circulation, moisture and heat budgets at selected parts over Arabian Sea. These studies were useful in understanding

to a certain extent, the origin and maintenance of the monsoon activity over the Arabian Sea. Logically, these studies on monsoons would be incomplete if no attempt is made to study the monsoon rainfall. The potential indicators for the rainfall estimation are being looked into by many. The most important indicator for the Indian monsoon rainfall has been identified as the SST over the Arabian Sea. Despite a number of attempts, no concrete results could be established, keeping the scope open for further investigations. These aspects in relation to some selected Indian West coast stations are presented in the next chapter.

CHAPTER - V

5.1 INTRODUCTION

Several studies [Bunker (1965), Ali (1980), Angell (1981), Joseph and Pillai (1954, 1986) and many others] have been carried out in recent years to find out the linkage of the oceanic parameters like sea surface temperature and their variations with the amount, and variability of Indian summer monsoon rainfall. Although these have enhanced the awareness on the influence of oceans on tropical weather, the contradicting results, still keep this field open for further investigations.

5.2 CORRELATION BETWEEN SEA SURFACE TEMPERATURE AND RAINFALL AT THE STATIONS ALONG WEST COAST OF INDIA.

An attempt is made in this chapter to obtain a relationship between SST of Arabian Sea and the summer monsoon rainfall along the West coast of India. The detailed methodology was presented in section 1.5.9. The results and discussions are presented here. As was already mentioned before, the Arabian Sea area between 8° and 25° N and 60° E and 77° E was divided into four quadrants (Fig.5.1) and the correlations between the weekly average sea surface temperature of these areas and the weekly total rainfall for thirteen West coast stations were studied in three different

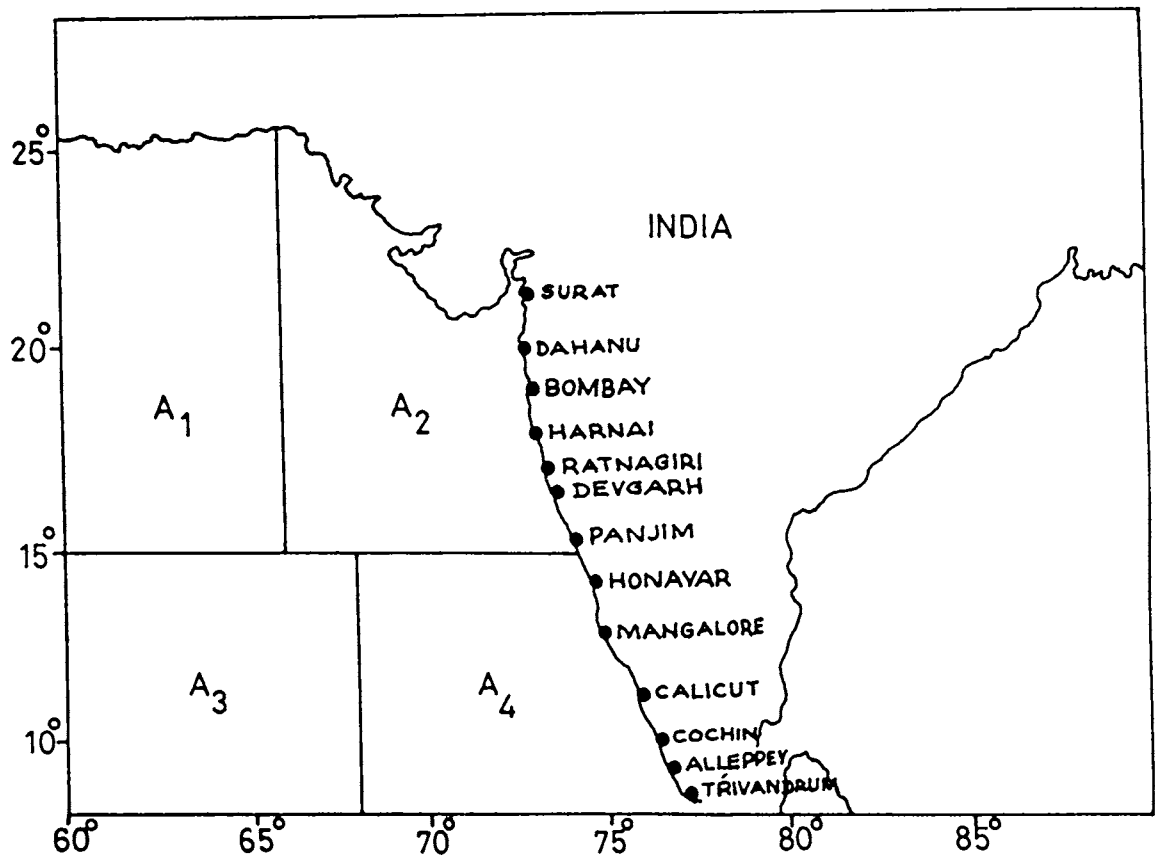


FIG.5.1 MAP SHOWING THE AREA OF STUDY

ways i.e., without any time lag between the SST data and rainfall data, with a lag of one week and with SST anomalies with a lag of one week.

5.2.1 Correlations without time lag

Table 5.1 gives the values of the correlation coefficients for all the stations for the four quadrants separately. It can be seen that, although the correlation values are not high, they are highly significant. The levels of significance had been obtained from the statistical Tables by Fisher and Yates (1936). For Trivandrum, Alleppey, Cochin and Kozhikode, the correlations are significant at 0.1% level (equivalent to a confidence level of 99.9%) at all the quadrants. Mangalore rainfall is significantly correlated with the SST's at 10% level. Rainfall of the other stations showed low correlation.

Examining in greater detail the above mentioned results, it was found that the coefficients are highest with the fourth quadrant followed by third, second and first quadrants respectively. It is natural, that the moisture supply for the west coast come from the western half of the Tropical Indian Ocean. Of the four stations selected along the Kerala Coast, Trivandrum showed the highest degree of correlation followed by Cochin, Kozhikode and Alleppey. One could also notice that the correlations are highly signi-

ficant for the stations south of 13°N and very poor for the stations north of 13°N . Moreover the south east (A₄) and south west (A₃) quadrants show highly significant correlations with the stations south of 13°N . It may be explained as due to the southwesterlies prevalent during the period of study. The influence being felt more in the southern stations because the impact would be felt immediately where the winds strike the coast first. Since the southwesterlies from the South Arabian Sea take some time to reach further northern latitudes, one has to look into this with a time lag between the oceanic temperature and rainfall. It is equally interesting to see that even quadrants A₁ and A₂ have influence on the Kerala coast rainfall. A close examination of the wind pattern over this region suggests that the winds are not always southwesterlies in the North Arabian Sea. Hence, the entire Arabian Sea area under consideration in the present study exhibits influence on the rainfall along the westcoast of India and especially the Kerala Coast.

5.2.2 Correlations with a lag of one week

Table 5.2 gives the correlation coefficients and levels of significance for the parameters with a lag of one week lag. As logically expected, the correlations have increased considerably for stations north of 13°N latitude along the west coast, while for the stations, south of 13°N ,

the correlation values have come down than that without lag. One third of the cases (33%) were significant at 0.1% level, 39% between 1 and 5% level and the rest (27%) of them were significant at 10% level. There was a considerable improvement for the correlation values over those computed without lag for the northern stations. Three stations gave negative correlations too. For the northern stations, the first quadrant has more influence followed by second, third and fourth respectively. Since it is natural to expect that the North Arabian Sea, which is closer to these stations would have more influence, the above results were not at all surprising.

It would be relevant to mention here, that the correlations might have been much better with a lag of 2 or 4 days also. But the non-availability of daily data prevented such a study.

5.2.3 Correlations with SST Anomalies

Table 5.3 gives the correlation between rainfall and sea surface temperature anomalies. The correlation values were not statistically significant for almost all the stations except Trivandrum. This may be probably because of their very small values and their difference in signs not being considered.

An intercomparison now reveals that the correlations are good between sea surface temperatures and rainfall of the subsequent week especially for stations north of 13°N latitude. This result indicates that one can estimate the expected rainfall a week before with sufficient accuracy using SST data. Tables 5.4, 5.5 and 5.6 give the constants (m and c) of the regression equations relating the rainfall and SST, for the three different cases described above. These values could be used with sufficient confidence for calculating the rainfall at the coastal stations.

The present study has revealed to some extent that the sea surface temperatures in the Arabian Sea have profound influence on the West coast rainfall. However, further studies should be carried out incorporating dynamics of the lower troposphere along with the Hadley and Walker circulations. Availability of daily SST values with sufficient accuracy would help us to understand the stress of these physical parameters on the Indian monsoon in greater detail.

STATION	QUADRANT A ₁		QUADRANT A ₂		QUADRANT A ₃		QUADRANT A ₄	
	r	Level of Signi. (%)	r	Level of Signi. (%)	r	Level of Signi. (%)	r	Level of Signi. (%)
TRIVANDRUM	0.32	0.1	0.34	0.1	0.42	0.1	0.49	0.1
ALLEPPEY	0.21	3.0	0.25	1.0	0.27	1.0	0.40	0.1
COCHIN	0.34	0.1	0.26	1.0	0.32	0.1	0.36	0.1
KOZHIKODE	0.30	0.1	0.26	1.0	0.25	1.0	0.31	0.5
MANGALORE	0.16	10.0	0.11	10.0	0.10	10.0	0.16	10.0
HONAVAR	0.04	Nil	0.17	10.0	-0.02	Nil	0.13	Nil
PANAJI	0.09	Nil	0.12	Nil	0.02	Nil	0.20	Nil
DEVAGARH	-	Nil	-0.03	Nil	0.07	Nil	0.10	Nil
RATNAGIRI	0.09	Nil	0.13	Nil	0.07	Nil	0.14	Nil
HARNAI	0.01	Nil	-0.001	Nil	-0.03	Nil	-0.02	Nil
BOMBAY	0.02	Nil	0.01	Nil	-0.02	Nil	-0.01	Nil
DAHANU	0.05	Nil	0.12	Nil	-0.02	Nil	0.05	Nil
SURAT	0.04	Nil						

Table 5.1 Values of Correlation Coefficients and levels of significance with SST and rainfall without lag.

STATION	QUADRANT A ₁		QUADRANT A ₂		QUADRANT A ₃		QUADRANT A ₄	
	r	Level of Signi. (%)	r	Level of Signi. (%)	r	Level of Signi. (%)	r	Level of Signi. (%)
TRIVANDRUM	0.35	0.1	0.29	0.5	0.4	0.1	0.39	0.1
ALLEPPEY	0.39	0.1	0.24	2.0	0.4	0.1	0.4	0.1
COCHIN	- 0.12	10.0	0.27	0.5	0.29	0.5	- 0.12	10.0
KOZHIKODE	0.34	0.1	0.25	2.0	0.29	0.5	0.26	2.0
MANGALORE	- 0.11	10.0	0.22	3.0	0.28	0.5	- 0.1	10.0
HONAVAR	- 0.11	10.0	0.26	1.0	0.17	10.0	- 0.11	10.0
PANAJI	0.33	0.1	0.23	5.0	0.27	1.0	0.28	1.0
DEVAGARH	0.31	0.5	0.1	10.0	0.23	2.0	0.22	5.0
RATNAGIRI	0.25	1.0	0.26	1.0	0.21	5.0	0.28	0.5
HARNAI	0.33	0.5	0.32	0.1	0.27	5.0	0.33	0.1
BOMBAY	0.22	2.0	0.14	10.0	0.16	10.0	0.19	10.0
DAHANU	0.21	3.0	0.23	2.0	0.15	10.0	0.21	5.0
SURAT	0.26	1.0	0.22	5.0	0.19	5.0	0.19	5.0

Table 5.2 Values of Correlation Coefficients and levels of significance with SST and rainfall with a lag of one week.

STATION	QUADRANT A ₁		QUADRANT A ₂		QUADRANT A ₃		QUADRANT A ₄	
	r	Level of Signi. (%)	r	Level of Signi. (%)	r	Level of Signi. (%)	r	Level of Signi. (%)
TRIVANDRUM	0.24	2.0	0.15	10.0	0.21	3.0	0.29	5.0
ALLEPPEY	0.17	10.0	- 0.01	Nil	0.12	10.0	0.15	Nil
COCHIN	0.17	10.0	- 0.03	Nil	0.10	10.0	0.097	Nil
KOZHICODE	0.17	10.0	0.004	Nil	0.07	Nil	0.0002	Nil
MANGALORE	0.01	Nil	- 0.09	Nil	0.02	Nil	- 0.001	Nil
HONAVAR	- 0.02	Nil	0.08	Nil	- 0.02	Nil	0.14	Nil
PANAJI	- 0.04	Nil	- 0.08	Nil	- 0.004	Nil	0.04	Nil
DEVAGARH	- 0.04	Nil	- 0.16	Nil	- 0.009	Nil	0.04	Nil
RATNAGIRI	- 0.04	Nil	- 0.04	Nil	0.003	Nil	0.03	Nil
HARNAI	0.12	Nil	0.04	Nil	0.09	Nil	0.014	Nil
BOMBAY	0.03	Nil	- 0.04	Nil	0.02	Nil	0.07	Nil
DAHANU	0.1	Nil	0.15	10.0	0.15	10.0	0.02	Nil
SURAT	0.18	10.0	0.05	Nil	0.11	Nil	0.168	10.0

Table 5.3 Values of Correlation Coefficients and levels of significance with SST anomalies and rainfall.

STATION	QUADRANT A ₁		QUADRANT A ₂		QUADRANT A ₃		QUADRANT A ₄	
	m	c	m	c	m	c	m	c
TRIVANDRUM	10.58	-237.30	14.70	-357.30	18.10	-443.00	29.30	-762.00
ALLEPPEY	10.80	-197.90	17.00	-377.00	17.80	-390.00	36.90	-927.00
COCHIN	20.07	-412.00	20.60	-441.80	25.60	-568.60	41.30	-1015.00
KOZHIKODE	19.60	-382.60	23.70	-509.90	20.50	-415.20	37.00	-804.00
MANGALORE	15.30	-229.00	14.20	-211.30	13.10	-175.90	28.60	-611.00
HONAVAR	03.60	83.70	22.80	-444.00	-2.60	-249.70	23.70	-472.00
PANAJI	08.40	-66.20	14.80	-249.00	14.70	-237.00	35.80	-828.00
DEVAGARH	-	-	-4.26	271.4	9.90	-115.2	19.20	-378.00
RATNAGIRI	09.10	-89.90	17.20	-319.00	9.90	-114.10	25.10	-539.00
HARNAI	01.29	85.60	-0.25	127.10	-4.40	-237.70	-3.50	-215.50
BOMBAY	01.76	76.70	0.72	103.00	-2.90	-200.60	-2.60	194.60
DAHANU	04.10	-04.90	12.90	-249.30	-2.10	-160.10	-7.80	-110.60
SURAT	-	-	-	-	-	-	-	-

Table 5.4 Values of the Constants m and c for the regression relation y (rainfall) = mx (SST) + C, Corresponding to x and y without lag.

STATION	QUADRANT A 1		QUADRANT A 2		QUADRANT A 3		QUADRANT A 4	
	m	C	m	C	m	C	m	C
TRIVANDRUM	10.50	-237.50	11.50	-273.20	15.30	-37.10	22.10	-566.10
ALLEPPEY	19.80	-433.70	16.50	-357.00	25.40	-591.10	37.80	-945.40
COCHIN	-	-	20.50	-449.00	21.70	-472.00	-	-
KOZHIKODE	2.90	-61.70	2.90	-64.60	3.10	-68.60	3.90	-94.70
MANGALORE	-	-	28.20	-599.20	36.20	-803.70	-	-
HONAVAR	-	-	34.30	-764.00	22.30	-422.90	20.10	159.20
PANAJI	31.90	-69.40	28.90	-633.00	34.80	-779.50	49.80	-1213.90
DEVAGARH	3.50	-78.20	1.50	-26.10	3.40	-75.50	4.50	-110.40
RATNAGIRI	23.90	-475.00	33.80	-785.00	25.90	-538.90	51.10	-1246.20
HARNAI	26.60	-59.00	40.90	-101.30	3.10	-71.80	5.10	-128.10
BOMBAY	21.30	-44.50	18.10	-372.00	20.00	-415.70	34.40	-824.50
DAHANU	17.00	-34.60	24.70	-568.40	15.90	-321.70	31.70	-766.30
SURAT	16.10	-358.50	18.50	-434.90	15.90	-359.40	22.40	-547.40

Table 5.5 Values of the Constant m and C for the regression relation y (rainfall) = mx (SST) + C, corresponding to x and y with a lag of one week.

STATION	QUADRANT A ₁		QUADRANT A ₂		QUADRANT A ₃		QUADRANT A ₄	
	m	c	m	c	m	c	m	c
TRIVANDRUM	9.90	46.80	6.90	47.40	11.90	44.80	22.00	43.90
ALLEPPEY	11.20	100.30	- 0.65	98.60	10.80	98.20	16.90	97.80
COCHIN	13.40	125.50	- 2.20	123.10	10.50	123.10	13.19	122.80
KOZHIKODE	14.90	136.60	- 0.43	130.20	7.50	130.50	0.03	130.40
MANGALORE	1.60	176.30	-11.90	172.80	3.40	175.90	0.27	176.10
HONAVAR	- 1.90	180.80	11.70	184.20	- 2.80	181.20	31.25	178.80
PANAJI	- 4.90	157.00	-10.90	154.70	- 0.66	157.70	9.46	156.90
DEVAGARH	- 5.10	154.70	-25.50	150.60	- 1.12	154.60	0.81	154.10
RATNAGIRI	- 5.50	150.70	- 5.90	149.80	0.46	151.40	2.95	151.20
HARNAI	11.80	112.80	5.20	111.70	12.85	110.80	12.20	109.40
BOMBAY	- 3.50	122.50	- 5.80	121.40	3.70	122.80	- 5.04	123.30
DAHANU	10.50	105.90	17.60	109.30	20.10	103.40	30.40	102.40
SURAT	14.50	71.90	4.40	71.20	11.96	69.40	10.90	89.30

Table 5.6 Values of the Constants m and c for the regression relation y (rainfall) = mx (SST anomalies) + C.

CHAPTER - VI

In view of the utmost importance the summer monsoon has, not only in shaping the economy of our country but also in influencing the general circulation of the atmosphere as a whole, numerous studies on this have been and are still being carried out. Because of certain inherent complexities in the behaviour of monsoon, it has not been possible to arrive at a thorough understanding of its characteristics. Lack of adequate data over the oceans has been one of the reasons for the insufficient understanding of the monsoon phenomena. The IIOE first provided relatively extensive coverage of data although not exhaustive and resulted in the emergence of a number of new findings, some of them conflicting too. The seventies saw the dawning of the new era in obtaining data over oceans from International Experiments such as ISMEX, MONSOON-1977, MONEX-1979 of which the last was the most important since, never before was such a huge experiment conducted with almost all the active groups all over the world participating in it. The number of scientific papers on the subject that appeared after 1979, perhaps outnumber those that appeared before it. Hence, the years 1977 and 1979 assume special importance and as such a composite study of these two monsoons in respect of some parameters is worth making.

The budget studies play a vital role in determining the actual heat and moisture sources and sinks for the maintenance of the monsoon circulation. The excellent data coverage in the years 1977 and 1979 over certain regions over Arabian Sea made it possible to undertake extensive studies on a sufficiently larger time scale varying from 12 to 15 days. Although many studies were carried out over these Arabian Sea regions, the diurnal and daily variations were not studied extensively. Since 1977 can be taken as a good monsoon year and 1979 a bad monsoon year, the comparisons between these two years represent contrasting monsoonal characteristics.

For a long time, people have been concerned with finding the potential predictors for monsoon rainfall on regional as well as large scale. The boundary forcings in the form of sea surface temperature play a dominant role in influencing the monsoon rainfall. Although several attempts have been made, the results have been very contrasting. This might probably be because of the differences in the areas of study and the techniques used.

The detailed review of literature (Chapter I) reveals that the scope is still wide open for further studies of these moisture and heat budgets of the marine atmosphere in view of the conflicting results most of which were men-

tioned in the review. Even though sea surface temperature studies in relation to rainfall have invited world wide attention, many gaps are yet to be filled in our understanding of the phenomena.

The methods to compute the various circulation parameters such as vorticity, divergence, vertical velocity, precipitable water vapour, moisture budget parameters such as evaporation, moisture flux, precipitation and heat budget parameters such as sensible heat, dry static energy were described in the Section 1.5. In addition, the method to find the correlations between sea surface temperature and rainfall for individual stations along the West coast of India is also described. The diurnal and daily variations of the above parameters are studied for the four phases indicated in the first chapter, during 1977 and 1979. The results and discussions of these studies are presented in the respective chapters. The conclusions and main results are summarised below.

The vertical variation of specific humidity and the zonal and meridional components Section-2 of wind reveal the following salient features: Irrespective of the phase and the day, the vertical variation of specific humidity remained the same with a consistent and rapid decrease upto the mid-troposphere and a gentle decrease thereafter. The

phase to phase variations of the specific humidity did not show any significant differences, the maximum variation at the surface being only 2gm/kg.

The studies of the zonal components of wind show that the westerly maximum was around 800 mb level and that the westerlies persisted upto very high altitudes when the monsoon was active as in Phase-I and in the later part of Phase-IV. During the above period, the easterly maximum was found around 200 mb level. The change of sign from westerlies to easterlies occurred at only one level when the monsoon was active. During the pre-monsoon period (For eg: Phase-III) or when the monsoon was weak (Phase-II) the westerlies were relatively weak and alternated with easterlies at two levels in the vertical. The maximum strength of easterlies was noticed around 400 mb, the magnitude being less than the maximum values (200 mb), in the active phase (Phase-I). The best indicator of the activity of the monsoon seems to be the vertical extent of westerlies and the number of times it changed sign in the vertical. The meridional component of wind were always of lower values than their zonal counterpart and irrespective of the activity of the monsoon and the phase, the meridional component of wind changed its sign twice in the vertical.

The amount of precipitable water vapour did not show any significant day-to-day or diurnal variations (Section 2.2). The amount of water vapour was relatively more in Phase-I when compared to that in Phase-II while, Phase-IV showed higher values than Phase-III.

Analysis of the kinetic energy values (Section 2.2) at the four levels, surface, 700, 500 and 200 mbs, indicated that there was no consistent variation of this parameter with the phases. In Phase-I the kinetic energy minimum was around 500 mb and maximum around 700 mb while the maximum was at 200 mb and minimum at 500 mb during Phase-II. During the IIIrd phase the maximum kinetic energy was observed at 500 mb and minimum around 600 mb especially so after 25th May. Kinetic energy was observed at 200 mb and the minimum at 700 upto 7th June 1979 and at 500 mb thereafter.

As detailed in Chapter II, the study of vertical time sections of vorticity, divergence and vertical velocity reveal the following features: During Phase-I, most of the period was dominated by cyclonic vorticity while anti-cyclonic vorticity dominated in the IInd Phase. The IIIrd and IVth phases experienced both cyclonic and anticyclonic vorticities. Divergence dominated all the phases except the first one where convergence and divergence are evenly distributed throughout this period. Upward as well as downward

motions were noticed in Phase-I with former dominating the latter. Phase-II and Phase-III were mostly dominated by downward motion. Both upward and downward motions were equally strong in Phase-III.

The moisture budget studies (Chapter III) for the four Phases revealed that the evaporation was relatively low in Phase-II and III than that in the other two. As far as moisture flux is concerned, considerable diurnal variations were noticed at all the boundaries of the polygon. In addition it was found that opposite walls of the polygon exhibited similar variabilities. The flux values were mostly positive at the west wall. The daily variation of this flux showed both positive and negative values alternately. Almost always, the values were higher through the zonal walls than that through the meridional walls. The convergence of net moisture flux was dominating the Phase-I and Phase-III while Phase-II showed divergence. In Phase-IV there were both divergence and convergence of moisture flux. Precipitation which was computed as a residual parameter from moisture budget computations, showed that the precipitation was positive almost always in Phase-I and Phase-II but it showed low values in the latter. May 25th in Phase-III and June 12th in Phase-IV showed prominent peaks of precipitation, and during these two phases, there were rarely negative values too.

Heat budget studies revealed that the sensible heat flux showed more positive values during Phase-I and in Phase-II it showed both positive and negative values. Phase-III and IV showed positive values. The heat flux did not differ significantly at the east and west walls, but at the north and south walls there was significant variations. Thus the convergence or divergence of heat flux into the polygon must be mostly contributed by the meridional transport although the meridional winds are much weaker than their zonal counterparts. The increases in the differences between the heat flux values of the meridional and the zonal walls always coincided with the presence of either a cyclonic storm or trough of low pressure while decreases coincided with the presence of a high pressure cell. The net heat flux showed convergence in Phase-I except on the 9th May and during Phase-II, heat divergence was predominant. During Phase III and IV divergence and convergence of net heat flux were noticed alternately. Radiative heating was observed almost all through in Phase-I except between the 9th and 11th June 1977. Phase-II showed both heating as well as cooling. Radiative cooling was dominating during Phase-III while heating was predominant in Phase-IV.

The relation between Arabian Sea surface temperature and rainfall along the west coast of India revealed the following: The correlations were good and highly significant

for the stations south of 13°N with the corresponding week's SST in all the four quadrants. For stations north of 13°N there was no relation at all, to the corresponding week's SST in any of the quadrants. The southern quadrants showed better correlations for the stations south of 13°N . The correlations with the weekly composites of SST and the subsequent week's rainfall (which means 1 week lag) were good and highly significant for almost all the stations along the West coast, although the levels of significance differed from one station to the other. An attempt at correlating SST anomalies and rainfall indicated that these two parameters have practically no relation at all. Although the conclusions drawn are good enough to indicate that monsoon rainfall predictors could be identified in some parameters over the Arabian Sea region, more extensive studies would have to be carried out over a much larger area in the Arabian Sea with extensive data for longer periods, in order to identify the best predictors.

REFERENCES

- Ali, E.L., 1980: Some aspects of the structure of the Summer Monsoon flow over the Arabian Sea, Summer MONEX Field Phase Research FGGE Operations Report, Vol.9, Part(A), PP.121-126.
- Ali, M.M., B. Simon and P.S. Desai, 1987: Heat Budget study of the equatorial Indian Ocean using Satellite data, S.Z. Qasim felicitation volume-contributions to Marine Science, PP.227-236.
- Ananthakrishnan, R., V. Srinivasan, A.R. Ramakrishnan and R. Jambunathan, 1968: Synoptic features associated with the onset of southwest monsoon over Kerala, Forecasting Manual, FMU Report No.IV-18,2, IMD, Pune, PP.46.
- Ananthakrishnan, R., J.A. Maliakal and M.K. Soman, 1984: Evaporation and water vapour transport over the Indian Ocean during the summer monsoon, Indo-US Workshop on Ocean Atmosphere Interaction - Meeting Report, PP.34.
- Angell, J.K., 1981: Comparisons of variations in atmospheric quantities with SST variations in the equatorial eastern Pacific, Monthly Weather Review, Vol.109, PP.230-243.

- Anjaneyulu, T.S.S., 1980: A study of the air and surface temperatures over the Indian Ocean, Mausam, Vol.31, PP.551-560.
- Appa Rao, G. and Bh.V. Ramanamurthy, 1977: Water vapour transport and vergence patterns over India during two contrasting summer monsoons, Pageoph, Vol.115, PP.491-502.
- Appa Rao, G., 1985: Moisture flux and Vergence of water vapour over India during drought and good monsoons, Mausam, Vol.36, No.1, PP.97-100.
- Barnett, T.P., 1978: Ocean temperatures: Precursors of climate change, Oceans, Vol.21, PP.27-32.
- Barnett, T.P., 1984: Long term trends in surface temperature over the oceans, Monthly Weather Review, Vol.112, PP.303-312.
- Basu, B.K., and K.C. Parel, 1984: Radiational Structure over Indian Sea during MONSOON-77 and MONEX-79, Mausam, Vol.35, No.4, PP.507-514.
- Bavadekar, S.N., 1982: Water vapour transport of the pre-monsoon period and the general performance of the Indian Summer Monsoon, Pageoph, Vol.120, PP.67-78.

- Bavadekar, S.N. and R.M. Khaladkar, 1982: Water vapour transport across the Section parallel to west coast of India during contrasting summer monsoon periods, Archives for Meteorology, Geophysics and Bioclimatology, Vol.31, PP.243-248.
- Bavadekar, S.N., 1984: Some aspects of large scale atmospheric motion with special reference to typical Indian Orography. Thesis submitted to the University of Poona, PP.239.
- Bhide, U.V., S.G. Nagar and D.R. Sikka, 1982a: Study of organised Convective systems observed over the Arabian Sea during the onset phase of summer Monex, GARP International Conference on the scientific results of Monsoon experiment - Indonesia, PP.3-69 to 3-73.
- Bhide, U.V., S.G. Nagar and D.R. Sikka, 1982b: Modulations of the Kinematic properties of heat and moisture fields in the troposphere over Equatorial Arabian Sea in the pre-onset and onset phases of the summer monsoon, Proceedings of the Regional Conference on Tropical Meteorology, Tsukuba, Japan, PP.91-96.
- Bhide, U.V., S.G. Nagar, P.M. Mahajan and D.R. Sikka, 1986: Fluxes of sensible and latent heat at the air-sea

interface over equatorial Arabian Sea during MONEX-79, Current Science, Vol.55, No.15, PP.699-701.

Bhumralkar, C.M., 1978: Relation between evaporation over the Arabian Sea and rainfall at the West coast of India during summer monsoon, Indian Journal of Meteorology and Geophysics, Vol.29, No.1, PP.150-161.

Brower, R.L., H.S. Gohrband, W.G. Pichel, T.I. Signore and C.C. Walton, 1976: Satellite derived sea surface temperature from NOAA spacecraft, NOAA Technical Memorandum NESS 78, U.S. Government Printing Office, Washington, D.C.

*Bunker, A.F., 1965: Interaction of summer monsoon air with the Arabian Sea, Proceedings of the Symposium on meteorological results of II OE, PP.3-16.

Cadet, D.L., 1981. Water vapour transport of the Indian Ocean during summer 1975, Tellus, Vol.33, PP.476-487.

Cadet, D.L., 1983: The monsoon over the Indian Ocean during summer 1975. Part 2: Break and active monsoons, Monthly Weather Review, Vol.III, PP.95-108.

- Cadet, D.L. and B.C. Diehl, 1984: International variability of surface fields over the Indian Ocean during recent decades, Monthly Weather Review, Vol.112, 1921-1935.
- Cadet, D.L. and G. Reverdin, 1981: The monsoon over the Indian Ocean during summer 1975. Part I: Mean field, Monthly Weather Review, Vol.103, PP.148-158.
- Chowdhury, M.H.K. and S. Karmakar, 1982: Diagnostic study on some aspects of the energetics and structural features of the troposphere over the Arabian Sea with advancement of South west monsoon, Results of Summer MONEX Field Phase Research (Part B). FGGE Operations Report Vol.9, PP.212-221.
- Chuchkalov, B.S., 1982: Vertical distribution of average dynamic features over the USSR ship polygons during summer MONEX, International conference on the scientific results of the Monsoon Experiment. Extended abstracts and panel session, PP.3.64-3.68.
- Colborn, J.G., 1975: The thermal structure of the Indian Ocean. The University Press of Hawaii, Honolulu, PP.173.

- Das, P.K., 1962, Mean Vertical motion and non-adiabatic heat sources over India during the Monsoon, *Tellus*, Vol.IV, PP.212-220.
- Das, P.K., 1968: *The Monsoons*, National Book Trust, New Delhi, P.162.
- Das, P.K., 1985: *The Monsoon Experiments*, *Mausam*, Vol.36, No.2, PP.150-158.
- Das, P.K., 1986: *Monsoons*, Fifth I.M.O. Lecture, World Meteorological Organisation Geneva, PP.41-46.
- Dewan, B.N., S.K. Subramanian and S.K. Dikshit, 1987: Moisture inflow over India and its contribution to rainfall during normal, good and bad monsoon years, *Proceedings of National Symposium on Hydrology*, PP.45-54.
- Druryan, L.M., 1982a: *Studies on the Indian Summer Monsoon with a Coarse-mesh general Circulation model, Part-I* *Journal of climatology*, Vol.1, PP.127-139.
- Druryan, L.M., 1982b: *Studies on the Indian Summer Monsoon with a Coarse-mesh general Circulation model, Part II*, *Journal of climatology*, 2:347-355.

- Duing, N. and A. Leetma, 1980: Arabian Sea Cooling - A preliminary heat budget, *Journal of Physical Oceanography*, Vol.10, PP.307-312.
- Fieux, M. and H. Stommel, 1977: Onset of southwest monsoon over the Arabian Sea and marine reports of surface winds: structure and variability, *Monthly Weather Review*, Vol.105, PP.231-236.
- Findlater, J., 1969a: A major low-level air current near the Indian Ocean during the northern summer, *Quarterly Journal of Royal Meteorological Society*, Vol.95, PP.362-380.
- *Findlater, J. 1969b: Interhemispheric transport of air in the lower troposphere over the western Indian Ocean, *Quarterly Journal of Royal Meteorological Society*, Vol.95, PP.400-403.
- Fisher, R.A. and F. Yates, 1936: *Statistical Tables*, Published by Oliver and Boyce Limited.
- Gadgil, S., P.V. Joseph and M.V. Joshi, 1984: Ocean-atmosphere coupling over monsoon regions, *Nature*, Vol.312, PP.141-143.
- Ghosh, S.K., M.C. Pant and B.N. Dewan, 1978: Influence of the Arabian Sea on the Indian Summer Monsoon, *Tellus*, Vol.30, PP.117-125.

- Gopinathan, C.K. and D.P. Rao, 1985: Surface temperature of the Indian Ocean before summer monsoon, *Mahasagar*, Vol.18, PP.281-292.
- Goswami, B.N., 1986: Preliminary analysis of 100 years SST data over Indian Ocean and Arabian Sea in relation to Monsoon variability (unpublished manuscript).
- Hastenrath, S. and P.J. Lamb, 1979: Climatic Atlas of the Indian Ocean, Part-II. The oceanic heat budget. The University of Wisconsin Press, Wisconsin, P.93.
- Hastenrath, S., 1980: Heat budget of tropical Ocean and atmosphere, *Journal of Physical Oceanography*, Vol.10, PP.159-170.
- Hastenrath, S., 1985: Climate and Circulation of the tropics, *Atmospheric Science Library*, D. Riehl Publishing Company, PP.72-103.
- Hastenrath, S. and P.J. Lamb, 1980: On the heat budget of hydrosphere and atmosphere in the Indian Ocean, *Journal of Physical Oceanography*, Vol.10, PP.694-708.
- Howland, M.R. and D.N. Sikdar, 1983: The moisture budget over the north eastern Arabian Sea during premonsoon and monsoon onset, 1979, *Monthly Weather Review*, Vol.III, PP.2255-2268.

- Jambunathan, . R. and K. Ramamurthy, 1975: Sea and air temperature distribution over the Arabian Sea during South west monsoon 1973, *Journal of Meteorology and Geophysics*, Vol.26, PP.465-478.
- Joseph, P.V.; 1981: Ocean-atmosphere interaction on a seasonal scale over north India Ocean and Indian monsoon rainfall and cyclone tracks - A preliminary study, *Mausam*, Vol.32, PP.237-246.
- Joseph, P.V. and P.V. Pillai, 1984: Air-sea interaction on a seasonal scale over the North Indian Ocean - Part-I: Interannual variations of sea surface temperature and Indian summer monsoon rainfall, *Mausam*, Vol.35, PP.323-330.
- Joseph, P.V. and P.V. Pillai, 1986: Air-sea interaction on a seasonal scale over north Indian Ocean - Part-II: Monthly mean atmospheric and oceanic parameters during 1972 and 1973, *Mausam*, Vol.37, PP.158-168.
- Kershaw, R., 1985: Onset of southwest monsoon and sea surface temperature anomalies in the Arabian Sea, *Nature*, Vol.315, PP.561-563.
- Keshavamurthy, R.N., J.M. Korkhao, S.K. Das and R.K. Mukhopadhyaya 1975: The Indian Summer monsoon and varia-

tion of ocean temperatures over the neighbouring seas, IMD, Scientific report No.220.

Keshavamurthy, R.N. 1982: Response of the atmosphere to sea surface temperature anomalies over the equatorial pacific and the teleconnections of the southern oscillation, Journal of atmospheric Science, Vol.39, PP.1241-1259.

Khalsa, Siri Jodha Singh, 1963: The role of SST in large scale air sea interaction, Monthly Weather Review, Vol.III, No.5, PP.954-966.

Kraus, E.B. and H.P. Hauson, 1983: Air-sea interaction as a propagator of equatorial Ocean surface temperature anomalies, Journal of physical Oceanography, Vol.13, PP.130-138.

Krishnamurthy, T.N. (Ed.), 1978: Monsoon Dynamics, Reprinted from Pure and Applied Geophysics, 115: PP.1087-1527.

Krishnamurthy, T.N. and H.N. Bhalme, 1979: Oscillations of a monsoon system. Part-I. Observational Aspects, Journal of Atmospheric Sciences, Vol.33, No.10, PP.1938-1954.

Kung, E.C. and T.A. Sharif, 1982: Long-range forecasting of the Indian summer monsoon onset and rainfall with

upper air parameters and sea surface temperature, Journal of Meteorological society of Japan, Vol.60, PP.672-681.

Michael, J.M., 1975: Variability in the Central Equatorial Indian Ocean, Part-III, Oceanic heat and turbulent energy balance, Marine Research, Vol.40, PP.405-420.

Mishra, D.K., 1981: Satellite derived SST distribution over the North Indian Ocean during the South West Monsoon season, Mausam, Vol.32, No.1, PP.59-60.

Mishra, D.K., Tiwari, V.S. and G.K. Bahuguna, 1981: The influence of SST over Indian sub-continent, Report of National Symposium on early results of monsoon experiment-IV, PP.4.

Mohanty, U.C., P.C. Sinha and S.K. Dube, 1982 (a) On the role of large scale energetics in the onset and maintenance of summer monsoon-I, Heat Budget, Mausam, Vol.33, No.2, PP.139-152.

Mohanty, U.C., P.C. Sinha and S.K. Dube, 1982(b): On the role of large Scale energetics in the onset and maintenance of summer monsoon-II, Moisture Budget, Mausam, Vol.33, No.3, PP.285-294.

Mohanty, U.C., S.K. Dube and M.P. Singh, 1983: A study of

heat and moisture budget over the Arabian Sea and their role in the onset and maintenance of summer monsoon, Journal of Meteorological Society of Japan, Vol.61, No.2, PP.208-221.

Mohanty, U.C., 1985: Monsoon Circulation Statistics: Inter-annual variability in relation to Heat and Moisture Budget, Report of Workshop on 'The Interannual Variability of Monsoons' by J. Shukla, PP.21.

Mooley, D.A. and B. Parthasarathy, 1983: Variability of Indian Summer monsoon and tropical circulation features, Monthly Weather Review, Vol.III, No.5, PP.967-978.

Murray, F.W., 1967: Computation of saturated vapour pressure, Journal of Applied Meteorology, Vol.6, PP.203-204.

Murthy, V.S.N., D.P. Rao and J.S. Sastry, 1983: The lowering of sea surface temperature in the east central Arabian Sea, Mahasagar, Vol.16, PP.67-71.

Nuzhdin, P.V., 1982. On laws covering fluctuations of Arabian Sea active layer thermodynamic properties and air-sea energy exchange characteristics during south west monsoon, GARP International Conference

on the scientific results of the Monsoon Experiment, Bali, Indonesia, ICSU/WMO, PP.7.24-7.27.

O'Brien, J.J., 1970: Alternate Solutions to the Classical Vertical velocity problem, Journal of Applied Meteorology, Vol.9, PP.197-203.

Oort, A., 1985: Annual and Interannual variations in the water vapour budget over the Asian Monsoon region, Report of workshop on 'The Interannual variability of Monsoons' by J. Shukla, PP.23.

Pant, M.C., 1977: Wind stress and fluxes of sensible and latent heat over the Arabian Sea during ISMEX-1973. Indian Journal of Meteorology Geophysics and Hydrology, Vol.28, No.2, PP.189-196.

Pant, D.S., 1983: A physical basis for the changes in the phases of the summer monsoon over India, Monthly Weather Review, 111: PP.487-495.

Pathak, P.N., 1982: Comparison of Sea surface temperature observations from TIROS-N and ships in the North Indian Ocean during MONEX (May-July 1979).

Peixoto, J.P. and A.H. Oort, 1983: The atmospheric branch of the hydrological cycle and climate in variations in the Global water budget. Edited by Street Perrot,

A.M. Beran and A. Ratcliffe, Reidel Publishing Co.,
Dordrecht, P.5-65.

Pisharoty, P.R., 1965: Evaporation from the Arabian Sea and
Indian Summer Monsoon, Proceedings of the symposium
on meteorological results of the IIOE, Bombay,
PP.43-54.

Pisharoty, P.R., 1981a: SST and the monsoon, Monsoon Dyna-
mics, Edited by J. Lighthill and R.P. Pearce, Cam-
bridge University Press, London, PP.237-251.

Pisharoty, P.R., 1981b: The Asiatic Summer Monsoon - A new
theory, International Conference on early results of
FGGE and large scale aspects of its Monsoon Experi-
ments, Tallahassee, USA, PP.43-47.

Raghavan, K., P.V. Puranik, V.R. Mujumdar, P.M.M. Ismail and
D.K. Paul, 1978: Interaction between the West
Arabian Sea and the Indian monsoon, Monthly Weather
Review, Vol.106, PP.719-724.

Ramage, C.S., 1966: The summer atmospheric circulation over
the Arabian Sea, Journal of Atmospheric Sciences,
Vol.23, No.2, PP.144-150.

Ramage, C.S., 1971: Monsoon Meteorology, International Geo-
physics Series, Vol.15, Academic Press, New York,
P.285.

- Ramage, C.S., 1977: SST and local weather, Monthly Weather Review, Vol.105, PP.540-544.
- Ramamurthi, K.M., 1972: On the activity of the Arabian Sea monsoon, Indian Journal of Meteorology and Geophysics, Vol.23, No.1, PP.1-14.
- Ramanadham, R., S.V.S. Somanadham and R.R. Rao, 1981: Heat Budget of the north Indian Oceanic surface during Monsoon-77, Monsoon Dynamics, Ed. James Lighthill and R.P. Pearce, PP.491-509.
- Ramanathan, Y., 1981: Onset of monsoon in the Arabian Sea during 1979, International Conference on Early Results of FGGE and large scale aspects of its Monsoon Experiments, Tallahassee, U.S.A., PP.34-37.
- Ramanathan, Y., 1982: A study of the atmosphere boundary layer over the Arabian Sea from MONEX-79, International Conference on the Scientific results of Monsoon experiment held at Bali, PP.3.39 to 3,43.
- Ramesh Babu, V., L.V.G. Rao, and Varadachari, V.V.R., 1981: Sea surface temperature variations in the north eastern Arabian Sea in relation to the South West Monsoon, Monsoon Dynamics, PP.481-489.

- Ramesh Babu, V., M.V. Rao and Y. Sadhuram, 1985: Relation between Arabian Sea surface temperature and monsoon rainfall on the west coast of India, Tropical Ocean - Atmosphere Newsletter, No.31, PP.6-9.
- Ramesh Babu, V., J.S. Sastry, 1984: Summer cooling in the East Central Arabian Sea - A process of dynamic response to the South west monsoon, Mausam, Vol.35, No.1, PP.17-26.
- Rameshkumar, M.R., S. Sathyendran, N.K. Viswambharan and L.V.G. Rao, 1986: SST variability over North Indian Ocean. A study of two contrasting monsoons, Proceedings of the Indian Academy of Sciences (Earth and Planetary Sciences), Vol., PP.
- Ranjit Singh, 1980: A study of SST and pressure patterns over Indian Ocean region in some years of contrasting southwest Monsoon rainfall in India, Mausam, Vol.31, No.4, PP.601-607.
- Rao, A.V.A.K., R.K. Datta, G.S. Mandal and Indu Bala, 1980: Certain aspects of SST and moisture distribution over the Arabian Sea during pre-onset phase of Monsoon 1979, Results of Summer Monex Field Phase Research (Part-B) FGGE Operations Report, Vol.9, PP.167-172.

- Rao, R.R., Somanadham, S.V.S. and Nizamuddin Syed, 1977: Study of the influence of the surface energy budget of the North Indian Ocean on the behaviour of the Indian Summer Monsoon. Presented at the International Symposium on Monsoons held at New Delhi, March 1977.
- Rao, R.R., Raman, K.V.S. and Santha Devi, M.R., 1981: Studies on energy budget of selected stations over North Indian Ocean during Monsoon-77, Monsoon Dynamics, Cambridge University Press, PP.509-521.
- Rao, D.P., R.V.N. Sarma, J.S. Sastry and K. Premchand, 1976: On the lowering of the surface temperature in the Arabian Sea, with the advance of the southwest monsoon. Proceedings of the symposium on Tropical Monsoons, I.I.T.M., Pune, PP.106-115.
- Rao, G.V. and C.T. Webdell, 1981: Preliminary estimates of divergence, vorticity and water vapour flux over different parts of the Arabian Sea employing MONEX-79 data, International conference on early results of FGGE and large scale aspects of its monsoon experiments - condensed papers and meeting report, PP.12.26-12.29.

- Rao, G.V., W.R. Schaub Jr., and Puetz, 1981: Evaporation and precipitation over the Arabian Sea during several monsoon seasons, Monthly Weather Review, Vol.109, PP.364-370.
- Rao, L.V.G., Ramesh Babu, V., Fernandes, A.A. and Vardachari, V.V.R., 1976: Studies on thermal structure of the north western Indian Ocean in relation to south west monsoon over the Indian peninsula, Proceedings of the symposium on Tropical monsoons, PP.219.
- Rao, R.R., S.V.S. Somanadham and D.V. Rama Raju, 1976: Study of energy exchange from Arabian Sea during a typical monsoon month, Proceedings of symposium on tropical monsoons, PP.322-332.
- Rao, R.R. and S.V.S. Somanadham, 1978: Study of the influence of surface energy budget of north Indian Ocean on the behaviour of Indian Summer Monsoon, Indian Journal of Meteorology and Geophysics, Vol.20, PP.190-197.
- Rao, R.R., K.V. Sunderraman and M.R. Santha Devi, 1981: The energy budget at selected stations over the north Indian Ocean during Monsoon-77, Monsoon Dynamics, Ed. J. Lighthill and R.P. Pearce, PP.509-523.

- Rao, Y.P., 1976: Southwest Monsoon, India Meteorological Department, Meteorological Monograph, Synoptic Meteorology No.1/1976, New Delhi, P.367.
- Sadhuram, Y., V.V. Gopalakrishna, V. Ramesh Babu and J.S. Sastry, 1987: The heat and moisture budgets of the atmosphere over central equatorial Indian Ocean during summer monsoon, Mausam, Vol.38, No.2, PP.227-232.
- Sadhuram, Y. and M.R. Ramesh Kumar, 1988: Does evaporation over the Arabian Sea play a crucial role in moisture transport across the west coast of India during an active monsoon period, Monthly weather review, Vol.116, No.2, PP.307-312.
- Saha, K.R., 1970: Zonal anomaly of SST in the equatorial Indian Ocean and its possible effect upon monsoon circulation, Tellus, Vol.22, PP.403-409.
- Saha, K.R., 1974: Some aspects of the Arabian Sea monsoon, Tellus, Vol.26, PP.464-476.
- Saha, K.R. and S.N. Bavadekar, 1973: Water vapour budget and precipitation over the Arabian Sea during the northern summer, Quarterly journal of the Royal Meteorological Society, Vol.33, PP.273-273.

- Saha, K.R. and S.N. Bavadekar, 1977: Moisture flux across the westcoast of India and rainfall during the SW monsoon, Quarterly Journal of Royal Meteorological Society, Vol.103, No.436, PP.370-374.
- Saha, K.R. and R. Suryanarayana, 1972: Mean monthly vertical fluxes of sensible and latent heat from the surface of the Arabian Sea, Journal of Marine Biological Association of India, Vol.14, PP.663-671.
- Saha, N., 1970: Air and Water transport across the equator in the Western Indian Ocean during northern summer, Tellus, Vol.22, PP.681-687.
- Sastry, J.S. and D'Souza, 1970: Oceanography of the Arabian Sea during Southwest monsoon season, Part-I, Thermal Structure, Indian Journal of Meteorology and Geophysics, Vol.21, No.3, PP.367-382.
- Sastry, J.S. and V. Ramesh Babu, 1985(b): Summer cooling of the Arabian Sea - A review, Proceedings of the Indian Academy of Sciences (Earth and Planetary Sciences), Vol.94, PP.117-128.
- Shetye, R.S., 1984: An analyses of the Arabian Sea mixed layer processes, Report of Indo-US workshop on Ocean atmosphere interaction, PP.42.

- Shukla, J., 1975: Effect of Arabian Sea SST anomaly on ISM: A numerical experiment with GFDL model, Journal of Atmospheric Science, Vol.32, PP.503-511.
- Shukla, J., 1986: International variability of monsoons. In Monsoons, Edited by T.S. Fein and P.L. Stephens, John Wiley Interscience Publishers, New York, PP.142.
- Shukla, J. and B.M. Mishra, 1977: Relationships between SST and wind speed over the Central Arabian Sea and Monsoon rainfall over India, Monthly Weather Review, Vol.105, PP.998-1002.
- Shukla, J. and P.P. Sajnani, 1971: A note on the magnitude of horizontal divergence, Indian Journal of Meteorology and Geophysics, Vol.22, No.3, PP.235-236.
- Sikka, D.R. and K. Raghavan, 1976: Comments on "Effect of SST anomaly on ISM: A numerical experiment with GFDL model", Journal of Atmospheric Science, Vol.33, PP.2252-2253.
- Sikka, D.R. and M.D. Mathur, 1965: Transport of water vapour over Arabian Sea and adjoining Indian region during an active monsoon situation, Proceedings of symposium on Meteorological results of the IIOE, PP.55-56.

- Simon, B. and P.S. Desai, 1986: Equatorial Indian Ocean evaporation estimates from Operational meteorological satellites and some inferences in the context of monsoon onset and activity, *Boundary Layer meteorology*, Vol.37, PP.37-52.
- Sinha, M.C. and O.P. Sharma, 1981: Vertical motion in the monsoon circulation, *Monsoon Dynamics*, PP.601-613.
- Singh, U.S. and R.S. Singh, 1988: Heat and momentum fluxes and their spectra over Western Coast during MONEX-79, *Mausam*, Vol.39, No.3, PP.291-295.
- Spiegel, M.R., 1961: *Schaum's outline of Theory and Problems of Statistics*, P.361.
- Subbaramayya, I. and M. Subba Rao, 1985: On the vagaries of the Indian South west monsoon *Mahasagar*, Vol.18, No.2, PP.180-185.
- Suppiah, Ramaswamy, 1988: Relationship between Indian Ocean sea surface temperature and the rainfall of Sri Lanka, *Meteorological Society of Japan*, PP.103-111.
- Varadhachari, V.V.R., V. Keshava Das and D. Sen gupta, 1987: Oceans and the Indian Summer Monsoon - A review, contribution in *Marine Sciences - Dr. S.Z. Qasim Felicitation Volume*, PP.141-174.

- Washington, W.M., R.M. Chervin and G.V. Rao, 1977: Effects of a variety of Indian Ocean Surface temperature pattern on the summer monsoon circulation: Experiments with NCAR General Circulation Model, Pure and Applied Geophysics, Vol.115, PP.1335-1356.
- Weare, B.C., 1979: A statistical study of the relationship between Ocean surface temperatures and the Indian Monsoon, Journal of Atmospheric Science, Vol.36, PP.2279-2291.
- Webster, P.J., 1983: Mechanism of monsoon low-frequency variability: Surface hydrological effects, Journal of Atmospheric Science, Vol.40, PP.2110-2124.
- WMO, 1975: The influence of the ocean on climate, WMO Report No.11, WMO No.472, PP.44
- Wyrtki, K., 1971: Oceanographic atlas of the International Indian Ocean Expedition, National Science Foundation, Washington, DC.

* not referred to in original

ANNEXURE

```

C ***** MAIN PROGRAM *****
PROGRAM BUDGET
C BUDGET COMPUTATIONS USING DATA FROM 4 SHIPS
PARAMETER (IM=59,JM=4,KM=17,KMP1=KM+1)
C IM => HOUR , JM => SHIP , KM => LEVEL
C ***** DIMENSION *****
DIMENSION DD(IM,KM,JM),FF(IM,KM,JM),TD(IM,KM,JM),T(IM,KM,JM),
1 SST(IM,JM),SDD(IM,JM),TDA(IM,JM),TA(IM,JM),U(KM,JM),
2 V(KM,JM),W(KM,JM),G12(KM,2),Q34(KM,2),QW(JM),QW1(2),
3 QW2(2),QA(JM),QSS(JM),PKM),PS(IM,JM),T12(IM,KM,2),
4 T34(IM,KM,2),Z(IM,KM,JM),Z12(IM,KM,2),Z34(IM,KM,2),
5 FH(JM),FH1(2),FH2(2),EL(JM),SF(JM),U12(KM,2),V34(KM,2),
6 US(JM),VS(JM),SFF(IM,JM),E(KM,JM),ESS(JM),EA(JM),
7 QQ(KM,JM),GAA(JM),QSSS(JM),QFLUX(KM,JM),QF12(KM,2),QF34(KM,2)
* HFLUX(KM,JM),HF12(KM,2),HF34(KM,2),OMEGA(IM,KM),DIV(IM,KMP1),
* VORT(IM,KMP1),AVORT(KMP1),ADIV(KMP1),AOMEGA(KM)
9 SED(KMP1,JM),SEM(KMP1,JM),PW(JM),EK(IM,KMP1),UBAR(IM,KMP1),
* VBAR(IM,KMP1),QBAR(IM,KMP1),AVSED(IM,KMP1),AVSEM(IM,KMP1),
* UAVER(KMP1),VAVER(KMP1),SEDM(KMP1),SEMM(KMP1),QAVER(KMP1),
* EKAVER(KMP1),QF700(JM),HF700(JM),QF712(2),QF734(2),HF712(2),
* HF734(2),QF200(JM),HF200(JM)
C ***** EQUIVALENCE *****
EQUIVALENCE (Q(1,1),Q12(1,1)),(Q(1,3),Q34(1,1)),(QW(1),QW1(1)),
1 (QW(3),GW2(1)),(T(1,1,1),T12(1,1,1)),(T(1,1,3),T34(1,1,1)),
2 (FH(1),FH1(1)),(FH(3),FH2(1)),(Z(1,1,1),Z12(1,1,1)),
3 (Z(1,1,3),Z34(1,1,1)),(U(1,1),U12(1,1)),(V(1,3),V34(1,1)),
4 (QFLUX(1,1),QF12(1,1)),(QFLUX(1,3),QF34(1,1)),
5 (HFLUX(1,1),HF12(1,1)),(HFLUX(1,3),HF34(1,1)),
6 (QF700(1),QF712(1)),(QF700(3),QF734(1)),
7 (HF700(1),HF712(1)),(HF700(3),HF734(1))
C *****
CHARACTER *80 TITLE(IM,JM)
DATA P /1000.,950.,900.,250.,800.,750.,700.,650.,600.,550.,
1 500.,450.,400.,350.,300.,250.,200./
OPEN (05,FILE='SHIPDATA',STATUS='UNKNOWN')
OPEN (06,FILE='OUTPUT',STATUS='UNKNOWN')
C ----- CONSTANTS -----
WL=4.05*110.E3
G=9.8 ; WL=4.05*110.E3 ; HL=2.5E6 ; CH=1.4E-3 ; PAI=22./7.
CP=1004. ; PHC=1.2 ; DP=50.E2 ; CON=PAI/180. ; DPG=DP/G
FACT=WL*DPG ; WL2=WL*WL ; DAY=24.*60.*60.
C ----- DATA INPUT -----
DO 100 J=1,JM ; DO 10 I=1,IM ; READ(05,9) TITLE(I,J)
READ(05,11) SDD(I,J),SFF(I,J),(DD(I,K,J),FF(I,K,J),K=1,KM)
READ(05,22) SST(I,J), TA(I,J),(T(I,K,J),K=1,KM)
READ(05,22) TDA(I,J),(TD(I,K,J),K=1,KM)
READ(05,33) PS(I,J), (Z(I,K,J),K=1,KM)
10 CONTINUE
120 CONTINUE
ZS=0.
9 FORMAT(A)
11 FORMAT(16(F3.0,F2.0))
C 11 FORMAT(16(F3.0,F2.0))
22 FORMAT(20F4.1)
33 FORMAT(16F5.0)
C 33 FORMAT(16F5.0)

```

```

C ----- TEMPERATURE CONVERSION TO DEGREE KELVIN -----
DO 111 J=1,JM ; DO 111 I=1,IM ; DO 111 K=1,KM
T(I,K,J)=T(I,K,J)+273.16 ; TD(I,K,J)=TD(I,K,J)+273.16
111 CONTINUE
DO 112 J=1,JM ; DO 112 I=1,IM ; TA(I,J)=TA(I,J)+273.16
TDA(I,J)=TDA(I,J)+273.16 ; SST(I,J)=SST(I,J)+273.16
112 CONTINUE
C ***** COMPUTATION OF U & V COMPONENTS FROM DDF *****
DO 200 I=1,IM ; DO 30 J=1,4
US(J)=-SFF(I,J)*SIN(SDD(I,J)*CON)
VS(J)=-SFF(I,J)*COS(SDD(I,J)*CON)
DO 30 K=1,KM
U(K,J)= -FF(I,K,J)*SIN(DD(I,K,J)*CON)
30 V(K,J)= -FF(I,K,J)*COS(DD(I,K,J)*CON)
C ----- DIVERGENCE, VORTICITY AND OMEGA COMPUTATION -----
C CALL VVERT(U,V,US,VS,WL,JM,KM,OMEGA, DIV, VORT, IM, I)
C ----- PART-1 ----- NET FLUX -----
C CALL SPHUM(TD, E, Q, QQ, P, IM, JM, KM, I)
CALL FLUX(QW1, FACT, Q12, U12, KM, QF12)
CALL FLUX(QW2, FACT, Q34, V34, KM, QF34)
C WRITE(06, '(4E10.6)') QW(1), QW(2), QW(3), QW(4)
C ----- CF 1000 - 700 MB -----
CALL FLUX1(QF712, FACT, Q12, U12, KM)
CALL FLUX1(QF734, FACT, Q34, V34, KM)
T2FLUX=QW(2)-QW(1)+QW(3)-QW(4)
C ----- PART-2 ----- SURFACE EVAPORATION -----
C CALL SPHUM1(TDA, EA, GA, GAA, PS, IM, JM, I)
CALL SPHUM1(SST, ESS, QSS, QSSS, PS, IM, JM, I)
CALL STATIC(SED, SEM, Z, T, Q, TA, ZS, QA, CP, HL, G, IM, JM, KM, I)
CALL TRANS
1 (PW, WVZT, WVMT, EK, UBAR, VBAR, QBAR, Q, U, V, US, VS, QA, DPG, JM, KM, IM, I)
WVZT=WVZT*WL ; WVMT=WVMT*WL
TOTPW=0.25*(PW(1)+PW(2)+PW(3)+PW(4))*WL2
C CALL BAR(UBAR, VBAR, U, V, JM, KM)
CALL XBAR(AVSED, SED, IM, JM, KMP1, I)
CALL XBAR(AVSEM, SEM, IM, JM, KMP1, I)
DO 50 J=1, JM
IF(SFF(I, J).GE.13.) THEN
CE=1.6E-3
ELSE
CE=1.4E-3
ENDIF
50 EL(J)=RHO*CE*SFF(I, J)*(QSS(J)-QA(J))
ELMEAN=0.25*(EL(1)+EL(2)+EL(3)+EL(4)) ; EAVER=ELMEAN*WL2
PL=EAVER-TQFLUX ; EDAY=EAVER*DAY
C --- CONVERSION EDAY(KG/DAY) & PL(KG/SEC) TO (CM/DAY) ---
EVDAY=EDAY*100./(WL2*1000.) ; PDAY=PL*DAY*100./(WL2*1000.)
C ----- PART-3 ----- HEAT BUDGET -----
C CALL FHEAT(FH1, FACT, T12, Z12, U12, IM, KM, CP, G, I, HF12)
CALL FHEAT(FH2, FACT, T34, Z34, V34, IM, KM, CP, G, I, HF34)
THEAT=FH(2)-FH(1)+FH(3)-FH(4)
C ----- HF 1000 - 700 MB COMPUTATION -----
CALL FHEAT1(HF712, FACT, T12, Z12, U12, IM, KM, CP, G, I)
CALL FHEAT1(HF734, FACT, T34, Z34, V34, IM, KM, CP, G, I)

```

```

C ----- GF 700 - 200 MB ; HF 700 - 200 MB -----
C DO 113 J=1,JM ; QF200(J)=QW(J)-QF700(J)
113 HF200(J)=FA(J)-HF700(J)
C ----- PAPT-4 ----- SURFACE HEAT -----
C DO 6J J=1,JM
C SF(J)=RHO*CH*CP*SFF(I,J)*(SST(I,J)-TA(I,J))
C SFMEAN=0.25*(SF(1)+SF(2)+SF(3)+SF(4)) ; SFAVER=SFMEAN*WLE
C RAD=-THEAT-SFAVER-PL*HL ; SFDAY=SFAVER*DAY
C ----- OUTPUT PRINTING -----
C WRITE(06,'(1X,A)')TITLE(I,1)
C DO 70 J=1,JM
C WRITE(06,'(1X,A)')TITLE(I,J)
C WRITE(06,'(1X,'QF700,QF200,HF700,HF200 ==>',E16.6)')
C 1 QF700(J),QF200(J),HF700(J),HF200(J)
C WRITE(06,'(1X,'DRY STATIC ENERGY (M**M/S**S) ==>',(7E14.4)')')
C 1 (SED(K,J), K=1,KMP1)
C WRITE(06,'(1X,'MOIST STATIC ENERGY ==>',(7E14.4)')(SEM(K,J),
C 1 K=1,KMP1)
C WRITE(06,'(1X,'PRECIPITABLE WATER (KG/M**M)='E14.4)')PW(J)
C WRITE(06,17) SST(I,J),ESS(J),QSSS(J),EL(J),GW(J),FH(J),SF(J)
17 FORMAT(1X,'SST ='FR.1,5X,'ESS(MB) ='FR.2,5X,'QSSS(G/KG) ='
1 FR.2,5X,'EVAP(KG/M**2/SEC) ='E16.6,1X,'QW(KG/SEC) ='E16.6,
2 4X,'FH(J/SEC) ='E10.0,4X,'SHFLUX(J/M**2/SEC) ='E16.6)
C WRITE(06,13)
C WRITE(06,14) PS(I,J),ZS,SDD(I,J),SFF(I,J),TA(I,J),TDA(I,J)
1 ,US(J),VS(J),EA(J),QAA(J)
C WRITE(06,14) (P(K),Z(I,K,J),DD(I,K,J),FF(I,K,J),T(I,K,J),
1 TD(I,K,J),L(K,J),V(K,J),E(K,J),QQ(K,J),QFLUX(K,J),HFLUX(K,J),
2 K=1,KM)
13 FORMAT(1X,'PRESSURE',3X,'HEIGHT',3X,' DD ',',',FF',4X,'T',7X,
1 'TD',0X,'U',8X,'V',7X,'E',7X,'G',7X,'QFLUX(KG/SEC)',
2 7X,'HFLUX(J/SEC)')
14 FORMAT(1X,2F5.0,3X,2F5.0,2F8.1,4F8.2,2E16.6)
70 CONTINUE
C WRITE(06,'(1X,A)')TITLE(I,1)
C WRITE(06,44) TQFLUX,EAVER,EDAY,PL,THEAT,SFAVER,SFDAY,RAD
44 FORMAT(1X,'TQFLUX(KG/SEC) ='E16.6,4X,'EAVER(KG/SEC) ='E16.6,3X,
1 'EDAY(KG/DAY) ='E16.6,3X,'PL(KG/SEC) ='E16.6,1X,
2 'THEAT(J/SEC) ='E16.6,4X,'SFAVER(J/SEC) ='E16.6,4X,
3 'SFDAY(J/DAY) ='E16.6,4X,'RAD(J/SEC) ='E16.6)
C WRITE(06,55) EVDAY,PDAY
55 FORMAT(1X,'EDAY='E12.4,3X,'PDAY='E12.4)
C WRITE(06,66)
66 FORMAT(1X,'PRESS',5X,'DIV(/SEC)',5X,'OMEGA(MB/SEC)')
C WRITE(06,'(1X,F6.0,2E14.4)')(P(K),DIV(K),OMEGA(K),K=1,KM)
C WRITE(06,'(1X,9E14.4)')(VCRT(I,K),K=1,KMP1)
C WRITE(06,'(1X,'MEAN U ==>',(17F7.2))')(UBAR(K),K=1,KM)
C WRITE(06,'(1X,'MEAN V ==>',(17F7.2))')(VBAR(K),K=1,KM)
C WRITE(06,'(1X,'MEAN K.E.(M**M/S**S) ==>',(7E14.4)')')
1 (EK(K),K=1,KMP1)
C WRITE(06,'(1X,'TOTAL PRECIPITABLE WATER (KG) ==>',E14.4)')TOTPW
C WRITE(06,'(1X,'ZONAL TRANSPORT OF WV (KG/S)**E14.4,5X,
C 1'MERIDIONAL TRANSPORT OF WV (KG/S)**E14.4)')WVZT,WVMT
C DO 233 K=1,KMP1
233 QBAR(I,K)=QBAR(I,K)*1000.
C WRITE(06,'(1X,'QBAR ==>',(17F7.2))')(QBAR(I,K),K=1,KMP1)
C WRITE(06,'(1X,'UBAR ==>',(17F7.2))')(UBAR(I,K),K=1,KMP1)
C WRITE(06,'(1X,'VBAR ==>',(17F7.2))')(VBAR(I,K),K=1,KMP1)
200 CONTINUE

```

```

C ----- COMPUTATION OF MEAN PROFILES FOR THE PHASE -----
C CALL AVER(SEDM,AVSED,IM,KMP1) ; CALL AVER(SEMM,AVSEM,IM,KMP1)
C CALL AVER(QAVER,UBAR,IM,KMP1) ; CALL AVER(VAVER,VBAR,IM,KMP1)
C CALL AVER(QAVER,QBAR,IM,KMP1) ; CALL AVER(EKAVER,EK,IM,KMP1)
C CALL AVER(AVORT,VORT,IM,KMP1) ; CALL AVER(ADIV,DIV,IM,KMP1)
C CALL AVER(AOMEGA,OMEGA,IM,KM)
C DO 114 K=1,KMP1
C 114 QAVER(K)=QAVER(K)*1000.
C WRITE(06,'(1X,'MEAN U ==>',(17F7.2))')(QAVER(K),K=1,KMP1)
C WRITE(06,'(1X,'MEAN V ==>',(17F7.2))')(VAVER(K),K=1,KMP1)
C WRITE(06,'(1X,'SP.HUM ==>',(17F7.2))')(QAVER(K),K=1,KMP1)
C WRITE(06,'(1X,'MEAN K.E.(M**M/S*S) ==>',(7E14.4))')
C 1 (EKAVER(K),K=1,KMP1)
C WRITE(06,'(1X,'AV. VORTICITY ==>',(8E14.4))')
C 1 (AVORT(K),K=1,KMP1)
C WRITE(06,'(1X,'AV. DIVERGENCE ==>',(8E14.4))')
C 1 (ADIV(K),K=1,KMP1)
C WRITE(06,'(1X,'AV. OMEGA ==>',(8E14.4))')(AOMEGA(K),K=1,KM)
C WRITE(06,'(1X,'DRY STATIC ENERGY (M**M/S*S) ==>',(7E14.4))')
C 1 (SEDM(K),K=1,KMP1)
C WRITE(06,'(1X,'MOIST STATIC ENERGY ==>',(7E14.4))')(SEMM(K),
C 1 K=1,KMP1)
C STOP
C END
C ***** SUBROUTINES *****
C SUBROUTINE SPHUF(TD,E,Q,QQ,P,IM,JM,KM,I)
C DIMENSION TD(IM,KM,JM),G(KM,JM),P(KM),E(KM,JM),QQ(KM,JM)
C DO 10 J=1,JM ; DO 10 K=1,KM ; TT=TD(I,K,J)
C IF(TT.LE.263.) THEN
C A=21.87 ; B=7.66
C ELSE
C A=17.26 ; B=35.36
C ENDOF
C E(K,J)=6.11*EXP(A*(TT-273.16)/(TT-B))
C Q(K,J)=0.622*E(K,J)/(P(K)-0.376*E(K,J))
C 10 QQ(K,J)=Q(K,J)*1000.
C RETURN
C END
C *****
C SUBROUTINE FLUX(QW,FACT,U,J,KM,PROD)
C DIMENSION QW(2),U(KM,2),PROD(KM,2)
C DO 10 J=1,2 ; SUM=0. ; DO 20 K=1,KM-1
C PROD(K,J)=(U(K,J)+U(K+1,J))*(Q(K,J)+Q(K+1,J))+0.25*FACT
C 20 SUM=SUM+PROD(K,J)
C 10 QW(J)=SUM
C RETURN
C END
C *****
C SUBROUTINE FHEAT(FH,FACT,T,U,IM,KM,CP,G,I,PROD)
C DIMENSION T(IM,KM,2),U(KM,2),Z(IM,KM,2),FH(2),PROD(KM,2)
C DO 10 J=1,2 ; SUM=0. ; DO 20 K=1,KM-1
C PRD=CP*(T(I,K,J)+T(I,K+1,J))+G*(Z(I,K,J)+Z(I,K+1,J))
C PROD(K,J)=(U(K,J)+U(K+1,J))*PRD+0.125*FACT
C 20 SUM=SUM+PROD(K,J)
C 10 FH(J)=SUM
C RETURN
C END
C *****

```

```

SUBROUTINE FLUX1(QF,FACT,G,U,KM)
DIMENSION WF(2),Q(KM,2),U(KM,2)
DO 10 J=1,2 ; SUM=0. ; DO 20 K=1,6
PRD=(U(K,J)+U(K+1,J))*(Q(K,J)+Q(K+1,J))=0.25*FACT
20 SUM=SUM+PRD
10 WF(J)=SUM
RETURN ; END
C *****
SUBROUTINE FHEAT1(HF,FACT,T,Z,U,IM,KM,CP,G,I)
DIMENSION T(IM,KM,2),U(KM,2),Z(IM,KM,2),HF(2)
DO 10 J=1,2 ; SUM=0. ; DO 20 K=1,6
PRD=CP*(T(I,K,J)+T(I,K+1,J))+G*(Z(I,K,J)+Z(I,K+1,J))
PRD=(U(K,J)+U(K+1,J))*PRD*0.125*FACT
20 SUM=SUM+PRD
10 HF(J)=SUM
RETURN ; END
C *****
SUBROUTINE SPHUM1(T,E,Q,QQ,P,IM,JM,I)
DIMENSION T(IM,JM),E(JM),Q(JM),P(IM,JM),QQ(JM)
DO 10 J=1,JM ; TT=T(I,J)
IF(TT.LE.263.) THEN
A=21.87 ; B=7.56
ELSE
A=17.26 ; B=35.86
ENDIF
E(J)=6.11*EXP(A-(TT-273.16)/(TT-B))
Q(J)=0.622*E(J)/(P(I,J)-0.378*E(J))
10 QQ(J)=Q(J)*1000.
RETURN
END
C *****
SUBROUTINE VVERT(U,V,US,VS,WL,JM,KM,W,DIV,VORT,IM,I)
DIMENSION U(KM,JM),V(KM,JM),W(DIV(IM,KM+1),ADIV(17)),W(IM,KM),
* US(JM),VS(JM),VORT(IM,KM+1)
K*1=KM-1 ; DP=50. ; DX=1./WL ; W(I,1)=0. ; W(1,KM)=0.
C ----- DIVERGENCE COMPUTATION -----
DIV(I,1)=DX*(US(2)-US(1)+VS(3)-VS(4))
DO 10 K=1,K*
10 DIV(I,K+1)=DX*(U(K,2)-U(K,1)+V(K,3)-V(K,4))
C ----- VORTICITY COMPUTATION -----
VORT(I,1)=DX*(VS(2)-VS(1)-US(3)+US(4))
DO 15 K=1,KM
15 VORT(I,K+1)=DX*(V(K,2)-V(K,1)-U(K,3)+U(K,4))
20 ADIV(K-1)=(DIV(I,K)+DIV(I,K+1))*0.5
SUM=0.
DO 30 K=1,KM+1
30 SUM=SUM+ADIV(K)
COR=SUM*DP/500.
DO 40 K=1,KM+1
40 ADIV(K)=(ADIV(K)-COR)*DP
SUM=0.
DO 45 K=1,KM
C 45 SUM=SUM+ADIV(K) ; W*TT=(06*(516.6)) SUM
DO 50 K=2,KM+1
50 W(I,K)=W(I,K-1)+ADIV(K-1)
RETURN
END

```

```

C *****
C   SUBROUTINE STATIC(SED,SEM,Z,T,G,TA,ZS,QA,CP,HL,G,IM,JM,KM,I)
C   COMPUTATION OF DRY STATIC ENERGY (:SED) & MOIST STATIC ENERGY (:SEM)
C   DIMENSION SED(KM+1,JM),SEK(KM+1,JM),Z(IM,KH/JM),T(IM,KH/JM),
1   Q(KH/JM),QA(JM),TA(IM,JM)
C   DO 10 J=1,JM ; SED(1,J)=G*ZS+CP*TA(I,J)
C   SEM(1,J)=SED(1,J)+QA(J)*HL
C   DO 10 K=1,KM ; SED(K+1,J)=G*Z(I,K,J)+CP*T(I,K,J)
17  SEI(K+1,J)=SEK(K+1,J)+Q(K,J)*HL
C   RETURN ; END
C *****
C   SUBROUTINE TRANS
C   1 (PW,WVZT,WVMT,EK,UBAR,VBAR,QBAR,Q,U,V,JS,VS,QS,DPG,JM,KM,IM,I)
C   COMPUTES PRECIPITABLE WATER (PW),ZONAL TRANSPORT OF WV (WVZT),
C   MERIDIONAL TRANSPORT OF WV (WVMT),MEAN K.E.(EK)
C   DIMENSION U(KM,JM),V(KM,JM),Q(KM,JM),PW(JM),EK(IM,KM+1),US(JM),
1   VS(JM),UBAR(IM,KM+1),VBAR(IM,KM+1),QBAR(IM,KM+1),QS(JM)
C   PRECIPITABLE WATER -----
C   DO 10 J=1,JM ; SUM=0. ; DO 10 K=1,KM-1
C   SUM=SUM+(Q(K,J)+Q(K+1,J))+0.5
10  PW(J)=SUM*DPG
C   ----- ZONAL / MERIDIONAL TRANSPORT OF WV /MEAN KE -----
C   WVZT=0. ; WVMT=0. ; DO 20 K=1,KM
C   QBAR(I,K+1)=0.25*(Q(K,1)+Q(K,2)+Q(K,3)+Q(K,4))
C   UBAR(I,K+1)=0.25*(U(K,1)+U(K,2)+U(K,3)+U(K,4))
C   VBAR(I,K+1)=0.25*(V(K,1)+V(K,2)+V(K,3)+V(K,4))
20  EK(I,K+1)=0.5*(UBAR(I,K+1)*UBAR(I,K+1)+VBAR(I,K+1)*VBAR(I,K+1))
C   DO 30 K=2,KM
C   WVZT=WVZT+(QBAR(I,K)+QBAR(I,K+1))*(UBAR(I,K)+UBAR(I,K+1))*0.25
30  WVMT=WVMT+(QBAR(I,K)+QBAR(I,K+1))*(VBAR(I,K)+VBAR(I,K+1))*0.25
C   WVZT=WVZT+DPG ; WVMT=WVMT+DPG
C   UBAR(I,1)=0.25*(US(1)+US(2)+US(3)+US(4))
C   VBAR(I,1)=0.25*(VS(1)+VS(2)+VS(3)+VS(4))
C   QBAR(I,1)=0.25*(QS(1)+QS(2)+QS(3)+QS(4))
C   EK(I,1)=0.5*(UBAR(I,1)*UBAR(I,1)+VBAR(I,1)*VBAR(I,1))
C   RETURN ; END
C *****
C   SUBROUTINE BAP(UB,VB,U,V,JM,KM)
C   DIMENSION UB(KM),VB(KM),U(KM,JM),V(KM,JM)
C   XJM=JM ; DO 10 K=1,KM ; USUM=0. ; VSUM=0. ; DO 20 J=1,JM
C   USUM=USUM+U(K,J) ; VSUM=VSUM+V(K,J)
20  CONTINUE ; UB(K)=USUM/XJM ; VB(K)=VSUM/XJM
10  CONTINUE ; RETURN ; END
C *****
C   SUBROUTINE XBAR(XA,X,IM,JM,KM,I)
C   DIMENSION XE(IM,KY),X(KM,JM)
C   DO 10 K=1,KM
10  XE(I,K)=0.25*(X(K,1)+X(K,2)+X(K,3)+X(K,4))
C   RETURN ; END
C *****
C   SUBROUTINE AVER(XAVER,X,IM,KM)
C   DIMENSION XAVER(KM),X(IM,KY)
C   XIM=IM ; DO 10 K=1,KM ; SUM=0. ; DO 20 I=1,IM
20  SUM=SUM+X(I,K)
10  XAVER(K)=SUM/XIM
C   RETURN ; END

```